Novel analytical approaches for biomarker detection in neonatology

Ángel Sánchez-Illana

Instituto de Investigación Sanitaria La Fe

Universitat de València

Programa de doctorado en Química (R.D. 99/2011)

Directed by: Dr. Máximo Vento Torres & Dra. Julia Kuligowski

Tutored by: Dr. Miguel de la Guardia Cirugeda

Universitat de València January 2021

D. Máximo Vento Torres, investigador principal del Grupo de Investigación en Perinatología y director científico del Instituto de Investigación Sanitaria la Fe; Doña Julia Kuligowski, investigadora postdoctoral en el Instituto de Investigación Sanitaria la Fe y D. Miguel de la Guardia Cirugeda, catedrático del departamento de Química Analítica de la Universidad de Valencia,

certifican

que la presente memoria titulada "**Novel analytical aproaches for biomarker detection in neonatology**", constituye la tesis doctoral de D. Ángel Sánchez Illana.

Asimismo, certifican haber dirigido, supervisado o tutorizado los distintos aspectos del trabajo y su redacción.

Y para que así conste a los efectos oportunos y a petición del interesado, firmamos la presente en Valencia, a 13 de enero de 2021.

Máximo Vento Torres

Julia Kuligowski

Miguel de la Guardia Cirugeda

A mi madre, que hubiera sido muy feliz de verme doctor y leer esta tesis.

Siempre recordaré todo lo que me enseñaste. Gracias, mamá.

Prefacio

La presente tesis doctoral se enmarca en la modalidad de compendio de publicaciones regulada en el reglamento sobre depósito, evaluación y defensa de la tesis doctoral de la Universitat de València, artículo 8. A continuación se detallan las publicaciones incluidas en la tesis doctoral en forma de los distintos capítulos.

Artículo 1.

Á. Sánchez-Illana, J.D. Piñeiro-Ramos, J. Kuligowski, Small molecule biomarkers for neonatal hypoxic ischemic encephalopathy, Seminars in Fetal and Neonatal Medicine. 25 (2020) 101084. https://doi.org/10.1016/j.siny.2020.101084.
Factor de impacto en el Journal Citation Reports (JCR) 2019: 3,540
Categoría y posición (JCR) 2019: Pediatrics, 11/128, D1

Artículo 2.

Á. Sánchez-Illana, R. Solberg, I. Lliso, L. Pankratov, G. Quintás, O.D. Saugstad, M. Vento, J. Kuligowski, Assessment of phospholipid synthesis related biomarkers for perinatal asphyxia: a piglet study, Sci Rep. 7 (2017) 40315. https://doi.org/10.1038/srep40315.
Factor de impacto en el Journal Citation Reports (JCR) 2017: 4,122
Categoría y posición (JCR) 2017: Multidisciplinary Sciences, 12/64, Q1

Artículo 3.

Á. Sánchez-Illana, A. Núñez-Ramiro, M. Cernada, A. Parra-Llorca, E. Valverde, D. Blanco, M.T. Moral-Pumarega, F. Cabañas, H. Boix, A. Pavon, M. Chaffanel, I. Benavente-Fernández, I. Tofe, B. Loureiro, J.R. Fernández-Lorenzo, B. Fernández-Colomer, A. García-Robles, J. Kuligowski, M. Vento, HYPOTOP Study Group, Evolution of Energy Related Metabolites in Plasma from Newborns with Hypoxic-Ischemic Encephalopathy during Hypothermia Treatment, Sci Rep. 7 (2017) 17039. https://doi.org/10.1038/s41598-017-17202-7.
Factor de impacto en el Journal Citation Reports (JCR) 2017: 4,122
Categoría y posición (JCR) 2017: Multidisciplinary Sciences, 12/64, Q1

Artículo 4.

Á. Sánchez-Illana, J.D. Piñeiro-Ramos, V. Ramos-Garcia, I. Ten-Doménech, M. Vento, J. Kuligowski, Oxidative stress biomarkers in the preterm infant, Advances in Clinical Chemistry. *Aceptado, sin número ni volumen* (2020).
https://doi.org/10.1016/bs.acc.2020.08.011
Factor de impacto en el Journal Citation Reports (JCR) 2019: 3,367
Categoría y posición (JCR) 2019: Medical laboratory technology, 6/29, Q1

Artículo 5.

Á. Sánchez-Illana, S. Thayyil, P. Montaldo, D. Jenkins, G. Quintás, C. Oger, J.-M. Galano, C. Vigor, T. Durand, M. Vento, J. Kuligowski, Novel free-radical mediated lipid peroxidation biomarkers in newborn plasma, Analytica Chimica Acta. 996 (2017) 88–97. https://doi.org/10.1016/j.aca.2017.09.026.
Factor de impacto en el Journal Citation Reports (JCR) 2017: 5,123
Categoría y posición (JCR) 2017: Chemistry, analytical, 8/81, D1

Artículo 6.

Á. Sánchez-Illana, V. Shah, J.D. Piñeiro-Ramos, J.M. Di Fiore, G. Quintás, T.M. Raffay, P.M. MacFarlane, R.J. Martin, J. Kuligowski, Adrenic acid non-enzymatic peroxidation products in biofluids of moderate preterm infants, Free Radical Biology and Medicine. 142 (2019) 107–112. https://doi.org/10.1016/j.freeradbiomed.2019.02.024.
Factor de impacto en el Journal Citation Reports (JCR) 2019: 6,170
Categoría y posición (JCR) 2019: Endocrinology & Metabolism 16/143, Q1

Artículo 7.

Á. Sánchez-Illana, A. Parra-Llorca, D. Escuder-Vieco, C.R. Pallás-Alonso, M. Cernada, M. Gormaz, M. Vento, J. Kuligowski, Biomarkers of oxidative stress derived damage to proteins and DNA in human breast milk, Analytica Chimica Acta. 1016 (2018) 78–85. https://doi.org/10.1016/j.aca.2018.01.054.
Factor de impacto en el Journal Citation Reports (JCR) 2018: 5,256
Categoría y posición (JCR) 2018: Multidisciplinary Sciences, 10/84, Q1

Artículo 8.

Á. Sánchez-Illana, F. Mayr, D. Cuesta-García, J.D. Piñeiro-Ramos, A. Cantarero, M. de la Guardia, M. Vento, B. Lendl, G. Quintás, J. Kuligowski, On-Capillary Surface-Enhanced Raman Spectroscopy: Determination of Glutathione in Whole Blood Microsamples, Anal. Chem. 90 (2018) 9093–9100. https://doi.org/10.1021/acs.analchem.8b01492.
Factor de impacto en el Journal Citation Reports (JCR) 2018: 6,350
Categoría y posición (JCR) 2018: Chemistry, analytical, 7/84, D1

Agradecimientos

Me gustaría trasladar un agradecimiento a las personas del Grupo de Investigación en Perinatología del Instituto de Investigación Sanitaria la Fe, a todo el personal del Servicio de Neonatología del Hospital la Fe y a los miembros de los equipos de nuestras colaboraciones nacionales e internacionales por su trabajo y ayuda a lo largo de todos estos años. Con una mención especial al Departamento de Pediatría del Instituto para la Investigación Quirúrgica del Hospital Universitario de Oslo; al Departamento de Pediatría del Hospital Vestfold de Tønsberg; al Instututo de Biomoléculas Max Mousseron de Montpelier; al Departamento de Pediatría del Hospital Universitario de Carolina del Sur; al Centro de Neurociencia Perinatal del *Imperial College* de Londres; al Departamento de Pediatría del *Rainbow Babies and Children's Hospital* y a la Facultad de Medicina de la Universidad *Case Western Reserve* de Cleveland; al Grupo de Investigación SOLINQUIANA del Departamento de Química Analítica de la Universidad de València; al equipo de la delegación de València de la división de Salud Humana, Medioambiental y Seguridad del Centro Tecnológico Leitat; al Área de Seguridad Alimentaria de FISABIO-Salud Pública de València y a todos los miembros de la Red de Salud Materno-Infantil y del Desarrollo (Red SAMID).

También quisiera transmitir mi reconocimiento, por sus diligentes servicios, al Servicio Central de Soporte a la Investigación Experimental (SCSIE) de la Universidad de València y a las plataformas y áreas de gestión del Instituto de Investigación Sanitaria La Fe.

Tampoco quisiera olvidar mis agradecimientos al Instituto de Salud Carlos III por la concesión del contrato predoctoral PFIS (FI16/00380) y la ayuda de movilidad M-AES (MV17/00024), gracias a las cuales he podido disfrutar de financiación personal. Así como los proyectos FISPI14/0433, EC11-244, CP16/00034, PI17/00127, RD12/0026/11 que han sido imprescindibles para la realización de esta tesis doctoral. También al grupo de Química Biológica y Aptámeros del LIMES-Institut y el Kekulé-Institut de la Universidad de Bonn por acogerme durante mi estancia como a uno más de su equipo.

Además, me gustaría agradecer a todos aquellos amigos que han estado a mi lado durante estos años, especialmente a Iván, mi ingeniero informático de cabecera.

Y por último y no por ello menos importante, agradecer a toda mi familia su ayuda y su apoyo y a Rebecca por todo lo que hace por mí cada segundo de nuestra vida juntos.

Contents

Resumen global

i. Introducción

A lo largo de los años, gran parte de los hitos en fisiología neonatal han estado íntimamente ligados a los avances en química analítica. Ejemplos de ello son las primeras medidas de oxihemoglobina en sangre de cordón realizadas por Zweifel a mediados del s. XIX empleando el recién inventado espectroscopio de Browning[1], los estudios de los gases sanguíneos en fetos y neonatos realizados por Huggett y Barcroft a principios del s. XX empleando manómetros de Van Slyke (y los propios aparatos inventados por Barcroft), los estudios del metabolismo de la glucosa de Hugget empleando por primera vez glucosa marcada con ^{14}C y determinaciones radiométricas[2] o los estudios de lactato en sangre de cordón de Eastman empleando sofisticadas volumetrías[3]. De igual manera, ya durante la segunda mitad del s. XX, la introducción de los ensayos enzimáticos, inmunoensayos y técnicas cromatográficas y electroforéticas permitieron estudiar en profundidad metabolitos, hormonas y proteínas de interés en neonatología[2]. Asimismo, en años más recientes, los avances en las tecnologías ómicas y bioinformáticas han permitido mejorar el conocimiento de los síndromes y enfermedades en el ámbito neonatal estableciendo patrones genómicos, epigenéticos, proteómicos y metabolómicos, permitiendo el acceso a una multitud de biomarcadores[2,4,5].

Una de las definiciones más reconocidas de biomarcador es la que ofrece la iniciativa conjunta de la *Food and Drug Administration* (FDA) y los *National Institutes of Health* (NIH) de Estados Unidos en su glosario BEST, que lo definen como una característica medible indicativa de normalidad, proceso patológico o respuesta a exposición o intervención. Además, la definición también clasifica a los diferentes tipos de biomarcadores en moleculares, radiográficos e incluso características fisiológicas[6]. En este sentido, no han sido únicamente las tecnologías ómicas las que han ido ampliando el número de biomarcadores en neonatología, pero sí las que han permitido el surgimiento de una plétora de moléculas candidatas a serlo y de prolíficos autores[4,5,7–11]. A modo de ejemplo, en la **Ilustración 1** puede observarse como el número de publicaciones sobre asfixia perinatal que incluye conceptos como biomarcador, metabolómica o algunos otros relacionados con otras ómicas ha experimentado un gran incremento en los últimos años.

De entre todas las ómicas, la metabolómica aborda el análisis exhaustivo de las moléculas pequeñas (<1 kDa) de una muestra biológica y tiene su razón de ser en el desarrollo de las técnicas instrumentales y, especialmente, las técnicas acopladas[12,13]. La resonancia

magnética nuclear (RMN) y la espectrometría de masas de alta resolución, esta última usualmente acoplada a cromatografía de gases o líquidos, han sido las técnicas más ampliamente utilizadas. Estas metodologías generan una ingente cantidad de datos multidimensionales por lo que el desarrollo de herramientas quimiométricas multivariantes que permitan lidiar con ellos ha sido igualmente crucial para el desarrollo de la metabolómica. Los análisis metabolómicos pueden dividirse en dirigidos, semidirigidos o no dirigidos y todos ellos juegan un papel en la búsqueda y validación de nuevos biomarcadores.

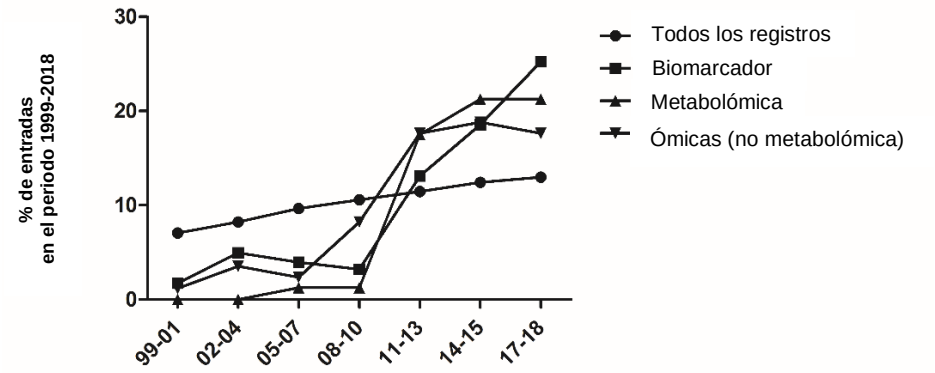

Ilustración 1 Porcentaje de los registros en la *Web of Science*® en el periodo 1999-2018 para cada intervalo de 3 años. Bases de datos empleadas: WOS, CCC, DIIDW, KJD, MEDLINE, RSCI, SCIELO. Las combinaciones de booleanas empleadas fueron: TS = (asphy* OR hypox* OR HIE OR anoxia) AND TS = (*perinatal* OR *pediatric* OR neonat* OR *newborn*) para el campo "todos los registros"; para los campos "biomarcador", "metabolómica" y "ómicas (no metabolómica)" se afinaron los resultados con los booleanos: *biomarker*, (metabolom or metabonom*), and ((*genomics or transcriptomics or proteomics or lipidomics or epigenomics*)), respectivamente.

Los métodos dirigidos fueron los primeros en desarrollarse y consisten en la cuantificación de un número relativamente pequeño de metabolitos (decenas de ellos), conocidos *a priori*. Al conocer las propiedades químicas de los analitos y las matrices de interés, es posible optimizar las variables experimentales para obtener unos parámetros de calidad analítica (selectividad, sensibilidad, precisión, exactitud, entre otros) adecuados. Además, es para los métodos dirigidos para los que existe un mayor desarrollo en cuanto a lo que validación analítica se refiere, existiendo diversas guías de organismos internacionales como la Agencia Europea del Medicamento y la FDA estadounidense[14,15]. Las determinaciones cuantitativas realizadas en los laboratorios clínicos empleando productos sanitarios para diagnóstico *in vitro* (*in vitro diagnostic tests, IVDs)*[16] hacen uso de métodos dirigidos y son también los métodos dirigidos los únicos que, a día de hoy, pueden enmarcarse en las normas internacionales de acreditación ISO 15189 e ISO/IEC 17025 para laboratorios clínicos y laboratorios generales de ensayo/calibración, respectivamente[17,18]. Sin embargo, la capacidad de los métodos dirigidos para descubrir nuevos biomarcadores y generar nuevas hipótesis es limitada ya que se encuentran circunscritos al panel de compuestos escogido.

Por su parte, los métodos no dirigidos consisten en el análisis simultáneo de tantos compuestos como sea posible en la muestra biológica en cuestión. Estos métodos proporcionan

información semicuantitativa (como p.ej. áreas de picos) en lugar de concentraciones absolutas[19] y la identidad de los compuestos no es conocida *a priori*, de hecho, el proceso de identificación es uno de los principales retos en los estudios de metabolómica no dirigida[20]. En este escenario se suele decir que el análisis es libre de hipótesis y las limitaciones son fundamentalmente instrumentales o computacionales.

Existe un enfoque intermedio entre el análisis no dirigido y el análisis dirigido denominado análisis semidirigido. En este tipo de análisis, se realiza un análisis de un gran número de compuestos, usualmente cientos de ellos. Estos números son accesibles gracias al desarrollo de los modernos equipos de cromatografía líquida-espectrometría de masas tándem (LC-MS/MS) y especialmente a las actuales interfases de *electrospray* (ESI). Estos métodos, suelen incluir simultáneamente determinaciones cuantitativas y otras semicuantitativas, empleando diferentes curvas de calibrado y múltiples calibraciones de patrón interno. Actualmente se comercializan varios kits comerciales como los desarrollados por Biocrates AG (Innsbruck, Austria), que permiten determinar por LC-MS/MS más de 500 metabolitos pertenecientes a 26 clases diferentes. Estos kits se han empleado para estudios en la población neonatal[21,22].

En cualquiera de sus modalidades, el análisis metabolómico aplicado a la población neonatal presenta una serie de peculiaridades que lo hacen especialmente delicado. En primer lugar, la obtención de cantidades suficientes de muestra suele ser complicado debido a que los procedimientos invasivos (venopunción, sondaje, canalización, entre otros) tienen mayores implicaciones en el neonato frente a una persona adulta. Y, además, hay que tener en cuenta que el momento del muestreo en muchas investigaciones se produce en situaciones extremadamente complejas, como puede ser un complicado ingreso en una unidad de cuidados intensivos neonatal (UCIN), en la camilla de reanimación del paritorio o durante complejos tratamientos como la hipotermia terapéutica o la oxigenación por membrana extracorpórea. Todo ello hace que el desarrollo de métodos analíticos *ad hoc* sea imprescindible para poder llevar a cabo validaciones satisfactorias.

De entre todas las patologías que son objeto de estudio en neonatología, en una de las que la metabolómica más se ha abierto paso es en la encefalopatía hipóxico-isquémica (EHI)[4,5,7–9,23]. La encefalopatía neonatal consecuencia de un evento intraparto, y más en concreto la EHI cuando existe una relación causal con un evento hipóxico isquémico, es una de las principales causas de morbimortalidad neonatal hoy en día[24]. Los procesos que desencadenan la EHI son complejos y pueden estudiarse sendas fases diferenciadas en las cuales suceden una serie de fallos en el metabolismo energético que pueden desembocar en necrosis y apoptosis de tejido neuronal[25]. El sistema nervioso central (SNC) junto con el miocardio puede considerarse tejidos oxireguladores en tanto en cuanto dependen del metabolismo aerobio en una mayor extensión que el resto de los tejidos. A lo que respecta al SNC, el mantenimiento de su homeostasis tisular es especialmente crítico. Una disfunción en la circulación cerebral puede ocasionar una falta de oxígeno y glucosa que conlleva un rápido agotamiento de las reservas energéticas y la muerte celular en pocos minutos[25]. En el caso de

la EHI, la asfixia aguda que la antecede causa una disminución en la perfusión cerebral y desencadena la secuencia de daño. En una primera fase aguda, esta falta de oxígeno y glucosa conduce al metabolismo anaerobio, ocasionando un drástico descenso en la producción de adenosín trifosfato (ATP) y un incremento en las concentraciones de ácido láctico. El agotamiento del ATP conlleva un transporte transmembrana defectuoso lo que inicia el proceso de excitotoxicidad provocando necrosis y la activación de cascadas apoptóticas. En función de la duración del evento hipóxico-isquémico y de la intervención clínica, una recuperación parcial ocurre entre los 30 min y los 60 min después de la fase aguda. Esta recuperación marca el comienzo de la fase latente, que puede durar entre 1 a 6 horas y está caracterizada por un restablecimiento del metabolismo oxidativo y el consiguiente daño por reperfusión en el que se desencadenan los procesos de estrés oxidativo. Para los casos severos y moderados, una segunda fase de la EHI ocurre desde las 6 horas del evento hipóxico-isquémico hasta las 15 horas. Esta segunda fase suele ser devastadora para el estado clínico del neonato, produciéndose un fallo energético secundario que se suma a los procesos iniciados en la fase latente, lo que supone la inactividad mitocondrial y muerte celular. En esta fase es cuando, con mayor frecuencia, ocurren las convulsiones. Por último, una tercera fase se describe para los días y meses posteriores al evento hipóxio-isquémico en la que aparece muerte celular tardía, una remodelación del cerebro dañado y astrogliosis[25,26]. En la actualidad, la EHI continúa siendo una de las causas más prevalentes de daño neurológico agudo y de afectación en el desarrollo suponiendo una mayor incidencia en parálisis cerebral, problemas cognitivos, retrasos en el crecimiento y epilepsia[24,27–29]. La magnitud de los fracasos en el metabolismo energético determina el daño histológico y la gravedad de la discapacidad neurológica posterior. El papel que juega la metabolómica y los biomarcadores en la EHI es, por un lado, mejorar el entendimiento de los procesos bioquímicos que ocurren en cada fase y, por otro, aportar información relevante que pueda guiar en el manejo clínico.

La prematuridad es otro de los contextos clínicos neonatales en los que la determinación de biomarcadores y los estudios metabolómicos han experimentado un gran auge[5,7]. Actualmente la prematuridad es la principal causa de mortalidad neonatal en los países desarrollados y en cuanto a morbilidad a largo plazo, se ha relacionado con un peor neurodesarrollo, mayores tasas de ingresos hospitalarios y dificultades de aprendizaje y socioemocionales. Por lo tanto, la prematuridad supone un gran impacto económico en las familias y en los sistemas sanitarios alrededor de todo el mundo[30]. Un nacimiento prematuro, según la Organización Mundial de la Salud, es aquél que ocurre antes de las 37 semanas de gestación o 259 días después del primer día del último periodo menstrual[31]. Adicionalmente, pueden clasificarse en diferentes categorías dependiendo de la edad gestacional como prematuros tardíos (entre 34 y 36+6/7 semanas), prematuros moderados (entre 32 y 33+6/7 semanas), muy prematuros (menor de 32 semanas) y prematuros extremos o grandes prematuros (menor de 28 semanas)[32], sin embargo no existen unos límites claros y coexisten diversas clasificaciones. En cualquier caso, incluso en el prematuro tardío, existe un mayor riesgo de complicaciones en comparación con un nacido a término. Este tipo de patologías incluyen al síndrome de distrés respiratorio, la broncodisplasia pulmonar, el ductus arterioso

persistente, la enterocolitis necrotizante, sepsis, la retinopatía del prematuro, la hemorragia intraperiventricular, la leucomalacia periventricular, y otras dolencias neurológicas junto con dificultades nutricionales, visuales y auditivas. Múltiples factores se han estudiado como parte de la etiología y la fisiopatología de la prematuridad entre los que destacan la susceptibilidad genética, el papel del estrés oxidativo, factores psicosociales y socioeconómicos, variables medioambientales al igual que infecciones. Sin embargo, en un gran número de nacimientos prematuros no puede encontrarse ningún factor claro[30].

Uno de los conceptos que por su papel clave más está siendo estudiado tanto en la EHI, la prematuridad y otros escenarios clínicos en el ámbito de la neonatología tales como la transición fetal-neonatal en sí misma, es el estrés oxidativo[33–42]. La definición más aceptada de este concepto es la elaborada por el Dr. Helmunt Sies que lo define como "un desbalance entre los oxidantes y los antioxidantes en favor de los oxidantes, conduciendo a una disrupción de la señalización redox y su control y/o a daño celular"[43]. Este desbalance, que no desequilibrio, supone una perturbación en los estados estacionarios redox. Tal y como se indica en la definición, se ha comprobado que el estrés oxidativo es parte de los mecanismos de señalización (p. ej. controla la expresión genética y la proliferación celular), pero que puede causar también daño a las biomoléculas induciendo apoptosis y afectando negativamente a los propios mecanismos de señalización redox[44]. Las especies reactivas oxidantes que participan en las reacciones redox biológicas pueden dividirse en especies reactivas de oxígeno (ROS, del inglés *Reactive Oxygen Species*); especies reactivas de cloro y bromo; especies reactivas de nitrógeno (RNS, del inglés *Reactive Nitrogen Species*); especies reactivas de azufre; carbonilos reactivos y especies reactivas de selenio. Las ROS son las más estudiadas y han sido las especies reactivas oxidantes por antonomasia. Estas especies se generan principalmente en la cadena de transporte electrónico y por la acción de diferentes enzimas oxidasas, pero también por el citocromo P450 microsomal y por la respuesta inmune. Las ROS comprenden un abanico de moléculas con diferente naturaleza química, desde los radicales libres ($^{\bullet}OH$, $O_2^{\bullet-}$, $^{\bullet}NO$) a moléculas no radicalarias (HOCl, H_2O_2, O_2 singlete) variando sus reactividades en hasta 11 órdenes de magnitud[43]. Para mantener la homeostasis redox, las células emplean una compleja red de mecanismos que comprende aquellos enzimáticos y no enzimáticos. Desde una perspectiva clínica, las enzimas antioxidantes más importantes son la superóxido dismutasa (*Superoxide Dismutase, SOD*), la catalasa (CAT), la glutatión peroxidasa y la glucosa 6-fosfato deshidrogenasa (G6PD). En cuanto a las especies no enzimáticas que juegan un papel fundamental en los sistemas antioxidantes destacan el tripéptido glutatión (GSH), proteínas encargadas del transporte y almacenamiento del hierro como la transferrina y la ceruloplasmina junto con otras moléculas como el ácido úrico, la bilirrubina, y las vitaminas (p.ej. la vitamina A, E y C)[45]. Estos mecanismos antioxidantes maduran en las últimas etapas de la gestación y, por lo tanto, los prematuros tienen mermada su capacidad de responder a los eventos antioxidantes lo que les hace especialmente susceptibles al daño oxidativo[33,34]. En la **Ilustración 2** se muestra un esquema de las diferentes implicaciones patológicas que se han descrito del estrés oxidativo en el prematuro.

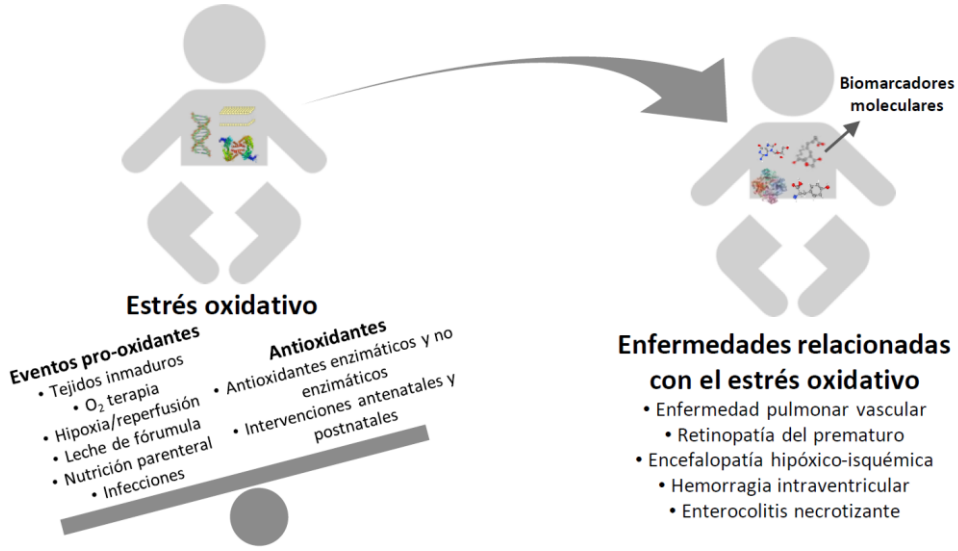

Ilustración 2 Esquema con el desbalance antioxidantes/oxidantes y su impacto en el prematuro.

El papel e impacto de los biomarcadores basados en moléculas pequeñas en el ámbito de la EHI, la prematuridad y el estrés oxidativo perinatales ha sido diverso, pero, sin embargo, hoy en día, únicamente unos pocos se utilizan sistemáticamente en la clínica. De hecho, en este contexto, los métodos dirigidos para determinar lactato y algunas vitaminas son los únicos que se encuentran implementados en IVDs y dispositivos médicos en los laboratorios clínicos. Esto contrasta con la ingente cantidad de métodos disponibles para evaluar diferentes biomarcadores basados en moléculas pequeñas que existen en la literatura, lo que pone de manifiesto el déficit de investigaciones traslacionales satisfactorias al respecto. Prueba de ello es que mientras existe un gran número de trabajos de revisión en los que se abordan estos biomarcadores desde un punto de vista clínico y bioquímico, los que lo hacen enfocados en una descripción y clasificación de la metodológica analítica son escasos.

ii. Hipótesis y objetivos

La hipótesis que se propone en la presente tesis doctoral es que el desarrollo de metodologías analíticas novedosas en el contexto neonatal permite mejorar la detección de diferentes biomarcadores de interés en diferentes biofluidos, facilitando su estudio en la toma de decisiones clínicas.

Así, se han planteado dos objetivos principales para verificar nuestra hipótesis de trabajo. El primer objetivo es realizar dos revisiones bibliográficas, una primera centrada en biomarcadores basados en moléculas pequeñas de EHI y otra para biomarcadores de estrés oxidativo en el prematuro. El segundo objetivo es el desarrollo de diferentes métodos analíticos basados en LC-MS/MS, GC-MS y espectroscopía Raman amplificada por superficie (SERS,

del inglés *Surface Enhanced Raman Spectroscopy*) para la determinación de biomarcadores de EHI y estrés oxidativo perinatal.

Los artículos que conforman la presente memoria de tesis doctoral por compendio de publicaciones se han dividido en dos secciones, introducida cada una de ellas por uno de los artículos de revisión y por sendos trabajos en los que se desarrollan distintos métodos analíticos.

En una primera sección, titulada "*Perinatal asphyxia biomarkers*" los métodos incluidos son:

- Un método mediante LC-MS/MS para la determinación cuantitativa de un panel de biomarcadores relacionados con la síntesis de fosfolípidos seleccionados a partir de estudios previos de metabolómica no dirigida. El método se emplea en el análisis de muestras de orina y plasma provenientes de un modelo animal de cerdo asfíctico.
- Un método cuantitativo mediante GC-MS y su validación conforme a la guía de la FDA para el análisis de compuestos relacionados con el metabolismo energético. En el mismo trabajo se realiza la determinación de estos compuestos en muestras provenientes de un ensayo clínico fase III en el contexto de la EHI y en neonatos sanos.

En una segunda sección, titulada "*Oxidative stress assessment*" se incluye los siguientes métodos:

- Un método mediante LC-MS/MS para la determinación cuantitativa de biomarcadores de peroxidación lipídica en plasma sanguíneo de niños que han sufrido EHI y su validación analítica conforme a la guía de la FDA.
- Un método mediante LC-MS/MS para el análisis semicuantitativo de una familia de biomarcadores de peroxidación del ácido adrénico en plasma y orina de prematuros.
- Un método mediante LC-MS/MS para la determinación cuantitativa de una familia de biomarcadores de daño oxidativo a DNA y proteínas en leche materna mediante LC-MS/MS y su validación parcial conforme a la guía de la FDA.
- Un método mediante SERS para la determinación directa de GSH en volúmenes muy pequeños (2 μL) de sangre de neonatos.

iii. Metodología

a. Obtención de las muestras: modelos animales y estudios clínicos

Las muestras empleadas en los diferentes métodos desarrollados a lo largo de esta tesis se han obtenido de un modelo animal de cerdo asfíctico, de voluntarios sanos y de diferentes estudios clínicos en los que se reclutaron neonatos prematuros o a término en distintos contextos. En todos los casos, se contó con los requerimientos éticos correspondientes habiéndose recibido la aprobación de los comités de las instituciones implicadas.

En el caso del modelo animal, se trata del consolidado modelo de cerdo recién nacido asfíctico del Departamento de Investigación Pediátrica del Hospital Universitario de Oslo (Noruega) cuyas características quirúrgicas se describen en el estudio de Andresen *et al*.[46]. En este modelo se emplean cerdos híbridos recién nacidos (12 a 36 horas) Noroc (LYxLD, es decir, híbrido Norwegian Landrace [L] ½, Yorkshire [Y] ¼ y Duroc [D] ¼)[47]. En el estudio del que obtuvimos las muestras, los animales tras haber sido anestesiados y estabilizados se dividieron en dos grupos: el grupo intervención (N = 26) y el grupo control (N = 6). A los cerdos del grupo intervención, se les produjo una hipoxia-isquemia ventilándolos con un 8% de O_2 hasta que alcanzaron una presión arterial media <20 mmHg o un exceso de bases de <-20 mM y, posteriormente, se les reanimó con O_2 al 21% durante 30 minutos. El otro grupo, el grupo control, fue sometido a los mismos procedimientos que el grupo intervención (cirugía y duración del estudio) pero no se le indujo la hipoxia-isquemia. Las muestras de sangre de ambos grupos fueron obtenidas en tubos Vacutainer® con ácido etilendiaminotetraacético (EDTA) como anticoagulante a distintos tiempos durante el estudio: al inicio y al final de la hipoxia, antes de la reoxigenación y 2 y 9 horas después de la reoxigenación. Inmediatamente a la extracción de la sangre, se tomó una alícuota mediante capilar para realizar la determinación de gases sanguíneos y lactato y, del resto, se aisló el plasma por centrifugación y se conservó a -80 ºC hasta su análisis. Por su parte, las muestras de orina se obtuvieron mediante punción vesical a los mismos tiempos e igualmente fueron conservadas a -80 ºC hasta su análisis.

Las muestras empleadas en el estudio cuantitativo de biomarcadores del metabolismo energético por GC-MS se obtuvieron de los pacientes de una subpoblación del ensayo clínico multicéntrico español HYPOTOP (194 muestras) y de una cohorte de neonatos sanos al alta (19 muestras). En el estudio HYPOTOP se trata de un ensayo fase III diseñado para comprobar la eficacia de un fármaco, el topiramato, como adyuvante al tratamiento de hipotermia terapéutica en neonatos con EHI moderada y severa. Las muestras de sangre se extrajeron empleando jeringas heparinizadas a diferentes tiempos: al nacimiento (por lo tanto, antes de la hipotermia) y a las 24, 48 y 72 horas. Inmediatamente a la extracción de la muestra se obtuvo el plasma mediante centrifugación y se conservaron las muestras a –80 ºC hasta su análisis.

Las muestras de plasma en las que se realizó la cuantificación de biomarcadores de peroxídación lipídica se obtuvieron, al igual que en el caso anterior, de un ensayo clínico de neonatos a término con EHI moderada y severa. El estudio se llevó a cabo en el Hospital Universitario de Carolina del Sur en Charleston (EE. UU.) y, en este caso, se trataba de un ensayo fase 0 para evaluar el tratamiento con N-acetilcisteína (NAC) y calcitriol como adyuvantes a la hipotermia terapéutica. Las muestras de sangre se recogieron en tubos con EDTA, y el plasma se obtuvo y se conservó de la misma manera que para el estudio anterior. Un total de 150 muestras de plasma de 20 neonatos se extrajeron a diferentes tiempos durante el tratamiento, durante la hipotermia y después de la hipotermia.

Las 75 muestras de plasma y 23 de orina empleadas en el estudio de los productos de oxidación a ácido adrénico se obtuvieron de una cohorte de prematuros moderados de entre 31 y 33 semanas reclutados en el *Rainbow Babies & Children's Hospital* de Cleveland (EE. UU.). Las muestras de sangre para obtener el plasma se recogieron empleando EDTA como anticoagulante y las muestras de orina mediante el empleo de bolsas Hollister o impregnación y exprimido de algodón. Las muestras de plasma y orina se conservaron a -80 ºC hasta su análisis.

Las muestras de leche materna empleadas en el desarrollo del método de análisis de productos de oxidación a ADN y proteínas se obtuvieron de dos estudios diferentes. En un primer estudio, se trataban de 59 muestras de leche materna de 31 madres con parto prematuro de ≤32 semanas de la Comunidad Valenciana reclutadas en el Hospital Universitario y Politécnico La Fe de València. Las participantes en el estudio se extrajeron un mínimo de 20 mL de leche (manualmente o con sacaleches) una vez por semana a partir del momento en el que se hubo establecido una nutrición enteral completa de aproximadamente 150 mL Kg^{-1} dia^{-1} de leche materna. El segundo estudio del que se obtuvieron las muestras se trataba de una evaluación de la pasteurización. En este último caso se utilizaron un total de 13 mezclas de muestras de leche materna donada almacenadas en el banco de leche Aladina-MGU del hospital 12 de octubre de Madrid antes y después de la pasteurización. Las muestras de ambos estudios se conservaron a -20 ºC hasta su análisis.

Las micromuetras de sangre (2 µL) recogidas para el desarrollo del método de determinación de GSH se obtuvieron de 20 adultos voluntarios, reclutados en el edificio de Investigación del Campus de Burjassot, mediante pinchazo en el dedo con lanceta. Para ese mismo estudio, también se emplearon 36 muestras de neonatos para realizar la comparación con el método de LC-MS/MS y para confirmar su desempeño con muestras neonatales. Para ello, se recogieron aproximadamente 60 µL de sangre sobrante de la prueba del talón de neonatos a término a 48 horas de nacimiento en el Hospital Universitario y Politécnico La Fe de València. De esas muestras, se tomaron 2 µL para realizar la determinación mediante SERS y 50 µL para la determinación por LC-MS/MS. El análisis mediante SERS se realizó inmediatamente y la muestra para el análisis mediante LC-MS/MS se conservó a -80 ºC tras adición de 10 µL de disolución acuosa de N-etilmaleimida (NEM) y dejar incubando a temperatura ambiente durante 5 minutos.

b. Biomarcadores analizados

En la **Ilustración 3** pueden observarse las estructuras moleculares de los diferentes biomarcadores analizados en cada capítulo. Asimismo, en la **Ilustración 4** se representan las estructuras de los compuestos empleados como patrones internos en cada una de las diferentes determinaciones. Estos compuestos puros fueron obtenidos de las casas comerciales Cayman Chemical (Ann Arbor, EE. UU.), Cambridge Isotope Laboratories Inc. (Tewksbury, EE. UU.), CDN Isotopes (Pointe-Claire, Canada), Toronto Research Chemicals (Toronto, Canada) o Merck (Darmstadt, Alemania). En cuanto a aquellos que no se encontraban disponibles comercialmente, fueron sintetizados por el grupo del Instututo de Biomoléculas Max Mousseron de Montpelier (Francia).

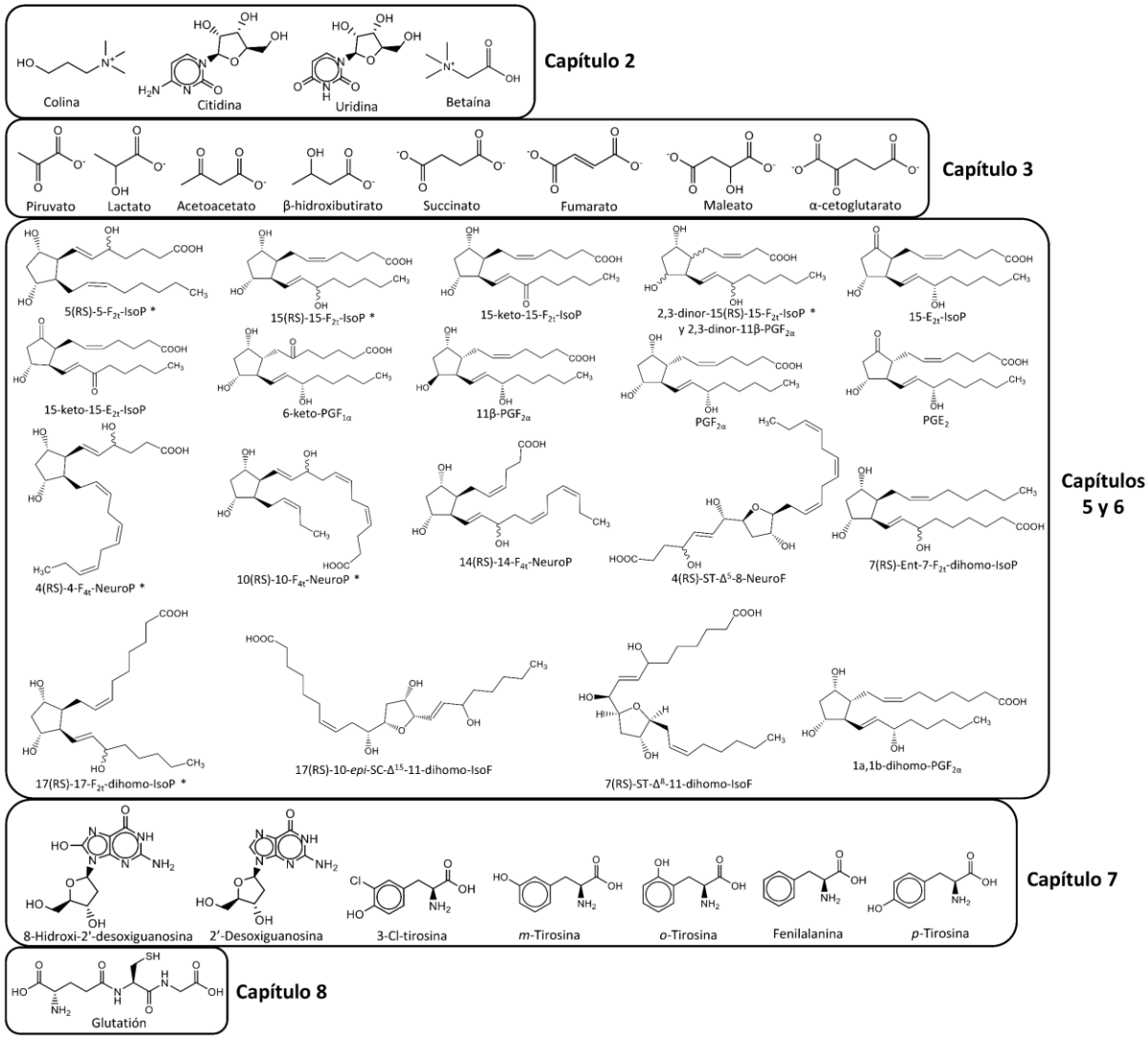

Ilustración 3 Estructuras moleculares de los diferentes biomarcadores analizados en esta tesis doctoral. Nota: para los compuestos señalados con * se incluyeron los diasteroisómeros R y S de la mezcla indicada en el análisis.

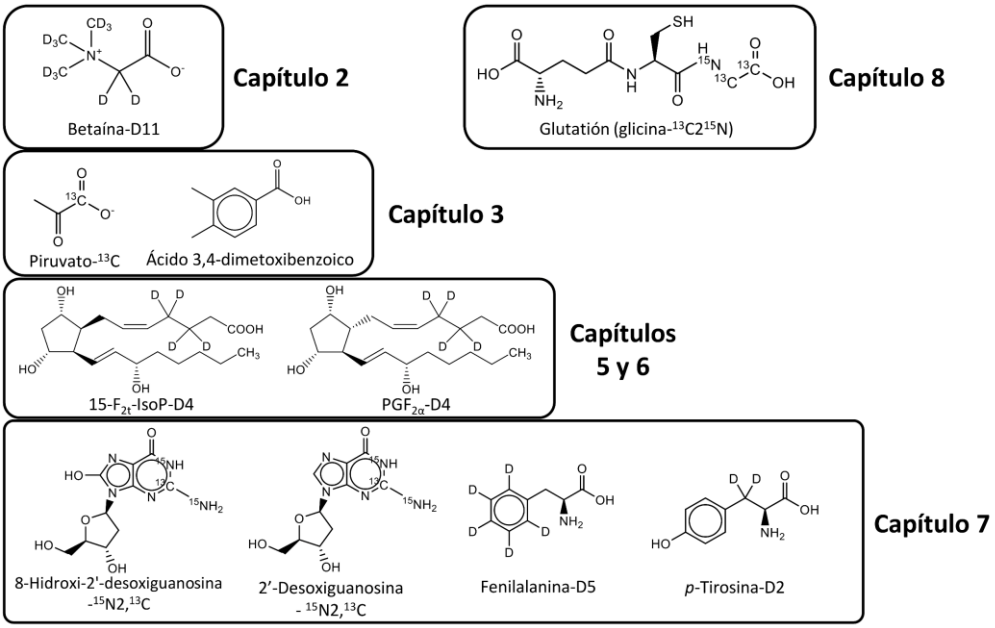

Ilustración 4 Patrones internos utilizados en cada uno de los métodos desarrollados en esta tesis.

c. Preparación de las muestras y análisis

Tal y como se ha indicado en **i**, las muestras provenientes de estudios clínicos centrados en el neonato presentan una serie de peculiaridades que resultan en la inaccesibilidad a grandes volúmenes de estas. Por ello, los métodos que se han desarrollado a lo largo de esta tesis han sido adaptados para trabajar con los menores volúmenes de muestra posibles, especialmente, en los análisis de plasma sanguíneo o sangre total. Asimismo, se han empleado diferentes preprocesados con el objetivo de hacer las muestras compatibles con las diferentes técnicas instrumentales empleadas. Dependiendo de la técnica, se ha requerido aumentar la concentración del analito, incrementar su estabilidad, adicionar patrones internos, eliminar la matriz u obtener al analito en una forma detectable por el sistema (p.ej. en forma iónica o neutra, en estado gaseoso, en disolución a un determinado pH, etc.). Para llevar esto a cabo se han empleado diferentes estrategias, las cuales se encuentran esquematizadas en la **Ilustración 5** para cada uno de los métodos desarrollados en los diferentes capítulos de la tesis.

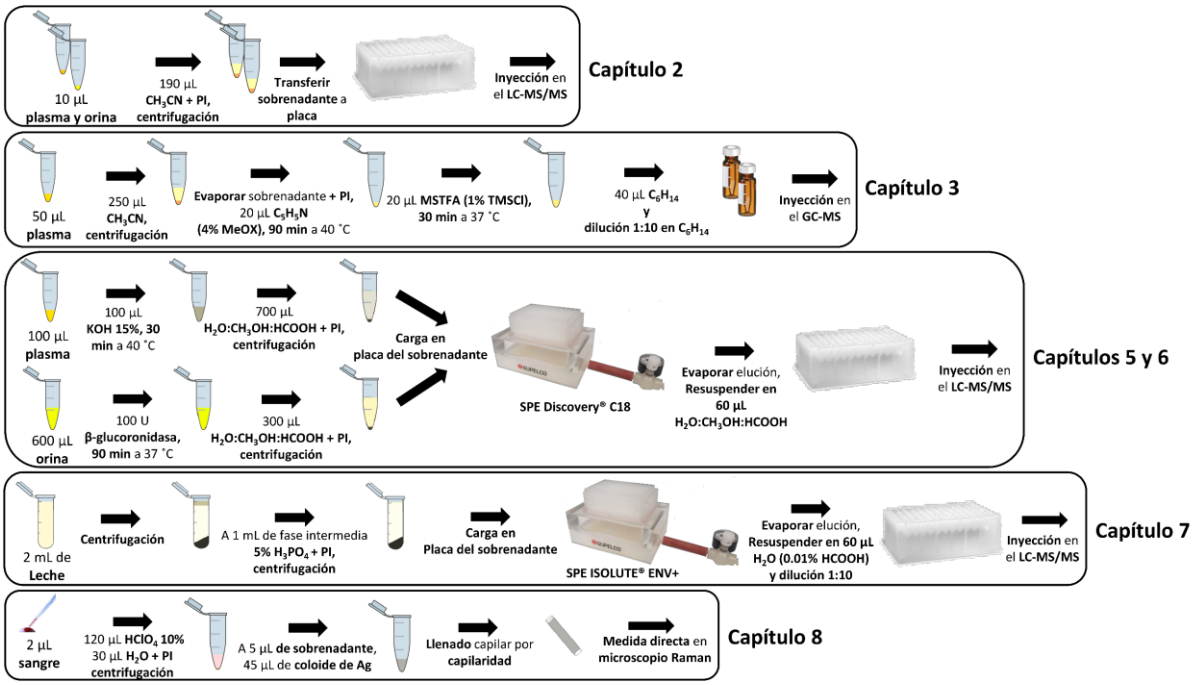

Ilustración 5 Esquema de los diferentes procesados de muestra empleados en los métodos desarrollados en esta tesis. Nota: PI = patrón interno, MeOX = metoxiamina, MSTFA = N-metil-N-(trimetilsilil)trifluoroacetamida, TMSCl = cloruro de trimetilsililo, SPE = extracción en fase sólida.

Uno de los pasos más utilizados en los procesados ha sido la desproteinización con disolvente orgánico o con disolución acuosa ácida como paso para eliminar parte de la matriz. Tal y como figura en el esquema de la **Ilustración 5**, para este propósito se ha empleado acetonitrilo (CH_3CN), ácido fosfórico (H_3PO_4) o ácido perclórico ($HClO_4$) seguido de centrifugación.

En el método desarrollado para el estudio de biomarcadores de la síntesis de fosfolípidos (capítulo 2), la desproteinización es el único paso del procesado. Posteriormente las muestras se inyectaron en el sistema de LC-MS/MS Acquity UPLC - Xevo TQS® de la casa Waters (Milford, EE. UU.). La separación cromatográfica se realizó empleando una columna de cromatografía líquida de interacción hidrofílica (HILIC) y las transiciones de MS/MS se seleccionaron inyectando los patrones correspondientes. La cuantificación se llevó a cabo empleando una calibración mediante patrón interno. Como control de calidad en cada secuencia de análisis se incluyó, cada 10 muestras, una muestra representativa de todas (muestra *quality control*, QC) preparada a partir de un pequeño volumen igual de cada una de ellas y fortificada con una mezcla de estándares de los analitos. Mediante esa muestra QC se comprobó que los valores de precisión y exactitud se encontraban con una desviación estándar máxima del 25% y una recuperación en el rango 75-125%, respectivamente. En cuanto a la determinación de lactato realizada en el quirófano, se emplearon las muestras de sangre recolectadas en capilar y se inyectaron en el sistema autoanalizador Blood Gas Analyzer 860 de Ciba Corning Diagnostics Corp. (Medfield, EE. UU).

Para el análisis de biomarcadores relacionados con el metabolismo energético por GC-MS (capítulo 3), una vez desproteinizada la muestra, se utilizó una derivatización por metoximación-sililación para aumentar la volatilidad y estabilidad, condiciones *sine qua non* para el análisis mediante GC-MS. Las muestras se inyectaron en el equipo 6890GC-5973N equipado con una columna HP-5MS, todo ello de la casa Agilent (Santa Clara, EE. UU.). La cuantificación se realizó empleando calibración mediante patrón interno y se procedió a la validación de acuerdo con la guía de la FDA[14]. Se realizaron las pruebas de estabilidad en patrones y en muestra y se comprobó la precisión y exactitud mediante el análisis de disoluciones patrón y de muestra adicionada. Asimismo, como control de calidad se emplearon igualmente disoluciones QC.

Por su parte, en el análisis de biomarcadores de peroxidación lipídica (capítulos 5 y 6) antes de la desproteinización se implementó un paso de hidrólisis tanto en las muestras de orina como en las de plasma para obtener los analitos en su forma analizable. En el caso del plasma se empleó una hidrólisis básica con KOH al 15% para obtener los analitos a partir de sus ésteres, es decir, una reacción de saponificación. Para las muestras de orina se empleó una hidrólisis enzimática mediante β-glucuronidasa para obtener los analitos a partir de sus glucurónidos. Tras la hidrólisis y desproteinización se sometieron las muestras a extracción en fase sólida (SPE, del inglés *Solid Phase Extraction*) empleando la fase estacionaria Discovery® C18 en su formato en placa de 96 pocillos, actualmente, de la casa comercial Merck (Darmstadt, Alemania). Las muestras se inyectaron en el sistema LC-MS/MS Acquity UPLC - Xevo TQS® de la casa Waters (Milford, EE. UU.). La separación cromatográfica se llevó a cabo empleando una columna BEH C18, también de Waters. Las condiciones cromatográficas y de espectrometría de masas se seleccionaron empleando patrones comerciales y de síntesis en el capítulo 5 y, en el capítulo 6, tras el análisis de una suspensión de ácido adrénico (AdA) oxidada *in vitro* con 2,2'-Azobis(2-amidinopropano) dihidrocloruro (AAPH). En el método cuantitativo del capítulo 5 la cuantificación se llevó a cabo empleando calibrados externos con patrón interno y se realizó una validación siguiendo la guía de la FDA[14], tal y como se ha indicado anteriormente.

El procesado de las muestras de leche (capítulo 7) resulta especialmente delicado por sus características de sistema coloidal. Para el método de análisis de biomarcadores de daño oxidativo a DNA y proteínas en esta matriz se ha empleado una combinación de centrifugaciones, una a baja velocidad (1200 g) y otra a alta (16000 g) junto con la desproteinización suave con H_3PO_4 al 5%. El sobrenadante resultante de este tratamiento se sometió a SPE empleando la fase estacionaria para compuestos polares ISOLUTE® ENV+ de la casa comercial Biotage (Uppsala, Suecia) en formato de placa de 96 pocillos, con el mismo objetivo que el indicado para el caso de los biomarcadores de peroxidación lipídica. El resultante se inyectó en el sistema LC-MS/MS Acquity UPLC - Xevo TQS® de la casa Waters. En la validación del método se siguió un esquema similar al del capítulo 5, seleccionando los parámetros instrumentales empleando disoluciones patrón y validando el método de acuerdo a la guía de la FDA[14].

Por último, en la determinación directa de GSH en sangre (capítulo 8) se desarrolló un procesado de muestra muy sencillo que permite realizar todos los pasos del análisis en unos pocos minutos por muestra. En este método un microvolumen de sangre (2 µL) se desproteinizó con $HClO_4$ al 10% y se le añadió un sustrato SERS de coloide de Ag sintetizado previamente mediante el método de Lepold et al.[48]. Esa mezcla con el coloide de Ag y muestra ácida desproteinizada se introdujo en el interior de un capilar de cuarzo transparente mediante capilaridad y se utilizó como celda de medida de la señal SERS empleando el microscopio Raman XploRA ONE de Horiba (Kioto, Japón). La determinación de la concentración se realizó mediante una calibración de patrón interno en la que tanto precisión como exactitud se evaluaron empleando réplicas de muestras adicionadas. Adicionalmente, un lote de muestras se analizó por este nuevo método y por un método de LC-MS/MS desarrollado anteriormente por nuestro grupo[49], para realizar la comparación entre ambos. El procesado de las muestras para el análisis de GSH por LC-MS/MS consistió en la precipitación de las proteínas con $HClO_4$ (empleando las alícuotas de 100 µL de sangre previamente tratadas con NEM) y en la dilución con H_2O (0,1% HCOOH).

d. Análisis de los datos

Para llevar a cabo el análisis de los datos generados en los diferentes experimentos, en primer lugar, se emplearon las diferentes suites de software de los equipos para realizar la integración de los cromatogramas, los calibrados y las interpolaciones en los métodos de LC-MS/MS y GC-MS o la adquisición de los espectros en el método de SERS. Estos programas fueron: MassLynx™ de Waters, MassHunter Workstation™ de Agilent (Santa Clara, EE. UU.) y Labspec™ de Horiba.

Para el resto de los cálculos se empleó la hoja de cálculo Microsoft Excel 2016 de Microsoft (Redmond, EE. UU.) y el sistema de cómputo numérico MATLAB de Mathworks (Natick, EE. UU) versiones 2015a-2017b a través de scripts y funciones desarrollas *ad hoc* y mediante el empleo de las funciones incluidas en el paquete PLS_Toolbox 8.0 de Eigenvector Research Inc. (Wenatchee, EE. UU.). Asimismo, exclusivamente para el cómputo de las curvas ROC multivariantes realizado en el capítulo 2, se empleó la herramienta en línea Metaboanalyst 3.0[50].

iv. Principales resultados

En el análisis de biomarcadores en plasma en el modelo de cerdo asfíctico del capítulo 2, se detectó un incremento significativo para la colina, la citidina y la uridina al comparar las concentraciones antes y después de la hipoxia y el valor de estos biomarcadores después de la hipoxia permaneció significativamente aumentado en comparación con el grupo control (prueba de la U de Mann-Whitney, $\alpha = 0.05$). Interesantemente, esa diferencia significativa permaneció, para el caso de la colina, incluso 2 horas después de la reoxigenación. También se

observó que las concentraciones de todos los biomarcadores estudiados se redujeron significativamente (prueba de la U de Mann-Whitney, $\alpha = 0.05$) tanto para el grupo intervención como para el grupo control al final del estudio (9 horas después de la reoxigenación. Para evaluar la capacidad de los diferentes biomarcadores para detectar la hipoxia se construyeron curvas ROC (del inglés, *Receiver Operating Characteristic*) para cada uno de ellos. Inmediatamente después de la hipoxia el área bajo la curva (AUC) para la colina, citidina y uridina resultó de >0.96 mostrando su poder predictor. También se construyeron curvas ROC multivariantes en las que se añadió las determinaciones de lactato realizadas en el quirófano y se observó una mejora en el poder predictor.

En cuanto al método de análisis del metabolismo energético desarrollado en el capítulo 3, se comprobó la resolución cromatográfica, los límites de cuantificación y la estabilidad de los patrones y muestras durante el análisis y almacenaje de estas, obteniéndose valores dentro de los márgenes de la guía de validación. Asimismo, del análisis de patrones y muestras adicionadas se calculó la precisión y exactitud obteniéndose igualmente valores adecuados. El análisis de las muestras de la cohorte HYPOTOP mostró como algunos metabolitos (acetoacetato, succinato, fumarato y α-cetoglutarato) permanecieron constantes a lo largo de los primeros días mientras que otros como el lactato, piruvato y β-hidroxibutirato disminuyeron y el maleato aumentó (prueba de la U de Mann-Whitney, $\alpha = 0.05$). Cuando se compararon las concentraciones de los biomarcadores entre ambas cohortes (control e HYPOTOP) para el mismo tiempo de vida del neonato se encontró que lactato y piruvato estaban significativamente aumentados en la cohorte HYPOTOP, mientras que acetoacetato y el β-hidroxibutirato se encontraban significativamente disminuidos en esa misma cohorte en comparación con la cohorte de niños sin EHI (prueba de la U de Mann-Whitney, $\alpha = 0.05$).

En el método desarrollado en el capítulo 5, de los 26 analitos incluidos en el análisis (ver **Ilustración 3**) se resolvieron 23 compuestos, sin embargo, fue imposible la resolución completa debido a la extremada similitud de los compuestos analizados. Aunque sí se consiguieron separar satisfactoriamente varios diasteroisómeros, mostrando la gran potencia de la técnica LC cuando se emplean columnas de alto rendimiento con tamaños de partícula <2 μm. En cuanto a la validación del método, en el análisis de patrones la exactitud y precisión fue adecuada para la mayoría de los compuestos con algunas excepciones para 17(RS)-10-*epi*-SC-Δ^{15}-11-dihomo-IsoF, 1a,1b-dihomo-$PGF_{2\alpha}$ y 15-E_{2t}-IsoP a algunos niveles. Por su parte, en el análisis de disoluciones adicionadas se evaluaron conjuntamente los efectos de la SPE y la hidrólisis básica a partir de las recuperaciones correspondientes y se encontró que 15-E_{2t}-IsoP, 15-keto-15-E_{2t}-IsoP, PGE_2 y 15-keto-15-F_{2t}-IsoP se degradaban completamente. De la observación de su estructura, hipotetizamos un mecanismo de degradación durante la hidrólisis. En cuanto a los 3 primeros, que comparten un sistema β-hidroxicetónico, proponemos una reacción de deshidratación del mismo, mientras que para el 15-keto-15-F_{2t}-IsoP hipotetizamos que se degrada a partir de su sistema δ-hidroxi-α,β-instaurado. También se observaron recuperaciones insatisfactorias para algunos dihomo-IsoPs y dihomo-IsoFs cuya causa no pudimos identificar. En el análisis de las muestras de plasma de neonatos los niveles detectados

fueron muy bajos y en la mayoría de las muestras analizadas, la mayoría de los compuestos permanecieron por debajo de límite de cuantificación. Sin embargo, los que sí pudieron detectarse mostraron un perfil de concentraciones temporal compatible con las observaciones realizadas hasta ahora en este tipo de compuestos[51,52].

En el desarrollo del método de análisis semicuantitativo de biomarcadores de peroxidación del AdA (capítulo 6), se identificaron las transiciones MS/MS relacionadas con una generación *in vitro* de dihomo-IsoPs y dihomo-IsoFs creciente con el tiempo, basándonos en la masa atómica de sus estructuras. Tanto el procesado de la muestra y las condiciones del método LC-MS/MS pudieron seleccionarse de manera que fuesen compatibles con la determinación de isoprostanoides e isofuranoides en plasma y orina implementadas en los diferentes métodos desarrollados en el grupo[51–55]. La determinación semicuantitativa de los dihomo-IsoPs y dihomo-IsoFs empleando este enfoque se realizó en un total de 75 muestras de plasma y 23 de orina de recién nacidos prematuros. La orina resultó ser la matriz donde el mayor número de muestras estuvo por encima de un umbral de 10 veces el área del blanco con un 70% y un 100% para los dihomo-IsoPs y dihomo-IsoFs, respectivamente. En cuanto a las muestras de plasma, únicamente en el caso de los dihomo-IsoFs se detectó señal por encima de ese umbral para el 12% de las muestras.

En el método desarrollado en el capítulo 7, para el análisis de biomarcadores de daño oxidativo a DNA y proteínas en leche materna, se cumplieron los requisitos de una validación parcial del método siguiendo los requerimientos de la guía de validación de la FDA. El valor de las recuperaciones sobre disoluciones de muestra fortificadas con analito estuvieron en el rango 90-100% con una desviación estándar relativa <20%, excepto para algunos analitos en algunos niveles que resultó del 30%. Teniendo en cuenta la complejidad de la muestra, consideramos satisfactorios estos niveles de exactitud y precisión. El análisis de las muestras de leche materna de madres con parto prematuro (59 muestras) resultó de una sensibilidad adecuada para cuantificar todos los biomarcadores en >90% de las muestras. Asimismo, el análisis de 13 muestras de leche humana antes y después de la pasteurización permitió evaluar el efecto de la pasteurización sobre la estabilidad de los diferentes biomarcadores. No encontrándose diferencias estadísticamente significativas antes y después de la pasteurización (prueba de los rangos con signo de Wilcoxon, $\alpha = 0.05$) para ningún biomarcador.

A lo que respecta al método de cuantificación de GSH mediante SERS desarrollado en el capítulo 8, se consiguió una ampliación de la señal del orden de 10^3-10^4 veces respecto a la señal Raman sin SERS, lo cual supuso una mejora sustancial respecto a estudios anteriores[56]. Asimismo, el uso conjunto de una calibración de patrón interno isotópicamente marcado y el de una celda de medida capilar de cuarzo permitió obtener también una reproducibilidad mejorada. En cuanto a la calibración, se empleó el desplazamiento de la banda 1710 cm^{-1} a 1765 cm^{-1} que aparece en el GSH-glicina$^{13}C2^{15}N$ como manera de detectar por separado las señales del patrón interno y analito en muestras y calibrado. Utilizando como respuesta la ratio entre la intensidad de la banda debida al GSH y la del patrón interno, se apreció una relación polinómica con la concentración, pero lineal con la fracción de analito respecto al total

analito+patrón interno. Esta relación lineal se empleó para construir los calibrados que mostraron una muy buena precisión inter- e intradía con una desviación estándar relativa <11%. La exactitud fue estimada mediante el cálculo de las recuperaciones en muestras fortificadas a diferentes niveles, resultando estas entre el 99 y el 103%. Por último, se analizó el GSH simultáneamente en muestras de neonatos a término mediante un método LC-MS/MS desarrollado previamente en nuestro grupo y mediante el nuevo método desarrollado por SERS no obteniéndose diferencias significativas entre ambos métodos. El resultado de ambas determinaciones, expresado como concentración media ± desviación estándar de GSH, fue de 1400 ± 400 μM para el método SERS y de 1200 ± 400 μM para el de LC-MS/MS.

v. Conclusiones y trabajo futuro

A lo largo de esta tesis doctoral, se ha demostrado la aplicabilidad de diferentes técnicas analíticas para abordar el análisis de biomarcadores en biofluidos en el contexto neonatal. Del desarrollo y el empleo de los diferentes métodos hemos extraído diferentes conclusiones que se resumen a continuación:

- En el plasma sanguíneo de un modelo animal de cerdo asfíctico pueden analizarse mediante LC-MS/MS la colina, la citidina, la uridina y la betaína y son un potencial biomarcador de EHI, que, combinadas con lactato, mejoran el poder predictivo del lactato solo.
- Puede validarse un método basado en GC-MS para el análisis de biomarcadores del metabolismo energético en plasma sanguíneo de neonatos. Asimismo, empleando ese método es posible obtener los perfiles de concentración de estos compuestos en neonatos con EHI sometidos a hipotermia terapéutica y en neonatos sanos.
- Es posible una validación completa, siguiendo las directrices de la FDA, de un método basado en extracción en fase sólida y LC-MS/MS para el análisis de un panel de isoprostanoides e isofuranoides en plasma de neonatos. Sin embargo, es necesario excluir del análisis los isómeros que sufren degradación durante el paso de hidrólisis en el procesado de la muestra. Este método permite el estudio del perfil de peroxidación lipídica en neonatos durante sus primeras semanas de vida.
- El análisis de la oxidación *in vitro* del ácido adrénico se puede emplear para identificar las señales de LC-MS/MS selectivas a esta oxidación y así analizarlas en muestras de plasma y orina. Mediante este enfoque se han detectado productos de oxidación de este ácido graso poliinsaturado en muestras de orina de prematuros y en una pequeña fracción de muestras de plasma.
- Es posible el análisis de biomarcadores de daño oxidativo a DNA y proteínas en muestras de leche materna empleando un método basado en LC-MS/MS y un preprocesado de extracción en fase sólida. Asimismo, hemos demostrado que

este método puede validarse de acuerdo con las directrices de la FDA. Con el método validado se ha estudiado el rango de concentración de estos compuestos en esas muestras y comprobado como la pasteurización de la leche no modifica significativamente la concentración de estos.

- El empleo de un patrón interno isotópicamente marcado y el uso de un capilar de cuarzo como celda de medida es una estrategia útil para aumentar la precisión en la determinación de GSH mediante SERS. De esta manera se puede desarrollar un método que permita la cuantificación de GSH en micromuestras de sangre de neonatos.

Además de los métodos analíticos, hemos realizado dos revisiones bibliográficas, una sobre los biomarcadores de EHI y otra sobre los de estrés oxidativo en prematuridad, con un enfoque más metodológico que clínico. Aportando a la literatura una información que creemos que todavía no había sido revisada en profundidad.

Por último, hay que destacar que también han ido surgiendo numerosos aspectos nuevos que han quedado abiertos, fruto de los trabajos de esta tesis y que están siendo objeto de estudio en la actualidad por nuestro grupo de investigación. Entre los que destacan:

- El análisis simultáneo en muestras de neonatos de los biomarcadores propuestos como fruto de los estudios en el modelo animal y su validación clínica. Para ello, se ha propuesto el desarrollo de un método que combine los hallazgos que se han hecho en otros trabajos de nuestro grupo, como es el uso del score metabólico[57].
- El estudio del metabolismo energético mediante GC-MS, incluyendo análisis de metabolómica dirigida y no dirigida, en un modelo animal de asfixia extrema para caracterizar los cambios que ocurren en ese contexto.
- El desarrollo de un método validado para los biomarcadores de peroxidación lipídica que solvente las limitaciones encontradas en la hidrólisis básica de la muestra, en el que se aumente la resolución cromatográfica y la sensibilidad.
- Estudiar con detalle las reacciones de oxidación de los ácidos grasos poliinsaturados *in vitro* bajo condiciones de interés en neonatología. Desarrollar un modelo de membrana lipídica.
- El desarrollo de un método de análisis a pie de cama (PoC, *Point of care*) de GSH basado en SERS en el que se pueda recolectar la muestra en papel (análisis de gota de sangre seca) y determinar el glutatión oxidado.
- El desarrollo de un sensor basado en aptámeros para la detección de los diferentes biomarcadores que han demostrado útiles en los diferentes contextos neonatales.

List of abbreviations

2-dG: 2'-Deoxyguanosine

3-Cl-Tyr: 3-Chlorotyrosine

3-NO_2-Tyr: 3-Nitrotyrosine

8-OHdG: 8-Hydroxydeoxyguanosine

AA: Arachidonic acid

AdA: Adrenic acid

aEEG: Amplitude integrated electroencephalography

AOPP: Advanced oxidation protein products

ASR: Absolute synthesis rate

ATP: Adenosine triphosphate

AUC: Area under the curve

BALF: Bronchoalveolar lavage fluid

BAP: Biological antioxidant potential

BBB: Blood–brain barrier

BCAA: Branched-chain amino acids

BD: Base deficit

BE: Base excess

BHT: Butylated hydroxytoluene

BPD: Bronchopulmonary dysplasia

CAT: Catalase

CDP: Cytidine diphosphate

CE: Capillary electrophoresis

CI: Confidence interval

CLD: Chronic lung disease

CoA: Coenzyme A

COX: Cyclooxygenase

Cyt^{+3}c: Cytochrome c (Fe^{+3})

DHA: Docosahexaenoic acid

DHM: Donor human milk

DHR: Dihydrorhodamine123

dihomo-IsoFs: Dihomo-isofuranes

dihomo-IsoPs: Dihomo-isoprostanes

DMBA: 3,4-Dimethoxybenzoic acid

DMPO: 5,5-Dimethyl-1-Pyrroline-N-Oxide

DNPH: 2,4-Dinitrophenylhydrazine

d-ROMs: Reactive oxygen metabolites

ECD: Electrochemical detection

EDTA: Ethylenediaminetetraacetic acid

EEG: Electroencephalography

ELISA: Enzyme-linked immunosorbent assay

EMA: European Medicines Agency

eNOS: Endothelial nitric oxide synthase

EPO: Erythropoietin

EPR: Electron paramagnetic resonance

FDA: Food and Drug Administration

FIA: Flow injection analysis

FiO_2: Fraction of inspired oxygen

fMLP: N-formyl-methionyl-leucyl-phenylalanine

FOX: Ferrous oxidation of xylenol

FRAP: Ferric-reducing antioxidant power

FT-ICR MS: Fourier-transform ion cyclotron resonance-mass spectrometry

G6PD: Glucose-6-phosphate dehydrogenase

GC-MS: Gas chromatography–mass spectrometry

GC-TOFMS: gas chromatography–time-of-flight mass spectrometr

GPx: Glutathione peroxidase

GSH: Glutathione

GSSG: Glutathione disulfide

GST: Glutathione S-transferase

HIE: Hypoxic ischemic encephalopathy

HIF-1α: Hypoxia-inducible factor 1-alpha

HRF: Hypoxemic respiratory failure

IGF-1: Insulin-like growth factor 1

IL: Interleukin

iNO: Inhaled nitric oxide

IsoFs: Isofuranes

IsoPs: Isoprostanes

IVD: In Vitro Diagnostic Devices

IVH: Intraventricular hemorrhage

KP: Kynurenine pathway

LC-ECD: Liquid chromatography-electrochemical detection

LC-MS/MS: Liquid chromatography-tandem mass spectrometry

LC-TOFMS: Liquid Chromatography Time-of-Flight Mass Spectrometry

LLOD: Lower limit of detection

LLOQ: Lower limit of quantitation

LOD: Limit of detection

LV: Latent variable

MABP: Mean arterial blood pressure

MCCV: Monte Carlo cross-validation

mchEEG: Multichannel EEG

MDA: Malondialdehyde

MPO: Myeloperoxidase

MRI: Magnetic resonance imaging

mRNA: Micro-ribonucleic acid

MSTFA: N-Methyl-N-(trimethylsilyl)trifluoroacetamide

m-Tyr: *meta*-Tyrosine

NAA: N-acetylaspartate

NAC: N-Acetyl-L-cysteine

NADPH: Nicotinamide adenine dinucleotide (reduced form)

NBPI: Non-bound protein iron

NEC: Necrotizing enterocolitis

NEM: N-Ethylmaleimide

NeuroFs: Neurofuranes

NeuroPs: Neuroprostanes

NF-κB: Nuclear factor kappa-light-chain-enhancer of activated B cells

NHPA: 3-nitro-4-hydroxyphenylacetic acid

NIH: National Institutes of Health

NMR: Nuclear magnetic resonance

NO_2-Tyr: 3-nitrotyrosine

OMM: Own mother's milk

OS: Oxidative stress

o-Tyr: *ortho*-Tyrosine

PaO_2: Partial pressure of oxygen

PGF: Prostaglandin-F

Phe: Phenylalanine

PLS: Partial least squares

PN: Parenteral nutrition

PoC: Point-of-care

PON1: Serum paraoxonase and arylesterase 1

PPHN: Parenteral nutrition

p-Tyr: *para*-Tyrosine

PUFAs: Polyunsaturated fatty acids

PVH: Periventricular haemorrhage

QC: Quality control

RDS: Respiratory Distress Syndrome

RNS: Reactive nitrogen species

ROC: Receiver Operating Characteristic

ROP: Retinopathy of prematurity

ROS: Reactive oxygen species

S100B: S100 calcium-binding protein B

SDF-1: Stromal cell-derived factor 1

SERS: Surface-enhanced Raman spectroscopy

SIM: Selected ion monitoring

SOD: Superoxide dismutase

SpO_2: Peripheral oxygen saturation

TAC (ABTS): Total antioxidant capacity with 2,2'-azino-bis(3-ethylbenz-thiazoline-6-sulfonic acid

TBA: Thiobarbituric acid

TBARS: Thiobarbituric acid reactive substances

TCA: Tricarboxylic acid

TH: Therapeutic hypothermia

TLR4: Toll Like Receptor 4

TMCS: Trimethylchlorosilane

TNFα: Tumor necrosis factor alpha

TOS: Total oxidant status

TPM: Topiramate

TPN: Total parenteral nutrition

UNICEF: United Nations International Children's Emergency Fund

UPLC: Ultra High Performance Liquid Chromatography

UV/Vis: Ultraviolet–visible spectroscopy

VEGFs: Vascular Endothelial Growth Factors

WHO: World Health Organization

Abstract

The main motivation of this PhD thesis is the assessment of small molecule biomarkers with relevance in the neonatal period, and more specifically, in situations of perinatal asphyxia and oxidative stress of the newborn.

Novel analytical methods have been developed and tailored to deal with the limitations of sampling in the neonatal population, employing minimally invasive approaches and small sample amounts. Different sample pre-processing steps are implemented within the workflows for the analysis of urine, blood, and human milk including Solid Phase Extraction and different deproteinizations. The employed analytical methods are based on Liquid Chromatography-tandem Mass Spectrometry (LC-MS/MS) for the analysis of phospholipid synthesis-related biomarkers, DNA & protein oxidative damage compounds, and lipid peroxidation products; Gas chromatography-Mass spectrometry (GC-MS) for the analysis of biomarkers of the energy metabolism; and Surface Enhanced Raman Spectroscopy (SERS) for the analysis of glutathione.

The different developed methods have been successfully applied in the early assessment of severity of perinatal asphyxia, the analysis of the energy metabolism-related compounds under therapeutic hypothermia treatment, the analysis of novel lipid peroxidation biomarkers after perinatal asphyxia, the analysis of oxidative stress in human milk, and the direct analysis of glutathione in blood microsamples. Therefore, it has been demonstrated the potential applicability of the advanced analytical technologies into the clinical decision-making.

Hypothesis and objectives

It was hypothesized that the development and implementation of novel analytical methods in the neonatal context offers an improved detection of biomarkers in biofluids, allowing their research in the clinical decision-making.

To confirm this hypothesis this PhD thesis was focused on two complementary objectives. The first objective was the review of the literature regarding the small molecule biomarkers for hypoxic ischemic encephalopathy and preterm oxidative stress. The other objective was the development of different analytical methods based on LC-MS/MS, GC-MS, and SERS for the determination of small molecule biomarkers of HIE and perinatal oxidative stress. Presented as a compendium of publications, the different chapters are divided into two main sections. Each section is introduced with a review article which reflects the state-of-the-art followed by articles corresponding to the different analytical methods developed during this PhD thesis within the scope of that section.

The first section, entitled 'Perinatal asphyxia biomarkers' consists of the following methods:

- LC-MS/MS determination of a panel of biomarkers related with the synthesis of phospholipids in urine and blood plasma from an animal model. These biomarkers were selected tacking into account the results of previous non-targeted metabolomic studies.
- Quantitative analysis by a validate GC-MS approach of energy metabolism-related metabolites in plasma samples from neonates with HIE.

The second section, entitled 'Oxidative stress assessment' includes:

- A validated LC-MS/MS method for the quantification of a panel of lipid peroxidation biomarkers in blood plasma from neonates with HIE.
- An LC-MS/MS approach for the semiquantitative analysis of lipid peroxidation products of adrenic acid in blood plasma and urine from preterm infants.
- A validated LC-MS/MS method for the quantification of a panel of biomarkers of oxidative damage to DNA and proteins in human milk samples.
- A novel method based on SERS for the quantification of GSH in blood microsamples from neonates.

Section I. Perinatal asphyxia biomarkers

Chapter 1 Small molecule biomarkers for neonatal hypoxic ischemic encephalopathy

1.1 Abstract

Hypoxic Ischemic Encephalopathy (HIE) is one of the most deleterious conditions in the perinatal period and the access to small molecule biomarkers aiding accurate diagnosis and disease staging, progress monitoring, and early outcome prognosis could provide relevant advances towards the development of personalized therapies. The emergence of metabolomics, the "omics" technology enabling the holistic study of small molecules, for biomarker discovery employing different analytical platforms, animal models and study populations has drastically increased the number and diversity of small molecules proposed as candidate biomarkers. However, the use of very few compounds has been implemented in clinical guidelines and authorized medical devices. In this work we review different approaches employed for discovering HIE-related small molecule biomarkers. Their role in associated biochemical disease mechanisms as well as the way towards their translation into the clinical practice are discussed.

1.2 Introduction

Neonatal encephalopathy (NE) following an intrapartum-related event is one of the leading causes of neonatal morbimortality worldwide. In situations where a causal relationship between NE and a hypoxic-ischemic insult is evidenced, it is referred to as perinatal hypoxic ischemic encephalopathy (HIE)[24]. Neonates that have suffered HIE have greater incidence of serious conditions such as cerebral palsy, cognitive impairment, growth restriction, and epilepsy[24,27–29]. Improvements in resuscitation[58,59], including the understanding of the role of the oxidative stress (OS)-related mechanisms[40,60], the introduction of therapeutic hypothermia (TH) as the standard-of-care treatment[61], and the employment of novel monitorization tools and biomarkers, represent the main landmarks in HIE management[28]. However, there is still a continuing need for early, accurate HIE diagnosis and prognosis biomarkers to enable the transition towards personalized treatment strategies.

The FDA-NIH Joint Leadership Council defined the term "biomarker" in the BEST (Biomarkers, EndpointS, and other Tools) glossary as: "A defined characteristic that is measured as an indicor of normal biological processes, pathogenic processes, or responses to an exposure or intervention, including therapeutic interventions. Molecular, histologic, radiographic, or physiologic characteristics are types of biomarkers."[6]. In this sense, biomarkers have helped in HIE assessment since the first half of the 20th century. Examples include the work of Eastman et al.[3] that reports the discovery of blood lactate increase during neonatal hypoxia, or the well-known Apgar[62] and more recent Sarnat[63] scores. The analytical methods available for biomarker discovery at that time and until the late 20th century were very limited in terms of selectivity and sensibility and hence, the discovery of new molecular biomarkers was troublesome. With the development of powerful analytical platforms, the range of accessible compounds was expanded, but the discovery of new biomarkers remained subordinated to the existing evidence sources. With the emergence of "omics" techniques in the last decades, the paradigm has shifted to the holistic study of biological systems, allowing to exploit the full potential of the increased analytical capabilities. In this sense, metabolomics, which is dedicated to the comprehensive analysis of small molecules, has been increasingly applied to the study of HIE[7,8,64,65]. Since metabolomics began to emerge, the number of literature reports on HIE-related biomarkers has grown rapidly as shown in **Figure 1.1**. However, despite the increasing number of candidate biomarkers of HIE, none of the biomarkers discovered employing metabolomics has been clinically validated and implemented in the current clinical practice. This fact is a hot topic in the metabolomics community and has been recently discussed elsewhere[66]. The proper design of biomarker discovery studies, and the data quality assessment and employed statistical approaches have been highlighted as the main challenges in successful biomarker discovery and their implementation[66,67].

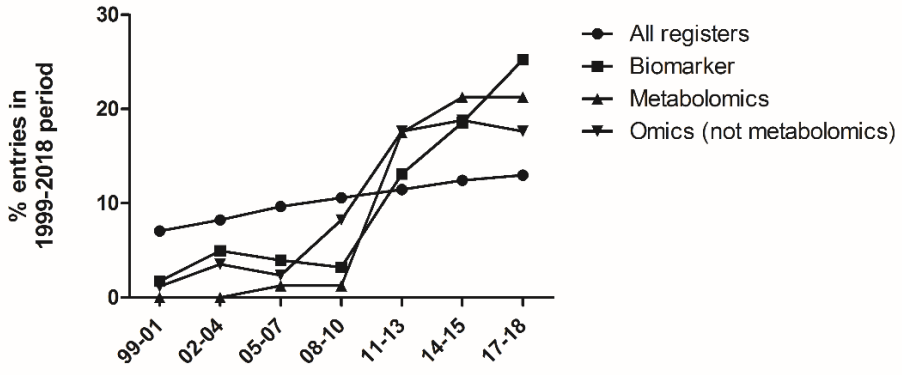

Figure 1.1 Percentage of the registered records in the Web of Science in the 1999–2018 period, for each 3-year interval. Databases: WOS, CCC, DIIDW, KJD, MEDLINE, RSCI, SCIELO. The boolean combinations employed were TS = (asphy* OR hypox* OR HIE OR anoxia) AND TS = (perinatal OR pediatric OR neonat* OR newborn) for all registers; biomarker, metabolomics, and omics (not metabolomics) fieldswere searched refining by biomarker, (metabolom or metabonom*), and ((genomics or transcriptomics or proteomics or lipidomics or epigenomics)), respectively.

We reviewed different approaches employed for small molecule biomarker discovery for HIE with a special focus on the most repeatedly reported compounds and their biochemical role in disease mechanisms. Furthermore, the clinical translation and how the candidate biomarkers fit into the recent U.S. Food and Drug Administration (FDA) and European Medicines Agency (EMA) programs and regulations were also discussed.

1.3 Biomarker discovery and assessment methods

A plethora of analytical techniques have been employed in pursuit of HIE small molecule biomarkers: classic titrations[3]; colorimetric reactions[68,69]; enzymatic assays and immunoassays with spectroscopic, electrochemical or radiometric detection[68–73]; binding assays[74]; nuclear magnetic resonance (NMR)[23,75–86]; Fourier-transform ion cyclotron resonance-mass spectrometry (FT-ICR MS)[87]; and separation techniques such as capillary electrophoresis (CE), liquid chromatography (LC, HPLC or UPLC), or gas chromatography (GC or GCxGC) coupled to different detectors including electrochemical detection (ECD), ultraviolet–visible (UV–Vis), or mass spectrometry (MS or MS/MS)[21,22,57,69,88–101]. The developed analytical methods can be divided into complementary metabolomics detection strategies, i.e. targeted, semi-targeted, and untargeted approaches.

1.3.1 Targeted biomarker determination

Targeted methods are optimized for the quantification of a relatively small number of biologically important metabolites with known chemical identities. Despite the limited number of metabolites that can be studied per experiment, employing targeted methods in human and animal studies several small molecules were discovered as relevant indicators for neonatal HIE. In 1931, lactate was the first described as a perinatal asphyxia biomarker[3], determined in cord blood by using a laborious titration, followed by hypoxanthine in the 1970ies[70]. Literature reports on the first discovery of different small molecule biomarkers for neonatal HIE are listed in **Table 1.1** in chronological order.

The most widely accepted small molecule biomarkers of perinatal asphyxia and HIE were first discovered and tested employing targeted methods. The main advantage offered by targeted approaches is the possibility of optimizing the analytical methods taking into account the (bio-)chemical properties of the biomarker under study in the biospecimen of interest (e.g. stability, complexity of the mixture, concentration range). This is of key importance in the perinatal field, where the sample volumes are limited and non-invasive or minimally-invasive sampling is required. In fact, targeted methods are the best choice for the determination of biomarkers presenting stability issues like, e.g. glutathione (GSH)[49,100,102] which is prone to enzymatic and nonenzymatic oxidation, or for biomarkers which are difficult to identify like, e.g. biomarkers of lipid peroxidation, where hundreds of molecules with highly similar structures can potentially be formed at concentrations in the nmol L^{-1} to pmol L^{-1} range[51–53,103].

Furthermore, targeted assays are the method of choice for providing quantitative results and establishing reference concentration ranges. During method development, the analytical figures of merit are systematically studied providing information about accuracy, precision, reproducibility, and robustness and the available EMA and the FDA regulator validation guidelines[14,15] are primarily focused on targeted methods. The main shortcoming of targeted methods is, however, their inherently limited potential for the discovery of previously unknown disease mechanisms and pathways and hence, new candidate biomarkers.

Table 1.1 Biomarkers discovered in the "pre-metabolomics era" employing targeted methods.

Biomarker (s)	First discovery					
	Main evidence source	Finding	Specie	Matrix	Method	Reference
Lactate	Previous studies in adults	Increases in hypoxia	**Human**	Blood	Oxidation - titration	Eastman NJ et al., 1931[3]
Hypoxanthine	Studies of the purine catabolism, oxidative phosphorylation and xanthine oxidation	Increases in hypoxia	**Human**	Blood	Enzymatic - electrochemical	Saugstad OD, 1975[70]
PGE_2 and $PGF_{2\alpha}$	Studies of PGE_2 and $PGF_{2\alpha}$ in adult insults	Increases in hypoxia	Gerbil	Brain tissue	Radioimmunoassay	Allen LG et al., 1982[71]
Glutamate, aspartate, γ-aminobutyric acid, taurine	Pathological studies in newborn autopsies and studies of glutamate and aspartate in adult brain	Increases in hypoxia	Lamb	Brain dialysates	HPLC-(on-line derivatization)-fluorescence detection	Hagberg H et al., 1987[89]
Phosphocreatinine (PCr), inorganic orthophosphate (Pi), adenosine triphosphate (ATP)	^{31}P-NRM abnormalities indicating altered oxidative phosphorylation were detectable in the brain after birth asphyxia	The reduced value of PCr/Pi indicates very poor prognosis and a reduction in ATP/total phosphorus indicates inevitable death	**Human**	Brain scan	NMR	Azzopardi D et al., 1989[75]
N-acetylaspartate (NAA), choline (Cho), creatinine+phosphocreatinine (Cr)	Findings in adults	Low NAA/Cho and NAA/Cr after hypoxia	**Human**	Brain scan	NMR	Peden CJ et al., 1990[76]
Uric acid/creatinine	Studies on the purine metabolism and their relation with hypoxanthine production	Uric acid normalized by creatinine increases in hypoxia	**Human**	Urine	Creatinine: colorimetric reaction. Uric acid: enzymatic – UV/Vis	Bader D et al., 1995[68]

Biomarker (s)	First discovery					
	Main evidence source	Finding	Specie	Matrix	Method	Reference
Hypoxanthine, xanthine, inosine, uric acid, malondialdehyde, hydroperoxides	Studies of the purine metabolism and their relationship with oxidative stress	Organic hydroperoxides (OHP) is a marker of free oxygen radical activity in the fetus and correlates with other evidences of hypoxia-reperfusion injury	**Human**	Blood	Purine metabolites: HPLC-UV/Vis. TBARS: Colorimetric reaction. OHP: enzymatic - UV/Vis	Rogers MS et al., 1997[69]
Dopamine (DA), 3,4-dihydroxyphenylacetic acid (DOPAC), homovanillic acid (HVA)	Studies of the central nervous system showing the importance of dopamine-containing pathways in the early brain development	Immediately after birth DA, its metabolites, and amino acid levels were increased by mild asphyxia periods, but not by extreme asphyxia in substantia nigra and ventral tegmental area	Rat	Brain dialysates	HPLC-electrochemical detection	Chen Y et al., 1997[88]
o-tyrosine/Phenylalanine (*o*-Tyr/Phe)	Studies of oxidative stress in cell cultures and animal models	An increase of *o*-Tyr/Phe was associated with oxygen treatment in neonates	**Human**	Urine	HPLC-fluorescence detection	Lubec G et al., 1997[97]
Coenzyme Q10, oxidized Coenzyme Q10 (CoQ10)	Reported low levels of antioxidant protection in newborns compared with adults	CoQ10 in infants with asphyxia was significantly elevated compared to normal infants	**Human**	Blood	HPLC-ECD	Hara K et al., 1999[98]
L-kynurenine, kynurenic acid, 3-hydroxy-kynurenine	Studies of excitatory amino acids implications in hypoxia and their relationship with the kynurenine metabolism	Time-dependent increase of kynurenines and kynurenic acid levels, a moderately delayed increase of 3-hydroxy-kynurenine, and a trend for a decrease of L-kynurenine content during asphyxia	Rats	Brain tissue	HPLC-fluorescence detection	Baran H et al., 2001[99]

Biomarker (s)	First discovery					
	Main evidence source	Finding	Specie	Matrix	Method	Reference
GSH/GSSG	Studies of oxidative stress in animals and humans	Neonates resuscitated with 100% oxygen exhibit protracted oxidative stress present even after 4 weeks of postnatal life	**Human**	Blood	Dinitrofluorobenzene derivatization - HPLC-fluorescence detection	Vento M et al., 2001[100]
15-F_{2t}-IsoP	Studies reporting changes in the CSF levels of F_2-IsoPs, an index of lipid peroxidation, in very low birth weight infants with white matter injury	15-F_{2t}-IsoP predicts delayed behavioral disturbances	Rats	Brain tissue	ELISA	Calamandrei G et al., 2004[72]
Serum free fatty acids (sFFA)	sFFA studies in adult hypoxia-ischemia	Low 1-minute Apgar score is associated with elevated levels of cord sFFA	**Human**	Blood	Fluorescent protein probe (ADIFAB2)	Yuvienco JMS et al., 2005[74]
NO_2-tyrosine	Animal experiments showing nitrosative stress during reperfusion	NO_2-tyrosine was found in brain tissue of full-term neonates, suggesting that nitric oxide toxicity might have a role in hypoxic-ischemic brain injury at term	**Human**	Brain	Immunohistochemistry	Groenendaal F et al., 2006[73]

1.3.2 Metabolic phenotyping

Metabolomics, or metabolic phenotyping, is a top-down approach for studying complex systems defined as the description of all low-molecular-weight (< 1 kDa) components in a biological sample[12,13]. Untargeted metabolomic fingerprinting aims at the simultaneous detection of as many metabolites as is feasible, providing semiquantitative data, e.g. peak areas, rather than absolute concentrations[19]. The chemical identity of the measured metabolites is not necessarily known before the initiation of the experiment and identification is performed *post hoc*. In this scenario the analysis is hypothesis-free and limitations in terms of metabolome coverage are solely instrumental.

Metabolomics has been employed for biomarker discovery in neonatal HIE taking full advantage of information rich datasets obtained from different analytical platforms such as

NMR, GC-MS, GCxGC-TOFMS or LC-TOFMS. For details on the use of metabolomics in clinical and experimental studies on perinatal asphyxia, the reader is referred to recent reviews from Denihan et al.[64], Fattuoni et al.[8], and Efstathiou et al.[65]. **Table 1.2** outlines candidate biomarkers for HIE that have been repeatedly described in three or more metabolomics studies, arranged in decreasing order of repeatability. Lactate is leading the list, being this the most repeated biomarker reported in metabolomics studies across different sample types including brain tissue, blood, urine, and cerebrospinal fluid, as well as species (i.e. primate, lamb, piglet, rat, mouse, and human). Metabolites related to the energetic metabolism such as succinate, glucose, pyruvate, citric acid, and fumarate, have also been frequently suggested as biomarkers of HIE outcomes. Furthermore, amino acids including alanine, taurine, and valine are also highly ranked in **Table 1.2**, together with other compounds like choline or hypoxanthine.

Within the field of metabolomics, semi-targeted assays act as an intermediate approach between untargeted and targeted methodologies. Here, a large panel of compounds with known chemical identity (i.e. low hundreds or metabolites) are targeted in one validated method. Semi-quantitative measurements are carried out typically by employing one calibration curve and internal standard for determining approximate concentrations for several metabolites belonging to a compound class. A major milestone in this regard was the development of commercial kits for LC-MS/MS platforms that to date enable the quantification of up to >500 metabolites belonging to 26 biochemical classes (Biocrates AG, Innsbruck, Austria). Such semi-targeted assays have been used to study HIE in an asphyxiated piglet animal model[21] and in human samples[22], providing a shortlist of compounds as candidate biomarkers for HIE diagnosis, duration of hypoxia or monitoring of reanimation parameters (see **Table 1.2**). Intermediates of the energy metabolism, amino acids, and acylcarnitines have been proposed as biomarkers in both, animal and human studies[21,22] employing semitargeted methods and these findings are in concordance with results obtained employing other approaches.

Table 1.2 Metabolites suggested as biomarkers of HIE outcomes in three or more untargeted or semi-targeted metabolomics studies. Note: BR: brain tissue; CSF: cerebrospinal fluid; B: blood; U: urine.

Biomarker	Specie	Sample	Analytical platform	References
Lactate	Primate, lamb, piglet, rat, mouse, **human**	BR, CSF, B, U	GCxGC-TOFMS, NMR, GC-MS, LC-MS/MS	21,78–80,82–86,91–93
Succinate	Primate, piglet, mouse, **human**	BR, B, U	GCxGC-TOFMS, FT-ICR MS, NMR, GC-MS, LC-MS/MS	21,78,80,82,84,87,91,92, 94
Alanine	Lamb, piglet, rat, mouse, **human**	BR, CSF, B, U	NMR, LC-MS/MS	22,78–80,84–86
Choline	Lamb, piglet, rat, mouse, **human**	BR, CSF, B	NMR, LC-TOFMS, CE-MS	79,80,84,86,90,96,104
Taurine	Rat, mouse, **human**	BR, B, U	NMR, GC-MS, LC-MS/MS	22,79–82,93
Acylcarnitines	**Human**	B, U	FT-ICR MS, NMR, LC-MS/MS	21,22,84,87,95
Creatinine	Primate, piglet, **human**	B, U	GCxGC-TOFMS, NMR	77,78,82,84,91
Glucose	Primate, piglet, **human**	B, U	GCxGC-TOFMS, NMR	78,82–84,91
Hypoxanthine	Lamb, piglet, **human**	CSF, B, U	FT-ICR MS, NMR, LC-TOFMS	23,82,86,87,96
Pyruvate	Piglet, rat, **human**	BR, B, U	NMR, CE-MS, LC-MS/MS	78,82,84,90,95
Valine	Piglet, rat, mouse, **human**	BR, B, U	NMR, LC-MS/MS	22,79,80,84,85
Carnitine	Piglet, rat, **human**	BR, B, U	CE-MS, LC-TOFMS, LC-MS/MS	21,90,94,96

Biomarker	Specie	Sample	Analytical platform	References
Citric acid	Primate, piglet, **human**	B, U	GCxGC-TOFMS, GC-MS, NMR	78,82,92,93
Fumarate	Primate, piglet, mouse	B, U	GCxGC-TOFMS, NMR, LC-MS/MS	21,80,85,92
Glutamate	Primate, rat, **human**	BR, B, U	GCxGC-TOFMS, NMR, LC-TOFMS, FT-ICR MS	79,87,91,94
Isoleucine	Rat, mouse, **human**	BR, B	NMR, LC-MS/MS	22,79,80,84
Leucine	Primate, rat, **human**	BR, B	GCxGC-TOFMS, NMR, LC-MS/MS	22,79,84,91
Phenylalanine	Lamb, **human**	CSF, CB, U	NMR, LC-MS/MS	22,84,86,95
Tyrosine	Lamb, rat, **human**	BR, CSF, B, U	NMR, LC-MS/MS	22,79,86,95
Acetone	**Human**	B, U	NMR, FT-ICR MS	82,84,87
Betaine	Piglet, **human**	B, U	NMR	82,84,85
Glutamine	Piglet, **human**	B, U	LC-TOFMS, NMR	82,94,96
Glycerol	Primate, **human**	B	GCxGC-TOFMS, NMR, FT-ICR MS	84,87,91
Malate	Primate, mouse	B	GCxGC-TOFMS, NMR	80,91,92
Myo-inositol	Primate, **human**	B, U	GCxGC-TOFMS, NMR	82,84,91
N-acetylaspartate	Rat, mouse, **human**	B, U	NMR, LC-MS/MS	79,80,95

1.3.3 Metabolic scores

HIE is a heterogeneous, multi-faceted disease entity which passes through different stages after the hypoxic insult. In addition, and in contrast to animal experiments, in newborns with HIE, the exact timing and duration of hypoxia are unknown. Hence, it cannot be expected that the use of a single biomarker will provide high selectivity and sensitivity for predicting clinical outcomes. For achieving the required adaptability, metabolic scores combining several metabolites into one multi-factorial model have been proposed.

A metabolic score based on LC-TOFMS measurements of plasma samples from an animal model was developed employing a partial least squares (PLS) multivariate model[57]. The plasma metabolic score combines the signals of three metabolites (choline, xanthine, and hypoxanthine) with lactate to estimate the duration of the hypoxic insult. Directly after an intense period of hypoxia its performance was similar as compared to lactate alone. However, an enhanced predictive capacity was provided 2 h after resuscitation. In another study involving human cord serum samples, the aim was to provide a direct and straightforward measure related to HIE severity employing NMR[101]. A “cord metabolite index”, y, defined as a quotient of signals of different metabolites, was established:

$$y = \frac{succinate * glycerol}{hydroxybutyrate * phosphocholine} \tag{1.1}$$

This metabolic score showed superior predictive capacity compared with other biochemical markers and could support clinical decision-making.

1.4 Biochemical mechanisms involving small molecule HIE

To date, knowledge of the underlying metabolic mechanisms and complex interactions of individual metabolic pathways involved in HIE is limited. Current understanding of HIE injury indicates that it is a dynamic, multi-factorial disease where hypoxia-ischemia sets in motion a biochemical cascade of events, which can be divided into distinct clinical phases. For a detailed description of the distinct phases, the reader is referred to a recent review on this topic[26].

In the following, the main biochemical mechanisms involved in hypoxic-ischemic injury, that have been reported in the context of metabolomics and small molecule biomarker studies outlined in section 1.3, are discussed. This is not intended to be a comprehensive list, but rather to give an overview of pathways and mechanisms that have repeatedly been deemed important in diverse studies on HIE in experimental model organisms, as well as humans.

1.4.1 Energy metabolism

The energy supply necessary for cell survival largely depends on aerobic metabolism involving the cleavage of glucose, fatty acids and amino acids with the purpose of generating energy via adenosine triphosphate (ATP) synthesis[105]. The first phase of HIE is characterized by a reduction of the blood flow that leads to hypoxic acidosis and brain damage as a result of primary energy failure. Under these circumstances, the cell reverts to anaerobic metabolism producing lactate to compensate the lack of oxygen and depletion of ATP[26,106]. Unsurprisingly, levels of lactate[21,78–80,82–86,91–93], and metabolites involved in the glycolysis pathway (e.g. glucose, pyruvate)[78,82–84,90,91,95] as well as the tricarboxylic acid (TCA) cycle (e.g. succinate, citric acid, fumarate, malate)[21,78,80,82,84,85,87,91–94] have been frequently reported to be altered in biomarker discovery studies. The TCA cycle is a central pathway of metabolism involved in a number of catabolic and anabolic reactions. Furthermore, intermediates of the TCA cycle can be replaced by amino acids and fatty acids through anaplerotic pathways. For example, glutamate is converted into α-ketoglurate, aspartate into oxaloacetate, and propionyl-CoA and amino acids are converted into succinyl-CoA via transamination[107]. Both, amino acid, and fatty acid levels, were also reported to be altered in HIE studies[22,74,78–82,84–87,91,93,95].

An alternative central energy production pathway is the oxidation of fatty acids to acetyl-CoA. Acetly-CoA is a key metabolic junction that fuels the TCA cycle and, in the heart, and liver fatty acids provide up to 80% of the energy needed in all physiological circumstances. Furthermore, in the liver acetyl-CoA can be converted into ketone bodies (i.e. acetoacetate and β-hydroxybutyrate), which are energy substrates transported to the brain and other tissues when glucose is not available[108]. In contrast to adults, where glucose is essentially the sole energy fuel for the brain, in neonates ketone bodies are thought to be equally important[90,109,110].

1.4.2 Oxidative and nitrosative stress

OS has a central role in the sequence of hypoxia-ischemia-derived perinatal injury[60]. The activation of oxidases, especially xanthine oxidase, leads to a burst of reactive oxygen species (ROS) that causes tissue damage. Purine metabolism has been repeatedly reported to be subjected to alterations in situations of hypoxia involving changing concentrations of xanthine, hypoxanthine, and uric acid among others[23,68–70,82,86,87,96]. In addition, nitric oxide formed in situations of OS can be combined with other reactive species forming reactive nitrogen species (RNS). ROS and RNS can attack lipids, proteins and nucleic acids and the resulting modifications can be detected and quantified[60]. For example, lipid peroxidation products (i.e. isoprostanes and isoprostanoids) were detected in tissue, plasma, and urine samples from animal models and infants with HIE[51,53,60,69,72,73,103,111]. Free-radical mediated protein oxidation products such as o-Tyr/Phe and NO_2-Tyr were identified as biomarker candidates in human studies[73,97].

The imbalance of the redox status has led to changes in the concentration of thiol/disulfide pairs, e.g. the reduced to oxidized glutathione ratio (GSH/GSSG). In newborns GSH/GSSG has been used to aid the optimization of resuscitation parameters employed for asphyxiated term infants[100]. Changes in this parameter have an impact on signaling, protein structure, and enzyme regulation. Besides, redox mechanisms control pro-inflammatory pathways, cell proliferation, and apoptotic processes[60].

1.4.3 Compounds related to brain injury

During HIE progression, a cascade of biochemical processes occurs including cellular bioenergetics failure followed by excitotoxicity, loss of mitochondrial activity, OS, and post-ischemic inflammation. These events cause cell death in the central nervous system and release of neurotransmitters such as glutamate, dopamine, NAA, choline and others[26,79,87,91,94]. Several tryptophan catabolites of the kynurenine pathway (KP) have the ability to modulate glutamatergic and nicotinic receptors, to regulate the response of the immune system after inflammation and/or infection, and even to modify the generation of ROS[112]. Therefore, different compounds of the KP and neurotransmitters are affected in HIE and are detectable as candidate biomarkers.

1.5 Validation and implementation into clinical practice

Despite the expanding list of candidate biomarkers, none of the newly discovered biomarkers has been implemented in the clinical management of HIE. To the best of our knowledge, and according to the Devices@FDA catalog[113], to date only medical devices for the analysis of lactate, creatinine, and uric acid have been approved by the FDA. We suggest that the main reasons for this are: 1) the lack of validation studies and clinical evidence of some

of the novel biomarkers and, 2) the absence of portable and validated analytical tools. The first shortcoming should be addressed in the forthcoming years by more powerful and better designed studies once quality standards are fully implemented in metabolomics studies[66]. Furthermore, regulators have also established biomarker qualification programs[114,115] to provide a framework for the review of biomarkers for use in regulatory decision-making. Regarding the second drawback, the use of spectroscopic tools (e.g. Raman spectroscopy[116,117]) could help to develop point of care devices (PoC) that can circumvent compound stability issues and might enable the performance verification of some biomarkers in the clinical scenario.

1.6 Conclusions

During the last years the number of proposed small molecule biomarkers for HIE reported in the literature has been growing without affecting the number of clinically exploited biomarkers. It is time to incorporate strict standards in study design and data quality assurance in the biomarker discovery stage. We identify a need for developing scalable methodologies and incorporate HIE biomarkers into regulator programs such as the FDA and EMA qualification programs, as well as medical devices to assure that the technical advances can be translated from the bench to the bedside and ultimately contribute to benefit the patients.

Chapter 2 Assessment of phospholipid synthesis related biomarkers for perinatal asphyxia: a piglet study

2.1 Abstract

The prompt and reliable identification of infants at risk of hypoxic-ischemic encephalopathy secondary to perinatal asphyxia in the first critical hours is important for clinical decision-making and yet still remains a challenge. This work strives for the evaluation of a panel of metabolic biomarkers that have been associated with the hypoxic-ischemic insult in the perinatal period. Plasma and urine samples from a consolidated newborn piglet model of hypoxia and withdrawn before and at different time points after a hypoxic insult were analyzed and compared to a control group. Time-dependent metabolic biomarker profiles were studied and observed patterns were similar to those of lactate levels, which are currently considered the gold standard for assessing hypoxia. Class prediction performance could be improved by the use of a combination of the whole panel of determined metabolites in plasma as compared to lactate values. Using a multivariate model including lactate together with the studied metabolic biomarkers allowed to improve the prediction performance of duration of hypoxia time, which correlates with the degree of brain damage. The present study evidences the usefulness of choline and related metabolites for improving the early assessment of the severity of the hypoxic insult.

2.2 Introduction

Both in the late preterm and term neonate, hypoxic-ischemic encephalopathy (HIE) secondary to perinatal asphyxia is a leading cause of mortality and acquired long-term neurologic co-morbidities. The overall incidence varies notably: while in developed countries between 1 and 8 per 1000 live births are affected, in low income areas it may account for 26 per 1000 live births[118].

Perinatal asphyxia is defined as the interruption of blood flow or blood gas exchange to and from the fetus in the perinatal period[119]. Hypoxic-ischemic injury is characterized by its evolution over time. The primary phase (i.e. the hypoxic insult) is followed by a partial recovery during reperfusion; however, in moderate to severe HIE a temporal sequence of injury is set in motion in the latent phase (from ~1–6 h) and the subsequent secondary phase (from ~6 h to > 3 days)[25,26].

Perceived prognosis greatly affects clinical management. The most successful intervention for the treatment of moderate to severe HIE is moderate whole body hypothermia. However, treatment has to be initiated within 6 hours from birth. Yet, as the clinical severity of HIE varies over time after the insult, assessments used for diagnosis are time-dependent and their accuracy may be reduced the earlier they are performed[119]. The prompt identification of infants who are most at risk of developing moderate to severe HIE in the critical first hours is desirable as it would help to guide clinical decision making and/or establish a prognosis. Yet, this still remains a challenge.

To date, the diagnosis of an asphyctic process that evolves to HIE is based on prenatal clinical information (sentinel events), and postnatal evaluation using serial Apgar score determinations with special emphasis on neurological assessment and cord blood gas analysis reflecting metabolic acidosis and increased lactate concentration6. Amplitude-integrated electroencephalography (EEG), brain magnetic resonance imaging (MRI) and multichannel EEG later on further confirm the diagnosis and the degree of severity[26,119]. A number of biochemical markers such as proteins apparently specific for neuronal tissue (creatine kinase brain band, protein S100B, neuron-specific enolase) and proteins involved in the pathogenesis of traumatic brain injury (e.g. glial fibrillary acidic protein, ubiquitin carboxyl-terminal hydrolase L1, phosphorylated axonal neurofilament heavy chain) as well as circulating pro-inflammatory cytokines (interleukin 1β and 6) and circulating mRNAs, among others, have been studied[26,119–122]. In most cases their usefulness has only been shown in pilot studies and currently none has entered into routine clinical use[122,123]. Furthermore, issues about the specificity of the reported markers have been raised[122] and information on correlation with long time outcomes is lacking[119].

Animal studies seeking after novel biomarkers which are able to provide improved performance have been carried out[8]. In a previous targeted metabolomic study in newborn piglets plasma it was shown that the duration and intensity of hypoxia were more accurately reflected by ratios of alanine to branched-chained amino acids (BCAA) and glycine to BCAA than by the traditionally employed plasma lactate concentration[21]. With the aim of discovering early biomarkers Solberg et al.[104] carried out an untargeted metabolomics study involving the analysis of retinal tissue samples from a piglet model of perinatal asphyxia. Retina is an integral neural tissue with a high metabolic demand for oxygen supported by an efficient vascular supply in which, under hypoxic conditions, a series of adaptive responses are induced including changes in the blood flow, angiogenesis, and protective metabolic adaptations[124]. After the hypoxic insult, elevated levels of CDP-choline, the limiting intermediate compound in the

major pathway of phosphatidyl-choline biosynthesis (i.e. the Kennedy pathway)[125] were found with concentrations correlating with the intensity of retinal hypoxia. In parallel, in vivo mouse[80] and rat models[90], revealed increased choline levels in brain tissue after hypoxia-ischemia in comparison to sham-controls. Earlier, in an ex-vivo rat model a decrease of choline in brain tissues after oxygen-glucose deprivation has been reported comparing hypothermia and normothermia groups[79].

Based on these findings in neuronal tissue, studies in minimal-invasively obtained biofluids were carried out. Choline and cytidine, two of the precursors of CDP-choline, were found among a set of 21 metabolites showing significant changes in a liquid chromatography-time-of-flight-mass spectrometry (LC-TOF-MS) untargeted metabolomics study on plasma samples from piglets subjected to hypoxia and reoxygenation in comparison to a non-asphyxiated control group[96]. Skappak et al.[85] found elevate levels of betaine, which is metabolically related to choline, in urine samples obtained from asphyxiated piglets vs. non-asphyxiated controls after 6 h of hypoxic insult. In concordance with the discussed results, a study involving the analysis of umbilical cord serum from newborns revealed an increase in choline and/or betaine levels in conditions of asphyxia and HIE[84].

Based on the above-cited observations a target study of three precursors of CDP-choline (choline, cytidine and uridine), together with betaine was incentivized. This work strives for the validation of candidate biomarkers in plasma and urine that have been associated with the hypoxic-ischemic insult in the perinatal period as they could potentially be of importance for grading the intensity and duration of tissue hypoxia in the clinical setting helping to stratify patients that could benefit from early moderate therapeutic hypothermia.

2.3 Material and methods

2.3.1 Animal model

Thirty-two 32 newborn Noroc (LYxLD) pigs aged between 12 h and 36 h, with hemoglobin (Hb) levels > 5 g dL^{-1} and good general conditions were included in the study. Anesthesia was induced with sevofluran 5%, then an ear vein was cannulated, sevofluran was disconnected and the piglets were given pentobarbital sodium 20 mg kg−1 and fentanyl 50 mg kg^{-1} intra venous (IV) as bolus injections. Continuous infusion of fentanyl (50 µ g kg^{-1} h^{-1}) and midazolam (0.25 mg kg^{-1} h^{-1}) was employed to maintain anesthesia. The piglets were orally intubated, ventilated and surgically prepared as described by Andresen et al.[46]. At the end of the observation time, the animals were given an overdose of pentobarbital (150 mg kg^{-1} h^{-1} IV).

After 1 h of stabilization, the piglets were randomly assigned either to the hypoxia and reoxygenation group (intervention group, n = 26) or the control group (n = 6) without exposure

to hypoxia, but maintaining the same procedures and observation times (anesthesia, surgery, ventilation and sample collection). In the intervention group, hypoxemia and subsequently hypoxia-ischemia was achieved by ventilation with a gas mixture of 8% O_2 in N_2 until either the mean arterial blood pressure (MABP) decreased to < 20 mmHg or the base excess (BE) reached − 20 mM L^{-1}. CO_2 was added during hypoxemia aiming at a pCO_2 of 8.0–9.5 kPa (60–71.3 mmHg) in order to imitate perinatal asphyxia. After 30 min of reoxygenation employing room air (21% O_2, n = 12) or 2.1% H_2 gas mixed into synthetic air (n = 14) all animals were kept normocapnic with pCO_2 between 4.5 and 5.5 kPa (33.8–41.3 mmHg) during 9 hours receiving room air. Continuous surveillance of blood pressure, saturation, pulse, temperature, and blood gas measurements were performed. In this study both reoxygenation groups were merged together (intervention group, n = 26) as no statistically significant differences could be found between animals from both groups in a previous untargeted metabolomics study[96].

Whole blood samples from piglets included in the hypoxia group were taken in ethylenediaminetetraacetic acid (EDTA) Vacutainer® blood collection tubes before start of hypoxia (t_0), at the end of hypoxia (t_1), after reoxygenation (t_2) and 2 and 9 hours after reoxygenation (t_3 and t_5, respectively). Blood volumes drawn for testing were replaced by 1.5× of saline. Plasma was obtained immediately after sampling by centrifugation of whole blood samples at 2000 × g for 10 min at 4 °C. For those piglets included in the control group plasma were also collected after 1 h stabilization. Besides, control plasma samples were collected at time points matching the mean values of the end of hypoxia (t_1), t_3 and t_5 for the comparison of the metabolic profiles in both groups of samples. Urine samples were withdrawn from piglets included in the hypoxia group 5 and 9 hours after reoxygenation (t_4 and t_5). Urine samples from piglets included in the control group were also collected at the same time point for the analysis of the effect of hypoxia and reoxygenation in the urinary metabolic profiles. Plasma and urine samples were stored at −80 °C until analysis. The experimental study design and sample collection time points are visualized in **Figure 2.1**.

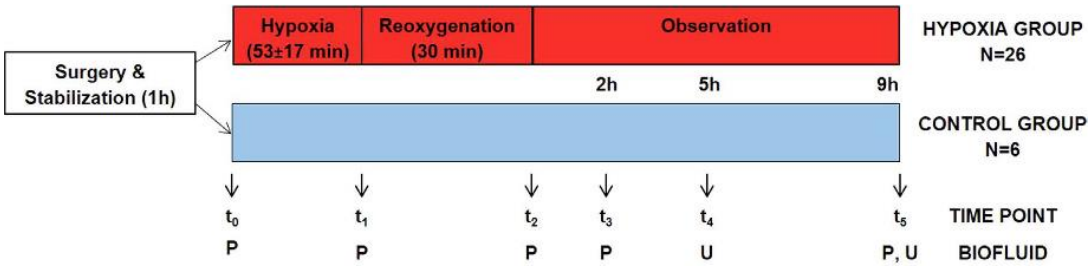

Figure 2.1 Overview of the study design. Note: P stands for plasma, U stands for urine; no plasma samples have been collected from animals included in the control group at t_2.

2.3.2 Chemical and reagents

Solvents of LC-MS grade and were purchased from Scharlau (Barcelona, Spain). Pure analytical standards (choline bitartrate, betaine, cytidine and uridine) and ammonium formate with purities ≥ 98% were from Sigma-Aldrich Química SA (Madrd, Spain) and betaine-D11 (98%) from Cambridge Isotope Laboratories Inc. (Tewksbury, MA, USA).

2.3.3 Sample preparation

Samples were thawed on ice and homogenized. 190 µL of cold acetonitrile (4 °C) and 10 µL of internal standard solution (betaine-D11) at a concentration of 10 µM were added to 10 µL of plasma or urine. Samples were centrifuged at 10000 × g for 10 min at 4 °C. 100 µL of supernatant were collected and transferred to a 96 well plate for LC-MS/MS analysis. During sample processing, samples were maintained on ice to prevent sample degradation. Blanks were prepared by replacing the sample volume with H_2O. Quality control (QC) samples for plasma and urine were prepared by mixing 5 µL of each sample. QCs were processed as described for samples.

In urine samples creatinine levels were determined for normalization of biomarker concentrations employing a MicroVue Creatinine Assay Kit from Quidel Corporation (San Diego, CA, USA).

2.3.4 Quantitative ultra-performance liquid chromatography coupled to tandem mass spectrometry (LC-MS/MS) analysis

Quantitative analysis of choline, betaine, cytidine and uridine was performed employing an Acquity UPLC system coupled to a Xevo-TQ triple quadrupole MS detector operating in the positive electrospray ionization mode (ESI+) (Waters, Manchester, UK). With a total runtime of 5 min, isocratic elution was performed using a Kinetex HILIC column (100 × 2.1 mm, 1.7 µm, 100 Å) from Phenomenex (Torrance, CA, USA) and a 30:70 v/v H_2O:CH_3CN mobile phase at pH 7 containing 5 mM ammonium formate. Flow rate, column temperature and injection volume were set at 0.4 ml min^{-1}, 30 °C and 5 µL, respectively. Detection conditions were set as follows: capillary voltage to 3.5 kV, source temperature to 120 °C and the cone, desolvation and collision gas flows were 50 L h^{-1}, 700 L h^{-1} and 0.2 mL min^{-1}, respectively. Dwell time was set to 5 ms ensuring a minimum of 10 data points per peak.

Stock solutions of standards were prepared in water by direct weighing. A set of 12 standard solutions was obtained by serial dilution of the stock solution in mobile phase covering the concentration ranges indicated in **Table 2.1**. For quantification, tandem MS detection was carried out by multiple reaction monitoring (MRM) applying the acquisition parameters shown in **Table 2.1**. Individual standard solutions at a concentration of 10 µM were

used for optimizing ionization and fragmentation parameters as wells as for confirming the absence of spectral interferences between the studied compounds.

Table 2.1 LC-MS/MS measurement conditions

Analyte	Cone [V]	CE [eV]	MRM	RT [min] (mean ± std)	Calibration range	R^2
Choline	40	15	104.1 > 60.2	2.318 ± 0.011	0.05-49	0.990
Betaine	30	20	118.0 > 59.0	1.528 ± 0.007	0.2-49	0.992
Cytidine	35	10	244.0 > 112.0	0.769 ± 0.011	0.06-15	0.950
Uridine	35	10	245.0 > 113.0	0.671 ± 0.008	0.11-15	0.990
Betaine-D11	10	25	129.0 > 66.0	1.530 ± 0.006	-	-

An initial system suitability test was carried out at the beginning of each batch involving the analysis of blank samples and solvent blanks to assure appropriate sensitivity levels and reproducible retention times (± 0.2 min). QC samples spiked with the stock solution were intercalated in the sample batch measurement to detect deficiencies in accuracy and precision levels prior to the release of results. Accordingly, at least 75% of the values found for the QC standards should be within ± 25% of their respective nominal values to accept the batch.

2.3.5 Data processing

Raw data were acquired and processed using MassLynx 4.1 and QuanLynx 4.1 (Waters, Milford, MA, USA), respectively. Linear response curves were obtained from UPLC-MS/MS peak area measurements employing betaine-D11 as internal standard. Further data processing was carried out in Matlab 2015a from Mathworks Inc. (Natick, MA, USA) using the PLS Toolbox 8.0 from Eigenvector Research Inc. (Wenatchee, WA, USA) and in-house written functions. ROCs and AUCs were computed employing MetaboAnalyst 3.0[50]. Missing values were estimated using k-nearest neighbors and data were autoscaled. For multivariate ROC curve based exploratory analysis all available features at each time point were employed. Feature ranking was based on univariate AUC values and random forests were used as a classification method. ROC curves were generated by Monte-Carlo cross validation (MCCV) using balanced subsampling where in each MCCV two thirds of the samples were used to evaluate the feature importance. Then, the model was validated using one third of the samples that were left out during model generation. For the calculation of the confidence interval (CI), this procedure was repeated 500 times.

2.4 Results

2.4.1 Characterization of the study cohorts

The experimental study design and sample collection time points are shown in **Figure 2.1**. **Table 2.2** summarizes parameters and variables continuously monitored during the animal experiments including hemoglobin, base excess (BE), mean arterial blood pressure (MABP),

partial O_2 arterial pressure (pO_2) and partial arterial CO_2 pressure (pCO_2). No differences between control and hypoxia groups were found neither for the basic biologic characteristics nor the clinical parameters after 1 h of stabilization. However, at the end of hypoxia in the intervention group significantly lower pH, BE, and MABP levels were found, while no difference in heart rate was observed (see **Table 2.2**). Resuscitation with room air rapidly improved clinical variables in the intervention group and at the end of resuscitation both groups showed comparable levels of pO_2, pCO_2 and MABP.

Table 2.2 Physiological background data. Characterization of the study cohort (intervention group) before (t_0), directly after asphyxia (t_1) and after reoxygenation (t_2–t_5) and at corresponding time points for the control group. Values are presented as mean ± standard deviation. Hb = hemoglobin; BE = base excess, MABP = mean arterial blood pressure; pO_2 = partial O_2 pressure; pCO_2 = partial CO_2 pressure.

Parameter	Time	Control group	Intervention group
Weight [kg]	All times	1.81 ± 0.17	1.90 ± 0.13
Age [h]	All times	29 ± 3	26 ± 4
Gender [male/female]	All times	3/3	12/14
Hypoxia time [min]	All times	0	53 ± 17
Hb [g/100mL]	t_0	7.2 ± 1.0	7.3 ± 1.1
	t_5	6.7 ± 0.8	6.80 ± 0.05
pH	t_0	7.41 ± 0.04	7.44 ± 0.07
	t_1	7.42 ± 0.03	6.84 ± 0.07
	t_2	7.44 ± 0.03	7.16 ± 0.07
	t_3	7.46 ± 0.03	7.39 ± 0.08
	t_4	7.42 ± 0.05	7.40 ± 0.09
	t_5	7.44 ± 0.08	7.40 ± 0.09
BE [mM]	t_0	2 ± 3	2 ± 3
	t_1	2 ± 3	19 ± 2
	t_2	2 ± 3	15 ± 2
	t_3	2 ± 3	0 ± 4
	t_4	1 ± 4	0 ± 5
	t_5	0 ± 5	0 ± 5
MABP [mmHg]	t_0	49 ± 5	54 ± 8
	t_1	48 ± 7	23 ± 8
	t_2	48 ± 7	42 ± 11
	t_3	47 ± 6	48 ± 11
	t_4	48 ± 8	44 ± 9
	t_5	47 ± 13	46 ± 11
Heart rate [b.p.m]	t_0	147 ± 11	140 ± 30
	t_1	156 ± 20	160 ± 50
	t_2	156 ± 20	200 ± 40
pO_2 [kPa]	t_0	9.9 ± 1.0	10.6 ± 1.7
	t_1	10.3 ± 0.8	5.0 ± 0.6
	t_2	10.3 ± 0.8	10.7 ± 1.4
pCO_2 [kPa]	t_0	5.4 ± 0.5	5.2 ± 0.8
	t_1	5.1 ± 0.3	9.3 ±1.1
	t_2	5.1 ± 0.3	4.7 ± 0.8

2.4.2 Effect of hypoxia on plasma and urine samples

Choline, betaine, cytidine and uridine were determined in plasma and urine samples employing UPLC-MS/MS. Representative chromatograms of samples from the control and hypoxia group obtained directly after asphyxia (t_1) are shown in **Figure 2.2** Concentrations of the studied metabolites in plasma and urine samples as determined employing the UPLC-MS/MS method at the different time points are represented in **Figure 2.3** and **Figure 2.4**, respectively. In addition, the plasma lactate profile at the same time points is shown in **Figure 2.3** for the sake of comparison. In plasma no significant changes in concentrations were detected in the control group with the exception of a decrease in betaine and cytidine between 2 and 9 h after reoxygenation (i.e. t_3 and t_5, respectively). In contrast, a highly significant, abrupt rise was observed in the intervention group for choline, cytidine and uridine levels when comparing plasmatic concentrations before and at the end of hypoxia (i.e. at t_0 and t_1, respectively) followed by a descent when comparing levels at the end of hypoxia to those found 2 h and 9 h after reoxygenation (i.e. t_3 and t_5, respectively). Consequently, at the end of hypoxia the intervention group showed significantly increased concentrations of choline, cytidine and uridine (Wilcoxon rank sum, p-value < 0.05) as compared to the control group. This difference remained significant (Wilcoxon rank sum, p-value < 0.05) for choline even after 2 h of reoxygenation (t_3). The profile of those three metabolites is similar to changes observed in lactate levels. For betaine a slightly different profile was obtained: the increase of betaine in the intervention group at t_1 was not found to be significant; this was followed by a decrease at t_2 and then an increase at t_3 yielding significantly higher concentrations (Wilcoxon rank sum, p-value < 0.05) in the intervention group. Besides, a significant decrease in the plasmatic concentrations was observed for both control and hypoxia groups in samples withdrawn 9 hours after reoxygenation (t_5). In urine samples no statistically significant changes were observed. However, choline concentrations in the intervention group showed a trend to higher concentrations and higher between-individuals variability.

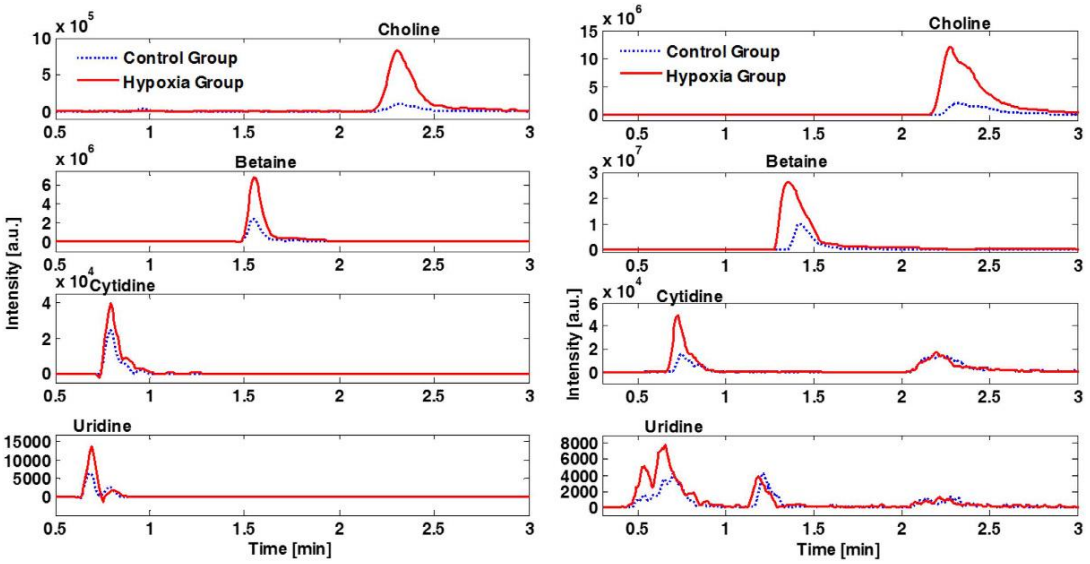

Figure 2.2 Representative chromatograms of plasma (left) and urine (right) samples from control and intervention (hypoxia) groups.

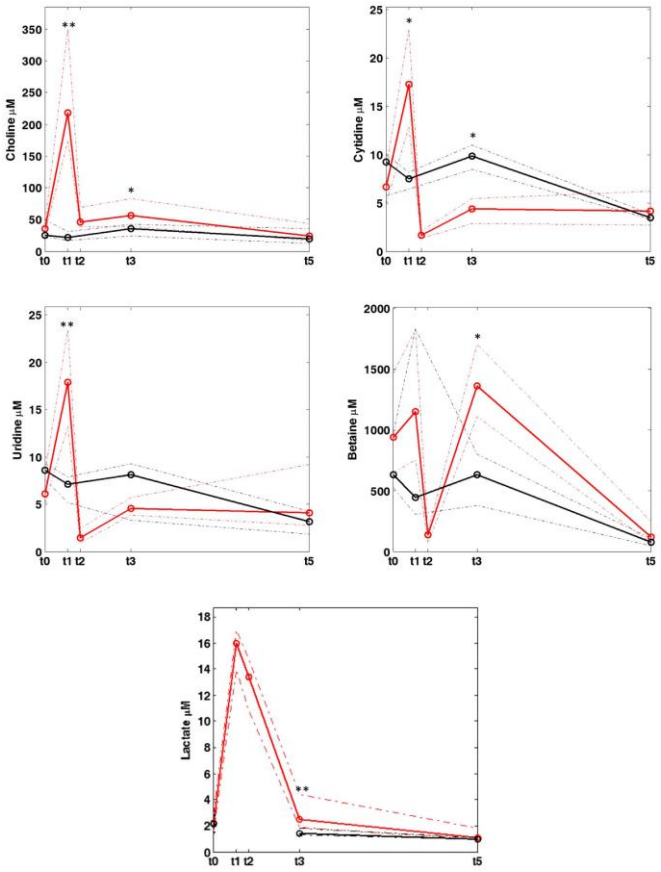

Figure 2.3 Concentrations of metabolites in plasma samples at different studied time points. Note: * and ** indicate significant differences (p-value < 0.05 and 0.01, respectively) between samples from the control (black line) and intervention groups (red line).

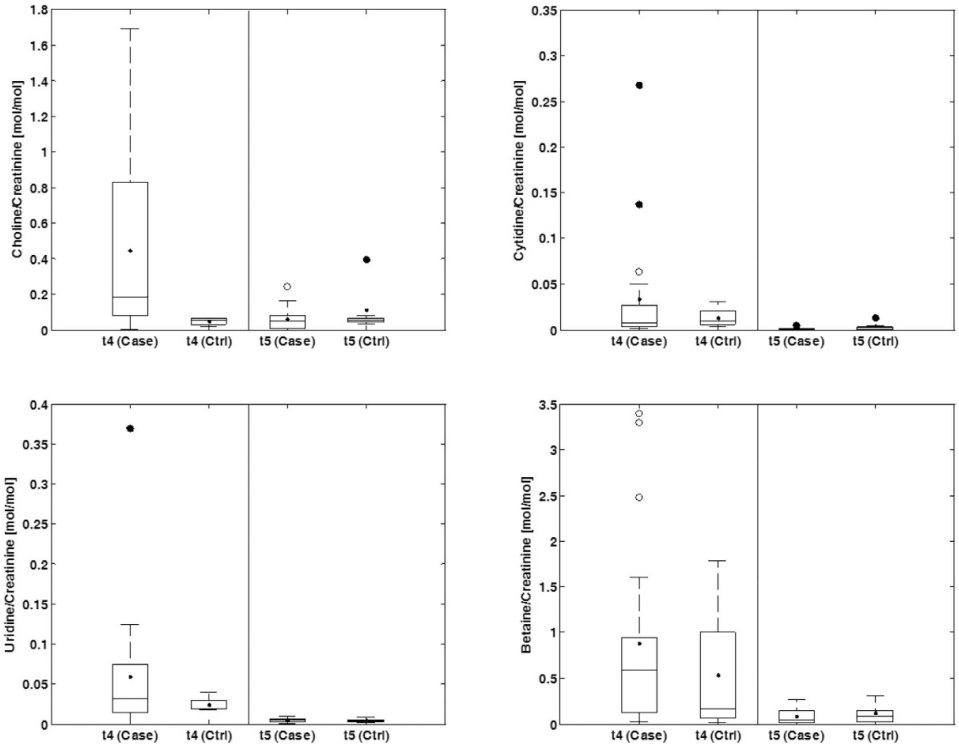

Figure 2.4 Boxplots representing concentrations of metabolites in urine. Note: Case = intervention group; Ctrl = control group; concentrations were normalized by creatinine.

2.4.3 Prognostic capacity of the studied metabolites

With the aim of assessing the prognostic capacity of the studied biomarkers, receiver operating characteristics (ROC) curves and areas under the ROC curve (AUC) were calculated for lactate, choline, cytidine, uridine and betaine comparing control vs intervention groups at each studied time point in urine and plasma samples[126]. The obtained AUC values and their 95% CI are listed in **Table 2.3**. In plasma collected before initiating hypoxia (t_0), no statistically significant models were obtained. Directly after hypoxic insult (t_1) choline, cytidine and uridine showed AUC values ≥0.969. As anticipated from the concentration profiles discussed above, the prognostic power was smaller 2 h after reoxygenation (t_3); however, for choline and cytidine, as well as lactate AUC of ≥ 0.814 were obtained. The effect of hypoxia on the studied metabolites 9 h after reoxygenation (t_5) was negligible and none of the calculated AUC values showed a better prediction performance than random models in both studied biofluids. In addition, choline concentrations determined in urine samples at t_4 showed a statistically significant prediction power.

Additionally to univariate ROC curves, multivariate ROC curves were calculated for each time point and biofluid using data from all available metabolites, thereby yielding optimum prediction properties. AUC (95% CI) values are shown in **Table 2.3**. Statistically significant models were obtained directly after asphyxia (t_1) and 2 h after reoxygenation (t_3). It is noteworthy that the predictive power 2 h after reoxygenation could be improved by the

multivariate approach. **Figure 2.5** shows ROC curves of multivariate models calculated for t_0, t_1, t_3 and t_5 in plasma samples. This figure illustrates the changing prediction power in dependence of the timing of blood sample collection.

Table 2.3 AUC (CI 95%) for biomarkers for hypoxia comparing control vs. intervention groups. Note: Lactate was not determined in plasma samples from the control group at t1 and in urine samples.

Metabolite	Plasma at t_0	Plasma at t_1	Plasma at t_3	Plasma at t_5	Urine at t_4	Urine at t_5
Lactate	0.518 (0.306–0.736)	–	0.989 (0.746–0.992)	0.561 (0.301–0.816)	–	–
Choline	0.615 (0.276–0.926)	1 (1–1)	0.814 (0.614–0.955)	0.577 (0.356–0.792)	0.829 (0.612–0.961)	0.630 (0.379–0.815)
Cytidine	0.679 (0.394–0.926)	0.969 (0.892–1)	0.826 (0.568–1)	0.574 (0.393–0.765)	0.592 (0.296–0.823)	0.713 (0.481–0.713)
Uridine	0.641 (0.372–0.878)	1 (0.969–1)	0.629 (0.326–0.909)	0.667 (0.429–0.866)	0.632 (0.414–0.842)	0.500 (0.231–0.787)
Betaine	0.615 (0.308–0.843)	0.708 (0.334–0.973)	0.788 (0.439–0.981)	0.673 (0.413–0.898)	0.671 (0.296–0.947)	0.602 (0.345–0.852)
Multivariate	0.549 (0.229–0.871)	0.976 (0.957–1)	0.932 (0.806–1)	0.525 (0.116–0.947)	0.815 (0.389–1)	0.463 (0.115–0.728)

2.4.4 Correlation with time of hypoxia 2h after reoxygenation (t_3)

The correlation of lactate levels in blood with the duration of hypoxia has been studied (see **Figure 2.6**, left) obtaining a coefficient of correlation (R) of 0.64, a slope significantly different from zero (p-value < 0.01) and a standard deviation of the residuals of ± 33 min. This result was compared to the performance of a Partial Least Squares (PLS) model using the plasma levels of lactate with choline, cytidine, uridine and betaine and 1 latent variable (LV) (see **Figure 2.6**, right). For the PLS predicted vs measured hypoxia time an R of 0.77 was obtained with a slope significantly different from zero (p-value < 0.01) and a standard deviation of the residuals of ± 14 min.

2.5 Discussion

Assessing the degree of perinatal asphyxia in the immediate postnatal period still remains a challenge. However, this information would be extremely valuable for optimizing therapy and reliably predicting short-and/or-long term outcomes especially in low-income countries with little access to hypothermia therapy.

An ideal biomarker is one that is easily and rapidly performed, its concentration is proportionately changed in the course of the disease according to the degree of injury and thus it can be used as an early predictor of long-term outcomes. Data presented in **Table 2.2** demonstrate that physiological variables do not provide sufficient predictive capacity as they return to normal values during resuscitation. In this study we assessed and compared the evolution of four metabolites, namely choline, betaine, cytidine and uridine, which have been identified as potential biomarkers of hypoxia in previous studies[84,85,96,104]. Levels of lactate,

which are currently considered the gold standard for assessing asphyxia in the clinics, were used throughout this work as reference for comparison.

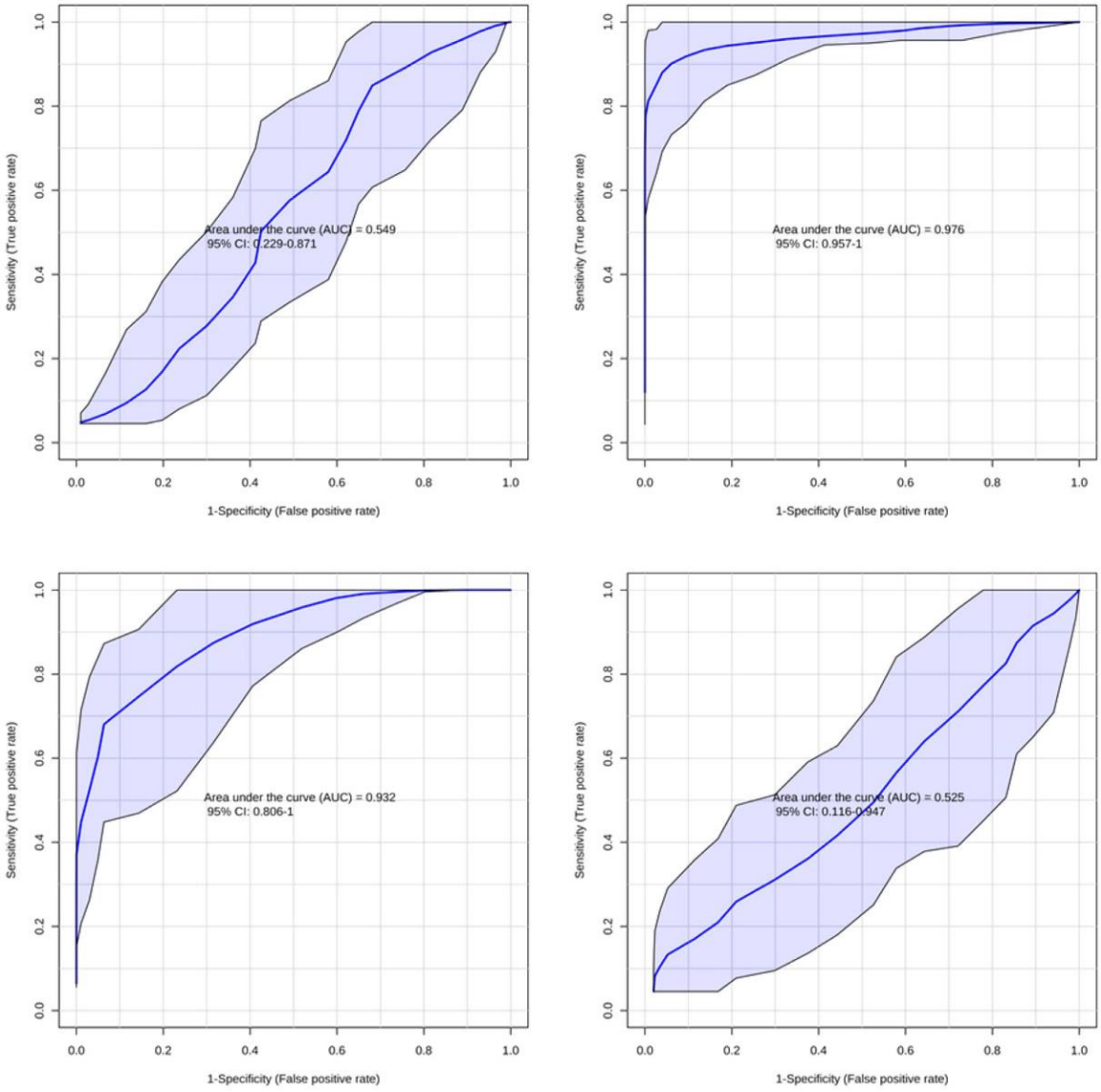

Figure 2.5 Multivariate ROC curves comparing cases and controls at t_0 (left, top), t_1 (right, top), t_3 (left, bottom) and t_5 (right, bottom).

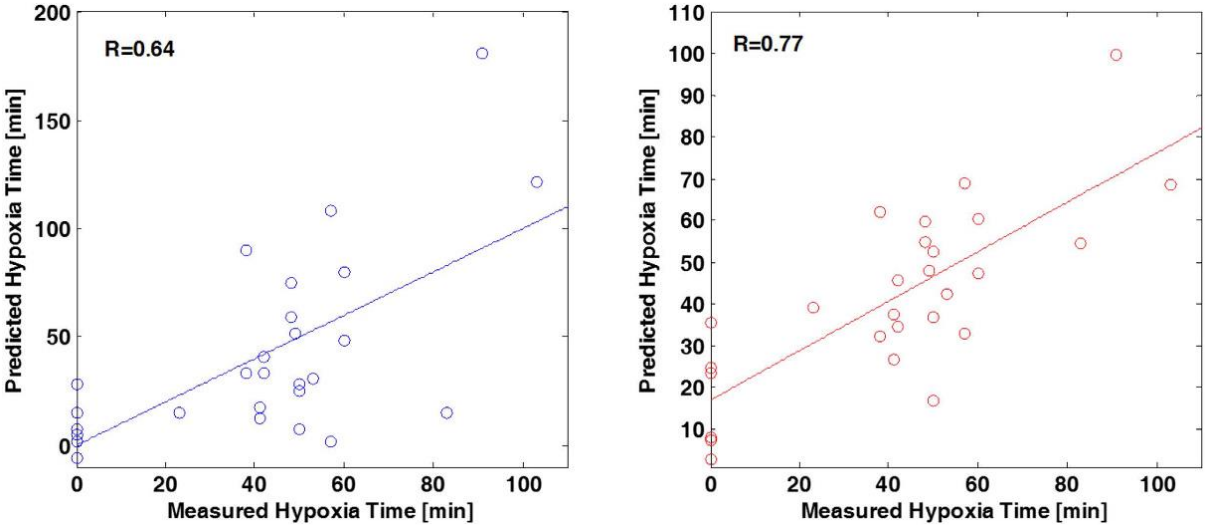

Figure 2.6 Correlation of lactate levels in blood with the duration of hypoxia (left) and predicted vs measured hypoxia time using a PLS multivariate model based on the levels of lactate, choline, cytidine, uridine and betaine (right) at t_3.

The present study shows significant transient changes in plasmatic levels of the studied metabolites in a piglet model of hypoxia-reoxygenation (see **Figure 2.3**). Whereas choline, cytidine and uridine followed a similar profile as compared to lactate levels, betaine, showed a slightly different pattern (see **Figure 2.3**). In urine samples collected 5 h after the insult (t_4), less pronounced differences in choline concentrations were found (see **Figure 2.4**). Choline is involved in a number of physiological processes. Hence, it is converted into betaine in a two-step enzymatic reaction taking place in the mitochondria of liver and kidney where it acts as an osmolyte to control physiologic osmotic pressure[127,128]. In the brain, choline together with the pyrimidines cytidine and uridine is incorporated into phosphatidylcholine following the cytidine 5-diphosphocholine pathway discovered by E.P. Kennedy in 1954[129]. Their uptake from the circulation into the brain's extracellular fluid is carried out by means of nucleoside transporters located at the blood-brain-barrier (BBB). The rate at which uptake occurs constitutes a major factor determining phosphatide synthesis[130]. Hence, these metabolites are precursors for the synthesis of membrane phospholipids including phosphatidylcholine, and thereby affect signaling and transport across membranes[125,128].

In newborns, both, the endogenous biosynthesis of phosphatidylcholine and the uptake from mother's milk have been studied[131]. In addition, choline's function as a part of the neurotransmitter acetylcholine has been discovered at the beginning of the 20th century[132,133]. Previous observations of elevated CDP-choline levels in retinal tissue support the alteration of the Kennedy pathway rather than the formation of acetylcholine as acetylcholine levels in the studied neuronal tissue remained unaffected during hypoxia-reoxygenation[104].

The evolution of the plasmatic profiles of these metabolites could potentially be related with the alteration of the Kennedy pathway together with the disturbance of the function of the

BBB which has been reported during HI insults in neonates[134]. In addition, a recent study on neonatal mouse brain has revealed the transient opening of the BBB within early hours after the insult[135]. Future studies will focus on the elucidation of the mechanism behind the reported observations.

Poor predictive capacity was observed before hypoxia (t_0) and 9 h after reoxygenation (t_5), whereas directly after asphyxia (t_1) and 2 h after reoxygenation (t_3) (in plasma) and at 5 h after reoxygenation (t_4) (in urine) significant models for the prediction of hypoxia were obtained (see **Table 2.3** and **Figure 2.5**). In view of the clinical applicability as valuable biomarkers of these metabolites, the time-course is of great importance. In the clinical setting, there is no access to blood samples before hypoxic insult for the sake of a relative comparison of metabolic changes. Hence, in this study all ROC curves were constructed comparing control and intervention groups at each time point. Furthermore, the selection of the most appropriate therapeutic strategy is limited by the therapeutic window of 6 h from birth for hypothermia treatment. At present, the gold standard of metabolic biomarkers for assessing the severity of hypoxia is lactate. In this study, lactate showed a good predictive power in plasma collected 2 h after reoxygenation (t_3) (see **Table 2.3**). However, it is noteworthy that the performance could be improved (AUC from 0.898 to 0.932 and CI reduced by > 20%) by the use of a combination of the whole panel of determined metabolites. An interesting finding from the viewpoint of a potential clinical application of these biomarkers is that the perturbation persists during at least a couple of hours in plasma and even longer in urine.

This offers the possibility to carry out serial determinations within the first hours of life, which could help to guide clinical decisions on treatment providing complementary information to other available diagnostic tools in the delivery room.

Another interesting finding of the present study is the prediction performance of choline in urine samples collected 5 h after reoxygenation (t_4) which to date, to the best of our knowledge, has not yet been reported in scientific literature. This finding is of special interest for the clinics, due to the non-invasive character of urine samples. However, metabolic fluctuations in urine reflect a much longer time span as compared to plasma samples and therefore, their interpretation and significance in the context of an acute process is more complex.

The duration of hypoxia is known to be directly proportional to the degree of brain damage[70]. Hence, the correlation of the studied biomarkers with the measured time of duration of hypoxia was assessed. By combining choline and its related metabolites with lactate levels measured 2 h after reoxygenation (t_3), the coefficient of correlation could be improved by > 20% from 0.64 to 0.77 as proven in **Figure 2.6**. Furthermore, the standard deviation of the residuals was reduced from 33 to 14 min thereby improving the prediction precision by 58%. This corroborates the usefulness of the described biomarkers for the clinical diagnosis within the first hours of life.

To summarize, the present study showed the potential of choline and related metabolites as biomarkers for hypoxia. The selected panel of metabolites was able to improve the predictive performance of lactate and further helped to improve the prediction precision of the duration of hypoxia. Their applicability for clinical diagnosis is to be confirmed in multicenter trials involving the analysis of blood and urine samples from newborns suffering from HIE. These studies will also focus on the assessment of their correlation with long-term neurodevelopmental outcomes.

Chapter 3 Evolution of Energy Related Metabolites in Plasma from Newborns with Hypoxic-Ischemic Encephalopathy during Hypothermia Treatment

3.1 Abstract

Therapeutic hypothermia (TH) initiated within 6 h from birth is the most effective therapeutic approach for moderate to severe hypoxic-ischemic encephalopathy (HIE). However, underlying mechanisms and effects on the human metabolism are not yet fully understood. This work aims at studying the evolution of several energy related key metabolites in newborns with HIE undergoing TH employing gas chromatography – mass spectrometry. The method was validated following stringent FDA requirements and applied to 194 samples from a subgroup of newborns with HIE (N = 61) enrolled in a multicenter clinical trial (HYPOTOP) for the determination of lactate, pyruvate, ketone bodies and several Krebs cycle metabolites at different sampling time points. The analysis of plasma samples from newborns with HIE revealed a decrease of lactate, pyruvate and β-hydroxybutyrate concentrations, whereas rising malate concentrations were observed. In healthy control newborns (N = 19) significantly lower levels of pyruvate and lactate were found in comparison to age-matched newborns with HIE undergoing TH, whereas acetoacetate and β-hydroxybutyrate levels were clearly increased. Access to a validated analytical method and a controlled cohort of newborns with HIE undergoing hypothermia treatment for the first time allowed the in-depth study of the evolution of key metabolites of metabolic junctions in this special population.

3.2 Introduction

Hypoxic-ischemic encephalopathy (HIE) secondary to perinatal asphyxia is a major cause of mortality and long-term neurologic co-morbidities especially occurring in the term neonate. Every year worldwide one million infants die and one million survive with neurological impairment. However, the overall incidence varies notably. Hence, while in developed countries the incidence of HIE ranges between 1 and 2 per 1000 live births, in low income areas it may account for 26 per 1000 live births[106].

Therapeutic hypothermia (TH) initiated within 6 hours from birth[119] was introduced to resuscitation guidelines in 2010[136] and involves a core temperature reduction to 33.5 ± 0.5°C for 72 h. Since then hypothermia treatment is standard of care for infants with HIE. To date this is the only treatment that has shown to reduce death and long-term disability for infants especially with moderate encephalopathy. However, in severe cases the combined outcome of death and/or severe disability has not been as successful and still affects around 45% of babies[137]. Therefore, in order to improve outcome of severely affected neonates, new synergistic therapies are being explored[26,138]. To this end, the HYPOTOP trial (EudraCT #2011-005696-17), a randomized, multicenter, double blinded placebo-control trial, aiming at the evaluation of the neuroprotective effect of topiramate (TPM) in addition to moderate total body hypothermia in patients with HIE, has been carried out. The HYPOTOP trial aimed at reducing the hyperexcitability component of HIE which leads to increased neuronal apoptosis. TPM has rendered good results in this regard in previously launched pilot studies[139]. New anticonvulsant drugs such as TPM or levetiracetam have shown not to foster apoptosis and even inhibit cascades of damage activated after hypoxic-ischemic insults at paediatric doses, indicating that they potentially act as neuroprotectors in addition to their antiseizure effects[140].

Both, early assessment of the severity of cerebral injury and the prediction of neurological outcomes are crucial for parental counselling, selection of the most appropriate early neuroprotective strategies and/or establishment of multidisciplinary interventions to lessen the severity of chronic morbidities. The diagnosis of an asphyxia process that evolves to HIE is based on prenatal clinical information (sentinel events), Apgar scores with special emphasis on neurological assessment of tone, response to stimuli or reflexes and cord blood gas analysis reflecting metabolic acidosis and increased lactate concentration. Amplitude-integrated electroencephalography (aEEG) in the first hours after birth and magnetic resonance imaging (MRI) of the brain and multichannel EEG (mchEEG) later on may further confirm the diagnosis[26].

Little is known about the evolution of most biochemical markers in newborns with HIE during TH. The secondary phase of injury is characterized by a failure of oxidative metabolism, which is associated with exhaustion of ATP reserves leading to cytotoxic edema, hyperexcitability, cerebral reperfusion and ultimately, cell death by necrosis and/or apoptosis. Clinical neurodevelopmental outcomes at 1 and 4 years of age are closely correlated with the severity of the secondary failure of oxidative metabolism at 15 h after birth[122]. Hence, the classical biochemical evaluation of the severity of asphyxia in the first hours of life is based on serial determinations of arterial pH, base deficit (BD) and blood lactate[141]. In practice, they showed reasonable precision for correctly identifying absent versus severe HIE. However, due to its remarkable ability to adapt to profound and prolonged hypoxia, the healthy foetus frequently is capable of tolerating such insults even without evidence of injury. Hence, BD and lactate provide rather imprecise relationship with neonatal encephalopathy for the intermediate group[122].

This study reports the evolution of eight metabolites including lactate, pyruvate, metabolites from the Krebs cycle and ketone bodies in plasma from newborns with HIE undergoing hypothermia treatment in comparison to a control group of samples collected from healthy term newborns. A gas chromatography – mass spectrometry (GC-MS) analytical method was developed and successfully validated, allowing the simultaneous quantification of the studied metabolites employing a sample volume of only 50 µL, thus enabling serial determinations from small volume blood samples. The availability of sound data from a controlled cohort of infants clears the way for studying the role of each metabolite in the clinical context of TH in newborns with HIE.

3.3 Material and methods

3.3.1 Standards and reagents

Sodium pyruvate, sodium lactate, lithium acetoacetate, sodium β-hydroxybutyrate, disodium succinate, sodium fumarate dibasic, malic acid and α-ketoglutaric acid potassium salt with purities >98%, as well as heparin sodium salt, methoxyamine hydrochloride (98%), pyrimidine (≥98%) and N-methyl-N-(trimethylsilyl)trifluoroacetamide with 1% trimethylchlorosilane (MSTFA + 1% TMCS), pyruvate-13C (Pyr13C) (99%) and 3,4-dimetoxibenzoic acid (DMBA) (99%) were purchased from Sigma-Aldrich Química SL (Madrid, Spain). Pyr^{13}C and DMBA were used as internal standards (IS). Mixture of C_7–C_{40} n-alkanes, each at 1000 g L^{-1} were acquired from Sigma-Aldrich Química SL (Madrid, Spain). Acetonitrile (analytical grade) and hexane (analytical grade) were obtained from J.T. Baker (Center Valley, USA) and Scharlau (Barcelona, Spain), respectively. Ultrapure H_2O was generated with a Milli-Q purification system from Merck Millipore (Darmstadt, Germany).

3.3.2 Population

A subgroup of newborns (N = 61) enrolled in the HYPOTOP trial (EU Clinical Trials Register: EudraCT 2011-005696-17, start date: 2013-06-18) was included in this study. The flow diagram presented in **Figure 3.1** summarizes the study protocol. Eligible patients were infants >36 weeks' gestational age that fulfilled the following criteria: (1) prenatal signs compatible with hypoxia-ischemia such as alterations of foetal cardiac monitoring, abnormal foetal scalp pH (<7.2) or sentinel events such as abruptio placenta, meconium stained amniotic fluid or cord prolapse; (2) objective assessment of postnatal depression which included: Apgar ≤5 at 5 min, need for resuscitation with positive pressure ventilation for >10 min after birth, cord pH ≤ 7.0 and BE ≥ −16 mEq L^{-1} in the worst blood gases obtained in the first 60 min after birth; (3) moderate to severe neurological status according to a modified Sarnat & Sarnat scale[63]. Exclusion criteria included gestational age < 36 weeks, birth weight < 2500 g, severe congenital malformations, chromosomopathies, or moribund status.

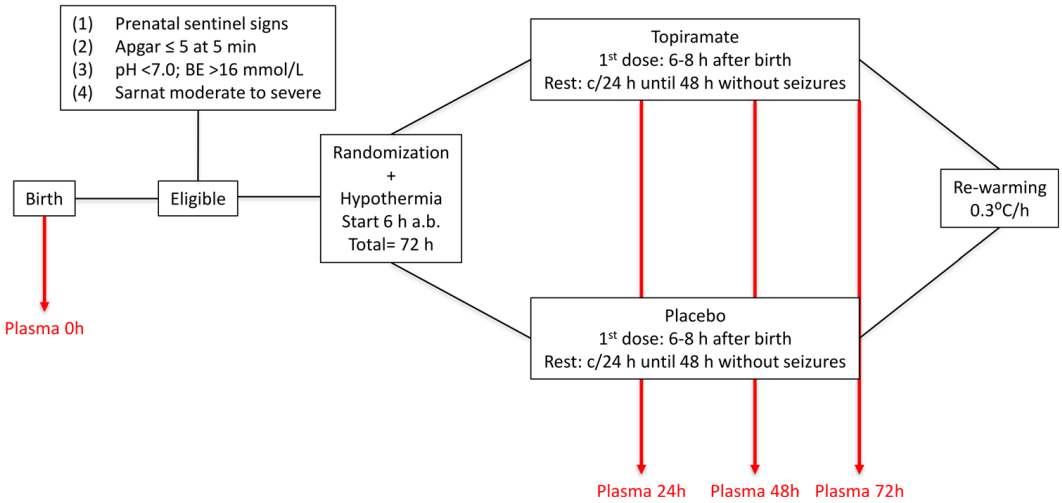

Figure 3.1 Flow diagram of the HYPOTOP trial.

A total of 194 plasma samples were withdrawn at birth (0 h, corresponding to umbilical cord blood or, if not available, the first extracted blood sample, N = 41) and 24 h (N = 51), 48 h (N = 51) and 72 h (N = 51) after the administration of the first dose of TPM or placebo. For plasma collection, 0.5 mL of blood was drawn by venipuncture employing a heparinized syringe (1% sodium heparin). Plasma was obtained immediately thereafter to avoid sample degradation, centrifuging the samples at 1800 g during 10 min at 20°C. Supernatants were immediately collected and stored at −80 °C until analysis. As a control group (N = 19), excess volumes from blood samples extracted 53 ± 13 h after birth for routine neonatal screening from healthy term newborns before hospital discharge were employed and plasma was extracted following the same protocol as described above. Patient characteristics are summarized in **Table 3.1**. The Ethics Committee for Biomedical Research of the Health Research Institute La Fe (Valencia, Spain) approved the study protocol. Informed consent was obtained from parents of all participants. All methods were performed in accordance with the relevant guidelines and regulations.

Table 3.1 Patients' characteristics. Note: p-value was computed employing a Mann–Whitney U test.

Parameter	Control (N=10)	HYPOTOP (N=61)	p-value
Gestational age (weeks, mean ± s)	38 ± 1	39 ± 2	>0.05
Gender (% male/female)	53/47	54/46	>0.05
Birth weight (g ± s)	3200 ± 500	3300 ± 600	>0.05
Type of delivery (% vaginal/C-section)	79/21	44/56	>0.01
Apgar 1 min (median (min–max))	10 (9–10)	1 (0–5)	>0.01
Apgar 5 min (median (min–max))	10 (10–10)	3 (0–8)	>0.01
Cord pH (mean ± s)	7.31 ± 0.06	6.8 ± 1.0	>0.01
Cord BE (mEq L−1, mean ± s)	−2.00 ± 0.04	−16 ± 7	>0.01
Cord lactate (mmol L−1, mean ± s)	4.5 ± 1.6	14 ± 4	>0.01
Positive pressure ventilation (% Yes/No)	0/100	98/2	>0.01
O_2>21% (% Yes/No)	0/100	97/3	>0.01
Cardiac Massage (% Yes/No)	0/100	56/44	>0.01
Adrenalin (% Yes/No)	0/100	49/51	>0.01

3.3.3 Preparation of stock, working and standard solutions

Five mL of individual stock solutions of pyruvate, lactate, acetoacetate, β-hydroxybutyrate, succinate, fumarate, malate and α-ketoglutarate at a concentration of 1 mmol L^{-1} were prepared in H_2O by weighing of pure solid analytical standards in volumetric flasks. 1 mL aliquots of each standard solution were stored at −20 °C in order to avoid freeze-thawing of standard solutions. 500 µL of a working solution containing 1000 µmol L^{-1} of lactate, 100 µmol L^{-1} of pyruvate, acetoacetate, and β-hydroxybutyrate and 25 µmol L^{-1} of succinate, fumarate, malate and α-ketoglutarate was prepared in H_2O:CH_3CN (1:4 v/v). 10 standard solutions were obtained by serial dilution from the working solution with H_2O: CH_3CN (1:4 v/v). Concentrations were ranging between 3.9 and 1000 µmol L^{-1} for lactate, 0.4 and 100 µmol L^{-1} for pyruvate, acetoacetate and β-hydroxybutyrate and 0.1 and 25 µmol L^{-1} for succinate, fumarate, malate and α-ketoglutarate. On each of the three validation days, 500 µL of spiking solution was prepared in H_2O:CH_3CN (1:4, v/v) containing 10 mmol L^{-1} of lactate, 800 µmol L^{-1} of pyruvate, 400 µmol L^{-1} of acetoacetate and β-hydroxybutyrate and 80 µmol L^{-1} of succinate, fumarate, malate and α-ketoglutarate.

3.3.4 Biomarker analysis of plasma samples

Prior to analysis, standards and samples were derivatized in a two-step oximation-silylation procedure. Blanks were prepared in the same way as plasma samples, replacing the plasma volume with H_2O.

Plasma samples were thawed on ice and homogenized on a vortex mixer during 30 s. 250 µL of cold (4 °C) CH_3CN were added to 50 µL of plasma. Samples were maintained on ice during 5 min followed by centrifugation at 11000 g during 10 min at 4 °C. 200 µL of supernatant or standard solution were transferred to an Eppendorf® tube and 8 and 4 µL of Pyr^{13}C and DMBA, both at a concentration of 1 mM were added, respectively. For the recovery test, spiked samples at three concentration levels (i.e. low, medium and high) were prepared by adding 2.5, 5 or 10 µL of spiking solution in addition to the IS. Samples and standards were evaporated on a SpeedVac concentrator from Genevac Ltd (Ipswich, UK) at 40 °C. Dry residues were suspended in 20 µL of a freshly prepared 4% (w/w) methoxyamine solution in pyridine. Samples and standards were incubated during 90 min at 30 °C on a thermomixer (MKR 13, Ditabis) under agitation. Then, 20 µL MSTFA + 1% TMCS were added. After 30 min of reaction time at 37 °C under agitation, samples and standards were diluted with 40 µL of hexane and placed in capped glass vials for GC-MS analysis. Samples were re-analysed after 1:10 dilution with hexane in case analyte concentrations exceed the established quantification range.

A 6890GC-5973N gas chromatography electron impact quadrupole mass spectrometric (GC-(EI)-Q-MS) system equipped with an autosampler and a HP-5MS column (0.25 mm × 30

m, film thickness 0.25 µm (5% Phenyl)-methylpolysiloxane) from Agilent Technologies (Santa Clara, CA, USA) were employed for sample analysis. The GC was operated at a constant He carrier gas flow at a flow rate of 1.2 mL min^{-1}. The injector temperature was set to 260 °C and 1 µL of sample was injected at a split ratio of 5:1. The oven temperature was maintained at 60 °C during 1 min followed by a linear gradient of 10 °C min^{-1} until reaching 310 °C which were held during 10 min. The total runtime was 36 min.

3.4 Results

3.4.1 Characteristics of the study population

Characteristics of the studied sub-population of the HYPOTOP trial as well as the control group are shown in **Table 3.1**. Between both groups, no significant differences were found for the gestational age, gender and birth weight. In the control group, the percentage of C-section was significantly lower. For all parameters used for the diagnosis of HIE in the delivery room (i.e. Apgar scores, cord pH, BE and lactate), highly significant differences were found as expected. Likewise, for treatments related to the resuscitation procedure (i.e. positive pressure ventilation, cardiac massage and use of O_2 and adrenalin) significant differences between both studied populations were obtained.

3.4.2 Quantification of metabolites in plasma samples

Full scan spectra of individual standard solutions were recorded during method optimization. Based on the results (data not shown), selected ion monitoring (SIM) parameters listed in **Table 3.2** were carefully chosen. Two m/z were recorded for each metabolite for quantification and confirmation.

After completing method optimization, analytical figures of merit were assessed during method validation including precision, selectivity, lower limit of detection (LLOD), lower limit of quantification (LLOQ), sample dilution, carry-over as well as sample and standard stabilities. Method validation was carried out following the recommendations of the US Food and Drug Administration (FDA) guidelines for bioanalytical method validation[15]. However, since the FDA guideline aims at the quantitative analysis of drugs and their metabolites it cannot be directly applied for the measurement of endogenous metabolites due to the lack of blank matrices. This drawback has been circumvented applying recovery tests of spiked plasma samples.

Table 3.2 summarizes the characteristics of the obtained calibration lines for each studied metabolite. When possible, linear regression was employed for calibration lines. However, for acetoacetate, succinate and α-ketoglutarate the use of a second order polynomial fit was necessary in order to cover a sufficiently wide concentration range. With the exception

of lactate, signal normalization employing an IS was necessary. All calibration curves had a coefficient of determination (R^2) of ≥0.990.

Figure 3.2 shows SIM chromatograms obtained during the analysis of a representative sample before and after spiking. It can be observed that in this plasma sample, all studied metabolites were detected with the exception of fumarate. Chromatographic resolution >1 from other unknown matrix compounds was achieved for all metabolites with the exception of malate. High retention time stability (see **Table 3.2**) combined with the use of two characteristic m/z was used to assure the specificity of the signal. In addition, the Retention Index reported in **Table 3.2** was determined for each metabolite and results fitted well with values reported in literature[142]. LLOQs listed in **Table 3.2** were established as the concentration of analyte that can be measured with an imprecision of less than 20% and a deviation from target of less than 20% and taking into account the preconcentration factor of 2.4 achieved during sample processing. The LLOQ was defined as three times the LLOD.

Table 3.3 shows intra- and inter-day accuracy and precision levels given as % recoveries ± standard deviations(s) obtained for standard solutions as well as spiked samples at low, medium and high concentration levels. For standard solutions, imprecision determined at each concentration level did not exceed 15%, except for the LLOQ, where it did not exceed 20%, while at the same time a deviation from the target concentration of less than 15% (20% at the LLOQ) was achieved. Results from the recovery study carried out with spiked plasma samples revealed the magnitude of matrix effect for each studied metabolite. No significant matrix effect was observed for pyruvate, succinate, malate and α-ketoglutarate. In case of the remaining metabolites, recoveries were ranging in a ±30% interval for precision as well as accuracy.

The stability of the studied metabolites in standards and samples was assayed under different conditions and compared to freshly prepared standards and samples. After three cycles of freeze-thawing, concentrations found in standards and samples remained unchanged with recoveries ranging between 81 and 120 and 80 and 114%, respectively. After 24 h at 4 °C, which are typical autosampler conditions, metabolites were stable in standards and plasma samples with recoveries of 86 to 112 and 93 to 115%, respectively, indicating that injection sequences of up to 24 h will not alter the obtained results. No alteration of the measured concentrations was observed (recoveries between 86 and 113%) from the analysis of individual aqueous standard solutions stored during 30 days at −20 °C. Analysis of samples collected and stored at −80 °C for at least two months did not show significant changes in determined concentrations ($N = 5$, $p > 0.05$), indicating that sample storage under the assayed conditions was appropriate, facilitating the application of the method in clinical trials as well as research studies.

Table 3.2 Data acquisition parameters and main figures of merit of the quantification method. Note: RT, Standard Error of Residuals (SER) measured on Day 1; LLOQs were established as the concentration of analyte that can be measured with an imprecision of less than 20% and a deviation from target of less than 20% and taking into account the preconcentration factor of 2.4 achieved during sample processing. The LLOQ is defined as three times the LOD. RI stands for Retention Index calculated as RI = 100 × n + 100 × (tc − tn)/(tn+1 − tn), where c stands for compound of interest, n stands for alkane with n carbon atoms eluting before compound c and n + 1 stands for alkane with n + 1 carbon atoms eluting after compound c. tc, tn and tn+1 represent their respective retention times.

Analyte	IS	m/z Quantification	m/z Confirmation	RT±s [min]	Calibration Range [µM]	$y=ax^2+bx+c$			SER	LLOD [µM]	LLOQ [µM]
						a ± s	b ± s	c ± s			
Pyruvate	Pyr-13C	174		6.00 ± 0.02	0.8-100	-	1.02 ± 0.04	0.0111 ± 0.0016	3	0.11	0.3
Lactate	-	191	117	6.20 ± 0.02	3.9-1000	-	12000 ± 2000	90000 ± 20000	0.3	0.5	1.6
Acetoacetate	DMBA	188	89	7.260 ± 0.003	3.1-100	0.011 ± 0.003	0.018 ± 0.008	-0.0007 ± 0.0005	0.003	0.4	1.3
β-hydroxybutyrate	DMBA	191	117	7.640 ± 0.008	0.4-100	-	0.4 ± 0.3	-0.0001 ± 0.0008	0.7	0.06	0.2
Succinate	DMBA	247	147	9.770 ± 0.002	0.1-25	0.17 ± 0.06	0.310 ± 0.014	0.00090 ± 0.00003	0.08	0.014	0.04
Fumarate	DMBA	245	147	10.200 ± 0.002	0.1-25	-	1.4 ± 0.7	0.0002 ± 0.0002	0.00007	0.014	0.04
Malate	DMBA	147	233	12.130 ± 0.002	0.1-25	-	1.18 ± 0.02	0 ± 0	0.02	0.014	0.04
α-ketoglutarate	DMBA	198	204	13.20 ± 0.05	0.1-25	0.1536 ± 0.0003	0.19 ± 0.04	0 ± 0	0.015	0.014	0.04
Pyr-13C	-	175	-	6.00 ± 0.02	-	-	-	-	-	-	-
DMBA	-	239	-	14.700 ± 0.004	-	-	-	-	-	-	-

Table 3.3 Back-calculated accuracy and precision of standard solutions and plasma sample at three spiking levels. Note: Values within brackets indicate the concentration of each metabolite in the standard solution/spiking concentration. *Measured in 1:10 diluted sample.

Analyte	Standard solutions - % Accuracy±s (conc µM)						Spiked plasma samples - % Accuracy ± s (conc µM)					
	Intra-day (N=3)			Inter-day (N=3)			Intra-day (N=3)			Inter-day (N=3)		
	Low	Medium	High	Low	Medium	High	Low	Medium	High	Low	Medium	High
Pyruvate	94 ± 20 (0.8)	109.4 ± 1.1 (25)	96.8 ± 0.12 (100)	90 ± 6 (0.8)	105 ± 4 (25)	96 ± 3 (100)	92 ± 10 (20)	92 ± 4 (40)	85 ± 1.0 (50)	94 ± 7 (20)	97 ± 5 (40)	89 ± 3 (50)
Lactate	115 ± 18 (3.9)	93 ± 7 (250)	97 ± 11 (1000)	114 ± 3 (3.9)	96 ± 3 (250)	99 ± 4 (1000)	69 ± 10 (250)	96 ± 14 (50)*	95 ± 5 (100)*	83 ± 14 (250)	120 ± 30 (50)*	100 ± 30 (100)*
Acetoacetate	108 ± 7 (3.1)	96 ± 4 (25)	100.9 ± 1.8 (100)	107.3 ± 0.5 (3.1)	102 ± 8 (25)	100.2 ± 1.6 (100)	70 ± 50 (10)	72 ± 18 (20)	69 ± 7 (50)	90 ± 20 (10)	68 ± 18 (20)	71 ± 14 (50)
β-hydroxybutyrate	112.6 ±1.8 (0.4)	103 ± 6 (25)	97 ± 4 (100)	103 ± 9 (0.4)	104 ± 3 (25)	97.8 ± 0.4 (100)	65 ± 17 (10)	69 ± 3 (20)	63 ± 3 (50)	77 ± 12 (10)	80 ± 30 (20)	74 ± 13 (50)
Succinate	119 ± 12 (0.1)	100 ± 2 (6.3)	97.9 ± 0.8 (25)	118 ± 9 (0.1)	102 ± 4 (6.3)	97.2 ± 0.6 (25)	85 ± 10 (2)	93 ± 7 (4)	87.0 ± 0.8 (10)	99 ± 16 (2)	100 ± 20 (4)	95 ± 11 (10)
Fumarate	96 ± 2 (0.1)	87 ± 2 (6.3)	105.9 ± 0.9 (25)	103 ± 6 (0.1)	95 ± 7 (6.3)	102 ± 3 (25)	74 ± 8 (2)	80 ± 6 (4)	62.2 ± 0.17 (10)	80 ± 30 (2)	100 ± 30 (4)	80 ± 30 (10)
Malate	94 ± 3 (0.1)	87 ± 2 (6.3)	104.5 ± 0.7 (25)	109 ± 13 (0.1)	94 ± 7 (6.3)	103 ± 3 (25)	82 ± 11 (2)	87 ± 7 (4)	97 ± 0.5 (10)	94 ± 17 (2)	100 ± 30 (4)	103 ± 17 (10)
α-ketoglutarate	93 ± 16 (0.1)	105 ± 3 (6.3)	96.5 ± 1.1 (25)	100 ± 7 (0.1)	107.6 ± 1.7 (6.3)	99 ± 2 (25)	97 ± 11 (2)	103 ± 9 (4)	98 ± 0.9 (10)	111 ± 12 (2)	111 ± 10 (4)	114 ± 17 (10)

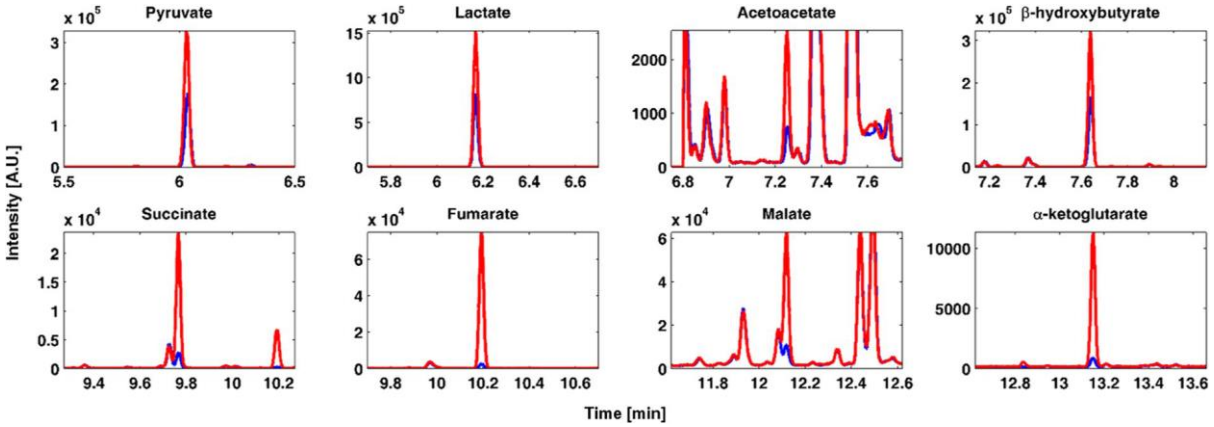

Figure 3.2 Chromatograms acquired during the injection of a plasma sample (blue line) and a spiked plasma sample (red line). Note: for lactate the 1:10 diluted sample is depicted.

3.4.3 Survey of clinical samples

The validated GC-MS method was applied for the analysis of 194 plasma samples drawn after birth at different points in time from newborns enrolled in the HYPOTOP trial. **Figure 3.3** represents metabolite concentrations at different sampling time points. Whereas some metabolites (i.e. acetoacetate, succinate, fumarate and α-ketoglutarate) remained constant throughout the first three days of life, others showed significant changes (two-tailed Wilcoxon rank sum test for equal medians, $\alpha = 0.05$, p-value for each metabolite shown in **Figure 3.3**) with time. Accordingly, lactate, pyruvate and β-hydroxybutyrate concentrations decreased, whereas rising malate concentrations were observed. When comparing metabolite concentrations of newborns treated with TPM or placebo stratified by sampling time points, no significant differences were observed at 24 h, 48 h or 72 h after the administration of the first dose (data not shown).

Furthermore, plasma samples from healthy, term newborns were collected and analysed for the sake of comparison. Main descriptors of the distribution of plasma metabolite concentrations of the control group in comparison to newborns subjected to hypothermia treatment 48 h after the administration of the first dose of TPM are summarized in **Table 3.4**. Significantly lower levels of pyruvate and lactate were found in healthy control newborns, whereas acetoacetate and β-hydroxybutyrate levels were clearly increased (two-tailed Wilcoxon rank sum test for equal medians, $\alpha = 0.05$, p-value for each metabolite shown in **Table 3.4**).

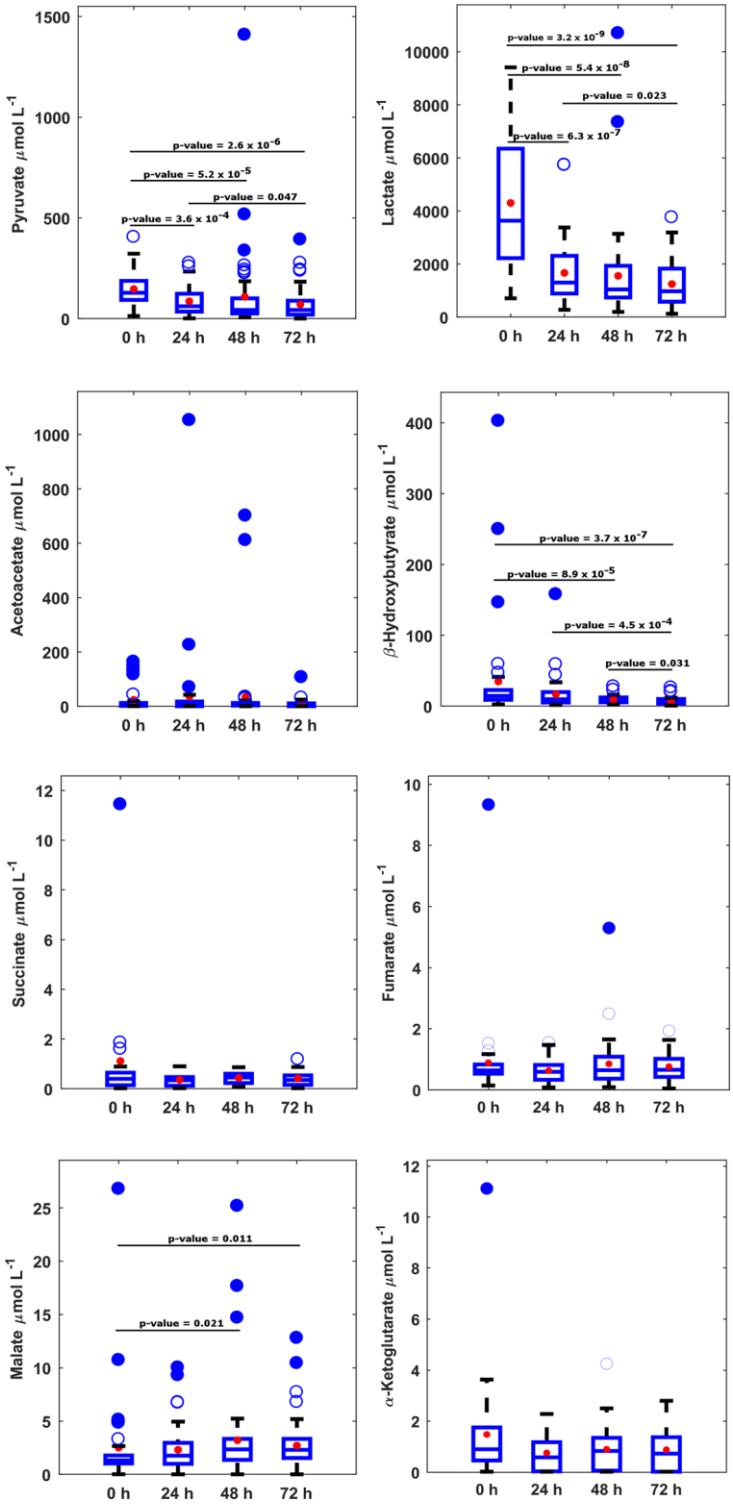

Figure 3.3 Boxplots of metabolite concentrations in plasma samples from newborns included in the HYPOTOP trial. Note: acetoacetate, succinate, malate and α-ketoglutarate detected in 77, 95, 92 and 60% and other analytes in 100% of samples, concentrations < LLOQ were set to ½ LLOQ; p-values calculated employing the two tailed Wilcoxon rank sum test for equal medians.

Table 3.4 Main descriptors of the distribution of concentrations (µmol L^{-1}) in plasma samples collected from the control group (N = 19) and newborns enrolled in the HYPOTOP trial 48 h after the administration of the first dose of TPM. Note: p-value calculated employing the two-tailed Wilcoxon rank sum test for equal medians (α = 0.05).

Metabolite	Control Group				HYPOTOP (48 h)				p-value
	Range P_{10}-P_{90}	Median [µmol L^{-1}]	Mean ± s [µmol L^{-1}]	>LLOQ (%)	Range P_{10}-P_{90}	Median [µmol L^{-1}]	Mean ± s [µmol L^{-1}]	>LLOQ (%)	
Pyruvate	6-5	11	100 ± 200	100	12-200	40	100 ± 200	100	1.6×10^{-5}
Lactate	300-1000	700	700 ± 400	100	500-3000	1000	1600 ± 2000	100	0.002
Acetoacetate	20–700	100	300 ± 300	100	0.7-30	7	35 ± 130	82	1.7×10^{-8}
β-Hydroxybutyrate	13–700	150	300 ± 300	100	4-15	8	9 ± 5	100	4.9×10^{-8}
Succinate	0.13–0.7	0.3	0.4 ± 0.3	95	0.11-0.8	0.5	0.4 ± 0.2	100	0.235
Fumarate	0.5–1.1	0.7	0.7 ± 0.2	79	0.3-1.3	0.6	0.8 ± 0.8	100	0.234
Malate	1.0–8	1.2	3 ± 4	100	0.7-5	2	3 ± 4	92	0.535
α-Ketoglutarate	0.5–2	1.2	1.3 ± 0.6	74	0.02-7	1.2	2 ± 4	81	0.672

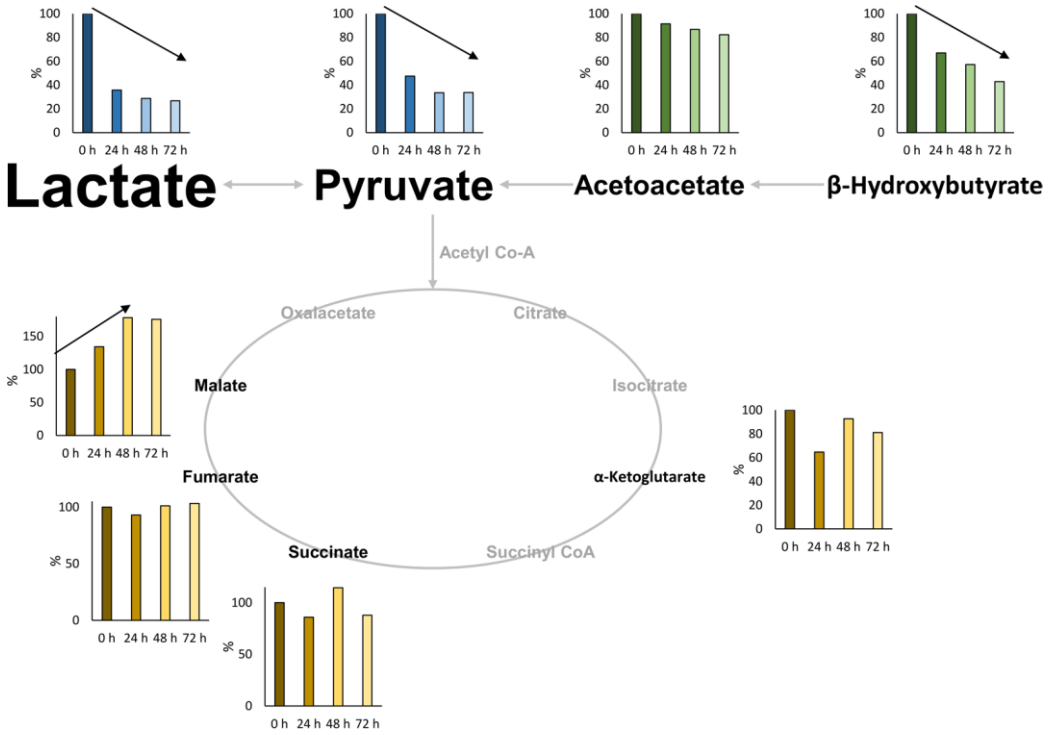

Figure 3.4 Relative changes of metabolites as a function of age of newborns with HIE enrolled in the HYPOTOP trial. Note: median values as a relative measure to median values at t_0; letter size proportional to concentration levels; arrows indicate tendencies.

3.5 Discussion

Evidence linking systemic aerobic metabolism and neurological disease in perinatal asphyxia and subsequent HIE has been reported in animal models[21,91] and in clinical studies[22,84]. Undoubtedly, whole body moderate hypothermia has substantially increased sequel free survival of newborn infants with moderate to severe HIE. A key beneficial physiologic effect of TH after perinatal asphyxia is the associated reduction in cerebral and whole-body metabolic rates by 5–8% for every 1 °C reduction of core temperature. Yet, a

decrease in corporal temperature does not simply provoke a slowdown of the metabolism, but alters diverse functions of many macromolecules simultaneously, including enzyme activities and transport efficiency, suggesting that cooling leads to coordinated effects on multiple regulatory processes[90]. It can therefore be considered to be of utmost importance to study the evolution of key metabolites of metabolic junctions in newborns with HIE undergoing TH in order to gain a better understanding of the physiological response of these babies for optimizing clinical monitoring and treatment. This work aimed at shedding light into the evolution of several key metabolites related to energy metabolism, including lactate, together with pyruvate, the ketone bodies acetoacetate and β-hydroxybutyrate as well as several Krebs cycle intermediates, in newborns with HIE receiving TH during the first 72 hours of life (see **Table 3.4**).

In recent years, several techniques have emerged that allow covering several of those metabolites in a single analysis in biological samples providing appropriate levels of sensitivity, accuracy and precision. In the literature, mainly GC-MS based methods have been reported[143–146]. Alternatively, nuclear magnetic resonance[84], liquid chromatography with fluorescence[147] or MS detection[148,149] or capillary electrophoresis-MS[150,151] have been employed. Here, a GC-MS based approach was developed for the quantification of metabolites in plasma samples from newborns. The validation study proved that the achieved levels of accuracy and precision were adequate for the simultaneous quantification of the set of metabolites in a sample volume of 50 µL.

Concerns about stability of ketone bodies and lactate in plasma samples have been raised and some authors propose the use of stabilizing agents for storage[109,152,153]. In this study metabolite stability in standards and samples was assessed and no significant alterations of concentrations were detected under the tested conditions. Hence, it can be concluded that the addition of stabilizing agents was not necessary and helps simplifying the sample collection process.

Under aerobic conditions glucose is metabolized through the glycolytic pathway and penetrates in the mitochondria where pyruvate is converted to acetyl coenzyme A, enters the tricarboxylic acid cycle and couples to the respiratory chain yielding energy in the form of adenosine triphosphate through oxidative phosphorylation[45]. In capillary blood drawn on day 4 from healthy full-term newborns, lactate and pyruvate were reported to range between 367 and 3245 and 10 and 141 µmol L^{-1}, respectively[154]. In this study, for healthy term newborns at two days of age ranges (percentile 10 to 90) between 300 and 1000 and 6 and 50 µmol L^{-1} (see **Table 3.4**) were obtained for lactate and pyruvate, respectively. During hypoxia-ischemia decreased cerebral perfusion reduces the delivery of oxygen and glucose to the brain. Oxidative phosphorylation is blocked and pyruvate is converted into L-lactate through the anaerobic metabolism[26,155]. Anaerobic metabolism is by far less energy efficient than aerobic metabolism leading to energy exhaustion in brain cells. Initial lactate levels are a useful biochemical marker to assess the degree of birth asphyxia[122,155,156]. It has been demonstrated that lactate levels took

longer to normalize in asphyxiated newborns with moderate to severe neonatal encephalopathy compared with newborns with mild neonatal encephalopathy[157]. In a retrospective case series Balushi et al.[155] suggest that lactate levels during the first 4 days of life should be carefully monitored in asphyxiated term newborns treated with hypothermia in order to optimize handling of those patients and alleviate brain injury. Furthermore, during hypothermia peripheral perfusion is significantly decreased and lactate production may indicate hypoxia at tissue level even in the absence of metabolic acidosis[158]. This study for the first time reports ranges and evolution of lactate values in newborns with HIE during TH. This knowledge is important for the interpretation of lactate values of babies during TH monitored in the neonatal intensive care unit. In the cohort studied in this clinical trial an increase in lactate levels was found in the acute stage and a decreasing tendency with time was observed as expected, revealing a partial restoring of aerobic metabolism upon clinical stabilization as a consequence of the energy saving mechanisms triggered by TH.

Pyruvate showed increased levels during the whole examined time period and concentrations also decreased with time although remaining elevated as compared to the control group at 48 h of life (see **Figure 3.3**). In rat brain tissue, the activation of the anaerobic flux during hypoxia-ischemia and increased glycolysis has been reported with all rate-limiting enzymes activated, being the transport of glucose across the blood-brain barrier the major rate-limiting step of this process. Consequently, the authors found increased pyruvate and lactate levels in brain during hypoxia-ischemia[159]. Here, reported results corroborate the accumulation of pyruvate during hypoxia-ischemia and show the evolution of its concentration profile during TH.

Whereas in adults glucose is essentially the sole energy fuel for the brain, in neonates the ketone bodies acetoacetate and β-hydroxybutyrate derived from ketogenesis in the liver are likely to be as important[90,109,110]. Furthermore ketones have been found to act as neuroprotectors[160]. In neonates suffering from severe HIE depletion of ketones has been reported suggesting that systemic metabolic responses such as ketogenesis may play a key role in preventing neurological injury during asphyxia[143]. Here, significantly higher levels of both metabolites were found in newborns from the control group presumably due to the high fat content of mother's milk consumed by healthy babies. In newborns with HIE, both metabolites showed a decrease with time (although not statistically significant for acetoacetate), which might probably be attributed to their consumption as energy fuels. A recent study[90] revealed that, hypothermia achieves its neuroprotective effects by mediating the cellular acetylation status through a coordinated suppression of acetyl-CoA, a metabolite that resides in metabolic junctions of glycolysis, amino-acid catabolism and ketosis. Both pyruvate and ketone bodies are major sources for acetyl-CoA and were found to decrease under hypothermia conditions in rat brain.

Succinate accumulation has been associated with severe HIE, possibly evidencing HIF-1α mediated neurological injury[84]. Chouchanie et al. showed that the malate/aspartate shuttle and purine nucleotide cycle pathways increase fumarate production, which is then converted

to succinate by succinate dehydrogenase reversal. The selective accumulation of succinate has been described as a universal metabolic signature of ischemia in a range of mouse and rat tissues and is thought to be responsible for mitochondrial ROS production that initiate ischemia-reperfusion injury[161].

The evolution of intermediates of the Krebs cycle has been studied in the HYPOTOP cohort. Determined levels of succinate, fumarate, malate, and α-ketoglutarate did not show statistically significant alterations in comparison to normal control babies. Malate showed an increasing tendency with time, although levels found at 48 h were not different from those found in the control group.

The HYPOTOP trial aimed at the assessment of the neuroprotective effects of the administration of TPM as compared to a placebo. Results presented in this study regarding metabolites involved in central metabolic pathways did not reveal any effect of the administration of TPM on metabolite levels. Ongoing studies will focus on the evaluation of the effect of TPM on other metabolic pathways as well as imaging (MRI) and short-and long-term clinical outcomes of the babies enrolled in the HYPOTOP trial.

This study has some limitations. Hypothermia for HIE has become a universally accepted standard of care. Therefore, energy metabolism derived metabolites in asphyxiated patients without cooling could not be studied and compared to patients undergoing hypothermia treatment. Moreover, patients are recruited shortly after birth in a severe clinical condition and submitted to acute resuscitation manoeuvres and cooled within 6 h after birth. Intriguingly, we did not find changes in energy-linked metabolites of the tricarboxylic cycle. Remarkably, most experimental models lack an active intervention to overcome asphyxia-derived damage. However, in our study human newborns were treated with hypothermia, sedation, analgesia and energy supplies in the form of parenteral nutrition to overcome the negative consequences of HIE. Altogether these interventions attenuated the rate of ATP consumption and enhanced its synthesis during the secondary energy failure phase. This allowed a satisfactory recovery of most organs of the body such as heart, kidney, intestine, muscle, and liver, while brain recovery depended on the initial degree of brain damage during primary energy failure. Determinations were carried out in plasma samples reflecting whole body dynamics and not specifically the brain. However, the value of the present study relates to the possibility of studying a big number of patients exquisitely controlled in a randomized controlled trial and opens a very valuable window for future studies.

In conclusion, this work presents data from a validated analytical approach for the determination of eight metabolites in small volume plasma samples. Furthermore, it reports for the first time the evolution of metabolite levels of newborns suffering from HIE with time during TH. The findings were discussed in the context of previously reported studies in animals and humans shedding light into the effect of TH on metabolite levels in newborns with HIE.

Section II. Oxidative stress assessment

Chapter 4 Oxidative stress biomarkers in the preterm infant

4.1 Abstract

Oxidative stress (OS) has a key role in the pathophysiology of the preterm infant and its proper assessment is an analytical challenge that has been partially addressed during the last decades. A plethora of approaches has been developed and applied to preterm biofluids showing the link between postnatal conditions of preterm infants and OS, giving rise to a set of widely employed biomarkers. However, the vast number of different analysis methods employed hampers the comparison of OS-related biomarkers between studies. In this chapter, we discuss approaches for the study of OS in prematurity considering methodological constraints, the metabolic source of the different biomarkers, and their role in clinical studies.

4.2 Introduction

Preterm birth, as defined by the World Health Organization (WHO), is any delivery that occurs before 37 completed weeks of gestation or fewer than 259 days from the first day of a woman's last menstrual period[31]. Hence, prematurity is a condition that is defined by the failure of gestation to reach a certain duration rather than by the presence of any specific symptoms. The estimated global preterm birth rate for 2014 was 10.6%, ascending to almost 15 million live preterm births worldwide[162]. Although preterm birth is a major complication of pregnancy, even in healthy women with low-risk pregnancies, a fraction of deliveries can be expected to take place preterm and the incidence varies geographically[163,164]. The highest regional preterm birth rates were found in North America, and the lowest in Europe while in absolute numbers, the vast majority of preterm babies were born in Asia and sub-Saharan Africa. The burden of preterm birth is therefore substantial and the incidence of preterm births is increasing[162,165].

For the newborn, preterm birth is a risk factor with an impact on health, welfare, and development even in adult life. On a global scale, preterm birth was the leading cause of death in children younger than 5 years accounting for approximately 16% of all deaths in this age group in 2018 and among newborns, prematurity was responsible for even 35% of deaths

according to the latest UNICEF report[166]. Moreover, prematurity in high-income countries is the leading cause of early neonatal death defined as deaths occurring during the first week after birth[106]. Neonatal outcomes are closely related to the gestational age at delivery and as such, preterm infants can be further classified as late preterm (between 34 and <36 and 6/7 weeks of gestation), moderate preterm (between 32 and <33 and 6/7 weeks of gestation) and early preterm (<32 weeks of gestation)[32]. Also, for gestations <28 weeks the term extreme preterm is generally employed. Even the late preterm has a significantly higher risk of adverse outcomes compared to term infants. Neonatal complications include increased risks of acute (Respiratory Distress Syndrome, RDS) or chronic (Bronchopulmonary Dysplasia, BPD) respiratory conditions, patent ductus arteriosus, necrotizing enterocolitis (NEC), sepsis, retinopathy of prematurity (ROP), intra-periventricular hemorrhage and periventricular leukomalacia and other neurological conditions, as well as feeding difficulties and visual and hearing problems. On the long term, prematurity has been linked to poorer neurodevelopmental outcomes, higher rates of hospital admissions as well as behavioral, socio-emotional, and learning difficulties in childhood. Furthermore premature birth also generates significant health system costs and it causes considerable psychological and financial hardship for affected families[30].

Multiple factors are involved in the etiology of preterm birth. Genetic susceptibility, race and ethnic origin, psychosocial and socio-economic factors, environmental and behavioral factors, as well as infections have all been associated with the development of preterm labor. Despite the myriad of reported risk factors, in most cases, preterm births cannot be associated with a single, specific risk factor, underlining the pathophysiologic heterogeneity of this complex syndrome[30]. Oxidative stress (OS) is thought to underlie several pathological processes relevant to preterm labor, including infection and vascular placental disease[167,168] and it has been repeatedly associated with preterm delivery[168] and pathologies of the preterm infant[169]. Although identifying associations between OS measurements and perinatal outcomes has become popular, knowledge-gaps in describing exact pathways involved in preterm birth and perinatal complications persist.

OS is defined as “the imbalance between oxidants and antioxidants in favor of the oxidants, leading to a disruption of redox signaling and control and/or molecular damage”[43]. The biological redox steady state is a nonequilibrium characterized by a flux through reactions with a specific set point of the redox potential of a given reaction at a certain location within the cell. Deviations from the set point in metabolic steady states are utilized for redox signaling (e.g. controlling gene expression and cell proliferation), while more pronounced deviations towards oxidation may ultimately cause damage to biomolecules or induce apoptosis, and hence modulate, and even disrupt physiological redox signaling[44,170].

Oxidation-reduction reactions in biological systems are mediated by reactive species acting as oxidizing agents, including reactive oxygen species (ROS), reactive chlorine and bromine species, reactive nitrogen species (RNS), reactive sulfur species, reactive carbonyl species, and reactive selenium species. More specifically, ROS are generated from metabolic

redox reactions mostly by the respiratory chain and oxidases, but also by the microsomal cytochrome P450 system and by the immune response[171]. Within ROS, molecules of different chemical nature are comprised, ranging from free radicals (e.g. the hydroxyl radical, $^{\bullet}OH$; superoxide anion, $O_2^{\bullet-}$; nitric oxide, NO) to non-radicals (e.g. hypochlorous acid, HOCl; singlet molecular oxygen; and hydrogen peroxide, H_2O_2), with chemical reactivities that vary by up to eleven orders of magnitude when assayed against a given target molecule[43].

To attain redox homeostasis, oxidant and antioxidant activities are interacting in complex networks. Living cells and organisms counteract oxidative challenge employing multiple strategies, jointly termed 'antioxidant defenses', that can be divided into three distinct protection mechanisms, i.e. prevention, interception and repair. The ensemble of antioxidant defense mechanisms involves enzymatic and nonenzymatic antioxidants, with the former preliminary countering the burden[43]. From a clinical perspective, the most important antioxidant enzymes are superoxide dismutase (SOD), catalase (CAT), glutathione peroxidase (GPx), and glucose 6-phosphate dehydrogenase (G6PD). The most abundant cytoplasmic non-enzymatic antioxidant is glutathione (GSH), a ubiquitous tripeptide (γ-glutamyl-cysteinylglycine). Other relevant non-enzymatic antioxidants are certain proteins (e.g. transferrin and ceruloplasmin), small molecules (e.g. uric acid and bilirubin), and vitamins (e.g. vitamins A, E, and C)[45]. Both, enzymatic and non-enzymatic antioxidant defense mechanisms mature late in gestation and hence, preterm infants are characterized by a limited capacity of response to a pro-oxidant aggression placing these infants at much higher risk of injury[33,34]. In fact, the antioxidant enzyme system is upregulated during the last 15% of gestation, while at the same time non-enzymatic antioxidants are crossing the placenta in increasing amounts. These developmental changes prime the infant for the transition from the relative hypoxia of intrauterine to the oxygen-rich extrauterine environment.

The transition from the intrauterine to the extrauterine world is characterized by a substantial increase in oxygen availability. At birth, placental gas exchange is abruptly interrupted and with the initiation of air breathing, arterial partial pressure of oxygen (PaO_2) rises gradually from 25 to 30 mm Hg (3.3 kPa) in the fetus to 75 to 85 mm Hg (10.5 kPa) in the newborn within the first minutes of life. This adaptation process has been studied in the delivery room employing non-invasive monitoring of the arterial oxygen saturation (SpO_2) with pulse oximetry and it has been shown that healthy term and near-term infants needed several minutes for achieving stable SpO_2 of ≈90%, with a high inter-individual variability. In comparison, late and moderate preterm infants need more time to achieve similar levels of SpO_2, while to date no target ranges for oxygen saturation are available for very preterm infants[36,37]. Physiologic OS caused by the burst of ROS due to an abrupt postnatal increase in oxygen availability is inherent to the normal fetal-to-neonatal transition. Oxidatively modified biomolecules can act as signaling molecules interfering in different pathways. For example, moderate OS at birth acts as a signal to up-regulate γ-cystathionase expression, which is the limiting enzyme involved in the synthesis of L-cysteine, a GSH precursor[38].

Preterm infants frequently need positive pressure ventilation with supplemental oxygen which adds to the risk of suffering from oxidative injury and associated health complications. Recent resuscitation guidelines for asphyxiated infants today no longer recommend the use of 100% O_2 for the resuscitation term and preterm infants[39], and experts rather recommend an initial inspired fraction of oxygen (FiO_2) ranging between 0.21 and 0.3 in dependence of the gestational age of the infant. The FiO_2 should be titrated to achieve target SpO_2 between 80 and 90% at 5 min after birth[40,41]. Controlling FiO_2 and SpO_2 seems to be important as hyperoxia, intermittent hypoxia as well as prolonged hypoxia followed by reoxygenation, especially using high FiO_2, are known to generate excessive amounts of ROS and hence, cause oxidative damage to cell structures[42]. **Figure 4.1** illustrates how the interplay of pro- and antioxidant conditions affects the oxidative balance of the preterm infant, as well as the consequences of pathologic levels of OS.

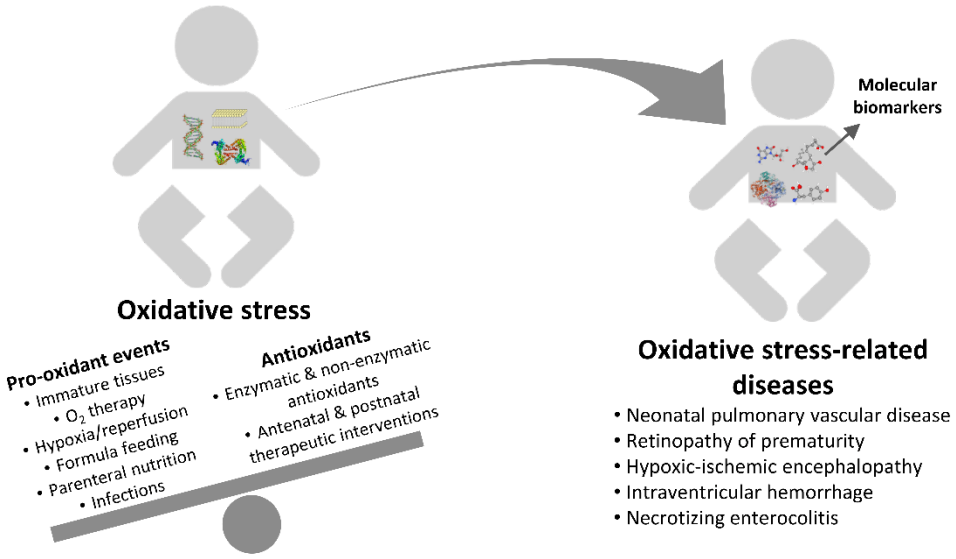

Figure 4.1 The impact of pro- and antioxidant conditions on the oxidative balance and their consequences for the preterm infant.

This chapter will give a comprehensive overview of available molecular biomarkers that have been proven useful for the monitoring of molecular damage and OS in in-vitro and in-vivo studies. Furthermore, current applications of biomarkers and their potential for control and assessment of events leading to a pro-oxidant status as well as interventions aiming at the reduction of OS in preterm infants will be discussed. Finally, the importance of OS biomarkers in the context of OS-related pathologies observed in the preterm infant will be reviewed.

4.3 Biomarkers and methods for the assessment of OS

Since the significance of OS —also referred to as oxygen toxicity prior to the definition of the term OS— in pulmonary, ophthalmologic and cerebral conditions of the preterm infant

was evidenced, OS assessment in prematurity has been carried out adopting different approaches[172–174]. Early clinical and histopathological studies were succeeded in the following decades by an in-depth study of oxygen physiology and biochemistry. Literature reports focused on antioxidant enzymes, non-enzymatic antioxidants, iron and purine metabolisms, and the damage to biomolecules promoted by OS[175,176], thereby expanding the number of described OS biomarkers. Different analytical methods have been employed according to the type of biofluid and studied biomarkers. Preterm biofluids commonly drawn for OS assessment are blood-derived (BD) samples (i.e. whole blood, plasma, serum, hemolysate, and isolated blood cells), urine, and bronchoalveolar lavage fluid (BALF), with each biofluid providing its characteristics regarding composition and stability. BD samples are more delicate in terms of stability as compared to urine samples, and their obtention is considered minimally invasive. Furthermore, in the preterm infant, the blood volume available for laboratory examinations is limited and repeated assessments are troublesome. BALF samples are no longer routinely collected for the assessment of OS in preterm infants and are not accessible, unless excess volumes of complementary examinations are available. In contrast, the non-invasive collection of several milliliters of urine is feasible using sterile plastic bags attached to the skin or cotton pads placed inside the diaper. The availability of higher sample volumes widens the range of pre-analytical procedures that can be employed for clean-up and biomarker preconcentration, thereby enhancing the analytical sensitivity given by the method's limit of detection (LOD). Moreover, the information provided by each biofluid is different: whereas BD samples allow to assess rapid changes occurring, e.g., during acute hypoxia or medical interventions such as resuscitation procedures, urine samples reflect the product of metabolism in a wider time window. **Figure 4.2** gives an overview of the biomarkers discussed in this chapter also indicating the most common biofluid(s) employed for the analysis of each compound.

The approaches available for the study of OS have gradually increased in number and diversity, but to date, no gold standard for OS assessment in preterm infants has been established and the evaluation of OS is not included in standard clinical analysis panels due to the lack of regulatory approval for their use as an in vitro diagnostic (IVD) test. **Table 4.1** gives an overview of diverse methods that have been repeatedly reported in the literature claiming a reliable OS evaluation in the context of prematurity. These methods, many of them available as commercial kits, have enabled a widespread use of OS-related parameters in clinical studies. However, in many literature reports the analytical procedures are a black box obviating methodological details and limitations. In contrast, other works present detailed descriptions of the optimization and analytical validation of specific OS biomarkers.

With the aim of discussing the present state-of-the-art of methods available for OS assessment in prematurity, in this chapter the diverse methodological approaches are detailed. According to the common classification in the OS-related literature[177], the methods are divided into two groups: the assessment of the redox steady state and the detection of biomolecule modifications promoted by OS.

4.3.1 Redox steady state assessment

The evaluation of the redox steady state involves the measurement of oxidant and antioxidant species. The accurate determination of oxidant species in biological matrices is certainly the most challenging OS-related analysis. The main reason is that these molecules are highly reactive, with very short half-lifes ($t_{1/2}$) and extremely low steady-state concentrations[178]. Notwithstanding these difficulties, employing electron paramagnetic resonance (EPR), chemical probes, and colorimetric reactions it is possible to detect and quantify ROS and RNS in biological samples[179]. However, the determination of ROS or RNS concentrations per se without an evaluation of their counterparts, i.e. the antioxidants, does not provide the full picture of the redox steady state. On the other hand, the determination of antioxidant species (i.e. antioxidant enzymes, cofactors, and small molecule antioxidants) is comparatively straightforward. These compounds are several orders of magnitude more stable than oxidant species and their concentrations are higher and hence, they are easily detectable employing different techniques as shown in **Table 4.1** and **Figure 4.2**.

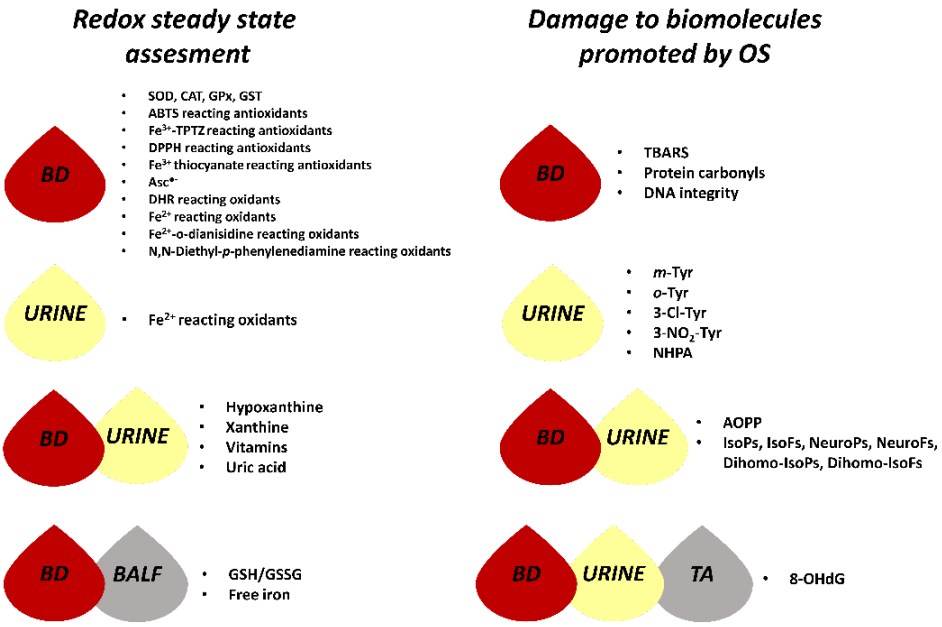

Figure 4.2 Compounds employed in the preterm oxidative stress assessment discussed in this chapter classified by the most usual biofluid employed in their analysis.

Table 4.1 Analytical techniques and assays employed for the evaluation of OS and related compounds.

Type of analytical technique	Analytical technique/assay	Type of OS assessment	Detected compounds	Examples of applications
Spectroscopic	EPR	Redox steady state	Ascorbyl radical	180
	UV/Vis	Damage to biomolecules	AOPP	181–186
Colorimetric	DMPO trapping-EPR	Redox steady state	•OH	187
	TAC (ABTS)-UV/Vis	Redox steady state	ABTS reacting antioxidants	188–192
	DPPH-UV/Vis	Redox steady state	DPPH reacting antioxidants	193
	FRAP-UV/Vis	Redox steady state	Fe^{3+}-TPTZ reacting antioxidants	191,193
	BAP-UV/Vis	Redox steady state	Fe^{3+} thiocyanate reacting antioxidants	194,195
	FOX-UV/Vis	Redox steady state	Fe^{2+} reacting oxidants (ROOH)	196
	TOS-UV/Vis	Redox steady state	Fe^{2+}–o-dianisidine reacting oxidants (ROOH)	188
	d-ROMs-UV/Vis	Redox steady state	N,N-Diethyl-*p*-phenylenediamine reacting oxidants (ROOH)	181–183,194,195,197
	DNPH-UV/Vis	Damage to biomolecules	Protein carbonyls	198–200
Fluorometric	Bleomycin-TBA-fluorescence	Redox steady state	Free iron	201
	DHR probe-fluorescence	Redox steady state	DHR probe reacting oxidants	202
	TBA-fluorescence (TBARS)	Damage to biomolecules	TBARS	198,203,204
	Comet assay	Damage to biomolecules	DNA damage	203
Enzymatic	Kinetic – UV/Vis	Redox steady state	SOD, CAT, GPx, GST	33,198,203–206
	Enzymatic – UV/Vis	Redox steady state	GSH/GSSG	207–210
	FIA-enzymatic assay	Redox steady state	GSH/GSSG	211,212
	Enzymatic-electrochemical	Redox steady state	Hypoxanthine	70
Immunoassay	ELISA	Damage to biomolecules	IsoPs, 8-OHdG, AOPP	180,213
	DNHP derivatization - ELISA	Damage to biomolecules	Protein carbonyls	214–216
Hyphenated separation techniques	LC-UV/Vis	Redox steady state	Hypoxanthine, xanthine, uric acid, vitamins	175,181–183,217–222
	Derivatization-LC-UV/Vis	Redox steady state	GSH/GSSG Iron	184,201,217,223,224
	CE-UV/Vis	Redox steady state	GSH/GSSG	225
	LC-ECD	Damage to biomolecules	8-OHdG	226–228
	Derivatization-LC-fluorescence	Damage to biomolecules	TBARS	214
	GC-MS	Damage to biomolecules	IsoPs, IsoFs, NeuroPs, NeuroFs	223,229
	LC-MS/MS	Damage to biomolecules & redox steady state	GSH/GSSG, IsoPs, IsoFs, NeuroPs, NeuroFs, Dihomo-IsoPs, Dihomo-IsoPs, 8OHdG/2dG, *m*-Tyr, *o*-Tyr, 3-Cl-Tyr, 3-NO_2-Tyr, NHPA	33,49,51–53,103,223,230,231

4.3.1.1 Antioxidant enzymes

The measurement of enzyme activity in BD samples has been the most frequently studied parameter for assessing antioxidant enzymes in prematurity. The enzyme activity is a biologically meaningful parameter as it yields a snapshot of the enzyme expression, amount, and integrity. However, since the units of activity (i.e. units [U] or katals [kat] in the International System of Units) are defined according to the analytical method employed, the comparability of the obtained quantitative information between experiments is limited.

In early determinations of SOD, GPx, glutathione S-transferase (GST), and CAT in samples from preterm infants, classic kinetic colorimetric assays were employed. In these assays, the reaction between the enzymes and selected substrates are spectrophotometrically monitored (i.e. UV/Vis detection)[232,233]. In the SOD activity assay, after the generation of $O_2^{\bullet-}$ in the presence of an oxidizable substrate with colored oxidized form (e.g. $Cyt^{+3}c$ or epinephrine), the rate of inhibition of the oxidation reaction is monitored at the corresponding wavelength, i.e. SOD competes with the oxidizable substrate for the $O_2^{\bullet-}$. For CAT, the activity is determined by measuring the rate of disappearance of H2O2 by monitoring the decrease in the absorbance at 240 nm. GPx activity is assessed coupling the reaction of glutathione reductase (GR) to the GPx reaction. GR consumes NADPH to reduce oxidized glutathione (GSSG) formed by GPx, and therefore the decrease of the NADPH absorbance signal at 340 nm is proportional to GPx activity. The classical method employed for the determination of GST activity is based on the S-conjugated formation between GSH and 1-chloro-2,4-dinitrobenzene (CDNB) that absorbs at 340 nm[232,234,235]. Furthermore, all these enzymatic assays have been improved to increase their sensitivities and specificities modifying the reactions with different substrates, probes, and dyes. The improved methods have been applied in clinical studies involving preterm infants following the published protocols or employing commercial kits[33,198,203,205,206]. Nevertheless, other recent studies in the preterm population employ some of the classical methods[204,205] demonstrating that there is no gold standard for antioxidant enzyme activity assessment. The choice of the method is mainly based on the laboratory's resources and experience rather than method performance.

4.3.1.2 GSH and glutathione disulfide (GSSG)

The analysis of redox pairs (i.e. couples of oxidized/reduced compounds) in biofluids has been employed for the evaluation of the oxidative status of preterm infants with the aim of measuring the overall redox potential. The thiol-disulfide pair GSH/GSSG is the most frequently employed biomarker. However, it should be noted that the primary antioxidant defense is not provided by small molecular antioxidants, but the enzymatic systems[43]. Therefore, the interpretation of the alteration of the GSH/GSSG should be discussed in the context of GSH metabolism and redox steady state. As emphasized elsewhere[43,236], the redox metabolism of the redox cells depends on kinetic instead of thermodynamic constraints. For a

detailed discussion on GSH metabolism, we encourage the readers to inquire a recent review article by Deponte et al.[236].

In early reports on preterm OS assessments, GSH was employed individually or as a sum of oxidized and reduced forms, inaccurately called 'total GSH'[207]. Once sensitivity and selectivity of the employed methods were improved, determinations were extended to the redox pair. GSH and GSSG are relatively stable compared to ROS or RNS, but they are paradigmatic examples of the challenges of OS-related determinations. GSH suffers enzymatic and non-enzymatic degradation during sample handling and storage and it is present in cells and fluids with high compartmentalization with its concentration differing several orders of magnitude depending on the cellular compartment[236,237]. For example, in blood, GSH is contained mainly inside the erythrocytes, whereas in plasma GSH is 200 times less concentrated. In whole blood samples, it has been shown that GSSG is 100 times less concentrated than GSH, and without proper sample treatment, GSH in blood hemolysate is oxidized to GSSG within minutes[237]. GSSG artifacts due to GSH oxidation were first addressed cleverly by Güntherberg et al. employing the Michael addition reaction for the alkylation of the SH group of GSH with N-ethylmaleimide (NEM)[238]. Alternative approaches for an accurate analysis of GSH and GSSG have been proposed elsewhere[237]. However, these procedures are difficult to apply in the clinical scenario, and they are very far from being implemented in a routine laboratory analysis. Even employing the most sophisticated methods, the ranges reported in similar preterm populations differ substantially. The actual evidence stands that an unbiased analysis of GSH/GSSG in blood samples is only possible if NEM is added instantly during the process of sample collection[239].

There are mainly three classes of analytical methods for the determination of GSH including (i) enzymatic methods with spectrophotometry detection, (ii) the use of a separation technique, i.e. liquid chromatography (LC) or capillary electrophoresis (CE), coupled to spectrophotometry or mass spectrometry (MS) detection, and (iii) direct spectroscopic methods. The preferred samples are blood hemolysate and the red blood cell fraction. Also, other samples like BALF have been employed for GSH analysis in preterm infants[207].

The first GSH determinations in preterm infants were based on the enzymatic method called recycling assay. The recycling assay is the most popular enzymatic method for GSH determination and was developed by Tietze in the 1960ies[240]. This method, with several modifications, is implemented in most of the available commercial kits for the determination of GSH and GSSG. The enzyme recycling assay exploits the Ellman's reagent (5-5'-dithiobis [2-nitrobenzoic acid], DTNB) and the enzyme GR. First, DTNB reacts with two moles of GSH generating the yellow compound 5-thionitrobenzoic acid (TNB) (max. absorption at 415 nm) and the glutathione-TNB adduct (GS-TNB). GS-TNB is now 'recycled' back to GSH by GR in the presence of NADPH increasing the assay's sensitivity. With this set-up, the rates of formation of DTNB are proportional to the GSH + GSSG content since GSSG reacts with GR too, yielding 2 moles of GSH. In the original work of Tietze it is also described how to measure the GSSG content by employing NEM to derivatize GSH to GS-NEM thereby avoiding its

participation in the reaction. However, a tedious extraction of the NEM excess is mandatory before carrying out the enzymatic reaction.

The recycling assay has been improved during the years and applied to the determination of GSH and GSSG in preterm infants[207–211]. Modern implementations allow to measure GSSG without extraction by replacing NEM by 2-vinylpyridine and additives such as sulfosalicylic acid (SSA) have been used in order to prevent enzymatic GSH oxidation[237]. Also, a dedicated flow injection analysis (FIA) method was developed based on the improved recycling assay and successfully employed to measure GSH and GSSG in preterm blood[211,212]. This FIA approach allows a straightforward automatization and hence, the measurement of large sample batches.

CE and LC coupled to different detection systems have been employed in several methods for the determination of redox pairs and applied successfully to the determination of GSH/GSSG in preterm biospecimens[33,223,225]. CE-UV has been employed for the analysis of preterm blood samples by Mohamed et al. In this method, whole blood is hemolyzed with metaphosphoric acid and subjected to CE analysis without derivatization detecting GSH and GSSG at 220 nm[225]. In LC methods with spectroscopic detection (absorbance and fluorescence), 2,4-dinitrofluorobenzene (FDNB) or monobromobimane are the most widely employed derivatizing agents[102,241]. The derivatization step is laborious and the stability of GSH, despite attempts of employing NEM or iodoacetic acid[102,241], is adversely affected[237].

LC coupled to tandem MS (MS/MS) is currently the most powerful technique for the determination of GSH and GSSG and their related compounds. LC-MS/MS provides adequate selectivity and sensitivity for a simultaneous multianalyte analysis. As an example, the analysis of a panel of different redox pairs (i.e. cysteine/cystine and homocysteine/homocystine) can be achieved in one analytical run from 100 µL of whole blood employing a recent method validated according to Food and Drug Administration (FDA) guidelines[49]. In this approach, samples are collected in NEM tubes, deproteinized and hemolyzed immediately with perchloric acid followed by centrifugation and stored at –80 °C with tested stability. Finally, samples are analyzed by LC-MS/MS after thawing and dilution in an isotopically labeled internal standard mixture.

Direct spectroscopic assessment has been proposed for the quantification of GSH. Employing Surface Enhanced Raman Spectroscopy (SERS) with a silver colloid and an isotopically labeled internal standard, it is possible to quantify GSH in 2 µL of blood from term newborns[116]. In this set-up, samples are collected in tubes with internal standard and deproteinized and hemolyzed with perchloric acid. Then, the silver colloid is added, and the samples are transferred to a quartz capillary for Raman measurements. This methodology is potentially applicable to the preterm population. Furthermore, it could be tailored to a point-of-care method allowing in-situ GSH determinations in preterm infants.

4.3.1.3 Hypoxanthine and purine metabolites

Hypoxanthine has been assessed repeatedly in order to evaluate OS during hypoxia-reoxygenation[4,217,242,243], as it is an ATP-breakdown product that increases its concentration in situations of oxygen limitation (i.e. hypoxic insult). Accumulated hypoxanthine is a potential generator of oxygen free radicals via endogenous enzymatic reactions, e.g. the conversion of hypoxanthine to xanthine and uric acid by xanthine oxidase, a form of the molybdoflavoenzyme xanthine oxyreductase[35,242]. Cord plasma is the preferred sample type for hypoxanthine determinations, since hypoxanthine assessment has been mainly employed during the study of neonatal resuscitation. Also, hypoxanthine has been monitored to study the inhibition of xanthine oxidase during the administration of purine analogues (e.g. allopurinol)[218].

The relevance of hypoxanthine in the perinatal context was first assessed by Saugstad et al.[70] in 1975 employing an enzymatic assay with electrochemical detection. At that time, this method provided a high advantage over other existing methods since only 150 µl of blood were necessary. Thereafter, different analytical approaches have been used for the analysis of hypoxanthine. The selectivity of enzymatic methods is very limited, and therefore, validated commercial kits available allow the determination of the "hypoxanthine/xanthine" parameter via consecutive enzymatic reactions hyphenated with colorimetric/florescence probes. LC-UV/Vis methods have been developed and validated for the analysis of hypoxanthine, xanthine, uric acid, and other purines in plasma and urine samples from preterm infants[175,181–183,217–222]. In general, the sample processing workflow consists in a centrifugation step followed by dilution prior the LC separation with UV detection of the chromatographic peaks being performed at different wavelengths (i.e. depending on the work considered) in the 220-260 nm interval.

Despite the availability of quantitative methods for hypoxanthine determination, some of the most recent studies do not provide concentration ranges[219,220]. This fact could be explained by the lack of reference ranges and IVD methods and it suggests reproducibility issues. Detailed analytical validation studies in the preterm population are warranted in order to establish a gold standard for hypoxanthine determinations and to validate the corresponding reference ranges.

4.3.1.4 Iron metabolism

The bound-iron transport is altered during a hypoxic event resulting in an iron release causing free radical production (mainly via $^{\bullet}OH$ Fenton reactions) in a cascade where other iron metabolism components are involved[217,242,244]. In addition, preterm infants are poorly endowed with metal transport proteins or they are dysfunctional and unable to keep transition metals bound. Free iron or other transition metals can be found circulating and the analysis of non-bound/bound iron and iron-binding proteins in BD samples have been employed for the assessment of the preterm oxidative status[217,224,242,244–249].

The analysis of free iron was carried out in the preterm population using the bleomycin-detectable iron (BDI) assay. In this method, the degradation of DNA promoted by bleomycin in the presence of iron is exploited. This reaction generates thiobarbituric acid reactive substances (TBARS) that can be quantified (for more information see section 'Lipid peroxidation') providing a signal proportional to the amount of non-protein bound iron (NPBI). The BDI assay has been replaced by more sensitive and selective determinations based on chelator agents and LC separations with UV/Vis detection. The latter approach has been employed for the development and validation of a method for free iron analysis in BD and BALF samples of preterm infants[201]. This analysis yields NPBI, also called non-transferrin bound iron (NTBI), employing a complexation in two steps: first with disodium nitryloacetic acid and, after filtration, with 3-hydroxyl-1-propyl-2-methyl-pyridin-4-one hydrochloride (CP22). The detection of the CP22-Fe complex is achieved by monitoring the absorbance at 450 nm[184,201,217,224].

The serum total iron, transferrin, ferritin, ceruloplasmin, total iron-binding capacity (TIBC), unsaturated iron-binding capacity (UIBC), and transferrin saturation are common parameters analyzed in clinical laboratories. Clinical laboratories employ commercial autoanalyzers for these determinations which are validated according to the regulator's requirements (i.e. approved as IVD test by FDA or European Medicines Agency).

4.3.1.5 Vitamins and carotenes

Within living organisms, the non-enzymatic interception of oxidant species is achieved by low-molecular-mass antioxidants such as vitamin A (retinol and carotenoids), vitamin C (water-soluble ascorbate), and vitamin E (α-tocopherol)[43]. These compounds have been analyzed repeatedly in preterm blood plasma and serum, especially in the context of nutrition, in order to evaluate the antioxidant status[204,208,211,242,250–257]. The first analysis of vitamins A, C, and E in preterm infants was carried out employing classical wet laboratory assays involving laborious sample treatments such as titrations and liquid-liquid extractions with visual, UV/Vis or fluorescence detection[256–258]. However, at present, those methods are considered obsolete and have been replaced by LC-UV/Vis or LC-fluorescence offering an increased sensitivity and specificity[253–255,259]. In fact, the separation of vitamins by LC is frequently employed with hundreds of methods available in the literature as it has been reviewed elsewhere[259]. In particular, the analysis of vitamins in clinical laboratories is carried out employing an LC-UV/Vis method approved as IVD test (e.g. ClinRep® HPLC method from RECIPE Chemicals, Munich, Germany).

Furthermore, the application of LC with MS detection to the analysis of vitamins is extended and several methods are also available, mainly circumscribed to the research context. Prior to LC-MS analysis for vitamin determination in biofluids, typically employed preprocessing steps aim at sample clean-up and analyte preconcentration. The most common approach is liquid-liquid extraction, but alternatives have been described such as ultrasonic assisted filtration, solid phase extraction (SPE), and deproteinization by solvent precipitation

and centrifugation[259]. Despite the myriad of available tools, there are recent clinical studies where classical methods for the determination of vitamins are still employed[199], exemplifying the gap between analytical developments and clinical implementation.

4.3.1.6 Total antioxidant assessment

In order to circumvent drawbacks associated to the determination of specific antioxidants, different methods have been developed to evaluate the totality of all antioxidants present in a redox steady state, i.e. the measurement of the total antioxidant status (TAS) or total antioxidant capacity (TAC). In these approaches, antioxidants present in the sample react with an oxidizing agent coupled with a detection set-up.

The 2,2'-azino-bis(3-ethylbenz-thiazoline-6-sulfonic acid) (ABTS) assay, also known as the Trolox equivalent antioxidant capacity or Erel's assay, is one of the most popular methods employed for the total OS assessment in the preterm population[188–192]. In this method, the oxidation of ABTS by H_2O_2 catalyzed by metmyoglobin yields an $ABTS^{\bullet+}$ cation that is measured by UV/Vis spectrophotometry (750 nm). In the presence of antioxidants originating from the biological sample, $ABTS^{\bullet+}$ is reduced to ABTS decreasing the absorbance indicating the TAS. In order to calibrate the ABTS assay, the Trolox® antioxidant (i.e. an analogue of vitamin E) is commonly employed.

The 2,2-diphenyl-1-picryl-hydrazyl ($DPPH^{\bullet}$) assay is another method based on the landmark work of Blois[260] that has been employed for the TAS evaluation in preterm infants[203]. For this analysis, the stable and colored (max. absorption at 520 nm) free radical DPPH• is reduced to yield a non-radical compound that does not present absorbance at 520 nm. Therefore, the amount of antioxidants that react with $DPPH^{\bullet}$ is proportional to the decrease in the absorption indicating the TAS. The result is usually given as % of DPPH reduction[203].

Other methods for the TAS assessment employed in the preterm population are the ferric-reducing antioxidant power (FRAP)[191,193] and the biological antioxidant potential (BAP)[194,195]. These methods exploit the redox properties of iron complexes. In the FRAP method, antioxidants present in the sample reduce the ferric tripyridyltriazine complex (Fe^{3+}-TPTZ) to the ferrous form Fe^{2+}-TPTZ that absorbs light in the visible spectral range at 593 nm. Likewise, in the BAP method, a colored thiocyanate ferric complex with maximum absorbance at 505 nm is reduced in the presence of the sample's antioxidants, thus decreasing the absorbance. Again, for calibration purposes Trolox or other antioxidants might be employed. However, in the case of FRAP, results are usually expressed as a Fe^{2+} equivalent concentration[193].

TAS methods have been implemented in several patented commercial systems[261] and kits that have been employed in preterm studies[194,195], but none of them has been approved as IVD test.

4.3.1.7 Radicals and other oxidant species

Despite their short $t_{1/2}$, the measurement of reactive oxidant species in biological samples has been demonstrated employing EPR, colorimetric reactions, and chemical probes[179,188,202]. In EPR, the interaction between the magnetic momentum of the unpaired electrons with an external magnetic field is exploited allowing the study of paramagnetic species (i.e. atoms or molecules with unpaired electrons) such as free radicals. This interaction generates different energy levels depending on the chemical environment of the electrons yielding a characteristic radiofrequency absorption pattern, proportional to the radical concentration. EPR has interesting advantages since it is partially non-destructive, sensitive, and only small sample volumes are required. However, the use of this technique is virtually limited to specialized laboratories and frequently it is outside of the researcher's scope[179]. Consequently, only very few examples of applications are available describing the analysis of free radicals in preterm biofluids. The $t_{1/2}$ of $^{\bullet}OH$, $O_2^{\bullet-}$, and $^{\bullet}NO$ is too short to analyze those radicals directly in biospecimens but they can be "trapped" by specific molecules called spin-trappers such as 5,5-Dimethyl-1-Pyrroline-N-Oxide (DMPO). Employing these trappers, the ability of a sample to generate certain radicals under defined conditions can be determined in-vitro. For example, this has been applied to the analysis of bronchoalveolar secretions, where the increase of the •OH formation due to the Fenton reaction was determined[187]. This approach is more specific than total antioxidant assessment methods since it provides information about the antioxidant scavenger system in the presence of certain reactive species. Another application of the use of EPR is the determination of the long-lived paramagnetic species such as the ascorbyl radical ($Asc^{\bullet-}$) in preterm plasma. The $Asc^{\bullet-}$ is the intermediate product of the antioxidant reaction of vitamin C (i.e. the ascorbate ion acts as a reducing agent). This radical is stable with a $t_{1/2}$ of 30-60 minutes in physiological conditions and over longer periods in frozen samples[262]. The ascorbate ion reacts with almost all reactive species to yield $Asc^{\bullet-}$, therefore, its determination offers a specific assessment of the vitamin C scavenger power and the oxidative status of the sample[179].

Further approaches for the assessment of oxidant species employed in preterm infants are based on colorimetric reactions, namely ferrous oxidation of xylenol (FOX), total oxidant status (TOS), and the reactive oxygen metabolites (d-ROMs). In these analyses, in the opposite way to TAS, the oxidant species present in the sample react with reducing agents coupled with a detection system. These assays measure mainly hydroperoxides (ROOH), that are formed in most reactions involving oxidant reactive species and therefore, these methods are also called total hydroperoxide (TH) assays. In FOX, hydroperoxides react with Fe^{2+} to yield Fe^{3+} that in the presence of butylated hydroxytoluene (BHT), xylenol orange, and sulfuric acid produces a colored complex (absorbance max. at 560 nm) which is measured by spectrophotometry and expressed as tert-butyl hydroperoxide (TBH) or H_2O_2 equivalents after calibration with these substances[196,197]. The TOS assay is a modification of FOX employing the Fe^{2+}–o-dianisidine complex instead of Fe^{2+} [188]. The d-ROMs assay is based on the method of Carratelli patented in the 1990is (patent expired)[263] and employs a N,N-Diethyl-p-phenylenediamine dye that

reacts with hydroperoxides[182,194]. It should be noted that some authors incorrectly refer to FOX, TOS, and d-ROMs as methods for the study of the impact of OS on biomolecules, since hydroperoxide can be formed during the reaction of ROS with structural molecules. However, these methods are unable to distinguish between hydroperoxide sources, and therefore, they cannot be considered specific biomarkers of molecular damage.

Chemical fluorescent probes are alternative techniques for the direct assessment of oxidant species. Here, the interaction between the probe and certain oxidant species is coupled with a fluorescent signal that is assessed spectroscopically. One example of the utility of fluorescent probes is the "oxidative burst assay" that was applied to blood samples of preterm infants to evaluate the $O_2^{\bullet-}$ production by neutrophils[202]. In this assay, whole blood is incubated with a dihydrorhodamine123 (DHR) probe and different oxidative burst generators such as E. coli or N-formyl-methionyl-leucyl-phenylalanine (fMLP) are added. The production of $O_2^{\bullet-}$ oxidizes the probe producing the fluorescent dye rhodamine123 that is monitored by flow cytometry (488 nm excitation, 530 nm emission)[264].

4.3.2 Damage to biomolecules by OS

Oxidant reactive species can react with lipids, proteins, nucleic acids, and carbohydrates resulting in damaged molecules with altered functions that may have an impact on signaling and other processes[43]. Consequently, the determination of damaged molecules is used as a measure of OS focused on its effects on metabolism.

4.3.2.1 Biomarkers of lipid peroxidation

The chemical mechanism of non-enzymatic lipid peroxidation has been studied and described in detail recently[265,266]. The main targets are polyunsaturated fatty acids (PUFAs), that have a key role because they are important structural elements of biological membranes where they are esterified within phospholipids. During PUFA peroxidation, the generation of hydroperoxides in a radical chain reaction yields labile bicyclic endoperoxides as one of the first products. These endoperoxides decompose in a plethora of compounds, some interspecific such as malondialdehyde (MDA), and others depending on the PUFA such as isoprostanes/isofurans (IsoPs/IsoFs), neuroprostanes/neurofurans (NeuroPs/NeuroFs), and dihomo-isoprostanes/dihomo-isofurans (dihomo-IsoPs/dihomo-IsoFs) deriving from arachidonic acid (AA), docosahexanoic acid (DHA), and adrenic acid (AdA), respectively[265–268].

In order to analyze the products of lipid peroxidation in preterm infant samples, diverse approaches have been developed for different biofluids. The TBARS assay has been employed repeatedly in preterm studies[198,203,204]. In this method, thiobarbituric acid (TBA) is mixed and heated with the sample in the presence of an acid to form a pink and fluorescent compound (maximum absorbance and emission at 532 and 553 nm, respectively) after the reaction with MDA and other lipid peroxidation products. The analysis of TBARS has also been tailored to

an LC-fluorescence method, employing the TBA reaction as a derivatization step[214]. In both cases, with or without LC separation, the signal is calibrated with MDA and expressed as MDA equivalents. Despite its popularity, the TBARS assay is nonspecific and different substances can interfere[266]. Several attempts have been made to improve the TBARS assay including the use of antioxidants such as BHT in order to avoid sample oxidation during the assay, and n-butanol extractions to increase the sensitivity and to eliminate interfering compounds[203].

A different approach for lipid peroxidation assessment is the direct analysis of isoprostanoids (i.e. IsoPs, NeuroPs, dihomo-IsoPs) and isofuranoids (i.e. IsoFs, NeuroFs, dihomo-IsoFs). These compounds are the most valuable biomarkers since they are end products of lipid peroxidation and reasonably resistant to metabolism (i.e. stable compounds) compared to MDA or hydroperoxides[266–268]. Also, it has been reported that their relative formation is dependent on the oxygen tension since the isofuranoid generation increases at high oxygen concentrations[267,268]. This fact can be exploited measuring the corresponding ratios (e.g. IsoPs to IsoFs). However, the analysis of isoprostanoids and isofuranoids is challenging as in biofluids a vast number of stereo- and regioisomers is present at low concentrations[53,269]. Consequently, sample clean-up and preconcentration are necessary and SPE or affinity columns need to be employed. In fact, lipid peroxidation products can be determined in biofluids in their free forms, but they are mainly present in esterified forms in blood or as glucuronides in urine, thus requiring their enzymatic or chemical hydrolysis during sample preparation. The analysis of these compounds in preterm biofluids has been addressed employing enzyme-linked immunosorbent assays (ELISAs)[262], GC-MS[223], and LC-MS/MS[51–53,103].

F2-isoprostanes derived from AA are the most studied isoprostanoids in preterm infant samples. ELISA methods allowing the determination of 15-F2t-Isoprostane (15-F2t-IsoP), also called 8-isoprostane or 8-iso-PGF2α, are popular since they are implemented in commercial kits and have been employed with preterm blood and urine samples[262,270]. However, ELISA methods present a considerable lack of selectivity due to cross-reactivity issues and therefore, reference methods for accurate IsoP determination rely on the use of GC-MS and LC-MS/MS[267]. GC-MS was initially employed for the determination of IsoPs and IsoFs in preterm urine samples[223] and it is still operational as shown in recent studies[229]. However, GC-MS requires tedious sample processing protocols including SPE extraction and pentafluorobenzyl (PFB)-ester/trimethylsilyl (TMS) derivatization. In contrast, LC-MS/MS methods do not require a derivatization step and they offer adequate selectivity and sensitivity in rapid chromatographic separations allowing the analysis of large batches of samples[51–53,103]. In addition, employing commercial and synthesized standards, quantitative determinations in urine and plasma samples have been satisfactorily developed and validated according to FDA guidelines[52,53]. On the other hand, a semi-quantitative analysis method has been developed for the measurement of total contents of isoprostanoids and isofuranoids[51,103]. It has been demonstrated that within the same analytical run it is feasible to obtain quantitative information of individual isoprostanoids and isofuranoids as well as relative levels of total contents

employing 100 μL of plasma or 600 μL of urine. The straightforward sample processing procedure includes a basic hydrolysis step employing KOH to hydrolyze the esters present in blood samples or an incubation with β-glucuronidase for the breakdown of glucuronides in urine samples. After hydrolyzation, SPE is applied and eluates are evaporated and re-dissolved in a small volume to preconcentrate the compounds before injection into an LC-MS/MS system[51–53,103,230].

4.3.2.2 Biomarkers of oxidative damage to DNA

DNA repair mechanisms of preterm infants, and especially very preterm infants, are immature, and are therefore predisposed to life-long lasting DNA structure alterations if DNA gets damaged in the immediate postnatal period[271]. The main DNA modifications promoted by OS are DNA oxidation, DNA hydrolysis and DNA methylation. Regarding DNA oxidation, the guanine base from the deoxyribonucleoside deoxyguanosine (2dG) is the most susceptible DNA component to modification[43]. Hence, the main products of ROS damage to DNA are the oxidized base 8-oxoguanine and the corresponding deoxyribonucleoside 8-oxo-2'-deoxyguanosine (8-oxo-dG) also known as 8-hydroxy-2'-deoxyguanosine (8-OHdG). LC coupled to electrochemical detection (ECD) was employed in the first characterization of 8-OHdG as an OS biomarker[272] and also in the analysis of preterm samples[226]. LC-ECD methods were improved employing column-switching techniques and they have been employed recently in the preterm population with adequate performance[227,228]. Alternatively, ELISA commercial kits were developed and they have become the most popular 8-OHdG determination method in blood, urine, tracheal aspirates, and other samples from preterm infants[185,199,205,213,273–282]. Recently, LC-MS/MS methods have emerged and have been validated according to FDA guidelines. These methods allow the analysis of 8-OHdG in conjunction with 2dG and other OS biomarkers such as protein oxidation products[223,231,283,284] in a fast, specific, accurate, and straightforward manner, especially in urine samples, where sample processing only consists in a centrifugation and dilution step.

The comet assay or single cell gel electrophoresis is a recently developed technique used for the evaluation of the total DNA integrity, and it has been employed in preterm infant samples[203]. Briefly, an electrophoresis of embedded, lysed cells is run in an agarose coated slide. After staining, the shape of the DNA migration is analyzed by an imaging software and related with the DNA integrity. The comet assay is not specific of oxidative damage, but it can be employed as a screening tool.

4.3.2.3 Biomarkers of protein oxidation

The oxidative damage to proteins is characterized by a variety of modifications of the amino acid side chains by different reactive species[43]. The formation of protein carbonyl derivatives is one of the main protein modifications by OS which may be produced by direct protein oxidation or by the reaction of proteins with previously oxidized compounds. The

protein carbonyl content has been employed as a general biomarker for oxidative damage to proteins[285] and studied in preterm samples repeatedly[198–200,214–216]. The most extended analytical method for the measurement of the protein carbonyl content in blood is based on the Braddy's test. In the classical implementation of this method, the reaction between 2,4-dinitrophenylhydrazine (DNPH) with protein carbonyls generates hydrazones via a condensation reaction that can be monitored spectrophotometrically at 370 nm. The lack of specificity of the DNPH reaction, that can react with other carbonyls present in the sample, as well as the low sensitivity of the method should be highlighted[286]. In order to improve the assay, extractions, filtrations, and washing steps have been included in sample processing protocols. Moreover, the Braddy's test can be used as a preprocessing step of a more sensitive ELISA method for the determination of protein carbonyls which is available in commercial kits. The latter approach has been employed for the determination of protein carbonyls in preterm blood samples[214–216].

The advanced oxidation protein products (AOPP) also called 'dityrosine containing cross-linked protein products' is another parameter employed to evaluate oxidative damage to proteins. The AOPP assessment is based on the early inconclusive finding that certain plasma protein-like species (i.e. 60 and 600 kDa), that are generated under oxidative conditions (i.e. treatment with HOCl), present ultraviolet absorption at 340 nm in acidic medium[287]. According to the original work, these AOPP species can be expressed as chloramine-T equivalents employing the reaction between chloramine-T and iodide to yield iodine monochloride (ICl) that shows an absorbance maximum at 340 nm, like AOPP. This approach is straightforward and it has been applied widely for OS assessment, also in preterm infant samples[181–186,213]. However, due to the lack of specificity, AOPP analysis based on the spectrophotometry assay can be considered obsolete. More recently, it has been replaced by immunoassays, which employ antibodies generated against specific protein oxidation products[288]. Although AOPP remains as a global measure of OS damage to proteins with limited molecular selectivity, different ELISA implementations are available in commercial kits and have been employed for studying AOPP in preterm biofluids[213].

The determination of molecules that are specific to OS mediated protein damage is an alternative approach. It involves the quantitation of meta- and orto-tyrosine (m-Tyr and o-Tyr)[223,231], 3-chlorotyrosine (3-Cl-Tyr)[231,289–292], 3-nitrotyrosine (3-NO_2-Tyr)[214,231,293], and 3-nitro-4-hydroxyphenylacetic acid (NHPA)[293]. The m-Tyr and o-Tyr isoforms are produced via the non-enzymatic hydroxylation of phenylalanine (Phe) by different oxidative species, with $^{\bullet}OH$ playing a key role[294]. 3-Cl-Tyr is generated from the reaction of hypochlorous acid originating from myeloperoxidase (MPO) reactions with para-tyrosine (p-Tyr) residues. Hence, 3-Cl-Tyr is an indicator of the activity of the neutrophils and monocytes that are present in MPO-containing cells[292]. On the other hand, 3-NO2-Tyr is generated by the nitration of p-Tyr promoted by different free radical-based reactions of $^{\bullet}NO$-derived oxidants[295]. Furthermore, NHPA is generated by the metabolization of 3-NO2-Tyr and nitration of para-hydroxyphenylacetic acid (PHPA), a metabolite of tyrosine. Thus, NHPA is also employed as

a biomarker of nitration in conjunction with 3-NO2-Tyr in preterm infant samples[293]. The analytical methods employed for the determination of m-Tyr, o-Tyr, 3-Cl-Tyr, 3-NO_2-Tyr, and NHPA in preterm biofluids are mainly based on LC-MS/MS with straightforward sample processing, especially for urine. As for 8-OHdG, only centrifugation followed by dilution with isotopically labeled internal standard mixture is necessary prior injection into the LC-MS/MS system. Therefore, multianalyte methods have been developed to determine m-Tyr, o-Tyr, 3-Cl-Tyr, and 3-NO_2-Tyr in conjunction with other biomarkers such as 8-OHdG and their corresponding precursors such as p-Tyr, Phe, and 2dG in small amounts of urine samples[223,230,231].

4.4 Perinatal events promoting pro-oxidant status in preterm infants

Preterm infants are exposed to events promoting a pro-oxidant status during, as well as after fetal-to-neonatal transition, that are intrinsically tied to their condition. Furthermore, external factors and medical interventions that need to be carried out in the delivery room and the neonatal intensive care unit do have a significant impact aggravating their pro-oxidant status. This is manifested in the presence of elevated levels of ROS, depletion of antioxidants and oxidative damage to structural molecules that can be assessed and measured employing the methods that have been described in the previous section. In the following, the main stressful perinatal events and the biomarkers employed for confirming the role of OS-related mechanisms in this context are outlined, including intermittent hypoxia and hypoxia/reperfusion, oxygen supplementation, infections, and preterm nutrition[296]. An overview of methods used for assessing the effect of perinatal events on OS and redox status in preterm infants is given in **Table 4.2**.

4.4.1 Hypoxia, reperfusion, and oxygen supplementation

It has been extensively studied that a deficiency in the amount of oxygen (hypoxia) or blood flow (ischemia) reaching the tissues can result in tissue damage and organ dysfunction. In addition, intermittent hypoxia in preterm infants is very common, as it is enhanced by an increased metabolic oxygen consumption and poor respiratory function[297]. Tissue damage is induced by the exhaustion of ATP and, consequently, an inactivation of the ATP-dependent ion pumps in the cells. The damage caused by this inactivation can be reduced by the restoration of blood flow (i.e. reperfusion). However, the expected benefits of early reperfusion on tissue recovery after ischemia have been questioned by several studies[298,299], outlining an intensification of the ischemic injury followed by reperfusion (reperfusion injury).

Table 4.2 Parameters and biomarkers used for assessing the effect of perinatal events on OS and redox status in preterm infants.

Implemented practice	Clinical Trial[1] *(phase, status)*	Targeted disease/event	OS assessment	References
HYPOXIA, REPERFUSION, AND OXYGEN SUPPLEMENTATION				
Resuscitation with 21% O_2	NCT01697904 *(N/A, c)*	BPD	Cord blood TH and BAP; oxidative balance ratio = BAP/TH	195
	NCT00369720 *(N/A, c)*	Preterm delivery	TAS Lipid peroxides	300
Resuscitation with 30% O_2	NCT00494702 *(III, c)*	OS, BPD, inflammation	Blood GSH/GSSG; urinary *o*-Tyr/Phe and 8-OH-dG/2dG; urinary IsoPs and IsoFs	223
iNO (2-10 ppm)	NCT00390065 *(IV, c)*	HRF	Plasma MDA and total GSH; intraerythrocyte GPx and GSR activity	301
NUTRITION				
Human milk fortifier	NCT03214822 *(N/A, c)*	Prematurity	Urinary F2-IsoPs	302
Preterm formula	-	OS	Urinary *o*-Tyr/Phe and 8-OH-dG/2dG	283
	-	OS, ROP, IVH, CLD, NEC	Urinary 8-OH-dG	303
Donor human milk	-	Prematurity	Urinary *o*-Tyr/Phe, 8-OH-dG/2dG, IsoPs and IsoFs	230
Light-protection of TPN solutions	NCT02694510 *(N/A, c)*	OS, BPD, sepsis, NEC, ROP	Urinary peroxides Plasma GSH/GSSG	304
	NCT00611546 *(*N/A, c*)*	CLD, NEC	Urinary peroxides	196
	NCT00328419 *(*N/A, c*)*	BPD, ROP, Sepsis, IVH, PVH, NEC	Urinary peroxides	305
PN rich in ω-3 and ω-6 fatty acids	-	Cholestasis, OS	Plasma CAT, SOD, GPx activity; TBARS	306
PN rich in ω-3 fatty acids	-	OS	Serum vitamin A and E; TAS	307
Trace elements in PN	NCT00611546 *(*N/A, c*)*	CLD, NEC, Sepsis	Urinary peroxides	196
PN rich in Se/ oral Se	NCT02066610 *(*N/A, c*)*	Prematurity	Plasma SOD and GPx activity; plasma amino acids	308
	-	CLD, ROP	Plasma protein carbonyls, MDA, GPx and fatty acids	309,310
PN rich in cysteine	ISRCTN82896385/ NTR243 (NA/c)	OS	Total GSH; plasma and cysteine; GSH FSR and ASR	311

[1] Phase: I, II, III, IV, not applicable (N/A). Status: completed (c).

ROS in general are the main mediators of reperfusion injury due to an imbalance in the ratio between pro-oxidants and antioxidants in the cells and the poor antioxidant system of preterm infants. During reperfusion, the activation of oxidases that metabolize purine derivatives generated as a consequence of the ATP exhaustion, triggers a burst of superoxide and/or hydrogen peroxide that causes a pro-oxidant status. Depending on the tissue and organ of the body, reperfusion injury has a wide diversity of responses. Nevertheless, there are several shared characteristics between organs such as necrosis, apoptosis, impaired microvascular function, and edema[35]. The main sources of ROS in post-ischemic tissue are enzymatic, such as xanthine oxidase, NADPH oxidase, and the mitochondrial electron transport chain and the uncoupled nitric oxide synthase[35]. However, recent studies have been focusing on the interactive activity between enzymatic sources, rather than on a single source. This is supported by the evidence that hydrogen peroxide, the product of all enzymatic sources, can act as an intracellular messenger that mediates redox signaling between ROS production sources[312].

The most frequently evaluated markers of hypoxia are plasma levels of TH, AOPP, hypoxanthine, xanthine, and uric acid. Several studies have shown that levels of these markers are higher in hypoxic preterm infants than in control term groups[182,183,219], demonstrating that OS in hypoxic preterm infants is higher in this vulnerable population.

As preterm infants frequently suffer from hypoxia due to respiratory insufficiency in the delivery room, they need oxygen supplementation and ventilatory support. In addition, their susceptibility to OS increases as lungs mature late in gestation[313,314]. Also, hyperoxia is associated with significant changes to genes related to the cell cycle, antioxidant defense enzymes, DNA repair, and inflammation[315]. Consequently, it is crucial to study the optimum amount of supplemental oxygenation that these infants require. In **Table 4.2**, different clinical trials regarding these interventions are summarized. FiO_2, i.e. percentage of oxygen in the gas mixture administrated to newborn infants, ranges from 0.21 (air) to 1.0 (pure oxygen). Current indications in neonatal resuscitation emphasize the importance of starting respiratory support with a low initial oxygen concentration in order to reduce OS. Several clinical trials have been conducted in this regard (e. g. NCT01697904, NCT00369720, NCT00494702, NCT00355875). In this sense, Kapadia et al.[195] observed that reducing the oxygen concentration for resuscitation in the delivery room ($FiO_2 = 0.21$) decreased TH and increased BAP within 1 hour of administration with respect to pure oxygen ($FiO_2 = 1.0$). Similarly, Vento et al.[223] followed the effect of resuscitation with an initial $FiO_2 = 0.3$ (low-oxygen group, Lox) vs $FiO_2 = 0.9$ (high-oxygen group, Hox) on several OS markers on day 1 and 7. Resuscitation in the Lox group resulted in a decrease in urinary o-Tyr/Phe, as well as 8-OHdG/2dG. Similarly, GSH/GSSG in blood and the plasma inflammatory cytokines TNFα and IL-8 decreased. However, on day 7, levels of lipid peroxidation markers (urinary IsoPs and IsoFs) were similar in both groups. Additionally, Lorente-Pozo et al.[316] studied changes in the DNA methylation profile before and after resuscitation, showing that oxygen loads of >500 mL O_2/kg modified the methylation pattern of different CpG sites involved in cell cycle progression, DNA repair, and oxidative stress. Despite new evidence, current resuscitation guidelines focusing on delivery room oxygen management do not provide clear recommendations for the optimum FiO_2 in preterm infants[317]. Hence, further studies supported by the determination of specific OS-related biomarkers are encouraged.

Alternatively, inhaled nitric oxide (iNO) is a pulmonary vasodilator that plays a major role in regulating vascular muscle tone. iNO therapy has emerged as a potential treatment for hypoxemic respiratory failure in newly born infants[318], and its effects on death, BPD, intraventricular hemorrhage (IVH) or other serious brain injury and on adverse long-term neurodevelopmental outcomes have been reviewed elsewhere[319]. Although safety and efficacy of iNO therapy in the term and late-preterm infant has been demonstrated in two large multi-center randomized clinical trials[320], neonatologists remain cautious regarding its use, since its long-term effects have not been fully studied[321]. Hamon et al.[301] measured plasma MDA, total plasmatic GSH, and intra-erythrocyte GPx and GR activity in infants with hypoxemic respiratory failure (HRF) before (T1) and 24 h after (T2) iNO treatment was initiated within

the first 72 h of life. A control and a reference group comprised of preterm infants with HRF but no iNO treatment, and without HFR, respectively, were enrolled for comparison. Levels of OS markers at T1 were similar in all three groups, whereas at T2 the rise in MDA was blunted in the iNO group compared with controls and was close to the reference infants and GSH was more stable in the iNO group, as there was no difference in GPx and GR activities.

4.4.2 Infections

Preterm infants are at particularly high risk of infections due to diverse factors, such as immaturity of the immune system, prolonged hospitalization, and frequent use of invasive procedures[322]. The activation of the immune system leads to a complex chain of redox processes known as the redox cascade[323]. Cytokines, mainly interleukin (IL)-6 and IL-8, are the compounds involved in the initiation of the sepsis redox cascade. These cytokines activate the nuclear factor kappa-light-chain-enhancer of activated B cells (NF-κB) that triggers the transcription of different genes that activate several stress-related pathways, leading to the generation of superoxide. Moreover, superoxide levels are increased due to the cytokine-induced activation of the NADPH oxidase[324].

Preterm infants often exhibit ambiguous clinical signs that complicate the diagnosis of sepsis and, due to the lack of biomarkers that show enough diagnostic accuracy to rule out sepsis at the time of clinical suspicion, diagnosis still relies on time-consuming microbiological tests. With the aim of developing new diagnostic biomarkers, several studies have been carried out studying differences between septic and non-septic infants. A recent work has compilated the profile of circulating markers of OS and enzymatic and non-enzymatic antioxidant defenses during neonatal sepsis[324]. In septic newborns, circulating levels of TNFα and MDA were shown to be significantly increased in comparison to healthy controls[325,326] along with the activity of the antioxidant enzymes, such as xanthine-oxidase, SOD, and GPx, while peroxidase and uric acid levels were suppressed[325]. In addition, both protein carbonyls and TBARS were increased along with IL-6 and IL-10 levels in patients with sepsis[327].

Interestingly, Cernada et al.[328] analyzed the gut microbiota and mucosal gene expression in septic preterm dizygotic twins and their non-septic twin (control group) to provide with an integrative perspective of host-microbe interactions in neonatal sepsis, concluding that an induction of inflammatory and OS pathways caused dysbiosis in the gut microbiota with predominance of Enterobacteria and reduction of Bacteroides and Bifidobacterium, leading to a global reduction of beneficial anaerobic bacteria.

4.4.3 Nutrition

4.4.3.1 Preterm formula and donor human milk (DHM)

Human milk is considered the gold standard for newborn nutrition and its short- and long-term benefits have been recognized worldwide. Regarding antioxidant defenses provided

through human milk, little is known about its OS and inflammatory profile and its impact on infant's trajectory[329,330]. However, OS has been assessed comparing formula fed infants vs infants on a human milk diet. Ledo et al.[283] compared urinary o-Tyr/Phe and 8-OHdG/2dG of stable preterm infants, that were either exclusively formula-fed or receiving human milk, with respect to a healthy breast-fed term control group. Higher levels of urinary oxidative metabolites in preterm groups than in term control group were found, but in the preterm formula-fed group, levels of o-Tyr/Phe and 8-OHdG/2dG were significantly higher than in the preterm group receiving human milk. These results were in agreement with the findings of Shoji et al.[303] and support the partially protective effect of human milk in counteracting OS in this at-risk population as compared to preterm formula.

On this behalf, Friel et al.[302] compared the redox status between formula-fed preterm infants and those fed with mother's milk fortified with a commercial human milk fortifier (i.e. Enfamil®). The second group was further subdivided according to human milk fortifier content into 0 –19, 20 – 49, and ≥50% groups. Urinary F2-IsoPs levels in formula-fed infants were higher than in infants receiving fortified mother's milk, except for the ≥50% fortification group, which presented the highest levels of these compounds (e. g. NCT03214822).

On the other hand, Parra-Llorca et al.[230] conducted a prospective, longitudinal, observational study with the aim of comparing the protective role of own mother's milk (OMM) vs donor human milk (DHM) against OS, as the latter is subjected to pasteurization. To this end, biomarkers of oxidative damage to DNA (8-OHdG/2dG) and proteins (o-Tyr/Phe), as well as individual and total free radical-mediated lipid peroxidation biomarkers (e.g. IsoPs, IsoFs, NeuroPs, NuroFs, dihomo-IsoPs, and dihomo-IsoFs) in urine samples from preterm infants exclusively fed either with OMM or DHM were measured. The results showed no significant differences in urinary OS biomarkers between groups, which reinforces human milk as a safeguard against OS, even if milk has undergone pasteurization.

4.4.3.2 Parenteral nutrition

Despite the fact that human milk is the best source of antioxidants for newborn infants, the inherent gastrointestinal immaturity of some premature infants requires the administration of parenteral nutrition (PN). Regardless of its benefits, PN is an important source of ROS and, therefore, it has been associated with OS[331]. Total parenteral nutrition (TPN) contains glucose, amino acids, lipids, vitamins and trace elements. These nutrients have the potential to influence the generation of oxidant molecules in the solution. The combination of lipids, which are strong electron donors, vitamin C, and dissolved oxygen acting as an electron acceptor, leads to the formation of lipid peroxides, dehydro-ascorbate, and the production of hydrogen peroxide[45]. Moreover, some of the light-sensitive molecules present in TPN, such as riboflavin, use energy from ambient light to accelerate the reaction between vitamin C and oxygen, increasing the formation of peroxides[332,333]. In this sense, light protection of TPN and coadministration of multivitamin preparations have been thoroughly evaluated in several clinical trials (e. g. NCT02694510, NCT00611546, NCT00328419) (see Table 2) in which urinary

peroxides[196,304,305] and other OS markers (e. g. plasma GSH/GSSG ratio[304]) have been measured. General outcomes of these studies revealed the value of photoprotection of TPN bags reflected in decreasing OS biomarker levels in preterm infants.

Compositional changes of TPN, such as the influence of trace elements, enrichment with ω-3 and ω-6 fatty acids, or cysteine enrichment, have been also studied. In order to assess the impact of these modifications on the antioxidant defenses, CAT, SOD, and GPx activity, lipid peroxidation products (TBARS), TAP, serum vitamin levels, and urinary peroxides have been measured in preterm infants[196,306,307]. In particular, for cysteine enrichment, total GSH and GSH synthesis rates were measured, but no significant changes were observed[311].

4.5 Interventions aiming at the reduction of OS in preterm infants

Preterm infants have profoundly disturbed antioxidant profiles with low levels of both, enzymatic antioxidants such as SOD, CAT, and GPx, and non-enzymatic antioxidants such as vitamin A, C, E, selenium or GSH. Current therapeutic interventions are aiming to reduce impact and severity of OS in preterm infants and they include both, antenatal and postnatal interventions. The former usually consists in drug administration during pregnancy when preterm birth risk becomes evident, whereas different strategies can be established for the latter as discussed in this section. The outcomes of antioxidant interventions and their effect on global redox status have been assessed thoroughly employing different methods and OS biomarkers as summarized in **Table 4.3**.

Table 4.3 Biomarkers used for assessing the effect of antioxidant interventions on OS and redoc status in preterm infants.

Intervention	Clinical Trial[1] *(phase, status)*	Targeted disease/event	OS assessment	References
		ANTENATAL INTERVENTIONS		
Prenatal corticosteroids (betamethasone)	NCT00791687 *(N/A, c)*	RDS, BPD, ROP, IVH	Blood GSH/GSSG; Blood GPx, GSR, GST, SOD, and CAT activity; urinary *o*-Tyr/Phe and 8-OHdG/2dG	33
NAC	NCT03596125 *(II/III, r)*	Preterm delivery	Plasma, RBCs, placenta and human milk GSH and related metabolites;	-
		POSTNATAL INTERVENTIONS		
rh-SOD	-	BPD, CLD	Plasma and urinary SOD activity and concentration	334–336
rh-EPO	NCT00593801 *(N/A, c)*	Anemia of prematurity, BPD, IVH, ROP, NEC	Plasma; RBCs SOD, CAT and GPx activity; plasma ferritin	337
Allopurinol	-	Anemia of prematurity	Serum MDA and ferritin; SOD, CAT and GPx activity	338
	-	PVL	Plasma hypoxanthine; TBARS	218
Melatonin	NCT04235673 *(N/A, not yet r)*	Brain impairment	Plasma MDA	-
	NCT03295162 *(I/II, c)*	Prematurity, Sepsis	Serum MDA	339
Vitamin A	NCT00417404 *(IV, c)*	CLD	Plasma vitamin A	340
			Serum vitamin A	341

Intervention	Clinical Trial[1] *(phase, status)*	Targeted disease/event	OS assessment	References
Vitamin E	NCT01193270 *(I, c)*	Prematurity, IVH	Serum vitamin E	342
Lutein	NCT02068807 *(I/II, c)*	-	Plasma TH, AOPP and BAP	343
	UMIN000007041 *(unk., c)*	TAS	TAS	344
Amino acids		-	Plasma AOPP	345
Surfactants		RDS	Serum TAC and TOS	188

[1] Phase: I, II, III, IV, not applicable (N/A), unknown (unk.), pharmacokinetically assessment (p. a.). Status: completed (c), recruiting (r)

4.5.1 Antenatal interventions

4.5.1.1 Corticosteroids

Antenatal steroid administration between 24 and 34 weeks of gestation is a routine protocol in pregnant women with risk of preterm delivery. The effectiveness in reducing the incidence and severity of many neonatal conditions such as RDS, BPD, ROP or NEC has been demonstrated. Vento et al.[33] established a direct relationship between steroid administration and redox status (GSH/GSSG), antioxidant enzyme activity of SOD, CAT, and GPx, GSH redox cycle enzymes (GR and GST), and markers of oxidative damage to proteins (urinary o-Tyr/Phe) and DNA (urinary 8-OHdG/2dG). Premature infants receiving prenatal corticosteroids had less OS reflected in higher GSH/GSSG, higher expression of SOD, CAT, and GSH redox cycle enzymes, and lower o-Tyr/Phe and 8-OHdG/2dG.

4.5.1.2 N-acetylcysteine (NAC)

NAC has antioxidant properties as it acts as an oxygen free radical scavenger through its thiol-reducing group and it is also a precursor for the synthesis of GSH. Pharmacodynamics and safety of NAC administration during pregnancy have been studied [196]. However, changes in OS markers in relation to NAC administration have not been explored to date. A randomized, single-blinded, placebo-controlled trial that aims to determine if NAC supplementation in women at risk of preterm labor (prior to 34 weeks of gestational age) may correct GSH deficiency in neonatal cord blood is ongoing (NCT03596125). In this study, GSH and related metabolites will be measured in plasma, blood, placenta, and human milk, together with metabolomic and lipidomic fingerprints.

4.5.2 Postnatal interventions

4.5.2.1 Superoxide dismutase (SOD)

SODs are endogenous antioxidant enzymes entrusted with converting reactive superoxide radicals ($O_2^{\bullet-}$) to hydrogen peroxide (H_2O_2) and oxygen (O_2). The effects of recombinant human CuZnSOD (rh-CuZnSOD or rh-SOD) administration to preterm infants on the incidence of BPD was studied by Davis and Rosenfeld throughout the 1990s[334–336]. After a single intratracheal administration of rh-SOD, an increase in both, concentration and activity

of the antioxidant enzyme in serum, tracheal aspirate fluid, and urine during the following two to three days was observed[336]. The authors concluded that rh-SOD administration was safe with no significant increase in any adverse outcome and the likelihood of an improved clinical status when measured at one-year corrected age was presented[335]. However, although cost-effectiveness analysis of rh-CuZnSOD treatment (not commercially available) supports its potential economic benefits[346], to date no results from follow-up studies are available[347].

4.5.2.2 Erythropoietin (EPO)

EPO is a glycoprotein hormone directly involved in the prevention of OS by generating antioxidant enzymes, inhibiting NO production, and decreasing lipid peroxidation [202]. It has been postulated that EPO enhances erythropoiesis. Mobilization of non-heme iron by EPO could inhibit iron-catalyzed reactions, thus reducing OS. For optimal erythropoiesis, recombinant human EPO (rh-EPO) is usually administrated with iron supplementation aiming at reducing anaemia of prematurity[348,349].

Regarding OS markers assessed in studies administrating rh-EPO to preterm infants, Akisu et al.[338] studied the effect on lipid peroxidation and the activity of erythrocyte antioxidant enzymes (e. g. SOD, CAT, and GPx). MDA levels were diminished in the rh-EPO group, but SOD, CAT and GPx activities were reported to be uncompromised. These results were confirmed by Loui et al.[337], who reported no change in trace element values after rh-EPO treatment. Benefits of rh-EPO treatment, however, remain inconclusive to date[350,351].

4.5.2.3 Allopurinol

As previously stated, allopurinol is a xanthine oxidase inhibitor, which is the enzyme involved in the production of superoxide radicals, especially during reperfusion damage. At high doses, allopurinol acts also as chelator agent of NBPI and as a direct free radical scavenger. The administration of allopurinol has been mainly focused on counteracting the neuronal damage of infants with hypoxic-ischemic encephalopathy (HIE). However, clinically important benefits of allopurinol administration for newborn infants with HIE remain unclear[352]. In this sense, a blinded randomized placebo-controlled parallel group multicenter phase III trial aiming at evaluating the effect of allopurinol as an adjuvant to therapeutic hypothermia in infants with moderate and severe encephalopathy is being carried out (NCT03162653)[353].

Regarding preterm infants, a randomized trial evaluated the effect of allopurinol on the incidence of periventricular leukomalacia in this population (24-32 weeks of gestation). In this study, hypoxanthine, oxypurine, allopurinol and its metabolite oxypurinol, as well as lipid peroxidation products (TBARS) were analyzed in plasma cord blood and on days 3 and 7. The results failed to show a protective effect of allopurinol against the prevention of periventricular leukomalacia, what the authors attributed to the concurrence of different factors[218]. Since then,

no additional studies involving allopurinol administration to preterm infants have been reported.

4.5.2.4 Melatonin

Melatonin is an endogenous pineal hormone with antioxidant properties due to its interaction with various ROS/RNS as well as organic radicals (e.g. •OH). Besides its ability to scavenge several radical species, melatonin stimulates the activity of antioxidant enzymes such as SOD and GPx, thus contributing indirectly to OS safeguard mechanisms[354,355]. Preterm infants are deprived of maternal melatonin secretion and for this reason, melatonin administration in this population is of clinical relevance[356]. Pharmacokinetic assessment of melatonin in preterm infants showed that the pharmacokinetic profile of this population differs from that of adults[357]. However, the effect of melatonin administration in infants with reference to OS markers has been scarcely studied[358,359]. Particularly, Gitto et al.[359] observed significantly lower levels of serum inflammatory cytokines IL-6, IL-8, and TNFα as well as nitrite/nitrate levels in preterm newborns with RDS treated with melatonin in comparison with a non-treated control group. Similarly, El-Kabbany et al.[339] studied the effect of melatonin administration by assessing the concentration of MDA at enrolment and 4 and 72 h after the administration of melatonin (e.g. NCT03295162). The concentration of MDA was doubled in the conventionally treated group while reduced in the melatonin treated group 72 h after intervention. Additionally, no side effects following melatonin administration were reported. All these data suggest that melatonin may be a promising drug against OS, which will be contrasted in further clinical trials (e. g. NCT04235673).

4.5.2.5 Vitamins

Vitamins A, C (ascorbic acid), and E (α, β, γ tocopherols) are essential nutrients considered as the most relevant antioxidant compounds obtained through the diet. Mechanisms of action and implications of vitamins are diverse[360], and antenatal and postnatal administration of vitamins has been widely studied[361–363]. Relatively low vitamin levels found in preterm infants compared to term infants have been related with several OS markers (e.g. higher levels of MDA)[204]. However, interventional studies with vitamins in preterm infants lack the measurement of OS biomarkers and focus mainly on establishing vitamin levels in plasma or serum after the corresponding treatment[340–342].

4.5.2.6 Carotenoids

Lutein, β-carotene, zeaxanthin or lycopene are dietary carotenoids with antioxidant properties present in human milk. In particular, the effectiveness of lutein to neutralize oxidants and to modulate inflammatory processes has been demonstrated in several experimental studies[364]. However, few data is available contrasting the effects of lutein supplementation on the antioxidant status of preterm infants[365]. In a pilot randomized trial, Perrone et al.[343]

observed an enhancement on the BAP after lutein supplementation in healthy term infants, jointly with a reduced level of plasma TH. However, results of this trial involving premature infants are not available so far. In this regard, Romagnoli et al.[366] observed that lutein was well-absorbed in the preterm gut after oral administration and that mean plasma lutein increased, whereas zeaxanthin levels remained unchanged. Conversely, Costa et al.[344] determined both, higher levels of plasma lutein and zeaxanthin in the test group with respect to a placebo group, although post-treatment mean changes were not different between groups. TAS was similar in both groups, but a significant positive correlation between TAS and plasma lutein, and between TAS and zeaxanthin was found.

4.5.2.7 Others

GSH constitutes an essential non-enzymatic antioxidant, whose inadequate sourcing is believed to contribute to the redox imbalance in preterm infants. In an attempt to stimulate GSH synthesis, te Braake et al.[345] administrated a mixture of amino acids directly after birth and the degree of OS was assessed by measuring concentrations of AOPP and di-tyrosine. Although they observed an increase in the absolute synthesis rate of GSH, the greater availability of GSH did not decrease OS biomarkers.

On the other hand, Dizdar et al.[188] studied the effect of surfactant administration on preterm infants with RDS by evaluating TAC and total oxidant status (TOS) in blood before and 48 h after surfactant treatment. Based on higher TAC levels and TAC/TOS found in the treatment group, the authors concluded that the oxidant–antioxidant balance shifted in favor of the antioxidant system after surfactant administration.

4.6 Pathologies of preterm infants associated to OS

Preterm infants are especially susceptible to OS and its consequences. Their antioxidant defense mechanisms are immature while at the same time they are exposed to elevated levels of OS due to the premature fetal-to-neonatal transition and the frequent use of supplemental oxygen in cases of respiratory insufficiency[296]. Pathologic levels of OS can affect a wide variety of organs, often simultaneously, and are involved in the pathogenesis and pathophysiology of a series of diseases including HIE[26], IVH[367], ROP[368], BPD[369], persistent pulmonary hypertension of the newborn (PPHN)[370], and NEC[371]. In this sense, biomarkers have been studied and applied in the context of OS-related diseases, thus providing diagnostic and prognostic information for clinicians enabling the monitoring of disease progression and the assessment of the efficacy of protective strategies and procedures in clinical trials. An array of different molecules such as tissue specific proteins, amino acids, lipid peroxidation products, and inflammatory markers have been proposed as candidate biomarkers in the principal diseases that relate preterm infants and OS.

4.6.1 Neonatal pulmonary vascular disease

Preterm birth exposes the lung to ambient oxygen concentrations that are several folds higher than fetal levels and supplemental oxygen is frequently required to support breathing. The importance of the hypoxic intrauterine environment suggests a potential role of transcriptional factor HIF in the regulation of normal fetal and neonatal lung development. Under hypoxic condition, HIF-1α induces expression of several transcriptional factors related to vasoconstriction and angiogenesis such as post-transcriptional regulation of growth factors including vascular endothelial growth factors (VEGFs), EPO, placental growth factor (PGF), and angiopoietins 1 and 2[372,373]. Therefore, formation of the pulmonary vasculature is dependent on vasculogenesis and the formation of new vessels from preexisting ones. However, preterm infants switch prematurely from the intrauterine hypoxic environment to normoxic conditions at birth, affecting the biochemical regulation of angiogenesis, with the lung being one of the organs most affected by OS.

BPD and PPHN are the most common conditions associated with lung development in preterm infants. BPD is a chronic respiratory disease and it is characterized by alveolar simplification on account of interruption of the lung maturation in the saccular and alveolar stage, loss of small pulmonary arteries and decrease of capillary density[374]. PPHN describes the failure of normal pulmonary vascular adaptation at birth and it is characterized by elevated pulmonary vascular resistance and right-to-left extrapulmonary shunting of deoxygenated blood that produces severe hypoxemia[375]. In both pathologies, endothelial nitric oxide synthase (eNOS) plays a critical role in the transition of pulmonary circulation by releasing NO[376,377]. This protein is the promoter of the growth of blood vessels in the pulmonary circulation in utero in response to VEGF. The exposure to hyperoxia increases lipid and protein oxidation products and disrupts normal parenchymal and vascular lung development. Moreover, the relevance of peroxynitrite in the generation of pulmonary vasoconstriction in PPHN via nitrosative stress has been described[378]. Under these circumstances, lipid peroxidation compounds (IsoPs, IsoFs, NeuroPs and NeuroFs) and $Asc^{\bullet-}$ were employed as biomarkers of OS[51,180,379,380]. These studies demonstrated that levels of lipid peroxidation compounds and $Asc^{\bullet-}$ were elevated in preterm infants who developed BPD or PPHN. Moreover, TAC and TOC were measured in a cohort of sixty-nine preterm infants with RDS before and 48 h after surfactant treatment. Hence, Dizdar et al.[188] propose that low TAC/TOC in preterm infants could be associated with increased mortality.

4.6.2 Retinopathy of prematurity

ROP is a common disease of preterm infants which was originally described in 1942 by Terry, who first connected the condition with premature birth[381]. This condition is the result of a two-phase injury characterized by an arrest of normal retinal vascular development associated with microvascular degeneration[382,383]. During the first physio-pathologic stage of ROP, preterm infants are exposed to increased oxygen tension after birth compared to in-utero

conditions. This hyperoxia suppresses VEGF and insulin growth factor-1 (IGF-1), which in turn inhibits normal vascularization. Therefore, the retinal vessel loss is generally attributed to hyperoxia inducing OS through the formation of ROS and the vaso-obliteration caused by apoptosis of vascular endothelial cells[368]. Subsequently, when blood vessel growth stops, the retina matures and the metabolic demand increases, which results in hypoxia and establishes the beginning of the second phase of ROP. In this phase, endothelial cells stimulate the expression of VEGF and EPO in the hypoxic retina, hence promoting a disorganized neovascularization. This pathological condition generates a chaotic growth of vessels, that produces a fibrous scar extending from the retina to the vitreous gel and lens[383,384]. Several parameters such as TOS, TAS, MDA and paraoxonase 1 (PON1) have been proposed as biomarkers of ROP[385]. This study showed that levels of OS correlated significantly with the development of ROP and according with the results, TOS and MDA have been proposed as candidate biomarkers for an early diagnosis of ROP.

4.6.3 Hypoxic-ischemic encephalopathy

The preterm brain is an oxyregulator tissue particularly vulnerable to OS. HIE associated with perinatal asphyxia is a leading cause of mortality and acquired long-term neurologic co-morbidities[26]. If preterm infants are subjected to periods of hypoxia and hyperoxia, this can produce OS affecting the developing brain through the activation of a cascade of biochemical processes. OS initiated by hypoxia/ischemia and reoxygenation produces irreversible damage to vital cellular structures in the brain. Cellular energy exhaustion is followed by excitotoxicity, OS, blood-brain barrier (BBB) dysfunction, neuroinflammation, and mitochondrial damage. Altogether these events cause neuronal cell death in the central nervous system and release neurotransmitters causing a burst of ROS[386,387]. As a result, a series of molecules may arise as possible candidates for biomarkers of HIE. OS biomarkers in preterm infants with HIE have been described in different studies. Buonocore et al.[224] demonstrated that NPBI levels in cord blood were significantly higher in preterm infants with a poor neurodevelopmental outcome than in those with normal outcome. The results suggest that NPBI could be a new early and reliable indicator of HIE. An ongoing clinical trial involving preterm infants (NCT02550054) aims to evaluate the role of EPO to prevent HIE. This trial does also include the assessment of biomarkers of OS through the measurement of stromal cell-derived factor (SDF-1), TNFα, and IL-1.

Table 4.4 Biomarkers of OS employed in preterm infants with different pathologies.

Pathology	Groups	Biomarkers of OS	References
BPD and PPHN	Preterm infants BPD or die (N = 29) vs. No BPD (N = 54)	8-IsoPs and $Asc^{\bullet-}$	180
	254 preterm infants LowOx (N = 133) vs. HiOx *(N = 120)*	IsoPs, IsoFs, NeuroPs and NeuroFs	51
	42 preterm infants PH (N = 21) vs. No PH (N = 21)	Untargeted metabolomic approach and evaluation of oxylipins (PGE1, PGE2, PGF2a, 9- and 13-HOTE, 9-and 13HODE and 9- and 13-KODE).	379
	40 preterm infants with BPD (N = 24) and without BPD (N = 16)	15-F_{2t}-IsoP	380
	69 preterm infants with RSD	TAC and TOC before and 48 h after surfactant treatment	188
ROP	59 preterm infants with ROP (N = 18) and without ROP (N =41)	TOS, TAS, MDA and PON1	385
HIE	384 newborns with GA from 24 to 42 weeks	NPBI	224
	312 preterm infants (estimated)	SDF-1, TNF_{α} and IL-1	388
IVH	Preterm infants receiving antenals steroids (CORT) (N = 37) or not (NOCORT) (N = 20)	GSH and GSSG, CAT, SOD, GST GPX and GSR	33
NEC	332 preterm infants with NEC (N = 29) and no NEC (N = 303)	TH, AOPP, protein carbonyls, NPBI	389
	31 preterm infants with FI	8OHdG	277

4.6.4 Intraventricular hemorrhage

IVH in preterm infants is a common disease associated with neurodevelopmental consequences. The pathophysiology is not well defined, but IVH has been attributed to changes in cardiovascular stability and impaired coagulation due to the immature germinal matrix microvasculature and secondary periventricular venous infarction[390–392]. In cerebral tissue, cyclooxygenase (COX) and prostaglandins play an important role modulating the inflammatory response and blood flow[393] and the expression of COX is induced by hypoxia, hypotension and inflammatory modulators including IL-6, IL-1β, TNFα, and NFκB[394,395]. These compounds lead to an increase of PUFA content, high O2 consumption and microglial activation that increase the generation of OS in the brain[396]. Protein and DNA damage and antioxidant activity were measured in cohorts of preterm infants. Both, o-tyr/Phe and 8OHdG/2dG indicated that neonates receiving high oxygen levels generated more OS[223]. Moreover, in another cohort that aimed the association between antenatal steroids and antioxidant activity and postnatal oxidative stress, the GSH/GSSG was decreased significantly and correlates with hyperoxia and reoxygenation damage. Thus, expression of the antioxidants enzymes SOD and CAT was significantly increased in preterm infants receiving antenatal corticosteroids[33].

4.6.5 Necrotizing enterocolitis

Despite advances in perinatal and neonatal research, NEC is still the most devastating gastrointestinal neonatal disease and remains a leading cause of morbidity and mortality in premature infants with mortality rates reaching approximately 30%[397]. NEC occurs with a frequency of 1 to 3 per 1000 live births and almost 90% of cases affect premature infants[371]. NEC is a multifactorial disease closely related with intestinal tract immaturity. Intestinal mucosa lesions in preterm infants appear due to the contribution of several factor such as hypoxia and nutrition. Furthermore, immunologic studies indicate that Toll Like Receptor 4 (TLR4) has a key role in the pathogenesis of NEC[398–400]. Preterm infants present immature intestinal epithelium, and therefore, excessive signaling in the epithelial TLR4 can occur in response to lipopolysaccharides produced by gram-negative bacteria in the gut[401]. This aggravated pathway activation leads to enterocyte and intestinal stem cell loss by apoptosis[400]. Altogether these events contribute to the release of bacteria and lipopolysaccharides into the blood flow, causing an increase in the production of proinflammatory cytokines, ROS, expression of induced nitric oxide synthase (iNOS) and deregulation of eNOS[402,403]. Hence, the pathogenesis of NEC is intrinsically tied to OS. In different studies, biomarkers of OS such as TH, AOPP, protein carbonyls, NPBI, and 8-OHdG were evaluated in cohorts of premature newborns[277,389]. Concentrations of AOPP, TH, and NPBI were markedly increased in preterm infants who developed NEC. Therefore, these studies could reaffirm the strong correlation between high levels of OS and the development of NEC.

4.7 Conclusions and future applications

During the last decades, an ample array of laboratory methods and commercial assays for the assessment of the redox state and OS damage to biomolecules have been developed. Many methods suit the needs of research studies and clinical trials in preterm infants helping to characterize the impact of pro-oxidant neonatal events and interventions aiming at the reduction of OS in this population. The available methods have also supported the study of common diseases in preterm infants that could be clearly associated to OS. However, due to the diversity of methods available employing different detection principles, the comparison of results between studies is challenging. For a transition from research to routine clinical use, an extensive analytical and clinical validation of laboratory methods and the approval of IVD methods is warranted. This would pave the way for establishing reference ranges in stable preterm infants and subsequently, the evaluation of the usefulness of OS measures as disease biomarkers in different conditions in a routine clinical setting. During this process, preference should be given to non-invasive tests, considering the special circumstances of preterm infants.

Chapter 5 Novel free-radical mediated lipid peroxidation biomarkers in newborn plasma

5.1 Abstract

Oxidative stress derived from perinatal asphyxia appears to be closely linked to neonatal brain damage and lipid peroxidation biomarkers have shown to provide predictive power of oxidative stress related pathologies in situations of hypoxia and reoxygenation in the newborn. The objective of this work was to develop and validate of a comprehensive liquid chromatography tandem mass spectrometry approach for the quantitative profiling of 28 isoprostanoids in newborn plasma samples covering a broad range of lipid peroxidation product classes. The method was developed taking into account the specific requirements for its use in neonatology (i.e. limited sample volumes, straightforward sample processing and high analytical throughput). The method was validated following stringent FDA guidelines and was then applied to the analysis of 150 plasma samples collected from newborns. Information obtained from the quantitative analysis of isoprostanoids was critically compared to that provided by a previously developed approach aiming at the semi-quantitative detection of total parameters of fatty acid derived lipid peroxidation biomarkers.

5.2 Introduction

Fetal life develops in a relatively hypoxic environment with an in utero arterial partial pressure of oxygen (paO_2) of approximately 3.3 kPa. After birth and with the initiation of spontaneous respiratory alveolar-capillary gas exchange, the situation changes abruptly and paO2 saturation in the circulating blood stream rises to approximately 10.5 kPa within the first minutes of life[170]. During the fetal-to-neonatal transition, a burden of reactive oxygen species (ROS) causes physiologic oxidative stress (OS) essential for the activation of specific metabolic pathways which enable an adequate adaptation to the extra-uterine environment[404].

Perinatal asphyxia is characterized by intermittent periods of hypoxia-ischemia and is considered an important cause of early neonatal death and severe neurological sequel such as hypoxic ischemic encephalopathy (HIE) and cerebral palsy[119]. Both hypoxia and reoxygenation can generate ROS exceeding the levels observed under physiologic conditions

during the fetal-to-neonatal transition which may react with non-radical macromolecules such as DNA, proteins and lipids[45]. OS appears to play a key role in neonatal brain damage, with the neonatal brain being especially susceptible because of its high concentration of unsaturated fatty acids, high rate of oxygen consumption, low concentration of antioxidants, and high iron levels[405].

Isoprostanes (IsoPs) are non-cyclooxygenase (COX) derived, prostaglandin-like molecules generated by the free radical-induced peroxidation of arachidonic acid (AA)[406]. Initially IsoPs are produced in esterified form attached to phospholipids, and then released into body fluids in free form. Today, they are considered the gold standard for in vivo assessment of lipid peroxidation due to their stability, selectivity and specificity[267,407]. Following similar mechanisms of non-enzymatic oxygenation, neuroprostanes (NeuroPs) and dihomo-IsoPs are generated from docosahexaenoic acid (DHA) and adrenic acid (AdA), respectively. In addition, when conditions switch to high oxygen tensions, isofurans (IsoFs) and neurofurans (NeuroFs) may be preferentially produced from AA and DHA, respectively[269,408].

The role of lipid peroxidation in pathologies of the neonate has been reviewed[217,409]. It was found that preterm infants with high urinary IsoFs levels in the first days after birth are more prone to develop chronic lung conditions such as bronchopulmonary dysplasia as compared to a control group[51]. In a preliminary case study, the potential of lipid peroxidation byproducts as biomarkers for HIE have been studied and significantly increased concentrations of IsoPs were found for newborns with severe postnatal acidemia[410].

Literature reports three primary analytical techniques for the determination of isoprostanoids in biological fluids and tissue extracts including (i) immunological methods such as radioimmunoassay and enzyme linked immunosorbent assay, (ii) gas chromatography coupled to mass spectrometry (MS) and (iii) liquid chromatography coupled to MS (LC-MS). Results obtained from immunoassays might be potentially biased due to the use of polyclonal antibodies and the high structural similarities between IsoPs and COX-derived prostaglandins as well as other related molecules.

Furthermore this technique is intrinsically limited as it does not allow differentiation between isomers. In contrast, MS-based assays are widely accepted as the most accurate methodologies[267,411,412]. LC coupled to tandem MS (LC-MS/MS) presents interesting advantages over GC-MS. It does not require long derivatization processes thus reducing the possibility of introducing additional sources of error. Moreover, the use of Ultra-high Performance Liquid Chromatography tandem mass spectrometry (UPLC-MS/MS) involves rapid chromatographic separations. UPLC-MS/MS offers suitable selectivity and sensitivity combined with a high sample throughput for which it has gained popularity recently in this field, especially for clinical applications[51,55,413].

In clinical studies, the choice of the biological fluid is of major concern. Urine samples are suitable for a long-term survey of lipid peroxidation biomarkers of up to several days or

weeks after an insult or intervention and allow repeated sampling, but the main pitfall is its limited time resolution and it might not be optimal when the objective is the analysis of early, fast responses in e.g. time-critical therapies. Conversely, blood reflects the dynamic metabolic response immediately improving time resolution. On the other hand, blood collection is an invasive procedure and the use of small volumes is mandatory, especially in the field of neonatology.

The objective of this work was the development and validation of a comprehensive analytical approach for isoprostanoids profiling in human plasma samples covering a broad range of lipid peroxidation product classes derived from AA, DHA and AdA. The method was developed to fulfill specific requirements to enable its clinical application in neonatology such as addressing the challenge of limited sample volumes, straightforward sample processing and high analytical throughput. In order to assess the usefulness of the developed method, it was employed for the analysis of 150 plasma samples collected from newborns. Information obtained from quantitative analysis was critically compared to that provided by a previously developed approach aiming at the semi-quantitative of total parameters of IsoPs, IsoFs, NeuroPs and NeuroFs, proposed as disease associated biomarkers in clinical applications.

5.3 Material and methods

5.3.1 Standards and reagents

Commercially available IsoPs (2,3-dinor-15-F_{2t}-IsoP, 15-keto-15-E_{2t}-IsoP, 15-keto-15-F_{2t}-IsoP, 15-epi-15-F_{2t}-IsoP, 15-E_{2t}-IsoP, 15-F_{2t}-IsoP), prostaglandins (PGs) (PGE_2, $PGF_{2\alpha}$, 2,3-dinor-11β-$PGF_{2\alpha}$, 11β-$PGF_{2\alpha}$, 6-keto-PGF_{1a}), dihomo-PG (1a,1b-dihomo-PGF_{2a}) were purchased from Cayman Chemical Company (Ann Arbor, MI, USA), with purities of 95% as well as deuterated internal standards (IS, PGF_{2a}-d4 and 15-F_{2t}-IsoP-d4) with purities of 98% and incorporation of 99% deuterated form (d1-d4); <1% d0.

Other analytical standards employed were F2-IsoPs (5-F_{2t}-IsoP, 5-epi-5-F_{2t}-IsoP, 15-epi-2,3-dinor-15-F_{2t}-IsoP), F4-NeuroPs (4-F_{4t}-NeuroP, 4-epi-4-F_{4t}-NeuroP, 10-epi-10-F_{4t}-NeuroP, 10-F_{4t}-NeuroP, 14(RS)-14-F_{4t}-NeuroP), F4-NeuroF (4(RS)-ST-Δ^5-8-NeuroF), F2-dihomo-IsoPs (17-F_{2t}-dihomo-IsoP, 17-epi-17-F_{2t}-dihomo-IsoP, Ent-7(RS)-F_{2t}-dihomo-IsoP), and F2-dihomo-IsoFs (17(RS)-10-epi-SC-Δ^{15}-11-dihomo-IsoF, 7(RS)-ST-Δ^8-11-dihomo-IsoF) synthesized at the Institut des Biomolecules Max Mosseron (Montpellier, France) according to previously published procedures[414–421], with purities of 99% and all physical data reported in those published articles confirmed the new structures[414–421].

Potassium hydroxide (KOH) was from Sigma Aldrich Química SA (Madrid, Spain). LC-MS grade solvents (methanol CH_3OH, ethanol, heptane and acetonitrile CH_3CN) were purchased from J.T. Baker (Phillipsburg, NJ, USA). Formic acid (HCOOH, 98%) and ethyl

acetate (analytical grade) were from Panreac (Barcelona, Spain). Ultrapure H_2O was generated on a milliQ system from Merck Millipore (Darmstadt, Germany).

5.3.2 Preparation of stock, working, and standard solutions

Individual stock solutions of solid pure analytical standards at a concentration of 1 mmol L^{-1} were prepared in ethanol. Individual stock solutions of 15-epi-15-F_{2t}-IsoP, 1a,1b-dihomo-PGF_{2a}, and 2,3-dinor-15-F_{2t}-IsoP standards were purchased in methyl acetate or at concentrations of 2.8, 2.6 and 0.3 mmol L^{-1}, respectively. A 5 mmol L^{-1} working solution of the set of target analytes was prepared by mixing adequate volumes of the individual stock solutions followed by evaporation to dryness and dissolution in H_2O (0.1% v/v HCOOH, pH 3):CH_3OH (85:15 v/v). Likewise, an IS working solution containing both IS (PGF_{2a}-d4 and 15-F_{2t}-IsoP-d4) at a concentration of 20 mmol L^{-1} each was prepared. Aliquots of the obtained stock and working solutions were stored in capped amber vials at -20 ˚C to avoid repeated freeze and thaw cycles. Standard solutions used for calibration were prepared on each measurement day from the working solution by serial dilution in H_2O (0.1% v/v HCOOH, pH 3):CH_3OH (85:15 v/v).

5.3.3 Population

After obtaining informed consent, twenty neonates ≥35 weeks gestation with HIE who qualified for cooling were recruited in a dose-finding, phase 0 clinical trial of N-acetylcysteine (NAC) and calcitriol. This study was approved by the Institutional Review Board at the Medical University of South Carolina, Charleston. Neonates with stage 2 or 3 HIE were enrolled within 6 h of birth. They received hypothermia (33 ˚C rectal temperature) for 72 h and intravenous administration of NAC 25 or 40 mg/kg by infusion over 1 h, q 12 h, and calcitriol 0.05 mcg/kg q 12 h from enrollment (3e6 h of age) until discharge or 10 days of life. Due to elevated ionized calcium in several subjects, calcitriol dose was decreased to 0.03 mcg/kg q 24 h for subjects 11-20. Characteristics of the HIE neonates are presented in **Table 5.1**.

Blood was collected in sodium EDTA tubes, centrifuged, and plasma was frozen at -80 ˚C within 15-20 min of collection. Samples were obtained before, 0.5 h, 1 h and 11.5 h after the 1st dose, and peak samples 1 h after the 3rd (24-30 h) dose during hypothermia. A second set of blood samples were obtained during normothermia before, and 0.5 h, 1 h and 11.5 h after the 10th or 11^{th} NAC dose on day of life 5-6 (>24 h after rewarming). Aliquots of plasma remained frozen at -80 ˚C and shipped on dry ice without thawing until analysis.

Table 5.1 Characteristics of the studied population.

Variable	Value
Male/female	11/9
Mean gestational age ± s [weeks]	38.3 ± 1.7
Mean birth weight ±s [g]	3300 ± 500
Vaginal/C-section	5/15
Mean cord pH ± s	6.9 ± 0.2
Mean base excess ± s [mEqL^{-1}]	-17 ± 9
Mean lactate ± s [mM]	9 ± 5
Mean Apgar score ± s at 1 min	1 ± 1
Mean Apgar score ± s at 5 min	3 ± 2
Mean Apgar score ± s at 10 min	5 ± 2

5.3.4 Processing of plasma samples

Samples were processed following previously described methods[51,52,54,55,422] with slight modifications. Briefly, 100 mL of plasma were thawed on ice, homogenized and 3 mL of IS working solution (20 mmol L^{-1}) were added. For basic hydrolysis 100 mL of KOH (15% w/v) were added to each sample followed by incubation for 30 min at 40 ˚C with gentle agitation in a WSB-18 water bath from Witeg (Wertheim, Germany). Thereafter, samples were diluted with 700 mL of H_2O:CH_3OH:HCOOH (82.6:14.6:2.8 v/v), homogenized on a Vortex mixer for 5 s and kept on ice for 10 min followed by centrifugation at 16000 g for 10 min at 4 ˚C.

Solid phase extraction (SPE) employing Discovery® DSC-18 SPE 96-well plates from Sigma-Aldrich (St. Louis, MO, USA) was carried out as follows: SPE cartridges were conditioned with 1 mL CH_3OH followed by 1 mL H_2O (0.1% v/v HCOOH, pH 3) and then diluted samples were loaded into the SPE wells. The washing steps included rinsing of each well with 1 mL H_2O (0.1% v/v HCOOH, pH 3) and 500 mL heptane. Cartridges were dried with room air and sample extracts were eluted with 4 100 mL ethyl acetate which were subsequently evaporated using a miVac centrifugal vacuum concentrator from Genevac LTD (Ipswich, UK). Sample extracts were dissolved in 60 mL of H_2O (0.1% v/v HCOOH, pH 3):CH_3OH (85:15 v/v) prior to UPLCMS/MS analysis.

5.3.5 UPLC-MS/MS analysis

UPLC-MS/MS analysis was carried out employing an Acquity-Xevo TQS system from Waters (Milford, MA, USA) using negative electrospray ionization (ESI$^-$). Instrumental conditions were selected as follows: capillary voltage was set to 2.9 kV, source temperature was 150 C, desolvation temperature was 395 ˚C and nitrogen cone and desolvation gas flows were set to 150 and 800 L h^{-1}, respectively. Dwell time was set to ensure a minimum of 10 data points per peak. Separation conditions were selected to achieve appropriate chromatographic retention and resolution by using a Waters BEH C18 reversed phase column (2.1 100 mm,1.7 mm) and a H_2O (0.1% v/v HCOOH):CH_3CN (0.1% v/v HCOOH) binary gradient. Flow rate, column temperature and injection volume were set at 450 mL min^{-1}, 45 C and 9 mL, respectively. The gradient with a total run time of 7.0 minwas as follows: from 0.0 to 0.1 min

15% v/v CH_3CN (0.1% v/v HCOOH) (i.e. channel B); from 0.1 to 5.0 min %B increased up to 40%; from 5.0 to 6.0 min %B increased up to 75%; between 6.0 and 6.15 conditions were held constant at 75% B followed by the return to initial conditions (i.e. 15% B) between 6.15 and 6.25 min; conditions were maintained for 0.75 min for system re-equilibration.

MS detection was carried out by multiple reaction monitoring (MRM) employing the acquisition parameters summarized in **Table 5.2**. The UPLC-MS/MS system was operated employing MassLynx software version 4.0 from Waters. Cone voltages and collision energy values were optimized by analysis of individual 1 mM standard solutions in the UPLC-ESI-MS/MS system. For quantification, linear regression curves with 1/x weighting were calculated including signal normalization with an IS. Concentrations found in plasma samples falling outside the calibration range or showing a shift in retention time bigger than ±0.05 min in comparison to standard solutions were not further considered. For total parameters (total IsoPs, IsoFs, NeuroPs and NeuroFs), MRM detection was carried out as previously described[51]. Here, relative signal intensities normalized using the IS signal were determined instead of absolute concentrations in order to avoid the need of pure analytical standards. Total parameters were considered when the area was >3 times the signal of a blank.

On each measurement day, prior to the launch of the analytical sequence, a system suitability test was carried out including the following criteria: (i) a backpressure ripple <2% at the beginning of the chromatographic run; (ii) absence of the IS peak in a non-spiked plasma sample; (iii) absence of analyte peaks during a blank injection (i.e. H_2O (0.1% v/v COOH)); (iv) appropriate sensitivity and precision during triplicate analysis of a standard solution at the LOQ. Accordingly, %RSD of peak area values should be ≤ 25% and the signal-to-noise ratios ≥9 for each studied analyte; and (v) retention times within ±0.05 min between consecutive batches.

Blank samples and solvent blanks were analyzed at the beginning of the sample batch, after a high concentration standard and repeatedly along the batch in order to check for contamination of the analytical system (i.e. column, mobile phase additives etc.), carryover and cross contamination. A representative quality control (QC) plasma sample was analyzed repeatedly throughout sample batches to detect deviations in accuracy and/or precision. An analysis batch was accepted if at least 75% of the values found for the QC standards were within ±25% of their respective nominal values.

5.3.6 Method validation

During method validation, figures of merit of the sample preparation and measurement procedure including the linearity range, precision, accuracy, selectivity, limit of detection (LOD), limit of quantification (LOQ) and carry-over were assessed. The method validation was based on the US Food and Drug Administration (FDA) guidelines for bioanalytical method validation[15]. However, the FDA guideline aims at the quantitative analysis of drugs and drug metabolites in biological matrices and it cannot be directly applied to the analysis of

endogenous metabolites due to the lack of blank matrices. To circumvent this, accuracy and precision of the method were established by calculating relative recovery values. Therefore, a non-spiked pooled plasma sample was analyzed by triplicate on each validation day. Duplicate analysis of standards at three concentration levels and triplicate analysis of plasma samples spiked before and after SPE at two concentration levels on two measurement days were carried out. The percentage of relative standard deviation (RSD) of replicate standards within one validation batch (intra-day) and between validation batches (inter-day) were calculated to assess precision. Inter-day and intraday extraction yields were calculated comparing absolute peak areas from samples spiked before and after SPE and the matrix effect was determined by comparing absolute peak areas of samples spiked after SPE to pure analytical standards. Furthermore, the method's overall accuracy and precision for the determination of the studied compounds in plasma were evaluated at two concentration levels by comparing the relative response of spiked samples and pure analytical standards. The LOD and LOQ levels were estimated as the concentrations providing a signal-to-noise ratio of 3 and 10, respectively also providing precision and accuracy levels within the FDA recommended ranges. Selectivity was evaluated by analyzing blanks and a non-spiked pooled plasma sample. The carry-over was determined from the analysis of a blank sample after to the measurement of a concentrated standard solution.

5.4 Results and discussion

5.4.1 UPLC-MS/MS method for the determination of lipid peroxidation biomarkers

Ionization and fragmentation conditions for the MS/MS quantification for the set of 28 analytical standards were optimized by analysis of 5 mmol L^{-1} individual standard solutions. Chemical structures of the studied compounds are shown in **Supplementary figure AI.1.1** and the selected MS/MS acquisition parameters are summarized in **Table 5.2**. Chromatographic conditions were also optimized employing a 5 mmol L^{-1} working solution. Specificity of the MRM transitions was assessed by analyzing a set of individual standards employing the proposed LC-MS/MS procedure, which included the recording of 16 MRM transitions. **Figure 5.1** displays representative LC-MS/MS chromatograms extracted from the analysis of a spiked plasma sample. As shown in the figure, symmetric peak shapes were obtained for the total of 23 resolved peaks, all eluting in a retention time window between 3.71 and 6.06 min. Nonetheless, due to high structural similarities, a reduced number of lipids showed a significant chromatographic and MS overlap that could not be resolved neither by MS/MS nor by changing the chromatographic conditions (see **Table 5.2**).

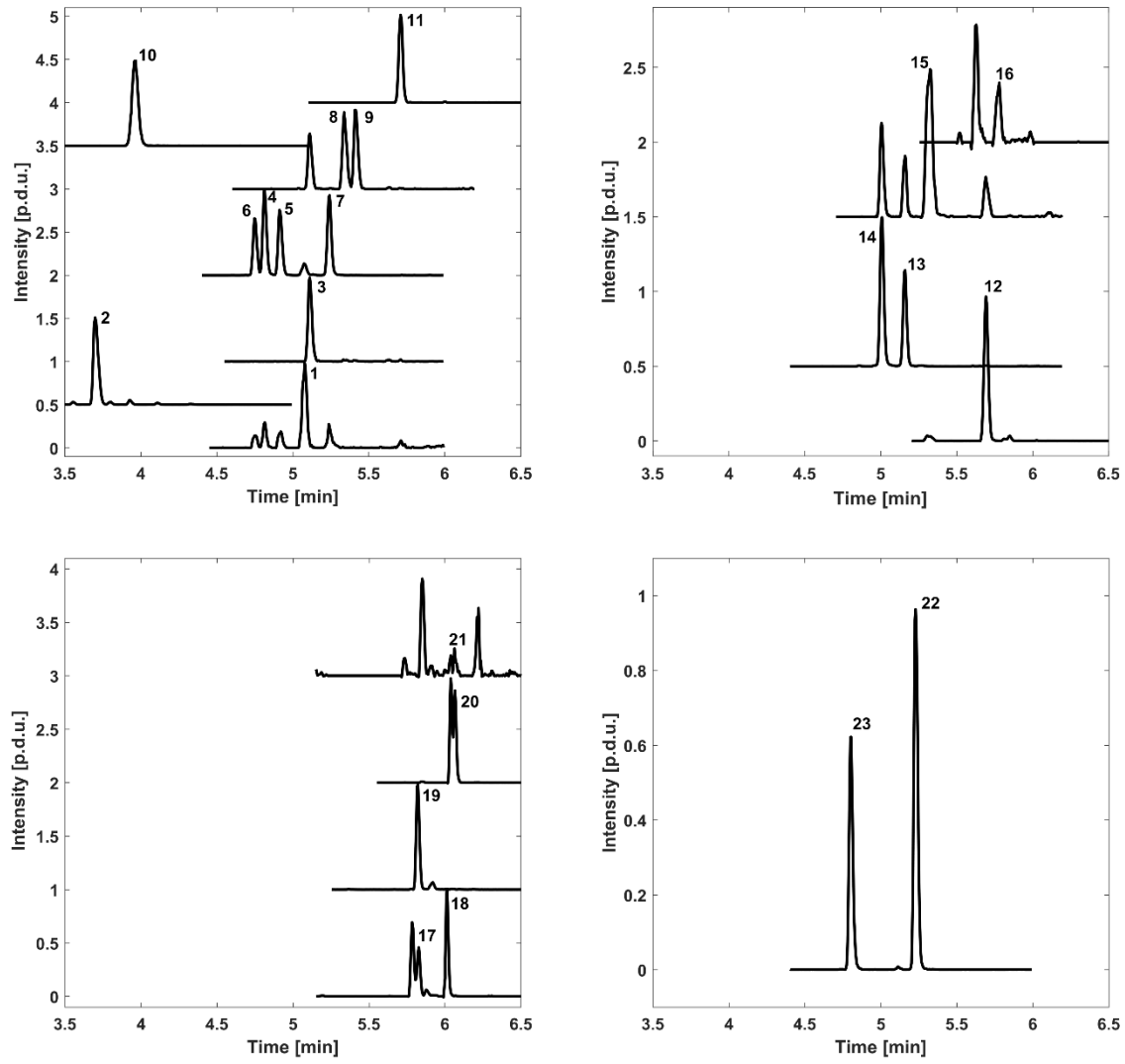

Figure 5.1 Chromatograms of lipid peroxidation products of AA+PGs (top, left), DHA (top, right), AdA (bottom, left) and IS (bottom, right) detected in a spiked plasma sample. Note: 1 = 5-F_{2t}-IsoP + 5-epi-5-F_{2t}-IsoP; 2 = 15-epi-2,3-dinor-15-F_{2t}-IsoP + 2,3-dinor-11β-$PGF_{2\alpha}$ + 2,3-dinor-15-$F_{2\alpha}$-IsoP; 3 = 15-keto-15-F_{2t}-IsoP; 4 = 15-epi-15-F_{2t}-IsoP; 5 = 15-F_{2t}-IsoP; 6 = 11β-$PGF_{2\alpha}$; 7 = $PGF_{2\alpha}$; 8 = 15-E_{2t}-IsoP; 9 = PGE_2; 10 = 6-keto-$PGF_{1\alpha}$; 11 = 15-keto-15-E_{2t}-IsoP; 12 = 4-F_{4t}-NeuroP + 4-epi-4-F_{4t}-NeuroP; 13 = 10-epi-10-F_{4t}-NeuroP; 14 = 10-F_{4t}-NeuroP; 15 = 14(RS)-14-F_{4t}-NeuroP; 16 = 4(RS)-ST-Δ^5-8-NeuroF; 17 = 17-F_{2t}-dihomo-IsoP + 17-epi-17-F_{2t}-dihomo-IsoP; 18 = 1a,1b-dihomo-$PGF_{2\alpha}$; 19 = Ent-7(RS)-F_{2t}-dihomo-IsoP; 20 = 17(RS)-10-epi-SC-Δ^{15}-11-dihomo-IsoF; 21 = 7(RS)-ST-Δ^8-11-dihomo-IsoF; 22 = $PGF_{2\alpha}$-d4; 23 = 15-F_{2t}-IsoP-d4; Chromatograms have been normalized to the maximum intensity of the highest detected peak; chromatograms have been shifted in the y-direction for a better visibility.

Table 5.2 Acquisition parameters and main figures of merit of the LC-MS/MS method.

#[a]	Analyte	m/z Parent ion	Cone [V]	CE [eV]	m/z Daughter Ions	RT ± s (min)	Calibration range (nM)	R^2	LOD (nM)	LOQ (nM)	Internal standard
1	**5-F_{2t}-IsoP + 5-*epi*-5-F_{2t}-IsoP**	353.20	35	30	115.00	5.09 ± 0.03	3.5 - 3562.5	0.991	0.6	2	$PGF_{2\alpha}$-d4
2	**15-*epi*-2,3-dinor-15-F_{2t}-IsoP + 2,3-dinor-11β-$PGF_{2\alpha}$ + 2,3-dinor-15-$F_{2\alpha}$-IsoP**	325.27	40	13	237.00	3.71 ± 0.04	1.7 - 3562.5	0.998	0.3	1.0	15-F2t-IsoP-d4
12	**4-F_{4t}-NeuroP + 4-*epi*-4-F_{4t}-NeuroP**	377.32	20	19	271.12	5.70 ± 0.03	1.7 - 3562.5	0.996	0.3	1.0	$PGF_{2\alpha}$-d4
13	**10-epi-10-F_{4t}-NeuroP**	377.32	10	19	153.00	5.17 ± 0.03	0.6 - 1187.5	0.994	0.11	0.4	$PGF_{2\alpha}$-d4
14	**10-F_{4t}-NeuroP**	377.32	10	19	153.00	5.02 ± 0.03	0.6 - 1187.5	0.998	0.11	0.4	15-F2t-IsoP-d4
15	**14(*RS*)-14-F_{4t}-NeuroP**	377.32	50	19	204.89	5.33 ± 0.03	9.3 - 1187.5	0.993	2	6	$PGF_{2\alpha}$-d4
16	**4(*RS*)-ST-Δ^5-8-NeuroF**	393.60	40	35	123.19	5.78 ± 0.03	296.9 - 4750	0.973	53	178	$PGF_{2\alpha}$-d4
17	**17-F_{2t}-dihomo-IsoP + 17-*epi*-17-F_{2t}-dihomo-IsoP**	381.30	20	25	337.15	5.80 ± 0.02	1.2 - 2375	0.997	0.2	0.7	$PGF_{2\alpha}$-d4
19	***ent*-7(*RS*)-F_{2t}-dihomo-IsoP**	381.30	50	25	142.98	5.83 ± 0.02	0.6 - 1187.5	0.990	0.11	0.4	$PGF_{2\alpha}$-d4
20	**17(*RS*)-10-*epi*-SC-Δ^{15}-11-dihomo-IsoF**	397.40	20	31	155.02	6.06 ± 0.01	0.6 - 1187.5	0.994	0.11	0.4	$PGF_{2\alpha}$-d4
21	**7(*RS*)-ST-Δ^8-11-dihomo-IsoF**	397.40	40	25	201.03	6.06 ± 0.01	148.4 - 4750	0.984	27	89	$PGF_{2\alpha}$-d4
3	**15-keto-15-F_{2t}-IsoP**	351.00	35	25	289.00	5.13 ± 0.04	1.2 - 1187.5	0.995	0.2	0.7	$PGF_{2\alpha}$-d4
18	**1a,1b-dihomo-$PGF_{2\alpha}$**	381.30	20	25	337.15	6.01 ± 0.01	1.2 - 1187.5	0.994	0.2	0.7	15-F2t-IsoP-d4
5	**15-F_{2t}-IsoP**	353.00	35	30	193.00	4.83 ± 0.03	2.3 - 1187.5	0.997	0.4	1.4	15-F2t-IsoP-d4
8	**15-E_{2t}-IsoP**	351.00	35	30	271.00	5.35 ± 0.03	9.2 - 1187.5	0.990	2	6	$PGF_{2\alpha}$-d4
6	**11β-$PGF_{2\alpha}$**	353.00	35	30	193.00	4.93 ± 0.03	1.2 - 1187.5	0.998	0.2	0.7	15-F2t-IsoP-d4
4	**15-epi-15-F_{2t}-IsoP**	353.00	35	30	193.00	4.76 ± 0.03	2.3 - 1187.5	0.998	0.4	1.4	15-F2t-IsoP-d4
10	**6-keto-$PGF_{1\alpha}$**	369.00	40	35	245.00	3.97 ± 0.03	0.6 - 1187.5	0.997	0.11	0.4	15-F2t-IsoP-d4
7	**$PGF_{2\alpha}$**	353.00	35	30	193.00	5.24 ± 0.03	0.6 - 1187.5	0.993	0.11	0.4	$PGF_{2\alpha}$-d4
11	**15-keto-15-E_{2t}-IsoP**	349.00	40	30	113.00	5.73 ± 0.03	2.3 - 1187.5	0.996	0.4	1.4	$PGF_{2\alpha}$-d4
9	**PGE_2**	351.00	35	30	271.00	5.42 ± 0.04	2.3 - 1187.5	0.992	0.4	1.4	$PGF_{2\alpha}$-d4
22	**$PGF_{2\alpha}$-d_4**	357.00	40	30	197.00	5.24 ± 0.03	-	-	-	-	-
23	**15-F_{2t}-IsoP -d_4**	357.00	40	30	197.00	4.81 ± 0.03	-	-	-	-	-
-	**Isoprostanes**	353.20	35	30	115.00	4.0-6.3	-	-	-	-	$PGF_{2\alpha}$-d4
-	**Isofurans**	369.20	45	20	115.00	1.9-6.3	-	-	-	-	$PGF_{2\alpha}$-d4
-	**Neuroprostanes**	377.00	35	20	101.00	2.0-6.2	-	-	-	-	$PGF_{2\alpha}$-d4
-	**Neurofurans**	393.00	35	20	193.00	2.4-6.2	-	-	-	-	$PGF_{2\alpha}$-d4

Note: a indicates the peak number according to **Figure 5.1**; LOQs were established as the concentration of analyte that can be measured with an imprecision of less than 20% and a deviation from target of less than 20% and taking into account the preconcentration factor achieved during sample processing. The LOD is defined as 3/10*LOQ.

Table 5.3 Back-calculated intra- and inter-day accuracy and precision of standard solutions.

#[a]	Analyte	Standard solutions - % Accuracy± RSD (conc nM)					
		Intra-day (N=3)			Inter-day (N=2)		
		Low	Medium	High	Low	Medium	High
1	**5-F_{2t}-IsoP + 5-*epi*-5-F_{2t}-IsoP**	96 ± 6 (3.5)	110 ± 10 (111.3)	98 ± 9 (3562.5)	100.6 ± 7 (3.5)	107 ± 9 (111.3)	100 ± 7 (3562.5)
2	**15-*epi*-2,3-dinor-15-F_{2t}-IsoP + 2,3-dinor-11β-$PGF_{2\alpha}$ + 2,3-dinor-15-$F_{2\alpha}$-IsoP**	89 ± 4 (1.7)	108 ± 2 (111.3)	101.8 ± 8 (3562.5)	93 ± 15 (1.7)	115 ± 8 (111.3)	98 ± 5 (3562.5)
12	**4-F_{4t}-NeuroP + 4-*epi*-4-F_{4t}-NeuroP**	80 ± 8 (1.7)	105 ± 5 (111.3)	97 ± 1 (3562.5)	82.6 ± 8 (1.7)	105 ± 5 (111.3)	98 ± 2 (3562.5)
13	**10-*epi*-10-F_{4t}-NeuroP**	110 ± 10 (0.6)	99.3 ± 5 (37.1)	101 ± 8 (1187.5)	111 ± 9 (0.6)	96 ± 5 (37.1)	104 ± 7 (1187.5)
14	**10-F_{4t}-NeuroP**	112 ± 12 (0.6)	103 ± 10 (37.1)	100 ± 5 (1187.5)	120 ± 14 (0.6)	100 ± 8 (37.1)	101.9 ± 7 (1187.5)
15	**14(*RS*)-14-F_{4t}-NeuroP**	110 ± 20 (9.3)	99 ± 2 (148.4)	98 ± 12 (1187.5)	109.4 ± 15 (9.3)	95 ± 7 (148.4)	102 ± 8 (1187.5)
16	**4(*RS*)-ST-Δ^5-8-NeuroF**	107 ± 10 (296.9)	95 ± 15 (1187.5)	94 ± 7 (4750)	109 ± 6 (296.9)	85 ± 14 (1187.5)	100 ± 13 (4750)
17	**17-F_{2t}-dihomo-IsoP + 17-*epi*-17-F_{2t}-dihomo-IsoP**	90± 14 (1.2)	97 ± 6 (74.2)	101 ± 3 (2375)	103 ± 12 (1.2)	95 ± 1 (74.2)	103 ± 3 (2375)
19	***ent*-7(*RS*)-F_{2t}-dihomo-IsoP**	86± 20 (0.6)	98 ± 10 (37.1)	101 ± 13 (1187.5)	99.1 ± 11 (0.6)	98 ± 7 (37.1)	101.8 ± 9 (1187.5)
20	**17(*RS*)-10-*epi*-SC-Δ^{15}-11-dihomo-IsoF**	120 ± 20 (0.6)	87 ± 8 (37.1)	107 ± 14 (1187.5)	130 ± 17 (0.6)	86 ± 5 (37.1)	106 ± 9 (1187.5)
21	**7(*RS*)-ST-Δ^8-11-dihomo-IsoF**	88 ± 15 (148.4)	88 ± 13 (1187.5)	112 ± 12 (4750)	95 ± 15 (148.4)	85 ± 12 (1187.5)	104 ± 11 (4750)
3	**15-keto-15-F_{2t}-IsoP**	99.1 ± 18 (1.2)	106 ± 5 (37.1)	98 ± 3 (1135.2)	103 ± 20 (1.2)	104 ± 5 (5.1)	100 ± 4 (1187.5)
18	**1a,1b-dihomo-$PGF_{2\alpha}$**	108 ± 20 (1.2)	80 ± 10 (10)	106 ± 1 (1187.5)	118 ± 15 (1.2)	81 ± 6 (37.1)	107 ± 3 (1187.5)
5	**15-F_{2t}-IsoP**	108 ± 18 (2.3)	108 ± 6 (37.1)	102 ± 4 (1187.5)	90± 20 (1.2)	107 ± 4 (37.1)	100 ± 4 (1187.5)
8	**15-E_{2t}-IsoP**	88 ± 2 (9.3)	97 ± 3 (74.2)	101 ± 4 (1187.5)	100 ± 20 (1.2)	102 ± 20 (74.2)	100 ± 3 (1187.5)
6	**11β-$PGF_{2\alpha}$**	103 ± 1 (1.2)	100 ± 2 (37.1)	103 ± 3 (1187.5)	93 ± 12 (1.2)	104 ± 5 (37.1)	100 ± 3 (1187.5)
4	**15-epi-15-F_{2t}-IsoP**	115 ± 1 (2.3)	101 ± 7 (74.2)	100 ± 2 (1187.5)	115 ± 17 (2.3)	100 ± 7 (74.2)	101 ± 2 (1187.5)
10	**6-keto-$PGF_{1\alpha}$**	82 ± 6 (0.6)	101 ± 3 (37.1)	102 ± 1 (1187.5)	84 ± 15 (0.6)	105 ± 5 (37.1)	100 ± 3 (1187.5)
7	**$PGF_{2\alpha}$**	112 ± 8 (9.3)	100 ± 1 (148.4)	97 ± 2 (1187.5)	120 ± 12 (9.3)	97 ± 3 (148.4)	99 ± 3 (1187.5)
11	**15-keto-15-E_{2t}-IsoP**	118 ± 9 (2.3)	102 ± 3 (74.2)	102 ± 4 (1187.5)	110 ± 20 (2.3)	104 ± 5 (74.2)	100 ± 4 (1187.5)
9	**PGE_2**	90 ± 12 (2.3)	98 ± 4 (74.2)	98 ± 2 (1187.5)	88 ± 8 (2.3)	102 ± 15 (74.2)	97 ± 2 (1187.5)

Note: Values within brackets indicate the added concentration of each metabolite; a indicates the peak number according to **Figure 5.1**

Table 5.2 summarizes the main analytical figures of merit obtained for the quantification of the selected set of compounds. Highly reproducible retention times with a standard deviation ≤0.04 min were observed for the set of metabolites and IS. Linear calibration lines calculated using either PGF2a-d4 or 15-F2t-IsoP-d4 as IS generally covering two to three orders of magnitude were obtained with coefficients of determination (R^2) >0.97 and homoscedastic residuals as assessed by visual inspection. LOD and LOQ expressed as nmol L^{-1} of plasma were in the 0.11-53 and 0.4-178 range, respectively. No carry-over was observed with peak areas of the blank injection remaining below 5% of the signal of the standard at the LOD.

Table 5.3 shows back-calculated recovery values in standard solutions for assessment of accuracy and precision. Adequate accuracies were obtained in standard solutions with the exception of 17(RS)-10-epi-SC-Δ^{15}-11-dihomo-IsoF and 1a,1b-dihomo-PGF_{2a}. Precision levels remained <20% at the LOQ and <15% for higher concentrations, with the exception of the intra-day precision obtained for 15-E_{2t}-IsoP. In **Table 5.4** the method's performance was further assessed by the analysis of spiked plasma samples and calculated recovery values taking into account the concentrations found in the non-spiked sample. The extraction yields were used for jointly assessing the effect of the KOH digestion procedure and the solid phase extraction sample clean-up. Good inter- and intraday extraction yields ranging between 82 and 115% and 79 and 131% were found for lipid peroxidation products derived from AA and DHA with the exception of four metabolites derived from AA (i.e. 15-keto-15-F_{2t}-IsoP, 15-E_{2t}-IsoP, 15-keto-15-E_{2t}-IsoP and PGE_2), which were not detected. It is suspected that during sample hydrolysis these analytes suffer dehydration within the β-hydroxy keto system in the cyclopentane ring (i.e. cyclopentenone PGs)[267] while the δ-hydroxy-α,β-unsaturated-keto system of 15-keto-15-F_{2t}-IsoP is degrading into a reactive conjugated keto-diene system. AdA derived lipid peroxidation products showed lower extraction yields ranging between 52 and 100% and 60 and 95% for inter- and intra-day accuracy, indicating that those compounds are either partially degraded during the digestion step or not completely recovered during the SPE. As observed from **Table 5.4**, for a total of seven compounds a notable matrix effect was observed whereas for the remaining compounds intra- and inter-day recoveries ranged between 78-129% and 75-123%, respectively. No pattern between different lipid peroxidation classes could be detected with respect to the matrix effect. Moreover, the overall accuracy and precision of the developed method was assessed for all metabolites which were not degraded during the hydrolysis procedure by means of relative recovery values employing deuterated ISs. For AA and DHA derived lipid peroxidation products obtained intra- and inter-day accuracy levels ranged between 79 and 120% and 80 and 113%, respectively, with the exception of 4(RS)-ST-Δ^5-8-NeuroF for which only a semiquantitative determination was achieved despite the use of an IS. Due to the low extraction yields observed for dihomo-IsoPs and dihomo-IsoFs a semiquantitative determination was proposed to enable the comparison of samples analyzed and extracted under the same conditions.

Table 5.4 Back-calculated intra- and inter-day accuracy and precision in spiked plasma samples.

		Extraction yield Accuracy ± RSD (conc nM)				Matrix effect % Accuracy ± RSD (conc nM)				Method Accuracy ± RSD (conc nM)			
#[a]	Analyte	Intra-day (N=3)		Inter-day (N=2)		Intra-day (N=3)		Inter-day (N=2)		Intra-day (N=3)		Inter-day (N=2)	
		Low	High	Low	High	Low	High	Low	High	Low	High	Low	High
1	**5-F_{2t}-IsoP + 5-*epi*-5-F_{2t}-IsoP**	104 ± 13 (15)	91 ± 14 (1800)	93 ± 16 (15)	87 ± 7 (1800)	83 ± 11 (15)	86 ± 13 (1800)	95 ± 20 (15)	109 ± 3 (1800)	110 ± 4 (15)	105 ± 4 (1800)	110 ± 4 (15)	105 ± 4 (1800)
2	**15-*epi*-2,3-dinor-15-F_{2t}-IsoP + 2,3-dinor-11β-$PGF_{2\alpha}$ + 2,3-dinor-15$F_{2\alpha}$-IsoP**	110 ± 13 (15)	95 ± 8 (1800)	98 ± 17 (15)	93 ± 2 (1800)	79 ± 9 (15)	92 ± 8 (15)	96 ± 20 (15)	100 ± 11 (1800)	95 ± 3 (15)	95 ± 4 (1800)	95 ± 8 (15)	97 ± 10 (1800)
12	**4-F_{4t}-NeuroP + 4-*epi*-4-F_{4t}-NeuroP**	89 ± 12 (15)	103 ± 18 (1800)	81 ± 14 (15)	94 ±14 (1800)	100 ± 15 (15)	89 ± 17 (1800)	109 ± 15 (15)	104 ± 20 (1800)	109 ± 5 (15)	119 ± 7 (1800)	100 ± 20 (15)	113 ± 12 (1800)
13	**10-*epi*-10-F_{4t}-NeuroP**	87 ± 13 (5)	95 ± 15 (600)	81 ± 9 (5)	91 ± 6 (600)	102 ± 19 (5)	96 ± 15 (600)	120 ± 20 (5)	109 ± 18 (600)	98 ± 14 (5)	116 ± 12 (600)	94 ± 17 (5)	113 ± 15 (600)
14	**10-F_{4t}-NeuroP**	90 ± 20 (5)	95 ± 15 (600)	81 ± 16 (5)	90 ± 8 (600)	83 ± 17 (5)	94 ± 16 (600)	97 ± 18 (5)	109 ± 19 (600)	87 ± 9 (5)	101 ± 3 (600)	89 ± 11 (5)	106 ± 13 (600)
15	**14(*RS*)-14-F_{4t}-NeuroP**	71 ± 30 (5)	94 ± 15 (600)	110 ± 51 (5)	89 ± 7 (600)	70 ± 30 (5)	86 ± 4 (600)	50 ± 27 (5)	80 ± 10 (600)	106 ± 41 (5)	94 ± 4 (600)	89 ± 36 (5)	90 ± 9 (600)
16	**4(*RS*)-ST-Δ^5-8-NeuroF**	<LOD (5)	105 ± 16 (600)	<LOD (5)	131 ± 30 (600)	<LOD (5)	70 ±30 (600)	<LOD (5)	80 ± 20 (600)	<LOQ (5)	70 ± 20 (600)	<LOQ (5)	110 ± 40 (600)
17	**17-F_{2t}-dihomo-IsoP + 17-*epi*-17-F_{2t}-dihomo-IsoP**	64 ± 9 (10)	73 ± 15 (1200)	61 ± 8 (10)	72 ± 2 (1200)	114 ± 14 (10)	90 ± 18 (1200)	123 ± 14 (10)	100 ± 16 (1200)	78 ± 8 (10)	85 ± 8 (1200)	67 ± 20 (10)	85 ± 9 (1200)
19	***ent*-7(*RS*)-F_{2t}-dihomo-IsoP**	70 ± 11 (5)	81 ± 14 (600)	64 ± 12 (5)	76 ± 9 (600)	89 ± 18 (5)	82 ± 14 (600)	92 ± 13 (5)	92 ± 15 (600)	65 ± 6 (5)	88 ± 8 (600)	59 ± 11 (5)	85 ± 9 (600)
20	**17(*RS*)-10-*epi*-SC-Δ^{15}-11-dihomo-IsoF**	78 ± 19 (5)	90 ± 15 (600)	73 ± 11 (5)	86 ± 7 (600)	110 ± 30 (5)	94 ± 17 (600)	116 ± 20 (5)	107 ± 18 (600)	83 ± 32 (5)	108 ± 9 (600)	78 ± 30 (5)	106 ± 11 (600)
21	**7(*RS*)-ST-Δ^8-11-dihomo-IsoF**	87 ± 17 (5)	100 ± 17 (600)	<LOD (5)	95 ± 6 (600)	<LOD (5)	116 ± 20 (600)	<LOD (5)	131 ± 30 (600)	<LOQ (5)	65 ± 20 (600)	<LOQ (5)	84 ± 30 (600)
3	**15-keto-15-F_{2t}-IsoP**	<LOD (5)	<LOD (600)	<LOD (5)	<LOD (600)	<LOD (5)	85 ± 13 (600)	<LOD (5)	101 ± 20 (600)	<LOQ (5)	<LOQ (600)	<LOQ (5)	<LOQ (600)
18	**1a,1b-dihomo-$PGF_{2\alpha}$**	52 ± 11 (5)	62 ± 11 (600)	<LOD (5)	60 ± 5 (600)	150 ± 40 (5)	107 ± 20 (600)	180 ±40 (5)	120 ± 20 (600)	33 ± 6 (5)	72 ± 5 (600)	38 ± 13 (5)	77 ± 11 (600)
5	**15-F_{2t}-IsoP**	82 ± 16 (5)	97 ± 11 (600)	79 ± 5 (5)	87 ± 16 (600)	95 ± 20 (5)	86 ± 10 (600)	101 ± 15 (5)	101 ± 18 (600)	87 ± 15 (5)	99 ± 1 (600)	86 ± 18 (5)	99 ± 9 (600)
8	**15-E_{2t}-IsoP**	<LOD (5)	<LOD (600)	<LOD (5)	<LOD (600)	<LOD (5)	83 ± 15 (600)	<LOD (5)	130 ± 9 (600)	<LOQ (5)	<LOQ (600)	<LOQ (5)	<LOQ (600)
6	**11β-$PGF_{2\alpha}$**	100 ± 20 (5)	96±14 (600)	80 ± 30 (5)	88 ± 13 (600)	100 ± 20 (5)	89 ± 14 (600)	120 ± 30 (5)	104 ± 19 (600)	89 ± 6 (5)	99 ± 1 (600)	84 ± 13 (5)	100 ± 10 (600)
4	**15-epi-15-F_{2t}-IsoP**	101 ± 15 (5)	106 ± 17 (600)	90 ± 20 (5)	95 ± 15 (600)	87 ± 10 (5)	125 ± 2 (600)	75 ± 15 (5)	100 ±20 (600)	111 ± 12 (5)	96 ± 5 (600)	102 ±13 (5)	101 ± 13 (600)
10	**6-keto-$PGF_{1\alpha}$**	107 ± 16 (5)	87 ± 13 (600)	95 ± 18 (5)	87 ± 1 (600)	97 ± 17 (5)	100 ± 2 (600)	85 ± 17 (5)	92 ± 10 (600)	79 ± 12 (5)	91 ± 2 (600)	80 ±8 (5)	94 ± 10 (600)
7	**$PGF_{2\alpha}$**	115 ± 11 (5)	94 ± 15 (600)	106 ± 12 (5)	86 ± 14 (600)	34 ± 8 (5)	82 ± 10 (600)	32 ± 10 (5)	100 ± 20 (600)	120 ±16 (5)	103 ± 6 (600)	100 ±18 (5)	102 ± 10 (600)
11	**15-keto-15-E_{2t}-IsoP**	<LOD (5)	<LOD (600)	<LOD (5)	<LOD (600)	119 ± 16 (5)	129 ± 1 (600)	110 ± 20 (5)	100 ± 30 (600)	<LOQ (5)	<LOQ (600)	<LOQ (5)	<LOQ (600)
9	**PGE_2**	<LOD (5)	<LOD (600)	<LOD (5)	<LOD (600)	90 ± 20 (5)	78 ± 11 (600)	100 ± 20 (5)	93 ± 17 (600)	<LOQ (5)	<LOQ (600)	<LOQ (5)	<LOQ (600)

Note: Values within brackets indicate the added concentration of each metabolite added to the plasma sample; a indicates the peak number according to **Figure 5.1**

Complementary approaches such as including isotopically labelled analogues of dihomo-IsoPs and dihomo-IsoFs as surrogates to improve the accuracy of the method are being evaluated. In summary, data shown in **Table 5.4** prove that the developed method is highly reproducible for the analysis of the majority of compounds while it gives insights in the analytical challenges for several other compounds which might be affected during sample processing and measurement.

5.4.2 Quantitative analysis of lipid peroxidation biomarkers in newborn plasma samples

Lipid peroxidation biomarkers were determined in 150 plasma samples from 20 term newborns suffering from HIE secondary to birth asphyxia (see **Table 5.1**) at 10 sampling time points covering from 3 h to 6 days after birth. Table 5 shows the main descriptors of the distribution of concentrations of the lipid peroxidation products found in the studied samples excluding the four metabolites which were not stable during the sample KOH hydrolysis process (i.e. 15-keto-15-F_{2t}-IsoP, 15-E_{2t}-IsoP, 15-keto-15-E_{2t}-IsoP and PGE_2). From the 17 remaining parameters, 11 (corresponding to 16 individual isoprostanoids) were detected in the studied samples. In addition to the determination of individual lipid peroxidation biomarkers, total relative IsoP, IsoF, NeuroP and NeuroF contents were measured following a procedure as described elsewhere[51]. Three out of the 11 compounds have been detected in a preliminary biomarker study involving a similar cohort of newborns (N = 20) [15]. In newborns with HIE undergoing TH concentrations determined were of the same order of magnitude as in this cohort with medians (IQRs) of 3 (12), 5(7) and 0 (3.4) for 5-F2t-IsoP, PGF_{2a} and 1a,1b-dihomo-PGF_{2a}, respectively.

Table 5.5 Main descriptors of the distribution of concentrations (nM) of the lipid peroxidation products in plasma samples with concentrations >LOQ from newborns with HIE.

#[a]	Analyte	Range	Median	IQR (25-75)	Mean ± s	>LOQ (%)
1	**5-F_{2t}-IsoP + 5-*epi*-5-F_{2t}-IsoP**	0.5 – 8.6	3.2	1.9	3.5 ± 1.3	44
2	**15-*epi*-2,3-dinor-15-F_{2t}-IsoP + 2,3-dinor-11β-$PGF_{2\alpha}$ + 2,3-dinor-15-$F_{2\alpha}$-IsoP**	-	-	-	-	0
12	**4-F_{4t}-NeuroP + 4-*epi*-4-F_{4t}-NeuroP**	1.1 – 1.6	1.3	0.2	1.3 ± 0.2	7
13	**10-*epi*-10-F_{4t}-NeuroP**	0.4 – 0.8	0.4	0.1	0.5 ± 0.1	9
14	**10-F_{4t}-NeuroP**	0.4 – 0.8	0.5	0.09	0.53 ± 0.12	13
15	**14(*RS*)-14-F_{4t}-NeuroP**	-	-	-	-	0
16	**4(*RS*)-ST-Δ^5-8-NeuroF**	-	-	-	-	0
17	**17-F_{2t}-dihomo-IsoP + 17-*epi*-17-F_{2t}-dihomo-IsoP**	0.5 – 1.1	0.8	0.1	0.8 ± 0.2	5
19	***ent*-7(*RS*)-F_{2t}-dihomo-IsoP**	0.3 – 1.0	0.5	0.1	0.5 ± 0.2	4
20	**17(*RS*)-10-*epi*-SC-Δ^{15}-11-dihomo-IsoF**	0.4 – 3.2	0.6	0.4	0.8 ± 0.6	61
21	**7(*RS*)-ST- Δ^8-11-dihomo-IsoF**	89.9 – 900.7	174.5	151.7	240 ±170	74
18	**1a,1b-dihomo-$PGF_{2\alpha}$**	0.8 -2.9	1.1	0.45	1.2 ± 0.4	37
5	**15-F_{2t}-IsoP**	-	-	-	-	0
6	**11β-$PGF_{2\alpha}$**	-	-	-	-	0
4	**15-epi-15-F_{2t}-IsoP**	-	-	-	-	0
10	**6-keto-$PGF_{1\alpha}$**	0.4 – 0.8	0.5	0.1	0.6 ± 0.1	3
7	**$PGF_{2\alpha}$**	0.8 – 10.8	2.5	1.2	2.6 ± 1.1	98
-	**Isoprostanes[b]**	-	-	-	-	0
-	**Isofurans[b]**	19.8 – 184.5	52.1	50	70 ± 40	76

#[a]	Analyte	Range	Median	IQR (25-75)	Mean ± s	>LOQ (%)
-	**Neuroprostanes[b]**	20 – 114	50.3	23	50 ± 20	29
-	**Neurofurans[b]**	8 – 27	14.5	7	15 ± 4	69

Note: [a] indicates the peak number according to **Figure 5.1**; [b] Values in area/area of internal standard x 1000.

Figure 5.2 shows boxplots of the results of isoprostanoids which were detected in more than 25% of samples. The results are stratified by two collection time windows, the first one comprising the first 30 h after birth during hypothermia and the second including samples collected on day 5-6 during normothermia. Interestingly, not all metabolites showed the same behavior with time. In a previous study the levels of total IsoPs, IsoFs, NeuroPs and NeuroFs were monitored in preterm infants throughout the whole neonatal period and nomograms of relative contents were established revealing the underlying changes of biomarker levels as a function of the infant's age[51]. This might be an important aspect to be taken into account during the experimental design of clinical studies as well as during the interpretation of the results. Here, a significant decrease with time was detected for some metabolites (i.e. 5-F_{2t}-IsoP þ 5-epi-5-F_{2t}-IsoP, PGF_{2a}, total NeuroFs), whereas others increased (i.e. 17(RS)-10-epi-SC-Δ^{15}-11-dihomo-IsoF, 7(RS)-ST-Δ^{8}-11-dihomo-IsoF, total NeuroPs) or remained unchanged (1a,1b-dihomo-PGF_{2a}, total IsoFs). This application illustrates the strengths of a detection method which is able to detect and quantify specific isomers as compared to the determination of total parameters. Also, the specific detection of isomers enables an absolute quantification, which at the same time improves the method's sensitivity. This is also demonstrated in the present study by the detection of IsoPs: whereas for total IsoPs the concentratons remained below the LOQ, some individual IsoPs could still be detected (i.e. 5-F_{2t}-IsoP and 5-epi-5-F_{2t}-IsoP).

Conversely, for IsoFs no analytical standard solutions were available and the determination of total IsoFs enabled the detection of these metabolites in plasma samples. Likewise, in case of NeuroPs and NeuroFs, individual isomers could not be detected in the majority of samples, whereas for the total parameters levels above the LOQ were found, indicating that the individual isomers included in this method might not be those which were formed primarily. Hence, the simultaneous determination of both, individual isomers and total parameters is recommended for studying lipid peroxidation biomarkers in biofluids. Whereas the individual isomers give a more detailed information on the lipid peroxidation process providing insight into the underlying mechanisms of action, total parameters are a straightforward alternative when no pure analytical standard solutions are available. Moreover, even if the determination of individual isomers was not limited by the availability of standards, it would not be feasible to resolve and determine all possible isomers in one analytical run. Therefore, it would first have to be established which lipid peroxidation biomarkers are of interest for monitoring in each study in dependence of the species, biofluid and pathophysiological situation.

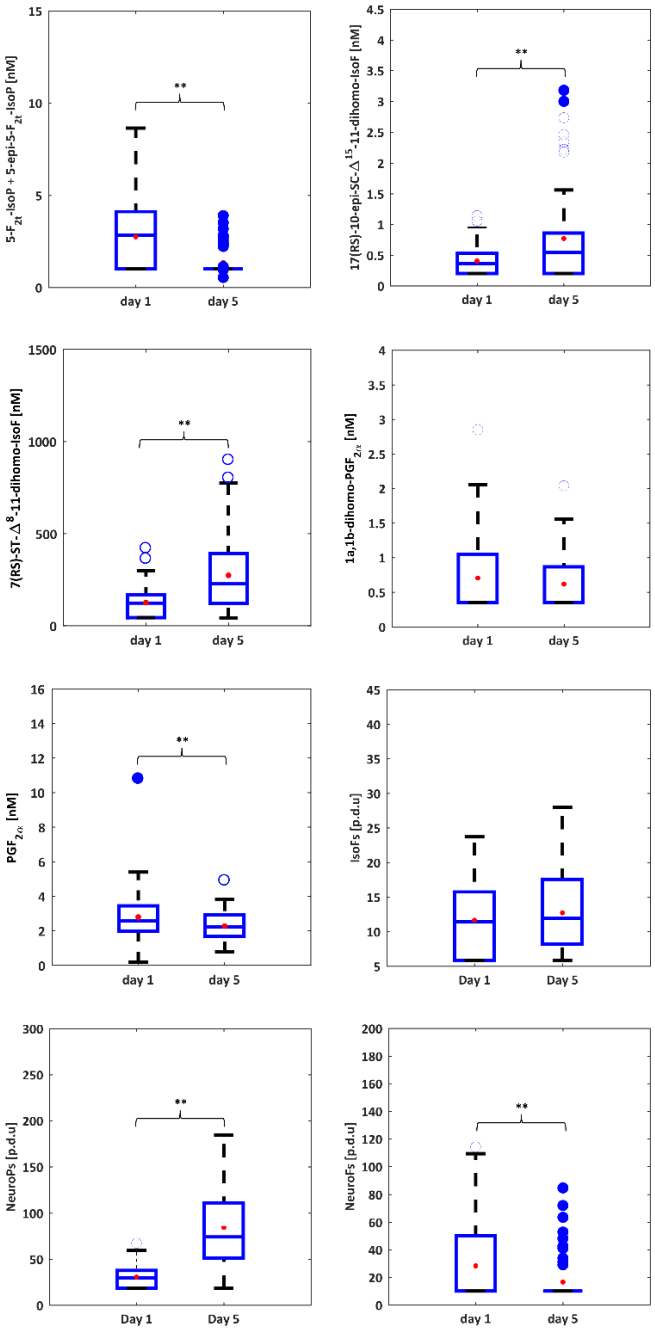

Figure 5.2 Boxplots of isoprostanoids in plasma samples from newborns on days 1 and 5. Boxes indicate the 1st and the 3rd quartiles, the median is shown as a blue line, whiskers mark the 9th and 91st percentiles, red triangles represent mean concentrations and blue circles are outliers Note: Values below LOQ were replaced by ½ LOQ; ** = p-value < 0.01

5.5 Conclusions

This work presents the first validated LC-MS/MS method for the simultaneous quantification of 28 lipid peroxidation biomarkers in addition to four total relative parameters in small volumes (100 mL) of plasma samples. The access to a considerable panel of different isomers allowed an in-depth study of the effect of analytical and pre-analytical conditions on the determination of the metabolites revealing stability issues in 4 metabolites during hydrolysis. Future studies will focus on the modification of the hydrolysis conditions e.g. using enzymatic hydrolysis. Furthermore, the use of isotopically labelled internal standards for each studied substance class as surrogates is recommended to improve the method's accuracy.

Chapter 6 Adrenic acid non-enzymatic peroxidation products in biofluids of moderate preterm infants

6.1 Abstract

Oxidative stress plays an essential role in processes of signaling and damage to biomolecules during early perinatal life. Isoprostanoids and isofuranoids from the free radical-catalyzed peroxidation of polyunsaturated fatty acids (PUFAs) are widely recognized as reliable biomarkers of oxidative stress. However, their quantification is not straightforward due to high structural similarity of the compounds formed. In this work, a semiquantitative method for the analysis of adrenic acid (AdA, C22:4 n-6) non-enzymatic peroxidation products (i.e. dihomo-isoprostanes and dihomo-isofurans) was developed. The proposed ultra-performance liquid chromatography - tandem mass spectrometry (UPLC-MS/MS) method was applied to the analysis of blood plasma and urine from preterm infants providing information about AdA peroxidation.

6.2 Introduction

The assessment of oxidative stress (OS) in the perinatal period, and particularly in prematurity is widely discussed elsewhere[176]. In both, physiological and pathological conditions, perinatal oxidative status provides highly valuable information and has helped to understand disease mechanisms and establish predictive or prognostic biomarkers.

One of the most studied OS-related reactions in the perinatal field is the free radical-catalyzed peroxidation of polyunsaturated fatty acids (PUFAs)[51–55]. Since the in-vivo free radical-catalyzed peroxidation of arachidonic acid (AA, C20:4 n-6) was discovered[406], numerous studies have been performed focusing on the mechanisms and biomedical implications of the formed compounds that were named isoprostanes (IsoPs) and isofurans (IsoFs). These implications have been recently reviewed by Milne et al.[267] including their employment as biomarkers of oxidative stress-related conditions and their biological activity

in the cardiovascular system. During the last decade, the study of lipid peroxidation (LPO) has been extended to other PUFAs thereby identifying different families of LPO products (i.e. isoprostanoids and isofuranoids) from docosahexanoic acid (DHA, C22:6 n-3) and adrenic acid (AdA, C22:4 n-6) among others[268,423–426]. The study of the AA, DHA and AdA peroxidations are particularly of interest in the neonatal field since these PUFAs play an essential role in the physical properties and function of membranes, influencing their packing and fluidity[427]. Moreover, AdA oxidation may be of particular interest during early human development given the high concentration of this PUFA in the retina and cerebral white matter[428].

Ultra-performance liquid chromatography - tandem mass spectrometry (UPLC-MS/MS) has proven its effectiveness to provide adequate sensitivity and selectivity for the analysis of isoprostanoids and isofuranoids in biological samples. Due to their clinical relevance, efforts have been made to chemically synthesize[414,420,425,429] different isomers of isoprostanoids and isofuranoids[268,425,430] for their use as analytical standards for quantification purposes. However, a comprehensive quantification of the complete set of potentially hundreds of isomers is complex because of the lack of analytical standards and the difficult resolution in the MS and chromatographic dimensions[269,420,425,431].

To circumvent these limitations, the semiquantitative analysis of IsoPs, IsoFs, neuroprostanes (NeuroPs) and neurofurans (NeuroFs) has been proposed recently[51,408,412,432]. In this approach, “total parameters” of IsoPs, IsoFs, NeuroPs, and NeuroFs are defined as the total relative response of LPO products that may be detected from the corresponding PUFA in-vitro lipid peroxidation at fixed conditions[51]. These conditions include the free radical generator and its concentration, the incubation time, the PUFA concentration, and the preprocessing performed to concentrate the generated compounds. Therefore, the analysis of the selected relative responses in a biological sample allows a straightforward assessment of the free radical attack to the PUFA.

Total parameters of IsoPs, IsoFs, NeuroPs, and NeuroFs were successfully implemented in a UPLC-MS/MS method that enabled their semiquantitative determination together with the quantification of 28 isoprostanoid isomers[53]. However, to the best of our knowledge, to date total parameters of dihomo-isoprostanes (dihomo-IsoPs) and dihomo-isofuranes (dihomo-IsoFs) formed by AdA peroxidation have not been studied yet.

This work assesses the potential of a relative quantification approach for total dihomo-IsoP and dihomo-IsoF isomers in biofluids. For method set-up and optimization AdA standards were subjected to an invitro peroxidation procedure and characterized employing UPLC-MS and UPLC-MS/MS. Detection parameters were optimized in terms of sensitivity and the method was applied to urine and plasma samples from preterm infants.

6.3 Material and methods

6.3.1 Standards and reagents

AAPH (2,2′-Azobis [2-methylpropionamidine] dihydrochloride), adrenic acid (AdA, 22:4 n-6), β-glucuronidase type IX-A from E. coli, and potassium hydroxide (KOH) were purchased from Sigma Aldrich Química S.A. (Madrid, Spain). Methanol (MeOH), ethanol (EtOH), n-heptane (C_7H_{16}), and acetonitrile (CH_3CN) at LC-MS grade were purchased from J.T. Baker (Phillipsburg, NJ, USA). Formic acid (98% w/w) and ethyl acetate (analytical grade) were from Panreac (Barcelona, Spain). Dulbecco's phosphate buffered saline (PBS) containing 137 mM of NaCl, 2.7 mM of KCl, 10 mM of sodium hydrogen phosphate, and 1.8 mM of potassium dihydrogenphosphate at pH 7.4 was prepared dissolving the pre-weighted tablet from VWR (Radnor, PA, USA) in 100 mL of water. Water was ultrapure H_2O generated on a Milli-Q® integral system from Merck Millipore (Darmstadt, Germany). Deuterated prostaglandin $F_{2\alpha}$ ($PGF_{2\alpha}$-D4) with purity ≥98% and deuterated incorporation ≥99% was purchased from Cayman Chemical Company (Ann Arbor, MI, USA) and employed as internal standard (IS).

6.3.2 Study population and sample collection

The samples employed to evaluate the method's performance were urine and plasma obtained from moderate preterm infants, defined as gestational age between >31 and ≤33 weeks at birth, collected at University Hospitals, Rainbow Babies & Children's Hospital, Cleveland Ohio, USA. Exclusion criteria included infants with congenital anomalies. Institutional review board approval was obtained for this study. Parents provided written consent at time of enrollment. A set of 75 plasma and 23 urine samples collected during the first 3 weeks of life (Days 7–10 and Days 13–17) were employed. For plasma, 500 µL of venous or capillary blood was collected in lithium heparin plasma separator tubes (BD Microtainer; Franklin Lakes, NJ, USA) and centrifuged at 1000 g for 10 min at 4 °C to obtain plasma that was then stored at –80 °C until analysis. One milliliter of urine was collected employing sterile cotton pads or a newborn Hollister bag and urine was extracted and stored at –80 °C until analysis. Samples were shipped on dry ice and arrived frozen for analysis.

6.3.3 AdA *in vitro* oxidation

AAPH was employed as a model generator of free radicals following previous works with slight modifications [1,8,24–26]. Eight aliquots of 500 µL of AdA (4.5 mg/mL) and AAPH (2.7 mg/mL) suspensions in PBS were incubated in 1.5 mL microcentrifuge tubes at 37 °C with mild shaking in a MKR13 thermoblock from Ditabis AG (Pforzheim, Germany). After 0, 2, 4, 6, 8, 10, 24, and 30 h, aliquots were withdrawn and stored at −20 °C until further

processing. Before analysis, each aliquot was thawed, homogenized on a Vortex S0200 mixer from LabNet (Edison, NJ, USA) for 30 s at maximum speed and diluted 1:9 (v/v) in H_2O:MeOH (85:15, 0.1% (v/v) HCOOH) to 900 µL. Blank samples were prepared following the same procedure in the absence of AdA. Diluted aliquots were centrifuged at 16000 g for 10 min at 4 °C using a Biocen 200r centrifuge from Orto Alresa (Madrid, Spain) and supernatants were extracted by solid phase extraction (SPE) following the procedure described for plasma and urine samples prior to UPLC-MS/MS analysis.

6.3.4 Sample preprocessing

Plasma samples were subjected to basic hydrolysis in order to obtain free isoprostanoids and isofuranoids by saponification from the corresponding esters as described in the literature[53,54,268,431]. A volume of 100 µL of plasma was thawed on ice and 100 µL of KOH solution at 15% (w/v) were added. The mixture was incubated at 40 °C for 30 min. For urine samples, the glucuronide conjugates were hydrolyzed using β-glucuronidase from E. coli to deconjugate glucuronides of isoprostanoids[433]. One hundred units of β-glucuronidase were added to 600 µL of urine and the mixture was incubated at 37 °C for 90 min.

A volume of 3 µL of aqueous IS solution (20 µM) was added to hydrolyzed samples and diluted to 900 µL with H_2O:MeOH (85:15, 2.8% (v/v) HCOOH) solution for plasma samples and H_2O:MeOH (85:15, 0.1% (v/v) HCOOH) solution for urine samples. Then, the samples were mixed for 30 s at maximum speed and centrifuged at 16000 g and 4 °C for 10 min. For clean-up and pre-concentration of the samples, an SPE procedure employing Discovery® DSC-18 SPE 96-well plates from Sigma Aldrich Química S.A. (Madrid, Spain) was applied following a protocol previously developed for the analysis of lipid peroxidation products[51–54]. Briefly, first the stationary phase was equilibrated with 1 mL of MeOH and 1 mL of water. Then, the supernatant of the centrifuged sample (approximately 900 µL) was loaded followed by washing with 1 mL of H_2O. Finally, the samples were eluted with 100 µL four times with ethyl acetate. The eluate was evaporated using a miVac centrifugal vacuum concentrator from Genevac LTD (Ipswich, UK) and dissolved in 60 µL solution of H_2O (0.1% v/v HCOOH, pH 3):CH_3OH (85:15 v/v).

6.3.5 UPLC-MS/MS analysis of dihomo-IsoPs and dihomo-IsoFs total parameters

An Acquity-Xevo TQS system from Waters (Milford, MA, USA) using negative electrospray ionization (ESI−) was employed for UPLC-MS/MS analysis. Chromatographic separation and ESI interface conditions were selected according to previously published methods[51–54]. A Waters BEH C18 reversed phase column (2.1×100 mm, 1.7 µm) was used. Flow rate, column temperature and injection volume were set at 450 µL min^{-1}, 45 °C and 9 µL, respectively. A binary mobile phase H_2O (0.1% v/v HCOOH):CH_3CN (0.1% v/v HCOOH) gradient with a total runtime of 7.0 min was run as follows: from 0.0 to 0.1 min 15% v/v

CH_3CN (0.1% v/v HCOOH) (i.e. mobile phase channel B); from 0.1 to 5.0 min %B increased up to 40%; from 5.0 to 6.0 min %B increased up to 75%; between 6.0 and 6.15 conditions were held constant at 75% B followed by the return to initial conditions (i.e. 15% B) between 6.15 and 6.25 min; conditions were maintained for 0.75 min for system reequilibration. ESI interface conditions were selected as follows: negative mode; capillary voltage to 2.9 kW; source and desolvation temperatures were 150 °C and 395 °C respectively; and nitrogen cone and desolvation gas flows were 150 and 800 L h^{-1}.

In order to determine the chromatographic profile of the in-vitro formation of dihomo-IsoPs and dihomo-IsoFs, the processed AdA oxidized samples (i.e. blank sample, 0, 2, 4, 6, 8, 10, 24, and 30 h) were injected into the UPLC-MS/MS system and detected in Selected Ion Monitoring (SIM) mode employing previously reported m/z ratios of parent ions for dihomo-IsoP and dihomo-IsoF isomer detection[53]. Once chromatographic profiles and parent ions of total parameters were established, the processed AdA oxidized samples were detected in daughter ion scan (i.e. product ion scan) mode (cone voltage: 30 V, collision energy: 30 eV, mass range: 105–397). The Collision Ion Dissociation (CID) patterns obtained were analyzed and the most intense product ions were identified for each total parameter. Thereafter, collision energy and cone voltages were optimized testing different combinations in a Multiple Reaction Monitoring (MRM) experiment. The MRM transition with the highest intensity after the optimization was selected for each total parameter. Extracts of plasma and urine samples were analyzed employing the parameters shown in **Table 6.1**. MassLynx™ 4.1 from Waters (Milford, MA, USA) was used for data acquisition and processing. Further data analysis was performed in Matlab R2017a (MathWorks, Natick, MA, USA).

Table 6.1 Mass spectrometric parameters and chromatographic window selected for the total parameters.

Analyte	m/z Parent ion	Cone [V]	CE [eV]	m/z Daughter Ions	Chromatografic window [min]	Internal standard
Dihomo-IsoPs	381.00	20	20	143.00	5.3 – 6.5	$PGF_{2\alpha}$-d4
Dihomo-IsoFs	397.00	35	25	155.00	3.5 – 6.5	$PGF_{2\alpha}$-d4
$PGF_{2\alpha}$-d4	357.00	40	30	197.00	4.97	-

6.4 Results and discussion

6.4.1 ULPC-MS/MS characterization of AdA non-enzymatic peroxidation products

Dihomo-IsoPs and dihomo-IsoFs formed by free-radical oxidation of AdA is a set of compounds with a vast number of isomers extensively studied in the literature[420,423,425,426,434]. They show similar chemical structures and only some of these isomers can be resolved chromatographically resulting in multiple and overlapping peaks. Furthermore, only a limited number of pure analytical standards for the quantitation of those isomers is commercially available or has been described in the literature[269,420,425,431]. It is also unclear to what extent of

knowledge on the augmentation of levels of specific isomers adds to the final interpretation in clinical studies[268]. In this work, an alternative top-down approach for the semi-quantitative measurement of total dihomo-IsoP and dihomo-IsoF isomers is presented. This approach potentially allows a straightforward determination of dihomo-IsoP and dihomo-IsoF substance classes in biological samples for their application as biomarkers in the clinical environment.

During analytical method development, the formation of AdA-derived lipid peroxidation products by free-radical attack in an in-vitro experiment with different reaction times was characterized by UPLCMS/MS. For this purpose, the ions $[C_{22}H_{38}O_5\text{-}H]^-$ (m/z=381) and $[C_{22}H_{38}O_6\text{-}H]^-$ (m/z=397) were monitored for dihomo-IsoPs and dihomo-IsoFs, respectively, taking into account the common molecular formulae of these compounds illustrated in **Figure 6.2**[420,423,434]. The chromatographic elution window for each total parameter under the employed chromatographic settings was assessed examining the SIM chromatograms of the parent ions for dihomo-IsoPs (m/z=381) and dihomo-IsoFs (m/z=397) as shown in **Figure 6.1**. For dihomo-IsoPs the intensities of the peaks between 5.3 and 6.5 min increased with incubation time. Likewise, for dihomo-IsoFs an increase was observed with a slight shift of the elution window between 3.5 and 6.5 min. The higher predicted logP for dihomo-IsoPs (i.e. 0.7 more than dihomo-IsoFs)[435] might explain the difference in the observed retention time windows. The above-mentioned ranges were established as elution windows for total dihomo-IsoPs and dihomo-IsoFs, respectively.

The oxidized AdA samples were re-injected in daughter ion scan mode to obtain CID patterns at different reaction times. The combined spectra of the scans acquired during the corresponding elution windows for each total parameter are shown in **Figure 6.1**. Regarding dihomo-IsoP product ions, the most abundant m/z were 139, 143, 157, and 155, while in the case of dihomo-IsoFs 139, 143, 155, and 183 m/z were the most intense product ions. For optimum sensitivity, different collision energies and cone voltages were tested (see **Supplementary figure AI.2.1** and **Supplementary figure AI.2.2**). In general, the collision energy had a great impact on the sensitivity, while the cone voltage showed to be less critical. For all values tested, the most sensitive MRM transitions (i.e. the pairs parent > daughter) were 381 > 143 for dihomo-IsoPs and 397 > 155 for dihomo-IsoFs. The selected transitions for both total parameters have been assigned to the 7-series dihomo-IsoPs[423] and 17-series dihomo-IsoFs[420] and have been employed previously for the quantification of certain dihomo-IsoP and dihomo-IsoF isomers[53,268,269,425,431,434]. The fragmentation patterns suggest a charge remote ion mechanism with previous 1 [3]-sigmatropic shift for the 7-series dihomo-IsoPs[436,437]. The structures with the proposed fragments are illustrated in **Figure 6.2**. The optimum MS detection conditions selected for the determination of total dihomo-IsoPs and dihomo-IsoFs based on the analysis of in-vitro oxidized AdA are shown in **Table 6.1**.

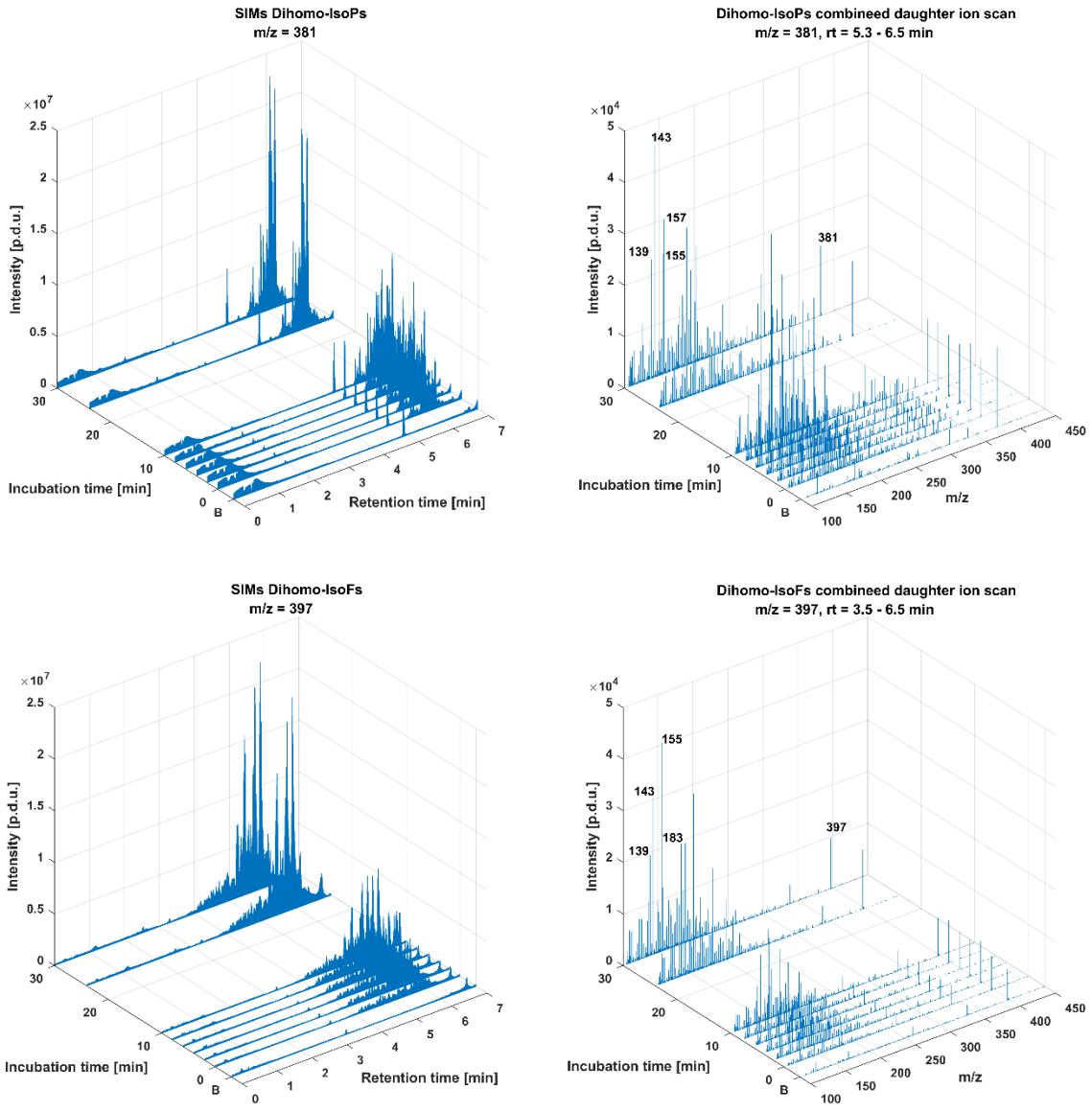

Figure 6.1 SIM (left) and daughter ion scan (right) chromatograms of dihomo-IsoPs (top) and dihomo-IsoFs (bottom) obtained at different reaction times from AdA.

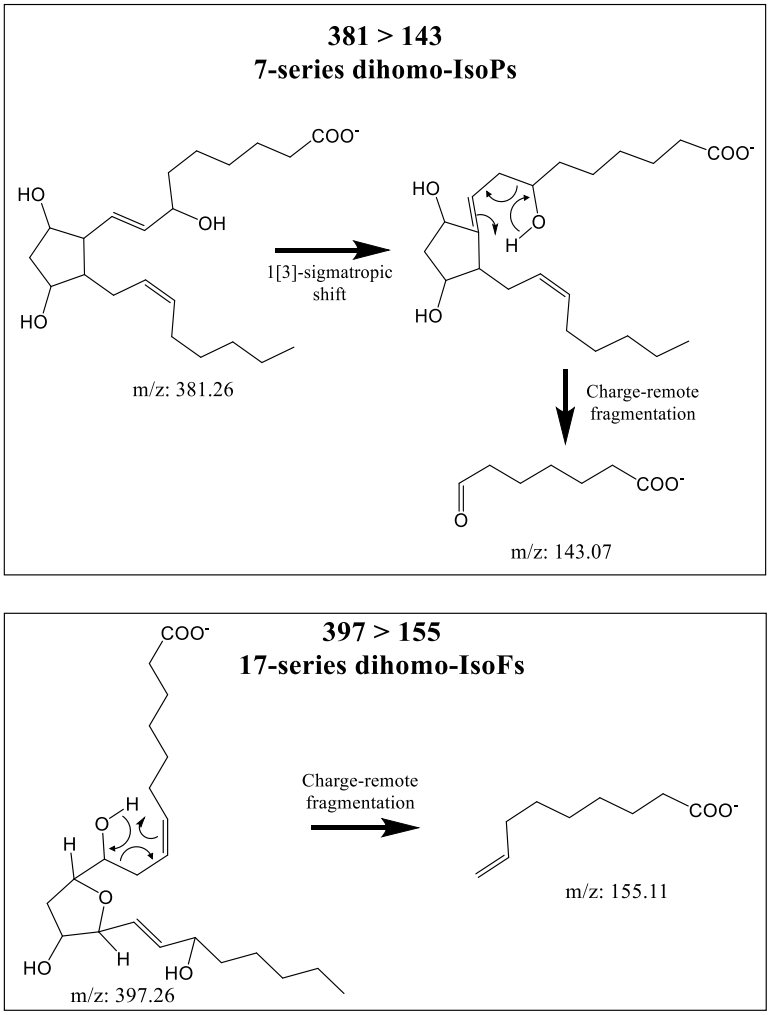

Figure 6.2 MRM transitions selected for the total parameters and proposed fragmentation mechanisms.

6.4.2 Total dihomo-IsoPs and dihomo-IsoFs in urine and plasma samples

A total of 75 plasma and 23 urine samples from preterm infants were analyzed by UPLC-MS/MS employing the parameters of the experimental conditions selected for dihomo-IsoP and dihomo-IsoF. Chromatographic profiles of representative samples for each matrix are plotted in **Figure 6.3** together with an in-vitro oxidized AdA standard solution and a blank. In urine samples, several peaks were observed at the same retention time and resolution as in-vitro oxidation products (i.e. peaks at ≈ 5.8, 6.1 and 6.2 min for dihomo-IsoPs and ≈5.5 and 5.75 for dihomo-IsoFs). Furthermore, additional peaks appear partially overlapped or at different retention times. In the case of plasma samples, no distinguishable dihomo-IsoP peaks were observed. In contrast, for dihomo-IsoFs two poorly resolved peaks at ≈ 5.5 min were measured.

The area of the entire chromatographic elution window, as determined during the analysis of oxidized AdA standards for each total parameter was selected as a response variable and the limit of quantification (LOQ) was defined as 10 times the blank area. With this cut-off value, both total parameters were detected in most of the urine samples (≥70%). However, for plasma samples only dihomo-IsoFs were detected in a small number of samples. The precision of the determinations was evaluated by the Relative Standard Deviation (RSD) of technical replicates of QC samples (i.e. pooled study samples) and satisfactory values ≤10% were obtained. The percentages of samples above the LOQ (> LOQ) and the precision measurements are shown in **Table 6.2**.

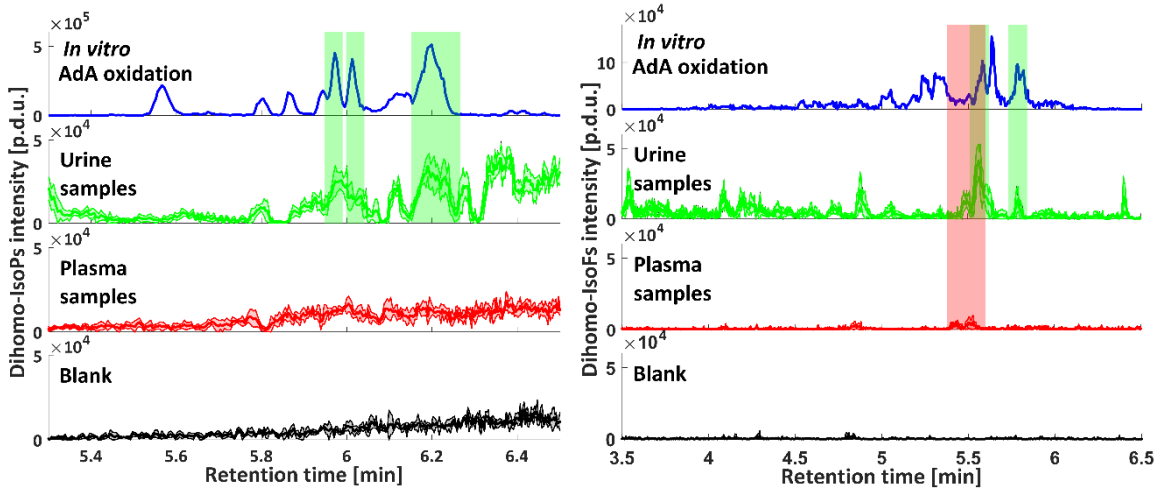

Figure 6.3 Chromatograms of total dihomo-IsoPs (left) and dihomo-IsoFs (right). AdA in-vitro non-enzymatic peroxidation products after t=2 hours and mean ± standard deviation (thick line and the light shade, respectively) of chromatograms of total parameters measured in 3 replicates of urine samples, plasma samples, and blanks.

In order to compensate signal fluctuations originating from instrumental noise and sample treatment, the areas detected in samples > LOQ were normalized by the area of the IS resulting in relative responses. The obtained relative responses given in procedure defined units (p.d.u.) allow a comparison of results between different batches of samples. Fig. 4 shows boxplots of relative responses obtained for both total parameters detected in blanks, urine and plasma samples. In urine samples, the dihomo-IsoPs mean relative response was 16 times higher than that found in the blanks. For dihomo-IsoFs, the mean relative response was 13 and 90 times higher than for blanks in plasma and urine samples, respectively. Urine samples showed a relatively large interquartile range compared to plasma samples. The fact that dihomo-IsoPs were <LOQ in plasma samples, while they could be detected in the majority of urine samples might be an indicator for the dynamics of dihomo-IsoP formation/excretion as it suggests that the maximum plasma concentration formed from oxidation of AdA remainsbelow the LOQ for the experimental methods used, whereas, dihomo-IsoPs were detected in excreted urine from the same infants. Conversely, dihomo-IsoFs showed a different profile: they were formed after dihomo-IsoPs at sustained oxygen tensions[420,425], and hence they were still present

in plasma at the time of sampling and were excreted at higher concentrations in a similar way as described for NeuroFs[51]. This observation is important for the design of future clinical study protocols that aim at targeting those biomarkers in biofluids.

Table 6.2 Percentage and number of samples >LOQ as well as RSD in % of QC sample replicates for each matrix and total parameter.

Analyte	Samples >LOQ [%]		RSD QCs [%]	
	Urine (N = 23)	Plasma (N = 75)	Urine (N = 3)	Plasma (N = 3)
Dihomo-IsoPs	70	0	10	-
Dihomo-IsoFs	100	12	4	9

The developed method allows the simultaneous relative determination of the total sum of 7-series dihomo-IsoPs and 17-series dihomo-IsoFs. In urine, this method proved sufficient sensitivity for detecting relevant concentrations in clinical samples, whereas sensitivity in plasma samples should be improved in order to enable detection of dihomo-IsoPs in the majority of samples. This could potentially be achieved by increasing the pre-concentration factor by using higher sample volumes or by modifying the hydrolyzation procedure. It should be noted that the basic/enzymatic hydrolysis employed during the preprocessing of biofluids allowed to detect the sum of free and esterified/glucuronide conjugated forms, however, this analytical method could be applied omitting the hydrolysis step in order to evaluate free forms independently. For clinical validation of the study parameters a larger study population needs to be tested and different sample collection time points are needed for a comprehensive assessment of dynamic concentration ranges. Finally, the sensitivity and selectivity of total dihomo-IsoPs and total dihomo-IsoFs for detecting brain injury in clinically relevant settings has to be studied.

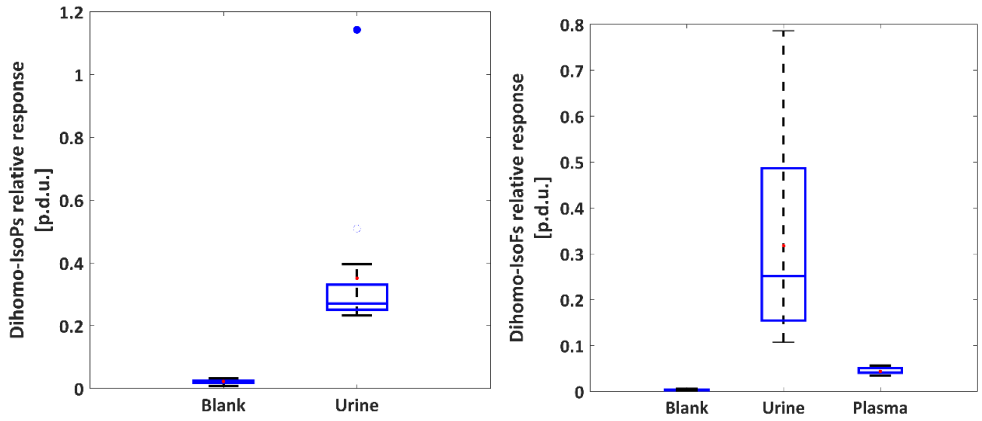

Figure 6.4 Boxplots of total dihomo-IsoPs (left) and dihomo-IsoFs (right) for blanks (N = 11), urine (N = 23) and plasma (N = 9) samples. Boxes indicate the 1st and the 3rd quartiles, the median is shown as a blue line, whiskers mark the 9th and 91st percentiles, red circles represent mean concentrations and blue circles are outliers.

6.5 Conclusions

In-vitro peroxidation of AdA was characterized by CID experiments allowing to select the most sensitive and selective MRM transitions for dihomo-IsoPs and dihomo-IsoFs (381 > 143 and 397 > 155, respectively). The selected measurement conditions were implemented in a UPLC-MS/MS method and applied to urine and plasma samples from preterm infants. Dihomo-IsoFs could be detected in both matrices (i.e. urine and plasma), however, dihomo-IsoPs were detected exclusively in a limited number (12%) of urine samples. This suggests that the plasmatic dihomo-IsoP concentration was low (i.e. below the LOQ) at the studied sampling time due to the formation and excretion rates. These results enable the design of future studies necessary to establish the accumulation and excretion patterns of total dihomo-IsoPs and total dihomo-IsoFs and compare them to the obtained regio- or stereoisomer profiles. The usefulness of the total parameters as biomarkers for brain injury will have to be assessed in bigger cohorts of study subjects with well-defined clinical conditions.

Chapter 7 Biomarkers of oxidative stress derived damage to proteins and DNA in human breast milk

7.1 Abstract

Oxidative stress derived biomarkers have been extensively studied for assessing pathological situations in the neonatal period and their usefulness for an early outcome prediction of oxidative stress related diseases in non-invasive biofluids could be demonstrated. This is the first report on a method for the simultaneous detection of a panel of oxidative stress related biomarkers for quantifying damage to proteins and DNA in human breast milk samples. A straightforward sample clean-up procedure using 1.5 mL of milk was developed and extracts were analyzed by ultra-performance liquid chromatography coupled to tandem mass spectrometry. The analytical method was validated and applied to human milk samples from a cohort of mothers of preterm infants, as well as donor human milk samples before and after pasteurization at a human milk bank. The results demonstrate the feasibility of this method for the analysis of a panel of oxidative stress related biomarkers, reporting ranges found in human milk.

7.2 Introduction

The most recent definition of oxidative stress (OS) has been provided by Sies et al.[43] as "an imbalance between oxidants and antioxidants in favor of the oxidants, leading to a disruption of redox signaling and control and/or molecular damage". In the field of perinatology, the role of OS is essential since the developing fetus, and then the newborn, are particularly susceptible to the effects of oxidants[60].

Fetal life elapses in a low oxygen atmosphere, and maturation of the lung, surfactant and antioxidant defense system only occurs very late in gestation. Therefore, babies born prematurely are not endowed with an adequate physiology to face a brisk increment in tissue oxygenation derived from respiration. Consequently, with the initiation of breathing immediately after birth and the need for oxygen supplementation for postnatal stabilization in the delivery room, a burst of oxygen free radicals is generated. Free radicals are extremely aggressive byproducts of incomplete oxygen reduction with an extremely short half-life that

cause structural and functional damage to nearby cellular components such as lipids, proteins, nucleic acids, etc. The consequences of oxidative stress can be damage to lung, myocardium, retina, intestine or brain[438].

Maternal OS has also been studied and both, maternal and perinatal OS were correlated with several pregnancy and perinatal conditions including prematurity[169,214,438–443]. At the same time, inflammatory processes are risk factors for preterm birth[60,444]. Indeed, OS and inflammation are interconnected and a paradigmatic example for this link is the action of neutrophils[43,445,446]. Neutrophils are the most abundant white blood cells in humans playing an essential role during the inflammatory response and they are key for killing bacteria and other microorganisms. The generation of a wide range of oxidant species by neutrophil myeloperoxidase (MPO) that destroy the pathogen is part of the complex mechanism of action of neutrophils[445]. Hypochlorous acid is one of these oxidant species which during MPO activity produces the chlorination of tyrosine residues forming 3-chlorotyrosine (3Cl-Tyr), which has been widely described as a biomarker of infection[284,445,447].

The assessment of OS may be carried out by quantification of the oxidants/antioxidants imbalance by measuring the oxidized-to-reduced ratio of selected antioxidants (e.g. glutathione). However, OS-mediated damage is a complex phenomenon that involves intricate repair pathways[43]. A complete appraisal of effects of OS on an organism can only be obtained by means of the analysis of biomarkers of damage to macromolecules such as lipids (e.g. peroxidation products), proteins or nucleic acids[43,60,438]. On the other hand, biomarkers of oxidative-related inflammation such as 3Cl-Tyr in addition to OS biomarkers, allow to obtain a more detailed vision of disruptions of the network of redox steady states[445].

Analytical methods for quantification of the above-mentioned biomarkers in perinatology have been reported in the literature during the last decades[60,438,448]. Gas Chromatography coupled to Mass Spectrometry (MS) and Liquid Chromatography coupled to tandem MS (LC-MS/MS) emerged as the most reliable techniques[438]. Recently, methods for analysis of lipid peroxidation products in urine[51,52], plasma[54], and serum[55] and biomarkers of damage to proteins and DNA in urine[231], plasma[449], amniotic fluid[284] and tissues[449] were developed employing Ultra Performance LC-MS/MS and applied to several studies related to the neonatal period involving biofluids and tissues from newborns and animal models.

Breast milk is a non-invasive and highly accessible biofluid that has been analyzed to quantify maternal OS[283,330,441,443,450–453]. However, multi-biomarker analysis of OS has not been reported in the scientific literature. Breastfeeding is the gold standard for newborn infant nutrition and especially for the high risk population of preterm infants[283,454]. Beyond nutritional aspects, human milk contains a wide spectrum of bioactive compounds which improves the regulation of the gastrointestinal tract and the immune system, contributing to disease prevention, infant growth, and development[454–457]. When own mother's milk is not available, the use of donor human milk (DHM) from human milk banks (HMB) is the best alternative for feeding of the (preterm) newborn[458]. DHM must be collected, processed, and stored in a way

that ensures its microbiological safety and nutritional quality. Holder pasteurization (62.5 ˚C, 30 min) is generally employed by HMBs to inactivate all non-spore forming and potentially pathogenic microorganisms. Processing (pasteurization and freezing) of expressed breast milk likely decreases the availability and function of a number of bioactive substances and microorganisms[458,459]. Antioxidants, enzymes and lipid peroxidation biomarker changes have been observed after pasteurization[460–463]. However, the effect of pasteurization on biomarkers of protein and DNA damage by OS has not been studied.

In this work we present the first method for the quantification of a panel of biomarkers of oxidative damage to proteins and DNA for assessing OS and inflammation in human breast milk samples employing a straightforward solid phase extraction (SPE) clean-up followed by ultra performance liquid chromatography (UPLC)-MS/MS analysis. The method was validated according to the FDA guidelines for bioanalytical method validation and then applied to samples of human milk from mothers of preterm infants and DHM samples from a milk bank before and after pasteurization.

7.3 Material and methods

7.3.1 Standards and reagents

Primary standards of o-tyrosine (o-Tyr), m-tyrosine (m-Tyr), phenylalanine (Phe), $3NO_2$-tyrosine (3NO2-Tyr), 3Cl-Tyr, p-tyrosine (p-Tyr), 8-Oxo-2'-deoxyguanosine (8OHdG) and 2-deoxyguanosine (2dG) (>96% w/w purity) were obtained from Sigma-Aldrich (St. Louis, MO, USA). Deuterated phenylalanine (Phe-D5) was purchased from CDN Isotopes (Pointe-Claire, Canada). 8-Oxo-20-deoxyguanosine-$^{13}C^{15}N_2$ (8OHdG-$^{13}C^{15}N_2$) and 20-deoxyguanosine-$^{13}C^{15}N_2$ (2dG-$^{13}C^{15}N_2$) were obtained from Toronto Research Chemicals (Toronto, Canada) and deuterated p-Tyrosine (p-Tyr-D2) from Cambridge Isotope Laboratories (Tewksbury, EEUU). Purities of all isotopically labeled compounds were >98% w/w.Water was Milli-Q® grade (>18.2 MU) dispensed from a Milli-Q® integral system (Darmstadt, Germany). Methanol and acetonitrile (LC-MS grade) where purchased from JT Baker (Deventer, Netherlands) and sodium hydroxide (NaOH), phosphoric acid and formic acid were acquired from PanReac Química (Barcelona, Spain).

7.3.2 Collection and storage of human milk samples

7.3.2.1 Human milk from mothers of preterm infants

Human milk samples from mothers of preterm infants were collected in a prospective, observational cohort study. Eligible infants were born at a gestational age ≤32 weeks and exclusively fed with own mother's milk. Exclusion criteria were severe congenital

malformations, intestinal surgery and chromosomopathies. The first aliquot of human milk was collected after achieving exclusive enteral nutrition of above 150 mL kg-1 day-1 and once per week thereafter. The mothers were followed for up to four weeks or until hospital discharge of the newborn. Milk was extracted manually or using a milk pump after receiving instructions from the nurse. Aliquots of the total volume of expressed breast milk collected during each extraction of ≥20 mL were placed in sterile glass vials and stored at -20 ºC until analysis. 59 human milk samples from 31 mothers were considered in this study. The Ethics Committee for Biomedical Research of the Health Research Institute La Fe (Valencia, Spain) approved the study protocol. Informed consent was obtained from all participants. All methods were performed in accordance with the relevant guidelines and regulations.

7.3.2.2 DHM samples before and after pasteurization

DHM samples were obtained from the Regional HMB "Aladina-MGU" located at the Hospital Universitario 12 de Octubre (Madrid, Spain). Milk collection was performed following a specific protocol for donor mothers approved by the local ethics committee (ethical approval code: 12/325) and informed consent was obtained from each donor. Milk was collected at home using either electric or manual pumps and transported to the HMB in an insulated box provided with ice packs. DHM samples from multiple donors were stored frozen (-20 ºC) until processing. DHM was thawed in a shaking water bath at 37 ºC and pooled in a sterile Pyrex bottle. An aliquot from each pool was separated before pasteurization, whereas the rest of the pool was pasteurized (62.5 ºC for 30 min). Then, milk samples were cooled in a shaking water bath providing temperature control (Jeio Tech BS-21; Lab Companion, Seoul, Korea) filled with ice-cold water. Once the temperature reached 4 ºC, DHM aliquots were stored at -20 ºC until analysis. A thermometer, coupled to an external temperature sensor (Mesa Labs, Inc., Lakewood, Colorado, USA), was dipped into a control bottle (cow's milk) and used to monitor the temperature of the milk batch during the whole heating/cooling process. The water bath maintained the required temperature with a precision of ±0.2 ºC. A total of 13 pools were processed following the procedure described above.

7.3.3 Preparation of stock, working and standard solutions

Stock solutions of o-Tyr (3 mmol L^{-1}), m-Tyr (3 mmol L^{-1}), Phe (60 mmol L^{-1}), 3NO_2-Tyr (2 mmol L^{-1}), 3Cl-Tyr (3 mmol L^{-1}), p-Tyr (4 mmol L^{-1}), 8OHdG (1 mmol L^{-1}), 2dG (1 mmol L^{-1}), Phe-D5 (1 mmol L^{-1}), 8OHdG-13C15N2 (1 mmol L^{-1}) and 2dG-$^{13}C^{15}N_2$ (1 mmol L^{-1}) were prepared by dissolving adequate amounts of pure, solid standards in H20 (0.1% HCOOH) and stored at -20 °C. Working solutions were obtained by dilution of stock solutions and were used for preparing mixtures for internal standards (IS), calibration and spiking solutions which were aliquoted and kept at -20 °C in capped vials and went through a single freeze-thaw cycle. Standard solutions were prepared by serial dilution of the calibration mixture in the concentration intervals summarized in **Table 7.1**.

7.3.4 Sample preparation

Frozen milk samples were thawed on ice. After that, samples were homogenized and centrifuged at 1200 g for 30 min at 4 °C. The top insoluble layer was discarded and 1 mL of supernatant were added to 1 mL of phosphoric acid solution (5 % w/v). 10 µL of IS mixture solution containing 20 µmol L^{-1} of Phe-D5, 8OHdG-$^{13}C^{15}N_2$ and 2dG-$^{13}C^{15}N_2$ were added followed by homogenization and centrifugation at 16000 g for 5 min at 4 °C. For extraction and pre-concentration of diluted samples, SPE was carried out employing ISOLUTE®-96 ENV+ (96 well, 40 mg) plates from Biotage (Uppsala, Sweden). Plate wells were conditioned with 1 mL of CH_3OH and 1 mL of H_2O. 2 x 800 µL of diluted human milk were loaded onto the plate wells at a flow rate of approximately 1 mL min^{-1}. Each well was washed with 2 x 300 µL of H_2O and samples were eluted using 300 µL of NaOH (0.1 mmol L^{-1}) aqueous solution and 2 x 300 µL of acetonitrile. Recovered eluates were evaporated and re-dissolved in 60 µL of H_2O (0.1% HCOOH v/v). Ten-fold dilutions were prepared by mixing 5 µL of sample extract with 45 µL of H_2O (0.1% HCOOH v/v) and both, the concentrated and diluted samples were analyzed by UPLC-MS/MS.

7.3.5 LC-MS/MS measurements

UPLC-MS/MS analysis was based on a validated method developed previously by our group[231]. It was carried out on an Acquity–Xevo TQ system (Waters, Milford, MA, USA) equipped with an electrospray ionization source working in positive mode (ESI+) and the following conditions: capillary 0.50 kV, cone 21.00 V, extractor 3.00 V, source temperature 120 °C, desolvation temperature 400 °C, nitrogen cone and desolvation gas flows were 50 and 750 L h^{-1}, respectively. Multiple reaction monitoring was performed using the instrumental parameters summarized in **Table 7.1**. The dwell time was set to 5 ms to ensure a minimum of 10 data points per peak. An Acquity UPLC BEH C18 reversed phase column (2.1x50 mm, 1.7 µm) from Waters and a CH_3OH (0.05% v/v HCOOH):H_2O (0.05% v/v HCOOH) binary gradient were used for chromatographic separation of compounds. Flow rate, column temperature and injection volume were set at 0.4 mL min-1, 30 °C and 5 µL, respectively. The gradient employed was as follows: from 0 to 1 min 0% v/v CH_3OH (0.05% v/v HCOOH) (i.e. channel B), from 1 to 2.5 min from 0 to 15% v/v B and from 2.5 to 4.5 from 15 to 99% v/v B. Conditions were maintained for 0.25 min followed by returning to initial conditions between 4.5 and 5.1, which were held for 0.9 min for system re-equilibration. During batch analysis, samples were kept at 4 °C in the autosampler. MassLynx 4.1 and QuanLynx 4.1 software (Waters) was used for data acquisition and processing, respectively. Linear response curves for each analyte were calculated employing IS indicated in **Table 7.1**.

Table 7.1 Acquisition parameters and main figures of merit of the method.

Analyte	m/z Parent ion	Cone [V]	CE [eV]	m/z Daughter Ions	RT ± s [min]	Calibration range [nmol L^{-1}]	R^2	LOD [nmol L^{-1}]	LOQ [nmol L^{-1}]	IS
8OHdG	284.10	20	15	168.10	3.22 ± 0.03	1.7 – 216.8	0.990	0.03	0.1	8OHdG-$^{13}C^{15}N$
2dG	268.00	15	10	152.00	2.55 ± 0.03	0.8 – 867.0	0.996	0.03	0.1	2dG-^{13}C
3Cl-Tyr	216.10	25	15	170.10	3.15 ± 0.05	13.5 – 867.0	0.999	0.3	1.0	Phe-D_5
3NO_2-Tyr	227.10	25	15	168.10	3.38 ± 0.06	27.1 – 867.0	0.988	0.6	2.0	Phe-D_5
o-Tyr	182.10	30	15	136.10	2.68 ± 0.02	13.5 – 867.0	0.994	0.3	1.0	Phe-D_5
m-Tyr					1.88 ± 0.03	6.8 – 216.8	0.98	0.2	0.5	p-Tyr-D_2
p-Tyr					1.42 ± 0.04	169.3 – 173400.0	0.993	4	12.7	p-Tyr-D_2
Phe	166.10	25	15	120.10	3.03 ± 0.03	169.3 – 173400.0	0.998	4	12.7	Phe-D_5
8OHdG-$^{13}C^{15}N$	287.00	25	10	171.00	3.22 ± 0.02	-	-		-	-
2dG-^{13}C	271.00	15	10	117.2	2.54 ± 0.02	-	-		-	-
p-Tyr-D_2	184.10	15	20	138.09	1.42 ± 0.02	-	-		-	-
Phe-D_5	171.10	35	10	125.00	3.00 ± 0.03	-	-		-	-

7.3.6 Partial validation

A partial validation of the analysis method originally developed for the determination of OS biomarkers in urine samples[231] was carried out following the FDA guidelines for bioanalytical method validation[15]. A written standard operation procedure was elaborated including the figures of merit assessed in the partial validation, i.e. accuracy, precision, selectivity, limit of detection (LOD) and quantification (LOQ) which was carried out employing a pooled human milk sample. All aliquots from the pooled human milk sample employed for method validation were prepared and analyzed by triplicate on each validation day. Supernatants of human milk obtained after centrifugation were fortified by adding standard mixtures at three concentration levels before sample clean-up employing SPE. Accuracy was assessed calculating % recoveries from spiked pooled milk samples by comparing measured concentrations to the spiking concentrations (see **Table 7.2**) taking into account the concentrations found in the same sample without spiking. Precision was determined in spiked samples by calculating the relative standard deviation (% RSD) of replicates (n = 3). Both parameters were assessed within one validation batch (intra-day) and between three measurement days (inter-day). Selectivity was evaluated by analyzing solvent blanks as well as non-spiked and spiked pooled human milk samples. The LOD and LOQ values of the studied metabolites in human milk were estimated as the concentrations providing a signal-to-noise ratio of three and ten in calibration standards, respectively; alternatively, for p-Tyr and Phe LOQs were set at the lowest concentration level studied.

7.4 Results and discussion

7.4.1 Quantification of OS biomarkers in human milk samples

Chromatographic as well as mass spectrometric parameters were optimized in our previous work[231] obtaining validated instrumental settings for UPLC-MS/MS analysis of the target compounds. The development of sample preparation and clean-up for human milk samples was guided by manufacturer's instructions of the employed SPE micro-well plates and a previous work describing the determination of 8OHdG in human milk[464]. In order to achieve suitable performance for the whole panel of target biomarkers, the washing and elution steps had to be optimized in terms of solvent types and volumes. Analytical figures of merit obtained for the determination of concentrations of selected OS biomarkers in human milk employing optimized conditions as described in section 2.4 are summarized in **Table 7.1**. Retention times were reproducible with standard deviations ≤ 0.06 min. Linear calibration lines calculated using Phe-D5, 8OHdG-$^{13}C^{15}N_2$ or 2dG-$^{13}C^{15}N_2$ as IS generally covering two to three orders of magnitude were obtained with coefficients of determination (R^2) ≥ 0.98 and homoscedastic residuals as assessed by visual inspection. LODs and LOQs in human breast milk ranged between 0.03 and 4 nmol L^{-1} and 0.1 and 12.7 nmol L^{-1}, respectively.

Figure 7.1 shows chromatograms obtained from a spiked and a non-spiked pooled human milk sample. From chromatograms obtained during the analysis of a non-spiked pooled human milk sample it can be appreciated that all analyte signals were apparently resolved from matrix compounds and symmetric peak shapes were obtained except for $3NO_2$-Tyr that was not detected. Back-calculated recovery values in spiked samples were used to assess accuracy and precision and are shown in **Table 7.2**. For all analytes intra-day recoveries in the range of 90–130% were obtained at all levels. As far as the intra-day precision was concerned, %RSD values ≤ 20 were obtained for all studied analytes except for 3Cl-Tyr at the high spiking level where the intra-day precision was 30% RSD. Obtained intra-day accuracies were similar to inter-day results covering values between 91 and 130%. Inter-day precisions generally also remained ≤ 20 %RSD, with the exception of 8OHdG (medium level), 3Cl-Tyr (medium and high level) and m-Tyr (high level). Taking into account the complexity of human milk and the relatively simple sample clean-up, we consider that the method's performance fits the purpose of simultaneously measuring a whole panel of OS related biomarkers in human milk especially considering that these biofluids are typically collected in clinical studies where a high sample throughput is essential.

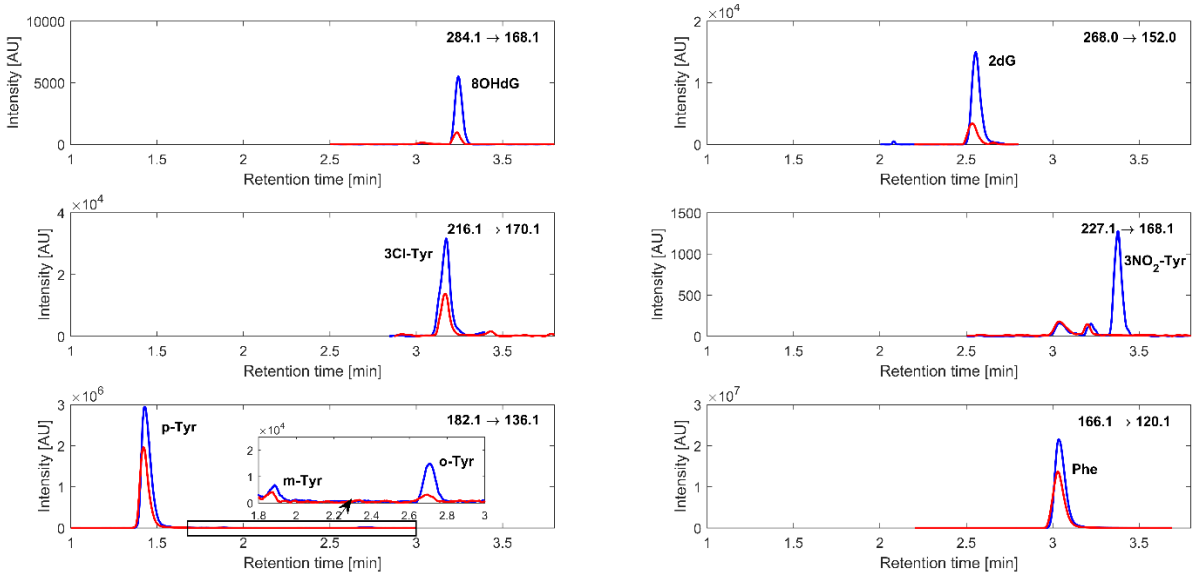

Figure 7.1 Chromatograms of the selected biomarkers obtained during the analysis of a pooled human milk sample extract (red) and a spiked pooled human milk sample extract (blue). Note: spiking concentrations were: 8OHdG: 50 nmol L^{-1}; 2dG: 755 nmol L^{-1}; 3Cl-Tyr: 360 nmol L^{-1}; $3NO_2$-Tyr: 125 nmol L^{-1}; m-Tyr: 60 nmol L^{-1}; o-Tyr: 200 nmol L^{-1}; p-Tyr and Phe: 7300 nmol L^{-1}.

Table 7.2 Back-calculated intra- and inter-day accuracy and precision in spiked milk samples.

Analyte	% Recovery ± s (µmol L^{-1})					
	Intra-day (N=3)			Inter-day (N=3)		
	Low	Medium	High	Low	Medium	High
8OHdG	120 ± 20 (8.3)	106 ± 8 (16.6)	94 ± 13 (24.9)	100 ± 20 (8.3)	120 ± 30 (16.6)	120 ± 20 (24.9)
2dG	92 ± 5 (8.3)	130 ± 20 (16.6)	110 ± 20 (24.9)	99 ± 17 (8.3)	120 ± 20 (16.6)	110 ± 20(24.9)
3Cl-Tyr	130 ± 11 (25.0)	120 ± 20 (49.9)	90 ± 30 (74.6)	122 ± 18 (25.0)	130 ± 30 (49.9)	130 ± 40 (74.6)
$3NO_2$-Tyr	90 ± 20 (25.0)	100 ± 20 (49.9)	100 ± 20 (74.6)	100 ± 20 (25.0)	114 ± 11 (49.9)	117 ± 19 (74.6)
m-Tyr	94 ± 8 (49.9)	110 ± 20 (99.8)	91 ± 6 (149.3)	108 ± 13 (49.9)	118 ± 9 (99.8)	120 ± 30 (149.3)
o-Tyr	100 ± 20 (25.0)	113 ± 7 (49.9)	108 ± 3 (74.6)	91 ± 11 (25.0)	100 ± 20 (49.9)	127 ± 17 (74.6)
Phe*	109 ± 11 (4993.8)	120 ± 14 (9975.1)	101 ± 14 (14925.4)	113 ± 8 (4993.8)	120 ± 20 (9975.1)	110 ± 20 (14925.4)
p-Tyr*	120 ± 20 (4993.8)	105 ± 15 (9975.1)	94 ± 19 (14925.4)	130 ± 20 (4993.8)	121 ± 16 (9975.1)	110 ± 14 (14925.4)

Note: Values within brackets indicate the spiking concentration [µmol L^{-1}] of each metabolite * measured in 1:10 diluted sample.

7.4.2 Analysis of human milk from mothers of preterm newborns

The validated method was applied to the measurement of OS biomarkers in 59 milk samples from 31 mothers of preterm newborns. The obtained concentration ranges are shown in Table 3. For 3Cl-Tyr, p-Tyr, and Phe concentrations >LOQ were found in all samples and 8OHdG, 2dG, m-Tyr, and o-Tyr were quantified in at least 93% of samples. Only in case of 3NO2-Tyr concentrations were <LOQ in all studied samples. Hence, the method's sensitivity proved its suitability for the quantification of OS related biomarkers in human breast milk. A

comparison of the determined metabolites with published concentrations has been carried out. To the best of our knowledge, only 8OHdG, Phe and p-Tyr were measured by other authors in milk samples. Recently, A. De Luca et al.[465] reported concentrations of 11 ± 5 and 13 ± 9 µmol L^{-1} for p-Tyr and Phe, respectively, and P.M.W Lam et al.[464] obtained 0.9 ± 0.3 nmol L^{-1} for 8OHdG employing LC-MS/MS based-methods. Both ranges were not significantly different from those reported in this work of 13 ± 5 and 18 ± 9 µmol L^{-1} for p-Tyr and Phe, and 0.9 ± 0.6 nmol L^{-1} for 8OHdG.

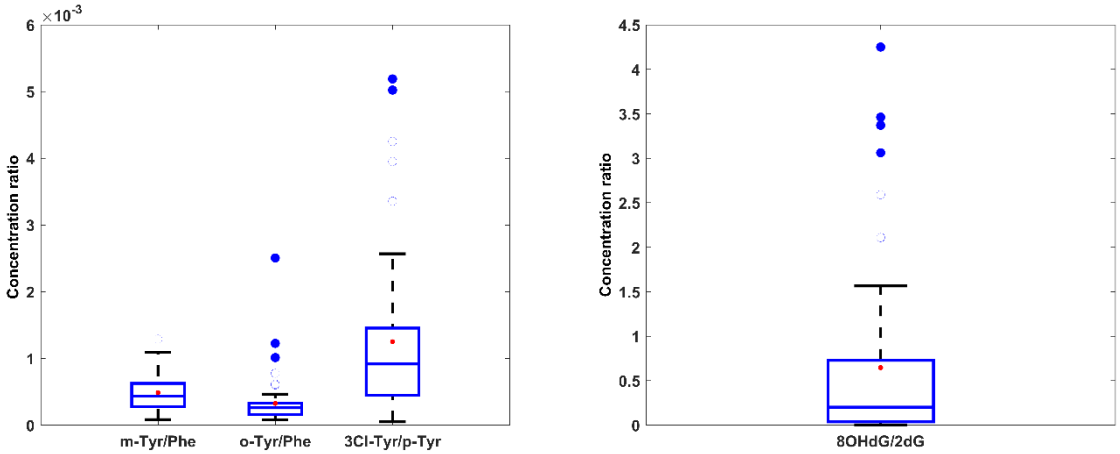

Figure 7.2 Boxplots of m-Tyr/Phe, o-Tyr/Phe and 3Cl-Tyr/p-Tyr ratios (left) and 8OHdG/2dG ratios (right) found in human milk from mothers of preterm infants. Note: boxes indicate the 1st and the 3rd quartiles, medians are shown as blue lines, whiskers mark the 9th and 91st percentiles, red triangles represent mean concentrations, standard (1.5*IQR) and extreme (3*IQR) outliers were plotted as open and closed circles, respectively.

Previously we observed changes in the levels of biomarkers of OS (lipid peroxidation) in urine samples from preterm infants, collected during the entire neonatal period, with the age of the infant[51]. Hence, the influence of sampling times (i.e. from the moment of reaching a stable ingestion above 150 mL of human milk per kg and day and once per week thereafter) on the determined levels of biomarkers of OS were studied. In contrast to our previously reported findings in urine samples, no significant differences in concentrations in dependence of the sample collection time point were found for m-Tyr/Phe, o-Tyr/Phe, 3Cl-Tyr and 8OHdG/2dG ratios in breast milk samples (data not shown).

Boxplots representing the determined ratios of biomarkers of OS to proteins (i.e. m-Tyr/Phe, o-Tyr/Phe, 3Cl-Tyr/p-Tyr) and DNA (i.e. 8OHdG/2dG) in 59 human milk samples are shown in **Figure 7.2**. None of the determined ratios followed a normal distribution (Shapiro-Wilk test, $\alpha = 0.05$) and the highest interquartile range (IQR) was found for 8OHdG/2dG ratio ($IQR_{8OHdG/2dG} = 0.7$) followed by 3Cl-Tyr/p-Tyr ratio ($IQR_{3Cl\text{-}Tyr/p\text{-}Tyr} = 9.9x10^{-4} = 2.8*IQR_{m\text{-}Tyr/Phe} = 5.8*IQR_{o\text{-}Tyr/Phe}$). This biomarker has been used for the assessment of inflammatory processes[284,445] and the correlation between inflammation and prematurity has been widely studied as was reviewed by Cappelletti et al.[444]. Moreover, inflammatory processes

such mastitis are a common condition in lactating women with incidences ranging between 3 % and 20 %[466,467]. Therefore, the detection of 3Cl-Tyr in the study cohort is in concordance with literature reports on inflammatory processes related to prematurity. Future studies with an appropriate study design need to be conducted to elucidate the correlation between the concentration of 3Cl-Tyr or other oxidative stress biomarkers in human milk and pathological conditions.

7.4.3 Analysis of DHM before and after pasteurization

Aliquots from 13 pools of DHM were analyzed before and after Holder pasteurization. NO_2-Tyr and 3Cl-Tyr were not detected in any sample and concentrations of 2dG and m-Tyr above the LOQ were found in 6 and 10 out of 13 samples, respectively. The remaining metabolites in raw and pasteurized human milk were detected in more than 11 samples.

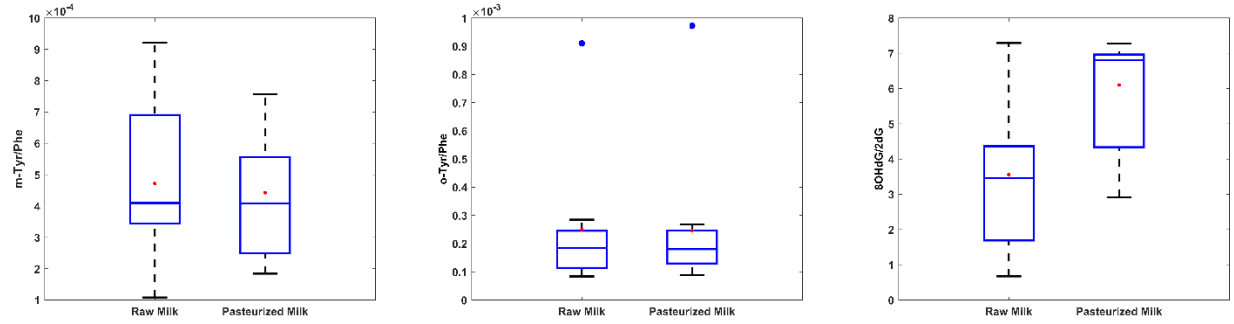

Figure 7.3 Boxplots of m-Tyr/Phe (left), o-Tyr/Phe (middle) and 8OHdG/2dG (right) ratios found in human milk pools before and after Holder pasteurization. Note: boxes indicate the 1st and the 3rd quartiles, medians are shown as blue lines, whiskers mark the 9th and 91st percentiles, red triangles represent mean concentrations, standard (1.5*IQR) and extreme (3*IQR) outliers were plotted as open and closed circles, respectively.

In order to assess the changes of measured ratios during heat treatment, samples measured before and after pasteurization were compared as shown in **Figure 7.3**. For the o-Tyr/Phe ratio, normal distributions with one extreme outlier for raw and pasteurized milk were obtained. The median in the case of raw milk was slightly lower than after pasteurization, but between both distributions no statistically significant differences were detected when a nonparametric paired test was performed (Wilcoxon signed-rank test, $\alpha = 0.05$). For m-Tyr/Phe and 8OHdG/2dG ratios higher IQRs were observed in both groups (i.e. raw milk and pasteurized milk). For m-Tyr/Phe ratios, medians remained unchanged (Wilcoxon signed-rank test, $\alpha = 0.05$). Regarding 8OHdG/2dG ratios, the median value for pasteurized milk was higher than for raw milk, but changes were not significant (Wilcoxon signed-rank test, $\alpha = 0.05$). In summary, we did not observe significant changes in any of the parameters under the studied pasteurization conditions. However, in the case of 8OHdG/2dG ratios, the detected increase in the median suggests a possible degradation of 2dG during the pasteurization process.

7.5 Conclusions

This work presents an analytical tool for the simultaneous determination of a panel of OS biomarkers suitable for the determination of free radical mediated damage to proteins and DNA in human milk samples. Small volumes (1.5 mL) were processed employing SPE allowing the simultaneous clean-up of 96 samples. Extracts were analyzed employing UPLC-MS/MS with a total runtime of 6 min per sample. Therefore, this analytical workflow is suitable for the analysis of human milk samples providing an acceptable throughput for large scale clinical studies. In addition, the method's performance was assessed following FDA guidelines of bioanalytical method validation.

The measurement of 59 human milk samples from 31 mothers of preterm infants was used to prove the usefulness of the developed analytical method. In the studied cohort, in general, the studied biomarkers could be quantified, with exception of $3NO_2$-Tyr, which was found below the LOQ. Concentrations were similar to those reported in literature for 8OHdG, Phe and p-Tyr. However, it has to be highlighted that for the majority of metabolites studied here (2dG, m-Tyr, o-Tyr, 3Cl-Tyr, $3NO_2$-Tyr) this is the first time that concentration ranges have been reported in human milk samples. From the results we conclude that determined ratios of biomarkers of OS do not vary during the neonatal period of the infant. Furthermore, the quantification of the 3Cl-Tyr/p-Tyr ratio in human milk samples could be of potential interest for the assessment of inflammation in different clinical scenarios.

The analysis of human milk samples before and after pasteurization did not reveal changes in the detected metabolite ratios, indicating that both raw and pasteurized milk may be used for the assessment of OS biomarkers. However, due to an increase in the medians of 8OHdG/2dG we recommend to carry out measurements in raw milk instead of pasteurized milk when possible.

Chapter 8 On-Capillary Surface-Enhanced Raman Spectroscopy: Determination of Glutathione in Whole Blood Microsamples

8.1 Abstract

Oxidative stress monitoring in the neonatal period supports early outcome prediction and treatment. Glutathione (GSH) is the most abundant antioxidant in most cells and tissues, including whole blood, and its usefulness as a biomarker has been known for decades. To date, the available methods for GSH determination require laborious sample processing and the use of sophisticated laboratory equipment. To the best of our knowledge, no tools suitable for point-of care (POC) sensing have been reported. Surface-enhanced Raman spectroscopy (SERS), performed in a microvolume capillary measurement cell, is proposed in this study as a robust approach for the quantification of GSH in human whole blood samples. The use of a silver colloid allowed a highly selective signal enhancement for GSH providing analytical enhancement factors of 3 to 4 orders of magnitude. A highly accurate determination of GSH in whole blood samples with recoveries ranging from 99 to 107% and relative standard deviations less than or equal to 18% were achieved by signal normalization with the intensity of an isotopically labeled internal standard. GSH concentrations were retrieved within 4 min using small-volume blood samples (2 μL). The developed procedure was applied to the analysis of blood of 20 healthy adults and 36 newborns, obtaining comparable results between literature and those found by SERS and a reference method. The characteristics of this novel tool are suitable for its implementation in a portable optical sensor device enabling POC testing of oxidative stress levels in newborns.

8.2 Introduction

Under normal conditions, arterial oxygen saturation in the fetal-to-neonatal transition rises from 55% in the fetus up to more than 95% in the newly born infant within ~10 min, generating physiologic oxidative stress[36,468]. However, in very preterm infants (i.e., <32 week gestation) postnatal stabilization is frequently required. This involves positive pressure

ventilation with an O_2-enriched gas admixture to achieve a normal heart rate and arterial oxygen saturation after birth[170]. Preterm infants are endowed with an immature lung and antioxidant defense system, and therefore supplementation with high oxygen concentrations leads to a pro-oxidant imbalance that causes oxidative stress, disruption of redox signaling and control, and/or molecular damage[43,170]. The consequences are increased morbidity and mortality[169]. Recent 2015 guidelines from the International Liaison Committee on Resuscitation6 recommend to initiate ventilation of term infants with an inspired fraction of oxygen (FiO_2) of 0.21 (i.e., room air) instead of 100% O_2 and preterm infants with an FiO_2 between 0.21 and 0.30. The use of oxygen has contributed to dramatically reduce mortality; however, the negative consequences of oxygen supplementation have been oxidative stress-related diseases such as retinopathy of prematurity, bronchopulmonary dysplasia, or intracranial hemorrhage[169,170]. Recently, we could link a panel of endogenous metabolic biomarkers to oxidative stress-related diseases of the preterm and show that their quantification in biofluids is useful for an early outcome prediction[51] facilitating treatment monitoring of newborns in neonatal intensive care units.

Reduced glutathione (GSH), a tripeptide (γ-glutamylcysteinyl-glycine), is the most abundant low molecular weight endogenous biothiol[236,469] and fulfills a wide range of functions in the metabolism including Phase II detoxification, synthesis of biomolecules, redox signaling, and a central role as part of the antioxidant defense system in charge of scavenging reactive oxygen species to maintain redox homeostasis[236,470]. Moreover, the reduced to oxidized glutathione redox couple (GSH/GSSG) is one of the main determinants of the cytoplasmic redox status[471] indispensable for an adequate cell reproduction, growth, and differentiation. Blood is a readily available biofluid frequently employed for clinical determinations. While GSH concentrations in blood plasma typically range between 2 and 20 μM, GSH concentrations in whole blood are notably high (mM range), as over 95% of GSH is located inside the erythrocytes[472]. GSH quantification in whole blood is hampered by the matrix complexity. Besides, GSH is easily oxidized under normal conditions[102,237,239,469,473], requiring laborious and time-consuming sample processing. The most widely used approaches involve a previous sample derivatization with, for example, N-ethylmaleimide followed by acidic protein precipitation[49,102,237,239,474,475] and a chromatographic or electrophoretic separation with different detectors[49,102,239,474]. Alternative approaches based on enzymatic assays[237] or electrochemical determinations[476] have also been reported. However, none of them enables a direct analysis of GSH, and they suffer from relevant limitations for their application in neonatal intensive care units such as the use of relatively large sample volumes (typically tens to hundreds of microliters of whole blood); time required for sample collection, pretreatment, and analysis; the use of expensive equipment and reagents; and the need of experienced personnel.

Surface-enhanced Raman spectroscopy (SERS) is a promising approach for the development of fast analytical methods. SERS combines the molecular specific information provided by Raman spectroscopy with high sensitivity due to the optical properties of

plasmonic metallic nanostructures[477]. The analytical enhancement factor (AEF), defined as the magnitude of increase in the apparent Raman cross-section of the molecules[478], depends on multiple factors including molecular binding, conformation, orientation, and distribution on the plasmonic substrates taking into account the absorption/desorption process[479]. Therefore, a precise control of atomic-scale parameters is needed to achieve reliable and reproducible quantitative SERS measurements. This is a challenging task, especially for the analysis of complex biofluids and the main limitation of SERS in biomedical applications. Several strategies, such as the use of an internal standard (IS)[480–483] or ratiometric calibrations[482] have been successfully implemented for compensating fluctuations in the SERS signal in aqueous solutions[484,485]. The determination of GSH using SERS in aqueous solutions has been proposed repeatedly[56,484–496], and a recent publication showed the correlation of SERS signal and biothiol concentration in umbilical cord blood samples[56]. However, no approach allowing a reproducible SERS-based quantification of GSH at physiologically relevant concentrations in blood droplets, complying with specifications suitable for clinical determinations, has been reported so far.

This study aimed at the development of a robust on-capillary SERS approach for the fast and direct quantification of GSH in whole blood. The developed approach enables a selective and reproducible GSH determination employing a silver colloid for SERS signal generation and an isotopically labeled IS for signal normalization. The method was developed to fulfill specific requirements enabling its application in neonatology including the use of very limited sample volumes. Results obtained provided adequate sensitivity, precision, and accuracy for the analysis of blood samples. The reduced sample pretreatment, analysis time (no incubation or drying required), and sample volume, especially critical in the field of neonatology, will facilitate the application of this SERS-based assay in the clinical environment and the development of a portable sensor device suitable for point-of-care (POC) testing in newborns.

8.3 Experimental section

8.3.1 Standards and reagents

GSH, glutathione-(glycine-$^{13}C_2$,^{15}N) trifluoroacetate salt (used as IS), L-alanine, Lasparagine, L-histidine, L-isoleucine, L-leucine, L-ornithine monohydrochloride, L-proline, sarcosine, L-serine, taurine, L-threonine, L-tryptophan, L-valine, L-glutamine, L-arginine, glycine, L-aspartic acid, L-creatinine, L-cystine, L-glutamic acid, L-lysine, L-phenylalanine, L-tyrosine, L-methionine, L-homocystine, L-cystathionine, L-cysteine, γ-L-glutamyl−L-cysteine, and L-homocysteine were obtained from Sigma-Aldrich. Phenylalanine-D5 (Phe-D5) was purchased from CDN Isotopes. All standards had purities of at least 97% except for γ-L-glutamyl−L-cysteine, L-cystathionine, and glutathione-(glycine-$^{13}C_2$,^{15}N) trifluoroacetate salt,

which were at least 80%, at least 90%, and at least 95%, respectively. Silver nitrate ($AgNO_3$), hydroxylamine hydrochloride, sodium hydroxide (NaOH), and Nethylmaleimide (NEM) were purchased from Sigma-Aldrich. Perchloric acid (70%) and formic acid (98%) were purchased from Panreac Quimica S.A.U. Ultrapure water was obtained from a Milli-Q Integral Water Purification System from Merck Millipore. Ethanol 96% was obtained from Labkem.

8.3.2 Silver colloid preparation

Silver colloids were synthesized as described elsewhere[48]. Briefly, hydroxylamine hydrochloride/NaOH (10 mL) was added rapidly to 90 mL of $AgNO_3$ at room temperature and under constant stirring, which produced a 1.5 mM hydroxylamine hydrochloride, 3 mM NaOH, and 1 mM $AgNO_3$ solution. The reaction (i.e., reduction of $AgNO_3$ by hydroxylamine hydrochloride at alkaline pH) was completed within seconds. A UV−vis spectrum of a 1:10 dilution of the colloid solution with H_2O was acquired (see **Supplementary figure AI 3.1**) employing a UV-1800 Spectrometer (Shimadzu). An absorption maximum at 416 nm and the full width at half-maximum of 116 nm were obtained giving an indication of the average particle size and particle size dispersion, respectively[497]. The results agreed well with those reported in the literature[48,56], indicating a successful synthesis of the silver colloid.

8.3.3 Preparation of standards

GSH and IS working solutions were freshly prepared on each measurement day. A 1 mM GSH working solution was prepared by accurately weighing solid GSH in polypropylene microcentrifuge tubes and dissolving it in adequate volumes of Milli-Q water. Six calibration standards were obtained by serial dilution of the working solution in Milli-Q water. For the IS, accurately weighed amounts of solid standard were prepared in ethanol. Aliquots were evaporated employing a miVac Centrifugal Vacuum Concentrator from Genevac LTD at room temperature, and dry residues were stored at −20 °C. On each measurement day, one aliquot of IS was dissolved in an appropriate amount of Milli-Q water. For SERS measurements, 24 µL of each GSH calibration standard was mixed with 16 µL of IS solution (286 µM) and 120 µL of perchloric acid solution (10% v/v in H_2O). Each solution (5 µL) was added to 45 µL of Ag colloid. With the blood samples being diluted by a factor of 800 during sample processing, a concentration of ∼1.25 µM GSH is expected in the measurement solution. Accordingly, GSH standard concentrations in the final measurement solutions ranged between 0.56 and 9 µM. Blanks were prepared by replacing GSH standard solutions with H_2O.

8.3.4 Blood sample processing

Blood samples from two study populations were collected: (i) finger-prick blood samples collected with lancets from 20 healthy adults and (ii) residual blood volumes from routine newborn screening of 36 healthy term infants extracted by venipuncture without anticoagulant. Characteristics of the study populations are shown in **Supplementary table AI**

3.1 and **Supplementary table AI 3.2**. Blood (2 μL) was mixed with 22 μL of H_2O and 16 μL of IS solution (286 μM). Then, 120 μL of perchloric acid solution (10% v/v in H_2O) was added for protein precipitation. The resulting solutions were centrifuged for 30 s at 2000 g at room temperature on a Sprout Mini Centrifuge (Heathrow Scientific). Supernatant (5 μL) was added to 45 μL of Ag colloid prior to SERS measurement.

This study was approved by the Ethics Committee of the Health Research Institute La Fe (Valencia, Spain), and all methods were performed in accordance with the relevant guidelines and regulations. Permission was obtained from each volunteer or legal representative by signing an informed consent form.

8.3.5 On-capillary SERS analysis

UV-transparent, fused silica capillary tubing from Molex with an inner diameter of 101 ± 4 μm and an outer diameter of 363 ± 10 μm was used. Manual injection was used to insert the sample into a 1 cm capillary placed on top of a microscopy glass slide. SERS spectra were recorded immediately employing an XploRA ONE confocal Raman microscope (Horiba) equipped with a laser emitting at 532 nm, a 10× objective, a 1200 grooves/mm grating, as well as a charge-coupled device detector. Slit width and hole were set to 200 and 500 μm, respectively, and for each spectrum, 10 scans, with an acquisition time of 3 s each, were accumulated in the range between 400 and 2000 cm^{-1}. Measurement parameters were optimized to minimize background fluorescence while maximizing the signal intensity.

8.3.6 Method validation

Analytical figures of merit were assessed following the Food and Drug Administration Guidelines for Bioanalytical Method Validation[15]. Accordingly, accuracy, precision, lower limit of quantification (LLOQ), selectivity, and on-bench stability were evaluated on three different measurement days. Because of the lack of blank matrices (i.e., blood sample without GSH), accuracy was assessed calculating recovery percentage values in samples spiked at three concentration levels. Concentration levels were chosen conveniently at 0.38, 0.75, and 1.50 μM in measurement solution, keeping total GSH concentrations in the measurement solution within the calibration range of the method. Spiked samples were prepared by adding 22 μL of GSH standard solutions to 2 μL blood samples before protein precipitation with perchloric acid. Precision was studied in spiked samples at three concentration levels, by calculating the relative standard deviation (% RSD) of replicates. Selectivity was tested by comparing the Raman and SERS signals of GSH and other endogenous metabolites with similar chemical structures including homocysteine (17.6 mM), γ-L-glutamyl−L-cysteine (32 mM), cysteine (20 mM), and other amino acids and related metabolites (600 μM) under the same experimental conditions. Stability of the signal acquired from blood supernatants after protein precipitation was monitored after 0.4, 1, 2, 4.3, and 7.1 h and compared to the results from the fresh blood sample.

GSH concentrations in blood samples from newborns were determined employing a validated Liquid Chromatography coupled to tandem Mass Spectrometry (LC-MS/MS) method[49]. Blood (50 µL) was added to 10 µL of aqueous 100 mM NEM solution. After 5 min of incubation at room temperature, 60 µL of perchloric acid (8% v/v) was added. After they were thoroughly mixed, samples were centrifuged at 10 000 g at 4 °C for 15 min. Supernatant (10 µL) was added to 90 µL of formic acid (0.1% v/v). After centrifugation at 10 000 g at 4 °C for 15 min, 95 µL of supernatant was added to 5 µL of Phe-D5 solution (12.5 µM, 0.1% v/v formic acid), and sample extracts were analyzed employing an Acquity-Xevo TQD system from Waters operating in the positive electro-spray ionization mode. Separations were performed using a Kinetex UPLC C8 column (2.1 × 100 mm, 1.7 µm) and precolumn (2.1 × 5 mm) from Phenomenex and a binary mobile phase gradient.

8.3.7 Data analysis and software

Labspec software (version 6, Horiba) was employed for spectra acquisition. Data analysis was performed in MATLAB 2015a (The Mathworks) using built-in as well as in-house written functions.

For GSH quantification, average values from six technical replicates of the relative intensities ($R_{GSH/IS}$) of the SERS signals measured at the maxima of specific peaks of GSH and IS located at 1738 and 1720 cm^{-1}, respectively, after a single point baseline correction at 1919 cm^{-1} were determined.

The AEF was determined using the following equation[498]:

$$AEF = \frac{I_{SERS}}{I_{Raman}} \tag{8.1}$$

where I_{SERS} and I_{Raman} stand for the relative intensities measured at 647, 715, 793 cm^{-1} (baseline correction at 860 cm^{-1}) and 1738 cm^{-1} (baseline correction at 1800 cm^{-1}) divided by concentration of GSH in the standard solutions employed for SERS and Raman measurements, respectively.

8.4 Results and discussion

8.4.1 On-capillary SERS analysis of GSH and IS

In this work, a fused silica capillary was employed as a measurement cell for liquid samples. This enables a straightforward signal acquisition of sample extracts on a Raman microscope avoiding the use of dried sample spots and overcoming associated issues concerning analyte stability and measurement reproducibility. **Figure 8.1** depicts Raman spectra obtained from an empty capillary segment as well as from the capillary filled with a

GSH standard solution containing perchloric acid. The empty capillary showed very weak Raman scattering with no distinguishable peaks. The signal obtained for the GSH standard solution was characterized by one predominant peak located at 925 cm^{-1} corresponding to the Raman shift observed for the ClO_4^- ion of perchloric acid. In view of the poor Raman activity of GSH in aqueous solution, an enhancement of the GSH signal intensity was indispensable to reach the sensitivity required for the direct quantification of GSH in blood. **Figure 8.1** shows the signal enhancement achieved when using a silver colloid substrate for SERS analysis of GSH and IS standard solutions containing perchloric acid as well as a perchloric acid (0.75% v/v) blank. In the blank spectrum only one distinguishable peak at 925 cm^{-1} assigned to ClO_4^- was observed. However, in agreement with previous works[56,485–488,491,493,496,499], information-rich SERS spectra were obtained from the GSH standard solution. The mechanism of the observed signal enhancement of GSH using silver substrates has been the subject of earlier studies[499,500]. A detailed peak assignment for GSH is summarized in **Table 8.1**. In this study a laser emission wavelength of 532 nm was selected for spectra acquisition due to the low signal intensity obtained using 785 nm and the intense background fluorescence observed when employing 638 nm.

Table 8.1 GSH peak assignment

Raman Shift [cm^{-1}]	Vibration	Intensity	Reference
647	$\nu_{(C-S)}$ from $-H_2C-S-$ group of Cys (P_H conformer)	s	499,501
715	$\nu_{(C-S)}$ from $-H_2C-S-$ group of Cys (P_C conformer)	m	499,501
793	$\nu_{(C=N)}$ Amide V	s	499,501
905	$\nu_{(C-COO-)}$	w	499,501
925	$\nu_{(ClO4-)}$	s	502
1007	$\nu_{(C-N)}$	w	499,501
1120	$\nu_{(ClO4-)}$	w	502
1245/1293	$\nu_{(C=N)}$ Amide III	m/m	499,503
1375	$\nu_{(COO)}$	m	499,501
1414	$\nu_{(COO-)}$	s	503
1567	$\nu_{(C=N)}$ Amide II	s	503
1629/1662	$\nu_{(C=N)}$ Amide I	w/m	499,503
1738	$\nu_{(C=O)}$	s	503

Note: w, m and s stands for weak, medium, and strong, respectively.

The SERS spectrum obtained from isotopically labeled GSH (used as IS) was almost identical in comparison to the GSH spectrum, with a single appreciable shift in the position of the $\nu_{(C=O)}$ peak from 1738 cm^{-1} for GSH to 1720 cm^{-1} for the IS (see **Figure 8.2**) attributed to the ^{13}C substitution of one of four C=O functional groups of the GSH molecule. Following the simple harmonic oscillator model, the frequency of Raman bands is inversely proportional to the square root of the mean atomic mass. Because of the mass difference between the ^{12}C and ^{13}C isotopes induced by isotopic substitution, the position of Raman peaks decreases with increasing ^{13}C concentration. Hence, the observed redshift of the $\nu_{(C=O)}$ peak is coherent with

the isotopic modification and in good agreement with previous results reported in the literature[504].

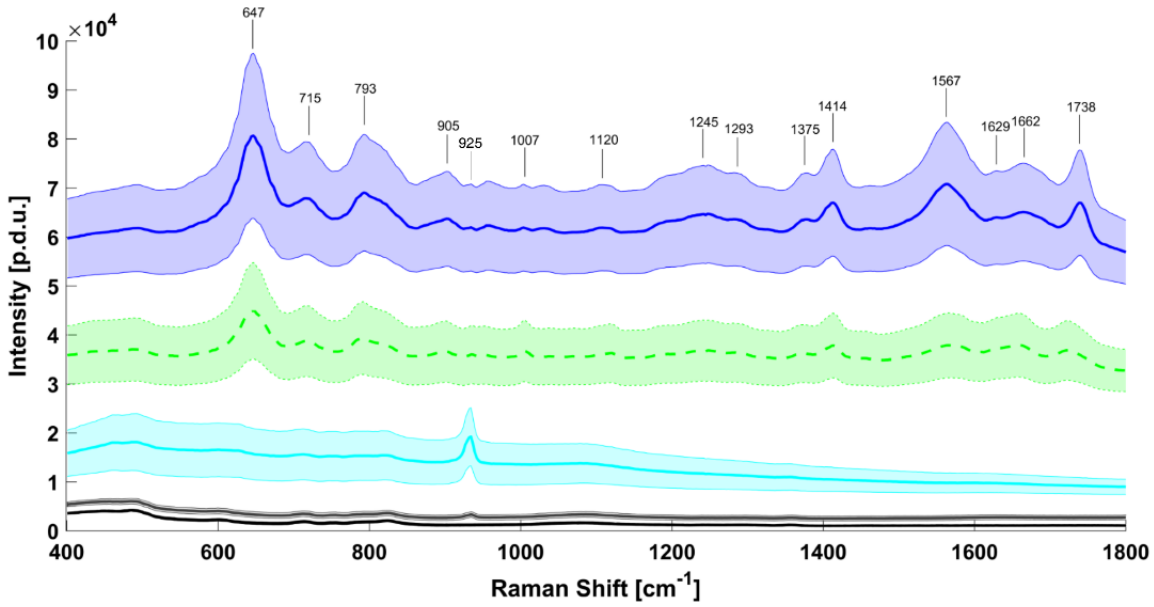

Figure 8.1 Raman and SERS spectra: Raman spectra of an empty capillary (black) and a GSH standard solution (6 µM) containing perchloric acid (cyan); SERS spectra of a GSH standard solution (6 µM, blue), IS solution (2.4 µM, green), and a perchloric acid blank (gray). Notes: spectra have been shifted for better visibility; spectra are shown as mean spectra ± standard deviation (n=6).

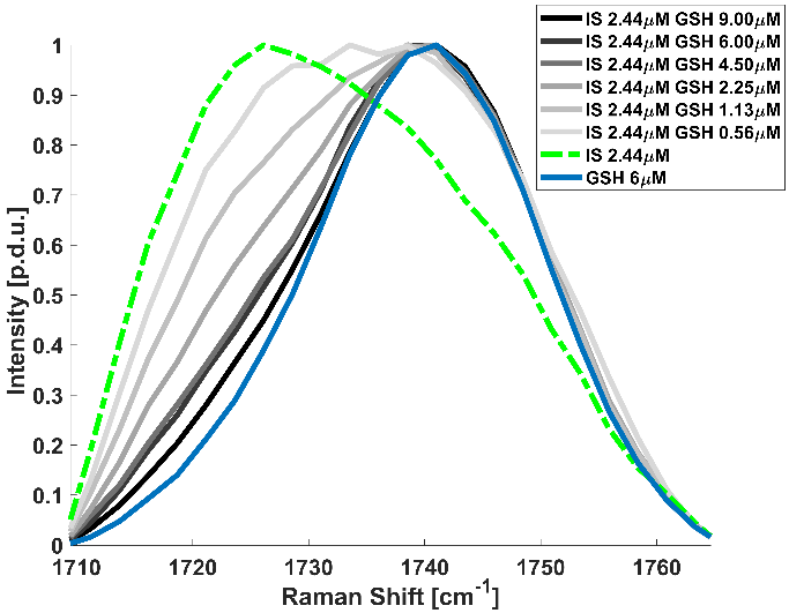

Figure 8.2 Normalized SERS spectra (maximum = 1) in the range between 1710 and 1765 cm-1 of GSH and IS standard mixtures

To optimize the SERS signal enhancement, different ratios of sample to SERS substrate were evaluated. With Raman and SERS spectra of two GSH standard solutions (2.4 mM and 6 µM, respectively), optimum AEFs were obtained using 5 µL of sample supernatant and 45 µL of Ag colloid (see **Figure 8.3**). The AEFs calculated for peaks located at 647, 715, 793, and 1738 cm^{-1} ranged between 2×10^3 and 1×10^4. The obtained AEFs are 3 orders of magnitude higher than those reported in a previous study[56] and provide appropriate sensitivity for GSH quantification in blood micro samples, where concentrations in the range of 1 mM are expected.

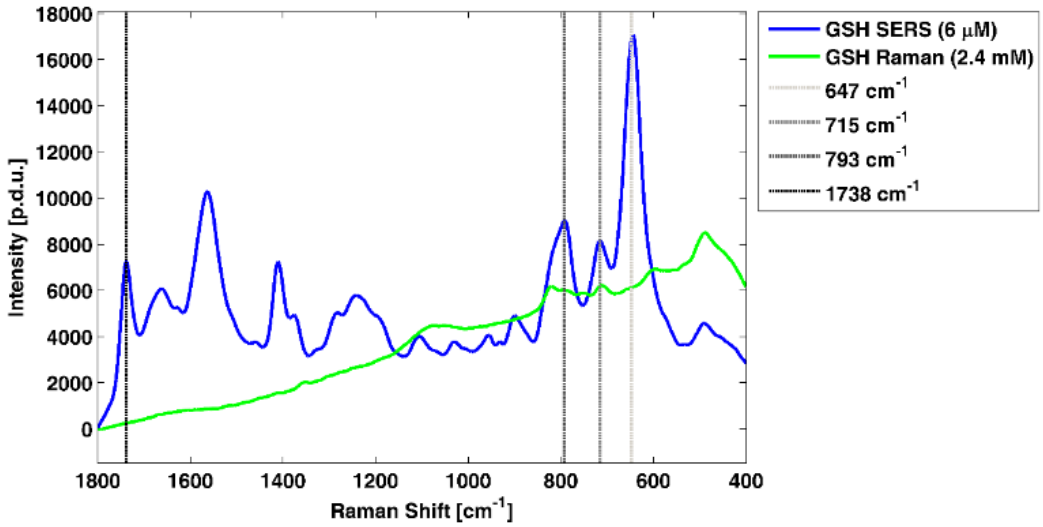

Figure 8.3 GSH spectra used for the calculation of AEFs. Note: spectra were baseline corrected at 1800 cm^{-1}; dashed vertical lines indicate the Raman shifts used for the calculation of AEFs; AEFs at 647, 715, 793 and 1738 cm^{-1} were $5x10^3$, $2x10^3$, $2x10^3$ and $1x10^4$, respectively.

To test the specificity of the SERS signal, spectra from relevant low molecular weight endogenous biothiols (homocysteine, γ-L-glutamyl−L-cysteine, and cysteine), present in blood and with molecular structures similar to GSH, were measured and compared to a GSH spectrum. The observed signal enhancement was very low (<10) for all tested metabolites. Besides, the correlation between the spectra of GSH and those of potentially interfering metabolites in the region between 600 and 1000 cm−1 was poor ($R^2 < 0.75$). Both observations support the specificity of the observed GSH SERS signal in blood samples.

In addition, SERS signals of other amino acids and related compounds that can be typically found in blood samples were examined. A detailed list of all obtained correlation coefficients can be found in the **Supplementary table AI 3.3**. Correlation coefficients calculated between GSH spectra and spectra of 27 studied compounds (600 µM) in the 600 to 1800 cm^{-1} region ranged between 0.09 and 0.4. Conversely, high correlation coefficients ranging between 0.6 and 0.99 in the 600 to 1800 cm^{-1} region were obtained when compared to a blank spectrum with the exception of L-arginine (R = 0.03). Hence, none of the tested

metabolites showed SERS features that could potentially interfere with the determination of GSH in blood sample extracts.

8.4.2 Quantification of GSH employing an isotopically labeled IS

As illustrated in **Figure 8.1**, SERS analysis suffers from a low precision characterized by a high RSD of ~40% for technical replicates. This shortcoming of the SERS approach is in agreement with previously reported results[56] and clearly hinders the direct use of peak intensities for quantitative measurements. To increase measurement precision and accuracy, a novel approach based on the use of isotopically labeled GSH as internal standard was employed. The calibration model exploited the peak shift between the $\nu_{(C=O)}$ peaks of GSH and the IS in the 1710−1765 cm^{-1} range. The changes in peak positions and relative intensities observed for GSH and IS are illustrated in **Figure 8.2**. Additionally, **Figure 8.4** (left) shows external calibration curves from data acquired on three different days. The relative intensity ratio of GSH and IS ($R_{GSH/IS}$) followed a rational function with the GSH concentration. However, it was found to vary linearly with the GSH concentration fraction χ, being

$$\chi = \frac{[GSH]}{[GSH] + [IS]} \tag{8.2}$$

where [GSH] and [IS] are the GSH and IS concentrations, respectively (see **Figure 8.4**, right). With this approach, [GSH] in samples could be easily determined after interpolation in the linear regression models as

$$[GSH] = \frac{\chi\,[IS]}{1-\chi}. \tag{8.3}$$

The accuracy and precision values were determined at the LLOQ (0.56 μM) and two concentration levels above the LLOQ (i.e., 2.25 and 9 μM) by replicate (n =3) analysis of GSH standard solutions on three measurement days providing recovery percentages ranging between 99 and 103% and RSDs ≤ 11% as shown in Table 2. These results demonstrate that the use of an isotopically labeled IS greatly improves the robustness of the method.

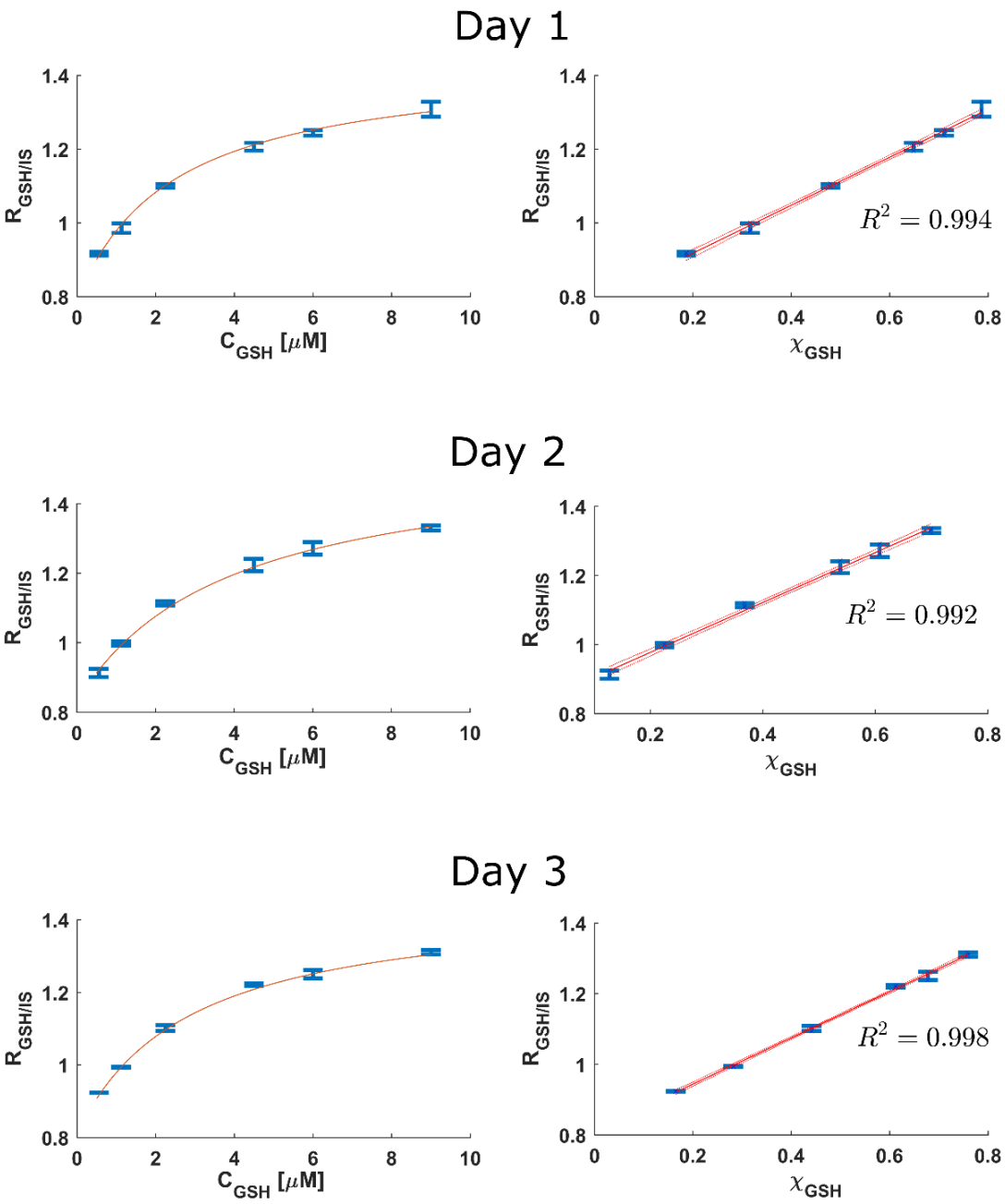

Figure 8.4 Calibration lines measured on different days of the validation study; intensity ratios ($R_{(GSH/IS)}$ vs. GSH concentrations (left) and vs. GSH concentration fractions χ (right) for each measurement day. Mean values (n=3) ± standard deviation are represented in blue; red lines are polynomic fits (left) or linear regression lines (+ 95% confidence interval) (right).

8.4.3 Determination of GSH in human blood samples

Figure 4 shows sample processing steps for SERS analysis and SERS spectra of a blood sample and a GSH standard solution, both containing IS. The characteristic peaks of GSH can

be clearly discerned in the blood spectrum, and both spectra were highly similar providing R^2 > 0.7 in the 400 to 1600 cm^{-1} region. Remarkably, the GSH and IS peaks at 1720 and 1738 cm^{-1}, respectively, were detected in blood enabling the use of the ratio $R_{GSH/IS}$ for GSH quantification as described in the foregoing section. To assess the robustness of the SERS quantification of GSH in blood samples, replicates (n = 3) of non-spiked and spiked samples at three levels were analyzed on three different days. GSH concentrations in samples and recovery percentages were calculated using the corresponding calibration equations acquired on each measurement day. Spiked and non-spiked sample concentrations were obtained with an adequate level of precision (i.e., <20% RSD), and accuracy ranged between 99 and 107% for all studied levels as summarized in **Table 8.2**.

Table 8.2 Accuracy and precision given as %recoveries and %RSD in GSH standard solutions and spiked blood samples.

		% Accuracy ± RSD (GSH concentration, µM)		
		Low	**Medium**	**High**
GSH standards	Intra-day (N=3)	103 ± 1 (0.56)	100 ± 5 (2.25)	101 ± 5 (9.00)
	Inter-day (N=3)	99 ± 11 (0.56)	103 ± 5 (2.25)	102 ± 8 (9.00)
Blood samples	Intra-day (N=3)	100 ± 6 (0.38)	99 ± 14 (0.75)	106 ± 11 (1.50)
	Inter-day (N=3)	102 ± 13 (0.38)	99 ± 15 (0.75)	107 ± 18 (1.50)

The proposed quantitative SERS method was sensitive and selective. The method requires a 2 µL blood sample, which was diluted during preprocessing, and finally, a small fraction of ~80 nL of the sample extract was introduced in the capillary for SERS measurement. Taking into account the diameter of the laser spot (~3 µm), an actual volume of ~25 pL of sample extract contributed to the final SERS signal. Hence, at the LLOQ of 0.56 µM, only 1.4 × 10−17 moles of GSH are located within the irradiated capillary volume, which corresponds to less than 8.4 million molecules, showing the high sensitivity of the SERS signal under the selected conditions.

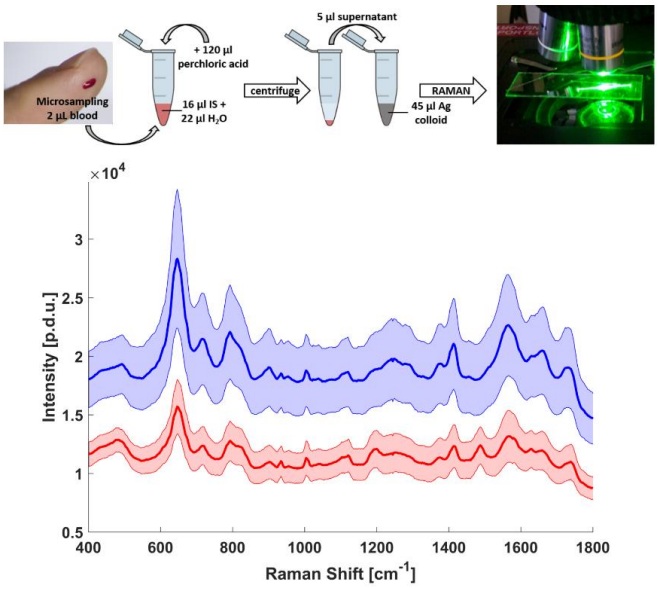

Figure 8.5 SERS determination of GSH in blood samples. Top: Schematic overview of the sample processing steps, bottom: Mean SERS spectra and their standard deviation (n = 6) of a GSH standard solution (6 µM, blue, top) and a blood sample (red, bottom). Note: Both, the GSH standard and the blood sample contained IS (2.4 µM) and perchloric acid. Spectra were shifted in the y-axis for a better visibility.

In the case of GSH analysis, stability of the target analyte was recognized as an important factor limiting reproducibility. Sample analysis might not always be performed immediately due to practical issues, and hence, storage of blood samples becomes necessary. Therefore, the on-bench stability of the blood sample extract after addition of perchloric acid and IS was performed covering a time period of over 7 h at 25 °C. Average differences between retrieved GSH concentrations were evaluated, and obtained results showed no statistically significant changes (Wilcoxon rank-sum test, two-tailed, pvalues >0.05) in the GSH concentration in the studied time interval, indicating that the sample extract was stable under the tested conditions.

The validated SERS method was applied to in situ obtained blood samples from 20 healthy adults. A median GSH concentration of 1055 µM was obtained, and the mean ± standard deviation was 1090 ± 190 µM. These observations were in good agreement with the range of 1020 µM ± 17% accepted as reference value in healthy adults.53 In addition, three independent blood samples were drawn from three volunteers to test repeatability. The mean GSH concentrations (µM) ± %RSD obtained for each volunteer were 968 ± 3%, 1007 ± 12%, and 1159 ± 10%. The %RSD represents variation arising from the sum of all steps including sample handling (i.e., sampling, preprocessing) as well as on-capillary SERS spectral acquisition. RSD values found in the replicate analysis of real samples supports the high repeatability of the approach.

The SERS approach was applied to the determination of GSH concentrations in blood samples from 36 newborns and compared to results obtained using a validated, LC-MS/MS

based reference method. Median GSH concentrations of 1412 and 1196 μM and mean concentrations ± standard deviation of 1360 ± 370 and 1200 ± 390 were obtained employing SERS and LC-MS/MS, respectively. Results are depicted in Figure S3. No significant differences were found between concentrations determined using both methods (Wilcoxon rank sum test, p-value = 0.1). The agreement between the results obtained with the SERS approach and the reference method further confirm the accuracy of GSH quantification in blood samples.

In summary, analytical figures of merit including selectivity, stability, precision, and accuracy were assessed in this study. The reported figures of merit for the quantification of GSH in blood samples are comparable and, in some cases, even outperformed other analytical approaches[49,102,474,505]. Specifically, the most recent work, focused on the determination of GSH in blood samples of newborns[49] employing LC-MS/MS and an isotopically labeled IS, yielded values for precision of up to 20% RSD and an accuracy of less than or equal to 90%. Furthermore, a sample volume of 100 μL was used, which is a limiting factor in neonatology and 50 times the volume needed for the SERS approach. It can be concluded that the developed approach presents important advantages over alternative standard methods based on LC-MS or GC-MS, as it significantly reduces the hands-on time required for sample analysis. The developed approach, including sample preparation and measurement, allowed to obtain GSH concentrations within ~4 min per sample.

8.5 Conclusions

This work describes a novel, fast, and highly robust SERS-based method for the quantification of GSH in whole blood samples. This approach relies on the use of a fused silica capillary employed as a measurement compartment for liquid blood extracts and the use of an isotopically labeled IS. The sample pretreatment steps of the proposed method have been minimized to reduce sources of variation that could affect the robustness of the analysis and affect its translation into clinical practice. The method avoids sample derivatization with toxic reagents, commonly employed in other validated approaches, and it provides a direct analysis setup potentially compatible with microfluidic or lab-on-a-chip devices. This work proves the applicability of the developed SERS approach for the determination of GSH in blood samples from two study populations (adults and newborns) and its capability of providing results comparable with an LC-MS reference method. The employed blood volume could be reduced 25 times (from 50 to 2 μL) with respect to previous work. This approach is especially valuable in the field of neonatology, where limited blood volumes are accessible and could potentially contribute to increase the understanding of the role of GSH in redox homeostasis in different scenarios relevant for neonatal care. Future work will focus on the possibility to allow a simultaneous determination of oxidized glutathione as well as on the automation and miniaturization of a Raman device specifically tailored to its application in a portable sensor device suitable for POC testing in newborns.

General conclusions and outlook

In this PhD thesis, the development and applicability of a range of analytical techniques for the analysis of biomarkers in biofluids relevant to the study of the newborn in different conditions has been shown. The following main conclusions can be drawn:

- The blood plasma from a pig model of perinatal asphyxia is a suitable matrix to analyze choline, cytidine, uridine, and betaine via LC-MS/MS. These compounds combined with lactate improve the predictive power of lactate in the assessment of asphyxia.
- The validation of a GC-MS based method for the analysis of biomarkers of energy metabolism in neonates that undergo HIE is feasible. With this method the concentration profiles of these compounds in neonates with HIE subjected to therapeutic hypothermia and healthy controls was measured.
- It is possible to develop and validate a method employing LC-MS/MS for the analysis of a panel of lipid peroxidation biomarkers (isoprostanes and isofuranes) in blood plasma from infants with HIE. However, it is necessary to exclude some compounds that suffer degradation during sample treatment from the analysis.
- The *in vitro* study of the oxidation of adrenic acid is suitable for identifying LC-MS/MS signals related to it. With this approach it was possible to identify oxidation products of adrenic acid that were found at detectable concentrations in urine and in a small proportion of plasma samples.
- It is possible to validate the analysis of biomarkers of oxidative damage to DNA and proteins in human milk employing LC-MS/MS. With this method the concentration ranges of several biomarkers were determined and it was shown that the pasteurization process did not affect their levels.
- The use of an isotopically labeled internal standard and a quartz capillary is a powerful approach to increase the measurement precision and accuracy of SERS methods. With this set-up it was possible to demonstrate the quantification of GSH in microsamples of blood from neonates.

Moreover, this Thesis comprises two review articles on biomarkers of HIE in the newborn and biomarkers of oxidative stress in preterm infants, respectively. These articles provide a novel approach, putting emphasis on the methodological and analytical aspects.

Finally, a series of questions that are being studied by our group have emerged from this PhD Thesis, resulting in the research lines summarized as follows:

- The clinical validation of candidate biomarkers found in the animal model of asphyxiated piglets. An LC-MS/MS method that combines the analysis of choline, cytidine, betaine, and uridine with other candidate biomarkers proposed by our group such as the "metabolite score"[57] is currently under development. The performance of this method will be tested on a cohort of newborn infants suffering from HIE.
- The study of the energy metabolism and related compounds in continuous and intermittent asphyxia in an animal model employing non-targeted and targeted approaches with the aim of controlling asphyxia conditions.
- The development of a comprehensive, quantitative analytical method for the analysis of lipid peroxidation products that circumvents the drawbacks found in sample processing, chromatographic resolution, and sensitivity.
- The *in vitro* study of peroxidation reactions of PUFAs under conditions of interest for neonatology (i.e. oxygen concentrations, matrix of interest, etc.) and the development of a lipid bilayer model.
- The development of a Point of Care approach for the analysis of GSH and GSSG in microvolume blood samples employing SERS.

References

1. Zweifel. Die Respiration des Fötus. *Arch. Gynak.* **9**, 291–305 (1876).
2. Longo, L. D. *The Rise of Fetal and Neonatal Physiology : Basic Science to Clinical Care*. (Springer-Verlag, 2018). doi:10.1007/978-1-4939-7483-2.
3. Eastman, N. J. & McLane, C. M. Foetal blood studies II. The lactic acid content of umbilical cord blood under various conditions. *Bulletin of the Johns Hopkins Hospital* **48**, 261–268 (1931).
4. Sánchez-Illana, Á., Piñeiro-Ramos, J. D. & Kuligowski, J. Small molecule biomarkers for neonatal hypoxic ischemic encephalopathy. *Seminars in Fetal and Neonatal Medicine* **25**, 101084 (2020).
5. Meyer, S., Zemlin, M. & Poryo, M. Editorial: Biomarkers in neonatology. *Early Human Development* **105**, 23–24 (2017).
6. FDA-NIH Biomarker Working Group. *BEST (Biomarkers, EndpointS, and other Tools) Resource*. (Food and Drug Administration (US), 2016).
7. Noto, A., Fanos, V. & Dessi, A. Metabolomics in Newborns. in *Advances in Clinical Chemistry, Vol 74* (ed. Makowski, G. S.) vol. 74 35–61 (Elsevier Academic Press Inc, 2016).
8. Fattuoni, C., Palmas, F., Noto, A., Fanos, V. & Barberini, L. Perinatal Asphyxia: A Review from a Metabolomics Perspective. *Molecules* **20**, 7000–7016 (2015).

9. Fanos, V., Atzori, L., Makarenko, K., Melis, G. B. & Ferrazzi, E. Metabolomics Application in Maternal-Fetal Medicine. *Biomed Res. Int.* 720514 (2013) doi:10.1155/2013/720514.
10. Fanos, V., Antonucci, R. & Atzori, L. Metabolomics in the developing infant. *CURR. OPIN. PEDIATR.* **25**, 604–611 (2013).
11. Bardanzellu, F. & Fanos, V. Omics in Neonatology: The Future? *Innovations and Frontiers in Neonatology* **22**, 169–183 (2020).
12. Holmes, E., Wilson, I. D. & Nicholson, J. K. Metabolic Phenotyping in Health and Disease. *Cell* **134**, 714–717 (2008).
13. Kosmides, A. K., Kamisoglu, K., Calvano, S. E., Corbett, S. A. & Androulakis, I. P. Metabolomic Fingerprinting: Challenges and Opportunities. *Crit Rev Biomed Eng* **41**, 205–221 (2013).
14. European Medicines Agency. Guideline on bioanalytical method validation. (2011).
15. U.S. Department of Health and Human Services, Food and Drug Administration, Center for Drug Evaluation and Research (CDER) & Center for Veterinary Medicine (CVM). Bioanalytical Method Validation Guidance for Industry. (2018).
16. Ministerio de Sanidad y Consumo. *Real Decreto 1662/2000, de 29 de septiembre, sobre productos sanitarios para diagnóstico 'in vitro'. Real Decreto 1662/2000*.
17. International Standarization Organization & International Electrotechnical Commission. *General requirements for the competence of testing and calibration laboratories*. *ISO/IEC 17025:2017*.
18. International Standarization Organization. *Medical laboratories - Requirements for quality and competence. ISO 15189:2013*.

19. Broadhurst, D. *et al.* Guidelines and considerations for the use of system suitability and quality control samples in mass spectrometry assays applied in untargeted clinical metabolomic studies. *Metabolomics* **14**, 72 (2018).
20. Domingo-Almenara, X., Montenegro-Burke, J. R., Benton, H. P. & Siuzdak, G. Annotation: a computational solution for streamlining metabolomics analysis. *Anal Chem* **90**, 480–489 (2018).
21. Solberg, R. *et al.* Metabolomic Analyses of Plasma Reveals New Insights into Asphyxia and Resuscitation in Pigs. *PLoS ONE* **5**, e9606 (2010).
22. Walsh, B. H. *et al.* The Metabolomic Profile of Umbilical Cord Blood in Neonatal Hypoxic Ischaemic Encephalopathy. *PLoS ONE* **7**, e50520 (2012).
23. Sachse, D., Solevåg, A. L., Berg, J. P. & Nakstad, B. The Role of Plasma and Urine Metabolomics in Identifying New Biomarkers in Severe Newborn Asphyxia: A Study of Asphyxiated Newborn Pigs following Cardiopulmonary Resuscitation. *PLOS ONE* **11**, e0161123 (2016).
24. Lee, A. C. *et al.* Intrapartum-related neonatal encephalopathy incidence and impairment at regional and global levels for 2010 with trends from 1990. *Pediatric Research* **74**, 50–72 (2013).
25. Wassink, G., Gunn, E. R., Drury, P. P., Bennet, L. & Gunn, A. J. The mechanisms and treatment of asphyxial encephalopathy. *Front. Neurosci.* **8**, (2014).
26. Douglas-Escobar, M. & Weiss, M. D. Hypoxic-ischemic encephalopathy: a review for the clinician. *JAMA Pediatr* **169**, 397–403 (2015).
27. Qin, X. *et al.* Mechanism and Treatment Related to Oxidative Stress in Neonatal Hypoxic-Ischemic Encephalopathy. *Front. Mol. Neurosci.* **12**, 88 (2019).

28. Martinello, K., Hart, A. R., Yap, S., Mitra, S. & Robertson, N. J. Management and investigation of neonatal encephalopathy: 2017 update. *Archives of Disease in Childhood - Fetal and Neonatal Edition* **102**, F346–F358 (2017).
29. Massaro, A. N. *et al.* Short-term outcomes after perinatal hypoxic ischemic encephalopathy: a report from the Children's Hospitals Neonatal Consortium HIE focus group. *J Perinatol* **35**, 290–296 (2015).
30. Vogel, J. P. *et al.* The global epidemiology of preterm birth. *Best Practice & Research Clinical Obstetrics & Gynaecology* **52**, 3–12 (2018).
31. Who: Recommended Definitions, Terminology and Format for Statistical Tables Related to The Perinatal Period And Use of A New Certificate For Cause of Perinatal Deaths. *Acta Obstetricia et Gynecologica Scandinavica* **56**, 247–253 (1977).
32. Purisch, S. E. & Gyamfi-Bannerman, C. Epidemiology of preterm birth. *Seminars in Perinatology* **41**, 387–391 (2017).
33. Vento, M. *et al.* Antenatal steroids and antioxidant enzyme activity in preterm infants: influence of gender and timing. *Antioxid Redox Signal* **11**, 2945–2955 (2009).
34. Davis, J. M. & Auten, R. L. Maturation of the antioxidant system and the effects on preterm birth. *Seminars in Fetal and Neonatal Medicine* **15**, 191–195 (2010).
35. Granger, D. N. & Kvietys, P. R. Reperfusion injury and reactive oxygen species: The evolution of a concept. *Redox Biology* **6**, 524–551 (2015).
36. Dawson, J. A. *et al.* Defining the Reference Range for Oxygen Saturation for Infants After Birth. *Pediatrics* **125**, E1340–E1347 (2010).
37. Dawson, J. A. & Morley, C. J. Monitoring oxygen saturation and heart rate in the early neonatal period. *Seminars in Fetal and Neonatal Medicine* **15**, 203–207 (2010).

38. Martín, J. A. *et al.* Oxidative stress as a signal to up-regulate gamma-cystathionase in the fetal-to-neonatal transition in rats. *Cell Mol Biol (Noisy-le-grand)* **53 Suppl**, OL1010-1017 (2007).
39. Wyckoff Myra H. *et al.* Part 13: Neonatal Resuscitation. *Circulation* **132**, S543–S560 (2015).
40. Saugstad, O. D., Oei, J.-L., Lakshminrusimha, S. & Vento, M. Oxygen therapy of the newborn from molecular understanding to clinical practice. *Pediatr. Res.* **85**, 20–29 (2019).
41. Thamrin, V. *et al.* Preterm Infant Outcomes after Randomization to Initial Resuscitation with FiO2 0.21 or 1.0. *The Journal of Pediatrics* **201**, 55-61.e1 (2018).
42. Vento, M. & Saugstad, O. D. Targeting Oxygen in Term and Preterm Infants Starting at Birth. *Clinics in Perinatology* **46**, 459–473 (2019).
43. Sies, H., Berndt, C. & Jones, D. P. Oxidative Stress. *Annual Review of Biochemistry* **86**, 715–748 (2017).
44. Sies, H. Oxidative stress: a concept in redox biology and medicine. *Redox Biology* **4**, 180–183 (2015).
45. Vento, M., Hummler, H., Dawson, J., Escobar, J. & Kuligowski, J. Use of Oxygen in the Resuscitation of Neonates. in *Perinatal and Prenatal Disorders* (eds. Dennery, P. A., Buonocore, G. & Saugstad, O. D.) 213–243 (Springer New York, 2014).
46. Andresen, J. H. *et al.* Newborn piglets exposed to hypoxia after nicotine or saline pretreatment: Long-term effects on brain and heart. *The Journal of Maternal-Fetal & Neonatal Medicine* **22**, 161–168 (2009).
47. Salvesen, B. Pathophysiological and Immunological Aspects of Meconium Aspiration Syndrome. (University of Oslo, 2009).

48. Leopold, N. & Lendl, B. A New Method for Fast Preparation of Highly Surface-Enhanced Raman Scattering (SERS) Active Silver Colloids at Room Temperature by Reduction of Silver Nitrate with Hydroxylamine Hydrochloride. *The Journal of Physical Chemistry B* **107**, 5723–5727 (2003).
49. Escobar, J. *et al.* Development of a reliable method based on ultra-performance liquid chromatography coupled to tandem mass spectrometry to measure thiol-associated oxidative stress in whole blood samples. *J Pharm Biomed Anal* **123**, 104–112 (2016).
50. Xia, J., Sinelnikov, I. V., Han, B. & Wishart, D. S. MetaboAnalyst 3.0—making metabolomics more meaningful. *Nucleic Acids Res* **43**, W251–W257 (2015).
51. Kuligowski, J. *et al.* Urinary Lipid Peroxidation Byproducts: Are They Relevant for Predicting Neonatal Morbidity in Preterm Infants? *Antioxid. Redox Signal.* **23**, 178–184 (2015).
52. Kuligowski, J. *et al.* Analysis of lipid peroxidation biomarkers in extremely low gestational age neonate urines by UPLC-MS/MS. *Anal Bioanal Chem* 1–12 (2014) doi:10.1007/s00216-014-7824-6.
53. Sánchez-Illana, Á. *et al.* Novel free-radical mediated lipid peroxidation biomarkers in newborn plasma. *Analytica Chimica Acta* **996**, 88–97 (2017).
54. Cháfer-Pericás, C. *et al.* Development of a reliable analytical method to determine lipid peroxidation biomarkers in newborn plasma samples. *Talanta* **153**, 152–157 (2016).
55. Cháfer-Pericás, C. *et al.* Ultra high performance liquid chromatography coupled to tandem mass spectrometry determination of lipid peroxidation biomarkers in newborn serum samples. *Analytica Chimica Acta* **886**, 214–220 (2015).

56. Kuligowski, J. *et al.* Surface enhanced Raman spectroscopic direct determination of low molecular weight biothiols in umbilical cord whole blood. *Analyst* **141**, 2165–2174 (2016).
57. Kuligowski, J. *et al.* Plasma metabolite score correlates with Hypoxia time in a newly born piglet model for asphyxia. *Redox Biology* **12**, 1–7 (2017).
58. Wyllie, J. *et al.* European Resuscitation Council Guidelines for Resuscitation 2015: Section 7. Resuscitation and support of transition of babies at birth. *Resuscitation* **95**, 249–263 (2015).
59. Perlman Jeffrey M. *et al.* Part 7: Neonatal Resuscitation. *Circulation* **132**, S204–S241 (2015).
60. *Perinatal and Prenatal Disorders*. (Humana Press, 2014).
61. Shankaran, S. *et al.* Whole-Body Hypothermia for Neonates with Hypoxic–Ischemic Encephalopathy. *New England Journal of Medicine* **353**, 1574–1584 (2005).
62. Apgar, V. A proposal for a new method of evaluation of the newborn infant. *Curr Res Anesth Analg* **32**, 260–267 (1953).
63. Sarnat, H. B. & Sarnat, M. S. Neonatal Encephalopathy Following Fetal Distress: A Clinical and Electroencephalographic Study. *Arch Neurol* **33**, 696–705 (1976).
64. Denihan, N. M., Boylan, G. B. & Murray, D. M. Metabolomic Profiling in Perinatal Asphyxia: A Promising New Field. *Biomed Res. Int.* 254076 (2015) doi:10.1155/2015/254076.
65. Efstathiou, N., Theodoridis, G. & Sarafidis, K. Understanding neonatal hypoxic-ischemic encephalopathy with metabolomics. *Hippokratia* **21**, 115–123 (2017).
66. Considine, E. C. The Search for Clinically Useful Biomarkers of Complex Disease: A Data Analysis Perspective. *Metabolites* **9**, 126 (2019).

67. Quintás, G., Sánchez-Illana, Á., Piñeiro-Ramos, J. D. & Kuligowski, J. Chapter Six - Data Quality Assessment in Untargeted LC-MS Metabolomics. in *Comprehensive Analytical Chemistry* (eds. Jaumot, J., Bedia, C. & Tauler, R.) vol. 82 137–164 (Elsevier, 2018).
68. Bader, D., Gozal, D., Weinger-Abend, M., Berger, A. & Lanir, A. Neonatal urinary uric acid/ceratinine ratio as an additional marker of perinatal asphyxia. *European Journal of Pediatrics* **154**, 747–749 (1995).
69. Rogers, M. S. *et al.* Lipid peroxidation in cord blood at birth: A marker of fetal hypoxia during labour. *Gynecol.Obstet.Invest.* **44**, 229–233 (1997).
70. Saugstad, O. D. Hypoxanthine as a Measurement of Hypoxia. *Pediatric Research* **9**, 158–161 (1975).
71. Allen, L. G., Louis, T. M. & Kopelman, A. E. Brain prostaglandins E2 and F2 alpha following neonatal asphyxia in the guinea pig. *Biol. Neonate* **42**, 8–14 (1982).
72. Calamandrei, G. *et al.* Increased Brain Levels of F2-Isoprostane Are an Early Marker of Behavioral Sequels in a Rat Model of Global Perinatal Asphyxia. *Pediatric Research* **55**, 85–92 (2004).
73. Groenendaal, F., Lammers, H., Smit, D. & Nikkels, P. G. J. Nitrotyrosine in brain tissue of neonates after perinatal asphyxia. *Archives of Disease in Childhood - Fetal and Neonatal Edition* **91**, F429–F433 (2006).
74. Yuvienco, J. M. S. *et al.* Umbilical Cord Unbound Free Fatty Acid Concentration and Low Apgar Score. *American Journal of Perinatology* **22**, 429–436 (2005).
75. Azzopardi, D. *et al.* Prognosis of Newborn Infants with Hypoxic-Ischemic Brain Injury Assessed by Phosphorus Magnetic Resonance Spectroscopy. *Pediatric Research* **25**, 445–451 (1989).

76. Peden, C. J. *et al.* Proton MR Spectroscopy of the Brain in Infants. *Journal of Computer Assisted Tomography* **14**, 886 (1990).

77. Atzori, L. *et al.* A metabolomic approach in an experimental model of hypoxia-reoxygenation in newborn piglets: urine predicts outcome. *The Journal of Maternal-Fetal & Neonatal Medicine* **23**, 134–137 (2010).

78. Fanos, V. *et al.* Metabolomics Network Characterization of Resuscitation after Normocapnic Hypoxia in a Newborn Piglet Model Supports the Hypothesis That Room Air Is Better. *BioMed Research International* **2014**, 1–7 (2014).

79. Liu, J. *et al.* Outcome-Related Metabolomic Patterns from 1H/31P NMR after Mild Hypothermia Treatments of Oxygen—Glucose Deprivation in a Neonatal Brain Slice Model of Asphyxia. *J Cereb Blood Flow Metab* **31**, 547–559 (2011).

80. Liu, J. *et al.* 1H nuclear magnetic resonance brain metabolomics in neonatal mice after hypoxia–ischemia distinguished normothermic recovery from mild hypothermia recoveries. *Pediatric Research* **74**, 170–179 (2013).

81. Liu, J. *et al.* 13C NMR Metabolomic Evaluation of Immediate and Delayed Mild Hypothermia in Cerebrocortical Slices after Oxygen–Glucose Deprivation: *Anesthesiology* **119**, 1120–1136 (2013).

82. Locci, E. *et al.* A longitudinal 1H-NMR metabolomics analysis of urine from newborns with hypoxic-ischemic encephalopathy undergoing hypothermia therapy. Clinical and medical legal insights. *PLOS ONE* **13**, e0194267 (2018).

83. Longini, M. *et al.* Proton nuclear magnetic resonance spectroscopy of urine samples in preterm asphyctic newborn: A metabolomic approach. *Clinica Chimica Acta* **444**, 250–256 (2015).

84. Reinke, S. N. *et al.* 1H NMR derived metabolomic profile of neonatal asphyxia in umbilical cord serum: implications for hypoxic ischemic encephalopathy. *J. Proteome Res.* **12**, 4230–4239 (2013).

85. Skappak, C., Regush, S., Cheung, P.-Y. & Adamko, D. J. Identifying Hypoxia in a Newborn Piglet Model Using Urinary NMR Metabolomic Profiling. *PLoS ONE* **8**, e65035 (2013).

86. Van Cappellen Van Walsum, A.-M. *et al.* Hypoxia in Fetal Lambs: A Study with 1H-NMR Spectroscopy of Cerebrospinal Fluid. *Pediatr Res* **49**, 698–704 (2001).

87. Denihan, N. M. *et al.* Untargeted metabolomic analysis and pathway discovery in perinatal asphyxia and hypoxic-ischaemic encephalopathy. *Journal of Cerebral Blood Flow & Metabolism* **39**, 147–162 (2019).

88. Chen, Y. *et al.* Short- and long-term effects of perinatal asphyxia on monoamine, amino acid and glycolysis product levels measured in the basal ganglia of the rat. *Developmental Brain Research* **104**, 19–30 (1997).

89. Hagberg, H., Andersson, P., Kjellmer, I., Thiringer, K. & Thordstein, M. Extracellular overflow of glutamate, aspartate, GABA and taurine in the cortex and basal ganglia of fetal lambs during hypoxia-ischemia. *Neuroscience Letters* **78**, 311–317 (1987).

90. Takenouchi, T. *et al.* Therapeutic Hypothermia Achieves Neuroprotection via a Decrease in Acetylcholine with a Concurrent Increase in Carnitine in the Neonatal Hypoxia-Ischemia. *J Cereb Blood Flow Metab* **35**, 794–805 (2015).

91. Beckstrom, A. C., Humston, E. M., Snyder, L. R., Synovec, R. E. & Juul, S. E. Application of comprehensive two-dimensional gas chromatography with time-of-flight mass spectrometry method to identify potential biomarkers of perinatal asphyxia in a non-human primate model. *Journal of Chromatography A* **1218**, 1899–1906 (2011).

92. Chun, P. T. *et al.* Serial Plasma Metabolites Following Hypoxic-Ischemic Encephalopathy in a Nonhuman Primate Model. *Developmental Neuroscience* **37**, 161–171 (2015).

93. Noto, A. *et al.* Urinary gas chromatography mass spectrometry metabolomics in asphyxiated newborns undergoing hypothermia: from the birth to the first month of life. *Annals of Translational Medicine* **4**, 417–417 (2016).

94. Lou, B.-S., Wu, P.-S., Liu, Y. & Wang, J.-S. Effects of Acute Systematic Hypoxia on Human Urinary Metabolites Using LC-MS-Based Metabolomics. *High Altitude Medicine & Biology* **15**, 192–202 (2014).

95. Sarafidis, K. *et al.* Urine metabolomic profile in neonates with hypoxic-ischemic encephalopa-thy. *Hippokratia* **21**, 80–84 (2017).

96. Solberg, R. *et al.* Changes of the plasma metabolome of newly born piglets subjected to postnatal hypoxia and resuscitation with air. *Pediatric Research* **80**, 284–292 (2016).

97. Lubec, G., Widness, J. A., Hayde, M., Menzel, D. & Pollak, A. Hydroxyl Radical Generation in Oxygen-treated Infants. *Pediatrics* **100**, 700–704 (1997).

98. Hara, K. *et al.* Oxidative Stress in Newborn Infants with and without Asphyxia as Measured by Plasma Antioxidants and Free Fatty Acids. *Biochemical and Biophysical Research Communications* **257**, 244–248 (1999).

99. Baran, H. *et al.* Increased kynurenic acid in the brain after neonatal asphyxia. *Life Sciences* **69**, 1249–1256 (2001).

100. Vento, M. *et al.* Resuscitation With Room Air Instead of 100% Oxygen Prevents Oxidative Stress in Moderately Asphyxiated Term Neonates. *Pediatrics* **107**, 642–647 (2001).

101. Ahearne, C. E. *et al.* Early Cord Metabolite Index and Outcome in Perinatal Asphyxia and Hypoxic-Ischaemic Encephalopathy. *Neonatology* **110**, 296–302 (2016).

102. Asensi, M. *et al.* A High-Performance Liquid Chromatography Method for Measurement of Oxidized Glutathione in Biological Samples. *Analytical Biochemistry* **217**, 323–328 (1994).

103. Sánchez-Illana, Á. *et al.* Adrenic acid non-enzymatic peroxidation products in biofluids of moderate preterm infants. *Free Radical Biology and Medicine* (2019) doi:10.1016/j.freeradbiomed.2019.02.024.

104. Solberg, R. *et al.* Metabolomic Analysis of the Effect of Postnatal Hypoxia on the Retina in a Newly Born Piglet Model. *PLoS ONE* **8**, e66540 (2013).

105. Buonocore, G., Perrone, S. & Tataranno, M. L. Oxygen toxicity: chemistry and biology of reactive oxygen species. *Seminars in Fetal and Neonatal Medicine* **15**, 186–190 (2010).

106. Lehtonen, L., Gimeno, A., Parra-Llorca, A. & Vento, M. Early neonatal death: A challenge worldwide. *Semin Fetal Neonatal Med* **22**, 153–160 (2017).

107. Sonnewald, U. Glutamate synthesis has to be matched by its degradation – where do all the carbons go? *Journal of Neurochemistry* **131**, 399–406 (2014).

108. Mulukutla, B. C., Yongky, A., Le, T., Mashek, D. G. & Hu, W.-S. Regulation of Glucose Metabolism – A Perspective From Cell Bioprocessing. *Trends in Biotechnology* **34**, 638–651 (2016).

109. McNeil, C. A., Pramfalk, C., Humphreys, S. M. & Hodson, L. The storage stability and concentration of acetoacetate differs between blood fractions. *Clinica Chimica Acta* **433**, 278–283 (2014).

110. Brekke, E., Berger, H. R., Widerøe, M., Sonnewald, U. & Morken, T. S. Glucose and Intermediary Metabolism and Astrocyte–Neuron Interactions Following Neonatal Hypoxia–Ischemia in Rat. *Neurochem Res* **42**, 115–132 (2017).

111. Nuñez-Ramiro, A. *et al.* Topiramate plus Cooling for Hypoxic-Ischemic Encephalopathy: A Randomized, Controlled, Multicenter, Double-Blinded Trial. *Neonatology* 76–84 (2019) doi:10.1159/000499084.

112. Badawy, A. A.-B. & Dougherty, D. M. Assessment of the Human Kynurenine Pathway: Comparisons and Clinical Implications of Ethnic and Gender Differences in Plasma Tryptophan, Kynurenine Metabolites, and Enzyme Expressions at Baseline and after Acute Tryptophan Loading and Depletion: *International Journal of Tryptophan Research* (2016) doi:10.4137/IJTR.S38189.

113. U.S. Food and Drug Administration. Devices@FDA Catalog. https://www.accessdata.fda.gov/scripts/cdrh/devicesatfda/index.cfm.

114. CDER Biomarker Qualification Program. *FDA* http://www.fda.gov/drugs/drug-development-tool-qualification-programs/cder-biomarker-qualification-program (2019).

115. European Medicines Agency. Qualification of novel methodologies for medicine development. *European Medicines Agency* https://www.ema.europa.eu/en/human-regulatory/research-development/scientific-advice-protocol-assistance/qualification-novel-methodologies-medicine-development (2018).

116. Sánchez-Illana, Á. *et al.* On-Capillary Surface-Enhanced Raman Spectroscopy: Determination of Glutathione in Whole Blood Microsamples. *Anal. Chem.* **90**, 9093–9100 (2018).

117. Westley, C., Xu, Y., Carnell, A. J., Turner, N. J. & Goodacre, R. Label-Free Surface Enhanced Raman Scattering Approach for High-Throughput Screening of Biocatalysts. *Anal. Chem.* **88**, 5898–5903 (2016).

118. Kurinczuk, J. J., White-Koning, M. & Badawi, N. Epidemiology of neonatal encephalopathy and hypoxic-ischaemic encephalopathy. *Early Hum. Dev.* **86**, 329–338 (2010).

119. Merchant, N. & Azzopardi, D. Early predictors of outcome in infants treated with hypothermia for hypoxic–ischaemic encephalopathy. *Developmental Medicine & Child Neurology* **57**, 8–16 (2015).

120. Aslam, S. & Molloy, E. J. Biomarkers of multiorgan injury in neonatal encephalopathy. *Biomark Med* **9**, 267–275 (2015).

121. Ahearne, C. E., Boylan, G. B. & Murray, D. M. Short and long term prognosis in perinatal asphyxia: An update. *World Journal of Clinical Pediatrics* **5**, 67–74 (2016).

122. Bennet, L., Booth, L. & Gunn, A. J. Potential biomarkers for hypoxic-ischemic encephalopathy. *Semin Fetal Neonatal Med* **15**, 253–260 (2010).

123. Ramaswamy, V. *et al.* Systematic Review of Biomarkers of Brain Injury in Term Neonatal Encephalopathy. *Pediatric Neurology* **40**, 215–226 (2009).

124. Lange, C. A. K. & Bainbridge, J. W. B. Oxygen Sensing in Retinal Health and Disease. *OPH* **227**, 115–131 (2012).

125. Gibellini, F. & Smith, T. K. The Kennedy pathway—De novo synthesis of phosphatidylethanolamine and phosphatidylcholine. *IUBMB Life* **62**, 414–428 (2010).

126. Xia, J., Broadhurst, D. I., Wilson, M. & Wishart, D. S. Translational biomarker discovery in clinical metabolomics: an introductory tutorial. *Metabolomics* **9**, 280–299 (2013).

127. Fagone, P. & Jackowski, S. Phosphatidylcholine and the CDP–choline cycle. *Biochimica et Biophysica Acta (BBA) - Molecular and Cell Biology of Lipids* **1831**, 523–532 (2013).

128. Ueland, P. M. Choline and betaine in health and disease. *Journal of Inherited Metabolic Disease* **34**, 3–15 (2011).

129. Kennedy, E. P. Synthesis of Phosphatides in Isolated Mitochondria Ii. Incorporation of Choline into Lecithin. *J. Biol. Chem.* **209**, 525–535 (1954).

130. Cansev, M. Uridine and cytidine in the brain: Their transport and utilization. *Brain Research Reviews* **52**, 389–397 (2006).

131. Zeisel, S. H. A Brief History of Choline. *ANM* **61**, 254–258 (2012).

132. Dale, H. H. The Action of Certain Esters and Ethers of Choline, and Their Relation to Muscarine. *J Pharmacol Exp Ther* **6**, 147–190 (1914).

133. Loewi, O. Über humorale übertragbarkeit der Herznervenwirkung. *Pflügers Arch.* **189**, 239–242 (1921).

134. Baburamani, A., Ek, C. J., Walker, D. W. & Castillo-Melendez, M. Vulnerability of the developing brain to hypoxic-ischemic damage: contribution of the cerebral vasculature to injury and repair? *Front. Physiol.* **3**, (2012).

135. Ek, C. J. *et al.* Brain Barrier Properties and Cerebral Blood Flow in Neonatal Mice Exposed to Cerebral Hypoxia-Ischemia: *Journal of Cerebral Blood Flow & Metabolism* (2015) doi:10.1038/jcbfm.2014.255.

136. Nolan, J. P. *et al.* European Resuscitation Council Guidelines for Resuscitation 2010 Section 1. Executive summary. *Resuscitation* **81**, 1219–1276 (2010).

137. Natarajan, G., Pappas, A. & Shankaran, S. Outcomes in childhood following therapeutic hypothermia for neonatal hypoxic-ischemic encephalopathy (HIE). *Seminars in Perinatology* **40**, 549–555 (2016).

138. Azzopardi, D. *et al.* Moderate hypothermia within 6 h of birth plus inhaled xenon versus moderate hypothermia alone after birth asphyxia (TOBY-Xe): a proof-of-concept, open-label, randomised controlled trial. *The Lancet Neurology* **15**, 145–153 (2016).

139. Juul, S. E. & Ferriero, D. M. Pharmacologic Neuroprotective Strategies in Neonatal Brain Injury. *Clinics in Perinatology* **41**, 119–131 (2014).

140. Blanco, D. *et al.* Neuroprotección con hipotermia en el recién nacido con encefalopatía hipóxico-isquémica. Guía de estándares para su aplicación clínica. *Anales de Pediatría* **75**, 341.e1-341.e20 (2011).

141. Saugstad, O. Is lactate a reliable indicator of tissue hypoxia in the neonatal period? *Acta Pædiatrica* **91**, 17–19 (2002).

142. Stein, S. E. Retention Indices. in *NIST Chemistry WebBook, NIST Standard Reference Database Number 69* (eds. Linstrom, P. J. & Mallard, W. G.) (National Institute of Standards and Technology, 2008).

143. Calderón-Santiago, M., Priego-Capote, F., Galache-Osuna, J. G. & Luque de Castro, M. D. Method based on GC–MS to study the influence of tricarboxylic acid cycle metabolites on cardiovascular risk factors. *Journal of Pharmaceutical and Biomedical Analysis* **74**, 178–185 (2013).

144. Paik, M.-J. *et al.* Simultaneous clinical monitoring of lactic acid, pyruvic acid and ketone bodies in plasma as methoxime/tert-butyldimethylsilyl derivatives by gas chromatography–mass spectrometry in selected ion monitoring mode. *Biomedical Chromatography* **22**, 450–453 (2008).

145. Mamer, O. *et al.* The complete targeted profile of the organic acid intermediates of the citric acid cycle using a single stable isotope dilution analysis, sodium borodeuteride reduction and selected ion monitoring GC/MS. *Metabolomics* **9**, 1019–1030 (2013).

146. Kombu, R. S., Brunengraber, H. & Puchowicz, M. A. Analysis of the Citric Acid Cycle Intermediates Using Gas Chromatography-Mass Spectrometry. in *Metabolic Profiling: Methods and Protocols* (ed. Metz, T. O.) 147–157 (Humana Press, 2011). doi:10.1007/978-1-61737-985-7_8.

147. Kubota, K. *et al.* Development of an HPLC-fluorescence determination method for carboxylic acids related to the tricarboxylic acid cycle as a metabolome tool. *Biomed. Chromatogr.* **19**, 788–795 (2005).

148. Luo, B., Groenke, K., Takors, R., Wandrey, C. & Oldiges, M. Simultaneous determination of multiple intracellular metabolites in glycolysis, pentose phosphate pathway and tricarboxylic acid cycle by liquid chromatography–mass spectrometry. *Journal of Chromatography A* **1147**, 153–164 (2007).

149. Koubaa, M., Cocuron, J.-C., Thomasset, B. & Alonso, A. P. Highlighting the tricarboxylic acid cycle: liquid and gas chromatography-mass spectrometry analyses of (13)C-labeled organic acids. *Anal. Biochem.* **436**, 151–159 (2013).

150. Soga, T. *et al.* Quantitative Metabolome Analysis Using Capillary Electrophoresis Mass Spectrometry. *J. Proteome Res.* **2**, 488–494 (2003).

151. Wakayama, M., Aoki, N., Sasaki, H. & Ohsugi, R. Simultaneous Analysis of Amino Acids and Carboxylic Acids by Capillary Electrophoresis−Mass Spectrometry Using an Acidic Electrolyte and Uncoated Fused-Silica Capillary. *Anal. Chem.* **82**, 9967–9976 (2010).

152. Astles, R., Williams, C. P. & Sedor, F. Stability of plasma lactate in vitro in the presence of antiglycolytic agents. *Clinical Chemistry* **40**, 1327–1330 (1994).

153. Dubé, M. P., Kitch, D. W., Parker, R. A., Alston-Smith, B. L. & Mulligan, K. The effect of long-term storage on measured plasma lactate concentrations and prospective lactate results from a multicenter trial of antiretroviral therapy. *Clinical Chemistry and Laboratory Medicine (CCLM)* **43**, 947–952 (2005).

154. Nielsen, J., Ytrebø, L. M. & Borud, O. Lactate and pyruvate concentrations in capillary blood from newborns. *Acta Paediatr.* **83**, 920–922 (1994).

155. Balushi, A. A., Guilbault, M.-P. & Wintermark, P. Secondary Increase of Lactate Levels in Asphyxiated Newborns during Hypothermia Treatment: Reflect of Suboptimal Hemodynamics (A Case Series and Review of the Literature). *AJP Rep* **06**, e48–e58 (2016).

156. Bracci, R., Perrone, S. & Buonocore, G. The timing of neonatal brain damage. *Biol. Neonate* **90**, 145–155 (2006).

157. Shah, S., Tracy, M. & Smyth, J. Postnatal Lactate as an Early Predictor of Short-Term Outcome after Intrapartum Asphyxia. *Journal of Perinatology* **24**, 16–20 (2004).

158. Wood, T. & Thoresen, M. Physiological responses to hypothermia. *Seminars in Fetal and Neonatal Medicine* **20**, 87–96 (2015).

159. Vannucci, R. C., Brucklacher, R. M. & Vannucci, S. J. Glycolysis and Perinatal Hypoxic-Ischemic Brain Damage. *DNE* **27**, 185–190 (2005).

160. Gasior, M., Rogawski, M. A. & Hartman, A. L. Neuroprotective and disease-modifying effects of the ketogenic diet. *Behavioural Pharmacology* **17**, 431–439 (2006).

161. Chouchani, E. T. *et al.* Ischaemic accumulation of succinate controls reperfusion injury through mitochondrial ROS. *Nature* **515**, 431–435 (2014).

162. Chawanpaiboon, S. *et al.* Global, regional, and national estimates of levels of preterm birth in 2014: a systematic review and modelling analysis. *The Lancet Global Health* **7**, e37–e46 (2019).

163. Kiserud, T. *et al.* The World Health Organization Fetal Growth Charts: A Multinational Longitudinal Study of Ultrasound Biometric Measurements and Estimated Fetal Weight. *PLOS Medicine* **14**, e1002220 (2017).

164. Papageorghiou, A. T. *et al.* International standards for fetal growth based on serial ultrasound measurements: the Fetal Growth Longitudinal Study of the INTERGROWTH-21st Project. *The Lancet* **384**, 869–879 (2014).

165. Blencowe, H. *et al.* National, regional, and worldwide estimates of preterm birth rates in the year 2010 with time trends since 1990 for selected countries: a systematic analysis and implications. *The Lancet* **379**, 2162–2172 (2012).

166. UNICEF, WHO & World Bank Group and United Nations. *Levels & Trends in Child Mortality. Report 2019*. https://www.unicef.org/media/60561/file/UN-IGME-child-mortality-report-2019.pdf (2019).

167. Menon, R. Oxidative Stress Damage as a Detrimental Factor in Preterm Birth Pathology. *Front. Immunol.* **5**, (2014).

168. Moore, T. A., Ahmad, I. M. & Zimmerman, M. C. Oxidative Stress and Preterm Birth: An Integrative Review: *Biological Research For Nursing* (2018) doi:10.1177/1099800418791028.

169. Torres-Cuevas, I. *et al.* Oxygen and oxidative stress in the perinatal period. *Redox Biol* **12**, 674–681 (2017).

170. Torres-Cuevas, I. *et al.* Oxygen Supplementation to Stabilize Preterm Infants in the Fetal to Neonatal Transition: No Satisfactory Answer. *Front. Pediatr.* **4**, (2016).

171. Panfoli, I. *et al.* Oxidative Stress as a Primary Risk Factor for Brain Damage in Preterm Newborns. *Front. Pediatr.* **6**, (2018).

172. Kinsey, V. E., Jacobus, J. T. & Hemphill, F. M. Retrolental Fibroplasia: Cooperative Study of Retrolental Fibroplasia and the Use of Oxygen. *AMA Arch Ophthalmol* **56**, 481–543 (1956).

173. Berfenstam, R., Edlund, T. & Zettergren, L. The Hyaline Membrane Disease. *Acta Paediatrica* **47**, 82–100 (1958).

174. Gyllensten, L. Oxygen Exposure and Brain Damage. *Nature* **183**, 1068–1069 (1959).

175. Perrone, S., Laschi, E. & Buonocore, G. Oxidative stress biomarkers in the perinatal period: Diagnostic and prognostic value. *Seminars in Fetal and Neonatal Medicine* 101087 (2020) doi:10.1016/j.siny.2020.101087.

176. Vento, M. Oxidative stress in the perinatal period. *Free Radical Biology and Medicine* **142**, 1–2 (2019).

177. Katerji, M., Filippova, M. & Duerksen-Hughes, P. Approaches and Methods to Measure Oxidative Stress in Clinical Samples: Research Applications in the Cancer Field. *Oxidative Medicine and Cellular Longevity* **2019**, 1–29 (2019).

178. Koopman, W. J. H. *et al.* Mammalian Mitochondrial Complex I: Biogenesis, Regulation, and Reactive Oxygen Species Generation. *Antioxidants & Redox Signaling* **12**, 1431–1470 (2010).

179. Spasojević, I. Free radicals and antioxidants at a glance using EPR spectroscopy. *Critical Reviews in Clinical Laboratory Sciences* **48**, 114–142 (2011).

180. Ahola, T., Fellman, V., Kjellmer, I., Raivio, K. O. & Lapatto, R. Plasma 8-Isoprostane Is Increased in Preterm Infants Who Develop Bronchopulmonary Dysplasia or Periventricular Leukomalacia. *Pediatr Res* **56**, 88–93 (2004).

181. Buonocore, G., Perrone, S., Longini, M., Terzuoli, L. & Bracci, R. Total Hydroperoxide and Advanced Oxidation Protein Products in Preterm Hypoxic Babies. *Pediatr Res* **47**, 221–221 (2000).

182. Perrone, S. *et al.* Oxidative kidney damage in preterm newborns during perinatal period. *Clinical Biochemistry* **40**, 656–660 (2007).

183. Buonocore, G. *et al.* Oxidative Stress in Preterm Neonates at Birth and on the Seventh Day of Life. *Pediatr Res* **52**, 46–49 (2002).

184. Tataranno, M. *et al.* Resuscitating preterm infants with 100% oxygen is associated with higher oxidative stress than room air. *Acta Paediatr* **104**, 759–765 (2015).

185. Tokuriki, S., Okuno, T., Ohta, G. & Ohshima, Y. Carboxyhemoglobin Formation in Preterm Infants Is Related to the Subsequent Development of Bronchopulmonary Dysplasia. *Disease Markers* https://www.hindawi.com/journals/dm/2015/620921/ (2015) doi:https://doi.org/10.1155/2015/620921.

186. Selmeci, L. *et al.* Human blood plasma advanced oxidation protein products (AOPP) correlates with fibrinogen levels. *Free Radical Research* **40**, 952–958 (2006).

187. Gerber, C. E., Bruchelt, G., Stegmann, H., Schweinsberg, F. & Speer, Ch. P. Presence of Bleomycin-Detectable Free Iron in the Alveolar System of Preterm Infants. *Biochemical and Biophysical Research Communications* **257**, 218–222 (1999).

188. Dizdar, E. A. *et al.* Total antioxidant capacity and total oxidant status after surfactant treatment in preterm infants with respiratory distress syndrome. *Ann Clin Biochem* **48**, 462–467 (2011).

189. Dursun, A., Okumuş, N., Erol, S., Bayrak, T. & Zenciroğlu, A. Effect of Ventilation Support on Oxidative Stress and Ischemia-Modified Albumin in Neonates. *Am J Perinatol* **33**, 136–142 (2016).

190. Rogers, S., Witz, G., Anwar, M., Hiatt, M. & Hegyi, T. Antioxidant capacity and oxygen radical diseases in the preterm newborn. *Arch Pediatr Adolesc Med* **154**, 544–548 (2000).

191. Musilova, I. *et al.* Umbilical cord blood markers of oxidative stress in pregnancies complicated by preterm prelabor rupture of membranes. *The Journal of Maternal-Fetal & Neonatal Medicine* **29**, 1900–1910 (2016).

192. Miller, N. J., Rice-Evans, C., Davies, M. J., Gopinathan, V. & Milner, A. A Novel Method for Measuring Antioxidant Capacity and its Application to Monitoring the Antioxidant Status in Premature Neonates. *Clinical Science* **84**, 407–412 (1993).

193. Wijnberger, L. D. E., Krediet, T. G., Visser, G. H. A., van Bel, F. & Egberts, J. Early neonatal antioxidant capacity after preexisting impaired placental function. *Early Human Development* **71**, 111–116 (2003).

194. Ezaki, S. *et al.* Resuscitation of Preterm Infants with Reduced Oxygen Results in Less Oxidative Stress than Resuscitation with 100% Oxygen. *Journal of Clinical Biochemistry and Nutrition* **44**, 111–118 (2009).

195. Kapadia, V. S. *et al.* Resuscitation of Preterm Neonates With Limited Versus High Oxygen Strategy. *Pediatrics* **132**, e1488–e1496 (2013).

196. Bassiouny, M. *et al.* A Randomized Controlled Trial on Parenteral Nutrition, Oxidative Stress, and Chronic Lung Diseases in Preterm Infants. *Journal of Pediatric Gastroenterology and Nutrition* **48**, 363–369 (2009).

197. Fabiano, A. *et al.* The development of lung biochemical monitoring can play a key role in the early prediction of bronchopulmonary dysplasia. *Acta Paediatrica* **105**, 535–541 (2016).

198. Lázár, R., Orvos, H., Szőllősi, R. & Varga, I. S. The quality of the antioxidant defence system in term and preterm twin neonates. *Redox Report* **20**, 103–108 (2015).

199. Negi, R., Pande, D., Kumar, A., Khanna, R. S. & Khanna, H. D. Evaluation of biomarkers of oxidative stress and antioxidant capacity in the cord blood of preterm low birth weight neonates. *The Journal of Maternal-Fetal & Neonatal Medicine* **25**, 1338–1341 (2012).

200. Berger, T. M. *et al.* Antioxidant Activity of Vitamin C in Iron-overloaded Human Plasma. *Journal of Biological Chemistry* **272**, 15656–15660 (1997).

201. Kime, R., Gibson, A., Yong, W., Hider, R. & Powers, H. Chromatographic Method for the Determination of Non-Transferrin-Bound Iron Suitable for Use on the Plasma and Bronchoalveolar Lavage Fluid of Preterm Babies. *Clinical Science* **91**, 633–638 (1996).

202. Abo, M. & Weerapana, E. Chemical Probes for Redox Signaling and Oxidative Stress. *Antioxidants & Redox Signaling* **30**, 1369–1386 (2019).

203. Norishadkam, M., Andishmand, S., Zavar reza, J., Zare Sakhvidi, M. J. & Hachesoo, V. R. Oxidative stress and DNA damage in the cord blood of preterm infants. *Mutation Research/Genetic Toxicology and Environmental Mutagenesis* **824**, 20–24 (2017).

204. Ghany, E. A. G. A., Alsharany, W., Ali, A. A., Youness, E. R. & Hussein, J. S. Anti-oxidant profiles and markers of oxidative stress in preterm neonates. *Paediatrics and International Child Health* **36**, 134–140 (2016).

205. Nassi, N., Ponziani, V., Becatti, M., Galvan, P. & Donzelli, G. Anti-oxidant enzymes and related elements in term and preterm newborns. *Pediatrics International* **51**, 183–187 (2009).

206. Inayat, M. *et al.* Antioxidants and Biomarkers of Oxidative Stress in Preterm Infants with Symptomatic Patent Ductus Arteriosus. *Amer J Perinatol* **32**, 895–904 (2015).

207. Grigg, J., Barber, A. & Silverman, M. Bronchoalveolar lavage fluid glutathione in intubated premature infants. *Archives of Disease in Childhood* **69**, 49–51 (1993).

208. Lee, Y.-S. & Chou, Y.-H. Antioxidant profiles in full term and preterm neonates. *Chang Gung Med J* **28**, 846–851 (2005).

209. Boda, D., Németh, I. & Pintér, S. Surface Tension, Glutathione Content and Redox Ratio of the Tracheal Aspirate Fluid of Premature Infants with IRDS. *NEO* **74**, 281–288 (1998).

210. Frosali, S. *et al.* Glutathione Recycling and Antioxidant Enzyme Activities in Erythrocytes of Term and Preterm Newborns at Birth. *Neonatology* **85**, 188–194 (2004).

211. Moison, R. M. W., Haasnoot, A. A., Zoeren-Grobben, D. van & Berger, H. M. Red blood cell glutathione and plasma sulfhydryls in chronic lung disease of the newborn. *Acta Paediatrica* **86**, 1363–1369 (1997).

212. Zoeren-Grobben, D. van *et al.* Markers of oxidative stress and antioxidant activity in plasma and erythrocytes in neonatal respiratory distress syndrome. *Acta Paediatrica* **86**, 1356–1362 (1997).

213. Elkabany, Z. A. *et al.* Oxidative stress markers in neonatal respiratory distress syndrome: advanced oxidation protein products and 8-hydroxy-2-deoxyguanosine in relation to disease severity. *Pediatr Res* **87**, 74–80 (2020).

214. Weber, D. *et al.* Oxidative stress markers and micronutrients in maternal and cord blood in relation to neonatal outcome. *Eur J Clin Nutr* **68**, 215–222 (2014).

215. Ahmed, A. E.-A., Abd-Elmawgood, E. A. & Hassan, M. H. Circulating Protein Carbonyls, Antioxidant Enzymes and Related Trace Minerals among Preterms with Respiratory Distress Syndrome. *J Clin Diagn Res* **11**, BC17–BC21 (2017).

216. Mocatta, T. J., Winterbourn, C. C., Inder, T. E. & Darlow, B. A. The Effect of Gestational Age and Labour on Markers of Lipid and Protein Oxidation in Cord Plasma. *Free Radical Research* **38**, 185–191 (2004).

217. Perrone, S., Laschi, E. & Buonocore, G. Biomarkers of oxidative stress in the fetus and in the newborn. *Free Radical Biology and Medicine* **142**, 23–31 (2019).

218. Russell, G. A. & Cooke, R. W. Randomised controlled trial of allopurinol prophylaxis in very preterm infants. *Archives of Disease in Childhood - Fetal and Neonatal Edition* **73**, F27–F31 (1995).

219. Holden, M. S. *et al.* Urinary Hypoxanthine as a Measure of Increased ATP Utilization in Late Preterm Infants. *ICAN: Infant, Child, & Adolescent Nutrition* **6**, 240–249 (2014).

220. Asmerom, Y. *et al.* Oral Sucrose for Heel Lance Increases Adenosine Triphosphate Use and Oxidative Stress in Preterm Neonates. *The Journal of Pediatrics* **163**, 29-35.e1 (2013).

221. Florio, P. *et al.* Activin A Plasma Levels at Birth: An Index of Fetal Hypoxia in Preterm Newborn. *Pediatr Res* **54**, 696–700 (2003).

222. Buonocore, G. *et al.* Hypoxia-induced free iron release in the red cells of newborn infants. *Acta Paediatrica* **87**, 77–81 (1997).

223. Vento, M. *et al.* Preterm resuscitation with low oxygen causes less oxidative stress, inflammation, and chronic lung disease. *Pediatrics* **124**, e439-449 (2009).

224. Buonocore, G. *et al.* Non protein bound iron as early predictive marker of neonatal brain damage. *Brain* **126**, 1224–1230 (2003).

225. Mohamed, I., Elremaly, W., Rouleau, T. & Lavoie, J.-C. Oxygen and parenteral nutrition two main oxidants for extremely preterm infants: 'It all adds up'. *Journal of Neonatal-Perinatal Medicine* **8**, 189–197 (2015).

226. Drury, J. A., Jeffers, G. & Cooke, R. W. Urinary 8-Hydroxydeoxyguanosine in Infants and Children. *Free Radical Research* **28**, 423–428 (1998).

227. Kato, E. *et al.* Effects of supplemental oxygen on urinary 8-hydroxy-2'-deoxyguanosine levels in extremely low birth weight infants. *Free Radical Research* **48**, 1285–1290 (2014).

228. Fusch, G. *et al.* Source and Quality of Enteral Nutrition Influences Oxidative Stress in Preterm Infants: A Prospective Cohort Study. *Journal of Parenteral and Enteral Nutrition* **42**, 1288–1294 (2018).

229. Matthews, M. A. *et al.* Increasing F2-isoprostanes in the first month after birth predicts poor respiratory and neurodevelopmental outcomes in very preterm infants. *J Perinatol* **36**, 779–783 (2016).

230. Parra-Llorca, A. *et al.* Does Pasteurized Donor Human Milk Efficiently Protect Preterm Infants Against Oxidative Stress? *Antioxidants & Redox Signaling* **31**, 791–799 (2019).

231. Kuligowski, J. *et al.* Assessment of oxidative damage to proteins and DNA in urine of newborn infants by a validated UPLC-MS/MS approach. *PLoS ONE* **9**, e93703 (2014).

232. Ripalda, M. J., Rudolph, N. & Wong, S. L. Developmental Patterns of Antioxidant Defense Mechanisms in Human Erythrocytes. *Pediatr Res* **26**, 366–369 (1989).

233. Vilas, N. N. *et al.* Copper, zinc and superoxide dismutase levels in cord blood. *Nutrition Research* **6**, 327–331 (1986).

234. Whaun, J. M. & Oski, F. A. Relation of red blood cell glutathione peroxidase to neonatal jaundice. *The Journal of Pediatrics* **76**, 555–560 (1970).

235. Wilson, D. C., Tubman, R., Bell, N., Halliday, H. L. & McMaster, D. Plasma manganese, selenium and glutathione peroxidase levels in the mother and newborn infant. *Early Human Development* **26**, 223–226 (1991).

236. Deponte, M. The Incomplete Glutathione Puzzle: Just Guessing at Numbers and Figures? *Antioxidants & Redox Signaling* **27**, 1130–1161 (2017).

237. Rossi, R. *et al.* Blood Glutathione Disulfide: In Vivo Factor or in Vitro Artifact? *Clinical Chemistry* **48**, 742–753 (2002).

238. Güntherberg, H. & Rost, J. The true oxidized glutathione content of red blood cells obtained by new enzymic and paper chromatographic methods. *Analytical Biochemistry* **15**, 205–210 (1966).

239. Giustarini, D., Dalle-Donne, I., Milzani, A., Fanti, P. & Rossi, R. Analysis of GSH and GSSG after derivatization with *N*-ethylmaleimide. *Nature Protocols* **8**, nprot.2013.095 (2013).

240. Tietze, F. Enzymic method for quantitative determination of nanogram amounts of total and oxidized glutathione: Applications to mammalian blood and other tissues. *Analytical Biochemistry* **27**, 502–522 (1969).

241. Rahman, I., Kode, A. & Biswas, S. K. Assay for quantitative determination of glutathione and glutathione disulfide levels using enzymatic recycling method. *Nat. Protocols* **1**, 3159–3165 (2007).

242. Perez, M., Robbins, M. E., Revhaug, C. & Saugstad, O. D. Oxygen radical disease in the newborn, revisited: Oxidative stress and disease in the newborn period. *Free Radical Biology and Medicine* **142**, 61–72 (2019).

243. Saugstad, O. D. Resuscitation of newborn infants: from oxygen to room air. *The Lancet* **376**, 1970–1971 (2010).

244. Wang, Y., Wu, Y., Li, T., Wang, X. & Zhu, C. Iron Metabolism and Brain Development in Premature Infants. *Front. Physiol.* **10**, (2019).

245. Lindeman, J. H. N., Houdkamp, E., Lentjes, G. W. M., Poorthuis, B. J. H. M. & Berger, H. M. Limited Protection Against Iron-Induced Lipid Peroxidation by Cord Blood Plasma. *Free Radical Research Communications* **16**, 285–294 (1992).

246. Sullivan, J. L. Iron, Plasma Antioxidants, and the 'Oxygen Radical Disease of Prematurity'. *Am J Dis Child* **142**, 1341–1344 (1988).

247. Lorenz, L., Peter, A., Poets, C. F. & Franz, A. R. A Review of Cord Blood Concentrations of Iron Status Parameters to Define Reference Ranges for Preterm Infants. *NEO* **104**, 194–202 (2013).

248. Signorini, C. *et al.* Plasma Esterified F 2 -Isoprostanes and Oxidative Stress in Newborns: Role of Nonprotein-Bound Iron. *Pediatr Res* **63**, 287–291 (2008).

249. Cooke, R. W. I., Drury, J. A., Yoxall, C. W. & James, C. Blood transfusion and chronic lung disease in preterm infants. *Eur J Pediatr* **156**, 47–50 (1996).

250. Baydas, G. *et al.* Antioxidant Vitamin Levels in Term and Preterm Infants and Their Relation to Maternal Vitamin Status. *Archives of Medical Research* **33**, 276–280 (2002).

251. Dallman, P. R. Iron, vitamin E, and folate in the preterm infant. *The Journal of Pediatrics* **85**, 742–752 (1974).

252. Galinier, A. *et al.* Reference range for micronutrients and nutritional marker proteins in cord blood of neonates appropriated for gestational ages. *Early Human Development* **81**, 583–593 (2005).

253. Heinonen, K. *et al.* Plasma vitamin C levels are low in premature infants fed human milk. *The American Journal of Clinical Nutrition* **43**, 923–924 (1986).

254. Huijbers, W. A., Schrijver, J., Speek, A. J., Deelstra, B. A. & Okken, A. Persistent low plasma vitamin E levels in premature infants surviving respiratory distress syndrome. *Eur. J. Pediatr.* **145**, 170–171 (1986).

255. Hustead, V. A., Gutcher, G. R., Anderson, S. A. & Zachman, R. D. Relationship of vitamin A (retinol) status to lung disease in the preterm infant. *The Journal of Pediatrics* **105**, 610–615 (1984).

256. Petrich, C., von Voss, H., Lietke, K. & Göbel, U. Vitamin E concentrations in term and preterm newborns and their clinical course. *Eur J Pediatr* **122**, 275–279 (1976).

257. Shenai, J. P., Chytil, F. & Stahlman, M. T. Vitamin A Status of Neonates with Bronchopulmonary Dysplasia. *Pediatr Res* **19**, 185–188 (1985).

258. Mohanram, M. & Kumar, A. Ascorbic acid and tyrosine metabolism in preterm and small-for-dates infants. *Archives of Disease in Childhood* **50**, 235–237 (1975).

259. Zhang, Y. *et al.* A Review of the Extraction and Determination Methods of Thirteen Essential Vitamins to the Human Body: An Update from 2010. *Molecules* **23**, 1484 (2018).

260. Blois, M. S. Antioxidant Determinations by the Use of a Stable Free Radical. *Nature* **181**, 1199–1200 (1958).

261. Mauro C. & マウロカラテッリ. 酸化ストレス度の分析装置. (2009).

262. Ahola, T., Levonen, A.-L., Fellman, V. & Lapatto, R. Thiol metabolism in preterm infants during the first week of life. *Scandinavian Journal of Clinical and Laboratory Investigation* **64**, 649–658 (2004).

263. Carratelli, M. Method for the determination of oxygen-centered free radicals. (2002).

264. Gessler, P., Nebe, T., Birle, A., Haas, N. & Kachel, W. Neutrophil respiratory burst in term and preterm neonates without signs of infection and in those with increased levels of C-reactive protein. *Pediatr. Res.* **39**, 843–848 (1996).

265. Zielinski, Z. A. M. & Pratt, D. A. Lipid Peroxidation: Kinetics, Mechanisms, and Products. *J. Org. Chem.* **82**, 2817–2825 (2017).

266. Yin, H., Xu, L. & Porter, N. A. Free Radical Lipid Peroxidation: Mechanisms and Analysis. *Chem. Rev.* **111**, 5944–5972 (2011).

267. Milne, G. L., Dai, Q. & Roberts, L. J. The isoprostanes—25 years later. *Biochimica et Biophysica Acta (BBA) - Molecular and Cell Biology of Lipids* **1851**, 433–445 (2015).

268. Galano, J.-M. *et al.* Isoprostanes, neuroprostanes and phytoprostanes: An overview of 25 years of research in chemistry and biology. *Progress in Lipid Research* **68**, 83–108 (2017).

269. Yen, H.-C., Wei, H.-J. & Lin, C.-L. Unresolved issues in the analysis of F_2-isoprostanes, F_4-neuroprostanes, isofurans, neurofurans, and F_2-dihomo-isoprostanes in body fluids and tissue using gas chromatography/negative-ion chemical-ionization mass spectrometry. *Free Radical Research* **49**, 861–880 (2015).

270. Chen, Y., Fantuzzi, G., Schoeny, M., Meier, P. & Patel, A. L. High-Dose Human Milk Feedings Decrease Oxidative Stress in Premature Infant. *Journal of Parenteral and Enteral Nutrition* **43**, 126–132 (2019).

271. Vande Loock, K. *et al.* Preterm newborns show slower repair of oxidative damage and paternal smoking associated DNA damage. *Mutagenesis* **27**, 573–580 (2012).

272. Shigenaga, M. K., Gimeno, C. J. & Ames, B. N. Urinary 8-hydroxy-2'-deoxyguanosine as a biological marker of in vivo oxidative DNA damage. *PNAS* **86**, 9697–9701 (1989).

273. Hsiao, C.-C. *et al.* Correlates of Elevated Interleukin-6 and 8-Hydroxy-2′-Deoxyguanosine Levels in Tracheal Aspirates from Very Low Birth Weight Infants Who Develop Bronchopulmonary Dysplasia. *Pediatrics & Neonatology* **58**, 63–69 (2017).

274. Tsukahara, H. *et al.* Oxidative stress in neonates: Evaluation using specific biomarkers. *Life Sciences* **75**, 933–938 (2004).

275. Tsukahara, H. *et al.* Quantification of L-type fatty acid binding protein in the urine of preterm neonates. *Early Human Development* **81**, 643–646 (2005).

276. Joung, K. E. *et al.* Correlation of urinary inflammatory and oxidative stress markers in very low birth weight infants with subsequent development of bronchopulmonary dysplasia. *Free Radical Research* **45**, 1024–1032 (2011).

277. Moore, T. *et al.* Relations Between Feeding Intolerance and Stress Biomarkers in Preterm Infants. *Journal of Pediatric Gastroenterology and Nutrition* **57**, 356–362 (2013).

278. Ferguson, K. K. *et al.* Repeated measures of urinary oxidative stress biomarkers during pregnancy and preterm birth. *Am. J. Obstet. Gynecol.* **212**, 208.e1–8 (2015).

279. Hattori, Y. *et al.* Catalytic ferrous iron in amniotic fluid as a predictive marker of human maternal-fetal disorders. *Journal of Clinical Biochemistry and Nutrition* **56**, 57–63 (2015).

280. Moore, T. A., Schmid, K. K., Anderson-Berry, A. & Berger, A. M. Lung Disease, Oxidative Stress, and Oxygen Requirements in Preterm Infants. *Biological Research For Nursing* **18**, 322–330 (2016).

281. Bandyopadhyay, T., Bhatia, B. D. & Khanna, H. D. A study of oxidative stress in neonates delivered through meconium-stained amniotic fluid. *Eur J Pediatr* **176**, 317–325 (2017).

282. Ferguson, K. K. *et al.* Urinary concentrations of phenols in association with biomarkers of oxidative stress in pregnancy: Assessment of effects independent of phthalates. *Environment International* **131**, 104903 (2019).

283. Ledo, A. *et al.* Human milk enhances antioxidant defenses against hydroxyl radical aggression in preterm infants. *Am J Clin Nutr* **89**, 210–215 (2009).

284. Cháfer-Pericás, C. *et al.* Novel biomarkers in amniotic fluid for early assessment of intraamniotic infection. *Free Radic. Biol. Med.* **89**, 734–740 (2015).

285. Dalle-Donne, I., Giustarini, D., Colombo, R., Rossi, R. & Milzani, A. Protein carbonylation in human diseases. *Trends in Molecular Medicine* **9**, 169–176 (2003).

286. Buss, H., Chan, T. P., Sluis, K. B., Domigan, N. M. & Winterbourn, C. C. Protein Carbonyl Measurement by a Sensitive ELISA Method. *Free Radical Biology and Medicine* **23**, 361–366 (1997).

287. Witko-Sarsat, V. *et al.* Advanced oxidation protein products as a novel marker of oxidative stress in uremia. *Kidney International* **49**, 1304–1313 (1996).

288. Liu, B. *et al.* Detection of advanced oxidation protein products in patients with chronic kidney disease by a novel monoclonal antibody. *Free Radical Research* **45**, 662–671 (2011).

289. Lorch, S. A. *et al.* Plasma 3-NITROTYROSINE and outcome in neonates with severe bronchopulmonary dysplasia after inhaled nitric oxide. *Free Radical Biology and Medicine* **34**, 1146–1152 (2003).

290. Harwood, D. T. *et al.* Biomarkers of neutrophil-mediated glutathione and protein oxidation in tracheal aspirates from preterm infants: association with bacterial infection. *Pediatr. Res.* **69**, 28–33 (2011).

291. Inder, T. *et al.* Elevated Free Radical Products in the Cerebrospinal Fluid of VLBW Infants with Cerebral White Matter Injury. *Pediatr Res* **52**, 213–218 (2002).

292. Buss, I. H. *et al.* 3-Chlorotyrosine as a Marker of Protein Damage by Myeloperoxidase in Tracheal Aspirates From Preterm Infants: Association With Adverse Respiratory Outcome. *Pediatric Research* **53**, 455–462 (2003).

293. Hoehn, T. *et al.* Urinary Excretion of the Nitrotyrosine Metabolite 3-Nitro-4-Hydroxyphenylacetic Acid in Preterm and Term Infants. *Neonatology* **93**, 73–76 (2008).

294. Ipson, B. R. & Fisher, A. L. Roles of the tyrosine isomers meta-tyrosine and ortho-tyrosine in oxidative stress. *Ageing Res Rev* **27**, 93–107 (2016).

295. Radi, R. Oxygen radicals, nitric oxide, and peroxynitrite: Redox pathways in molecular medicine. *Proc Natl Acad Sci USA* **115**, 5839–5848 (2018).

296. Di Fiore, J. M. & Vento, M. Intermittent hypoxemia and oxidative stress in preterm infants. *Respiratory Physiology & Neurobiology* **266**, 121–129 (2019).

297. Sands, S. A. *et al.* Mechanism Underlying Accelerated Arterial Oxygen Desaturation during Recurrent Apnea. *Am J Respir Crit Care Med* **182**, 961–969 (2010).

298. Reimer K A, Lowe J E, Rasmussen M M & Jennings R B. The wavefront phenomenon of ischemic cell death. 1. Myocardial infarct size vs duration of coronary occlusion in dogs. *Circulation* **56**, 786–794 (1977).

299. Hearse, D. J., Humphrey, S. M. & Chain, E. B. Abrupt reoxygenation of the anoxic potassium-arrested perfused rat heart: A study of myocardial enzyme release. *Journal of Molecular and Cellular Cardiology* **5**, 395–407 (1973).

300. Wang, C. L. *et al.* Resuscitation of Preterm Neonates by Using Room Air or 100% Oxygen. *PEDIATRICS* **121**, 1083–1089 (2008).

301. Hamon, I. *et al.* Early Inhaled Nitric Oxide Improves Oxidative Balance in Very Preterm Infants. *Pediatric Research* **57**, 637–643 (2005).

302. Friel, J. K. *et al.* Evidence of Oxidative Stress in Relation to Feeding Type During Early Life in Premature Infants. *Pediatric Research* **69**, 160–164 (2011).

303. Shoji, H. *et al.* Suppressive effects of breast milk on oxidative DNA damage in very low birthweight infants. *Archives of Disease in Childhood - Fetal and Neonatal Edition* **89**, F136–F138 (2004).

304. Mosa, S. & Nasef, N. Light-Exposed Parenteral Nutrition Solutions and Implications for Preterm Infants. in *Diet and Nutrition in Critical Care* (eds. Rajendram, R., Preedy, V. R. & Patel, V. B.) 2019–2035 (Springer, 2015). doi:10.1007/978-1-4614-7836-2_98.

305. Laborie, S., Lavoie, J.-C. & Chessex, P. Increased urinary peroxides in newborn infants receiving parenteral nutrition exposed to light. *The Journal of Pediatrics* **136**, 628–632 (2000).

306. Yildizdas, H. Y. *et al.* Effects of two different lipid emulsions on antioxidant status, lipid peroxidation and parenteral nutrition- related cholestasis in premature babies, a randomized-controlled study. *Pediatrics & Neonatology* **60**, 359–367 (2019).

307. Skouroliakou, M. *et al.* A double-blind, randomized clinical trial of the effect of ω-3 fatty acids on the oxidative stress of preterm neonates fed through parenteral nutrition. *European Journal of Clinical Nutrition* **64**, 940–947 (2010).

308. Huston, R. K., Jelen, B. J., Ray, L. K. & Borschel, M. W. Parenteral and Enteral Selenium Supplementation in Low Birthweight Preterm Infants. ▲ 1853. *Pediatric Research* **39**, 311–311 (1996).

309. Winterbourn, C. C. *et al.* Protein Carbonyls and Lipid Peroxidation Products as Oxidation Markers in Preterm Infant Plasma: Associations with Chronic Lung Disease

and Retinopathy and Effects of Selenium Supplementation. *Pediatr Res* **48**, 84–90 (2000).

310. Darlow, B. A. *et al.* The effect of selenium supplementation on outcome in very low birth weight infants: A randomized controlled trial. *The Journal of Pediatrics* **136**, 473–480 (2000).

311. Braake, F. W. J. te, Schierbeek, H., Vermes, A., Huijmans, J. G. M. & Goudoever, J. B. van. High-Dose Cysteine Administration Does Not Increase Synthesis of the Antioxidant Glutathione Preterm Infants. *Pediatrics* **124**, e978–e984 (2009).

312. Cai Hua. NAD(P)H Oxidase–Dependent Self-Propagation of Hydrogen Peroxide and Vascular Disease. *Circulation Research* **96**, 818–822 (2005).

313. Almaas, R., Saugstad, O. D., Pleasure, D. & Rootwelt, T. Effect of Barbiturates on Hydroxyl Radicals, Lipid Peroxidation, and Hypoxic Cell Death in Human NT2-N Neurons. *Anesthesiology* **92**, 764–774 (2000).

314. Gidday, J. M., Beetsch, J. W. & Park, T. s. Endogenous Glutathione Protects Cerebral Endothelial Cells From Traumatic Injury. *Journal of Neurotrauma* **16**, 27–36 (1999).

315. Saugstad, O. D. Update on oxygen radical disease in neonatology. *Current Opinion in Obstetrics and Gynecology* **13**, 147–153 (2001).

316. Lorente-Pozo, S. *et al.* The Oxygen Load Supplied during Delivery Room Stabilization of Preterm Infants Modifies the DNA Methylation Profile. *The Journal of Pediatrics* **202**, 70-76.e2 (2018).

317. Oei, J. L. & Vento, M. Is There a “Right” Amount of Oxygen for Preterm Infant Stabilization at Birth? *Front. Pediatr.* **7**, (2019).

318. Peliowski, A., Society, C. P., Committee, F. and N. & Committee, F. and N. Inhaled nitric oxide use in newborns. *Paediatr Child Health* **17**, 95–97 (2012).

319. Barrington, K. J. & Finer, N. Inhaled nitric oxide for respiratory failure in preterm infants. *Cochrane Database of Systematic Reviews* (2010) doi:10.1002/14651858.CD000509.pub4.

320. Sokol, G. M., Konduri, G. G. & Van Meurs, K. P. Inhaled nitric oxide therapy for pulmonary disorders of the term and preterm infant. *Seminars in Perinatology* **40**, 356–369 (2016).

321. Vento, M. & Sánchez-Illana, Á. Nitric oxide and preterm resuscitation: some words of caution. *Pediatric Research* **87**, 438–440 (2020).

322. Greenberg, R. G. *et al.* Late-onset Sepsis in Extremely Premature Infants: 2000–2011. *The Pediatric Infectious Disease Journal* **36**, 774–779 (2017).

323. Spasojević, I., Obradović, B. & Spasić, S. Bench-to-bedside review: Neonatal sepsis - redox processes in pathogenesis. *Critical Care* **16**, 221 (2012).

324. Poggi, C. & Dani, C. Sepsis and Oxidative Stress in the Newborn: From Pathogenesis to Novel Therapeutic Targets. *Oxidative Medicine and Cellular Longevity* vol. 2018 e9390140 https://www.hindawi.com/journals/omcl/2018/9390140/ (2018).

325. Batra, S., Kumar, R., Seema, Kapoor, A. K. & Ray, G. Alterations in antioxidant status during neonatal sepsis. *Annals of Tropical Paediatrics* **20**, 27–33 (2000).

326. Seema *et al.* Serum TNF-alpha and free radical scavengers in neonatal septicemia. *Indian J Pediatr* **66**, 511–516 (1999).

327. Cancelier, A. C. *et al.* Inflammatory and oxidative parameters in cord blood as diagnostic of early-onset neonatal sepsis: A case-control study. *Pediatric Critical Care Medicine* **10**, 467–471 (2009).

328. Cernada, M. *et al.* Sepsis in preterm infants causes alterations in mucosal gene expression and microbiota profiles compared to non-septic twins. *Scientific Reports* **6**, 25497 (2016).

329. Sánchez-Illana, Á. *et al.* Biomarkers of oxidative stress derived damage to proteins and DNA in human breast milk. *Analytica Chimica Acta* **1016**, 78–85 (2018).

330. Young, B. E. *et al.* Markers of Oxidative Stress in Human Milk do not Differ by Maternal BMI But are Related to Infant Growth Trajectories. *Maternal and Child Health Journal* **21**, 1367–1376 (2017).

331. Lavoie, J.-C. & Chessex, P. Parenteral nutrition and oxidant stress in the newborn: A narrative review. *Free Radical Biology and Medicine* **142**, 155–167 (2019).

332. Lavoie, J.-C., Bélanger, S., Spalinger, M. & Chessex, P. Admixture of a Multivitamin Preparation to Parenteral Nutrition: The Major Contributor to In Vitro Generation of Peroxides. *Pediatrics* **99**, e6–e6 (1997).

333. Dupertuis, Y. M. *et al.* Physical characteristics of total parenteral nutrition bags significantly affect the stability of vitamins C and B1: a controlled prospective study. *Journal of Parenteral and Enteral Nutrition* **26**, 310–316 (2002).

334. Davis, J. M. *et al.* Safety and Pharmacokinetics of Multiple Doses of Recombinant Human CuZn Superoxide Dismutase Administered Intratracheally to Premature Neonates With Respiratory Distress Syndrome. *Pediatrics* **100**, 24–30 (1997).

335. Davis, J. M. *et al.* Pulmonary Outcome at 1 Year Corrected Age in Premature Infants Treated at Birth With Recombinant Human CuZn Superoxide Dismutase. *Pediatrics* **111**, 469–476 (2003).

336. Rosenfeld, W. N. *et al.* Safety and Pharmacokinetics of Recombinant Human Superoxide Dismutase Administered Intratracheally to Premature Neonates With Respiratory Distress Syndrome. *Pediatrics* **97**, 811–817 (1996).

337. Loui, A., Raab, A., Maier, R. F., Brätter, P. & Obladen, M. Trace elements and antioxidant enzymes in extremely low birthweight infants. *Journal of Trace Elements in Medicine and Biology* **24**, 111–118 (2010).

338. Akisu, M., Tuzun, S., Arslanoglu, S., Yalaz, M. & Kultursay, N. Effect of recombinant human erythropoietin administration on lipid peroxidation and antioxidant enzyme(s) activities in preterm infants. *Acta Med Okayama* **55**, 357–362 (2001).

339. El-Kabbany, Z. A. *et al.* Melatonin as an adjuvant therapy in preterm infants with neonatal sepsis, randomized trial. *Egypt Pediatric Association Gaz* **68**, 2 (2020).

340. Mactier, H. *et al.* Vitamin A Supplementation Improves Retinal Function in Infants at Risk of Retinopathy of Prematurity. *The Journal of Pediatrics* **160**, 954-959.e1 (2012).

341. Wardle, S. P. Randomised controlled trial of oral vitamin A supplementation in preterm infants to prevent chronic lung disease. *Archives of Disease in Childhood - Fetal and Neonatal Edition* **84**, 9F – 13 (2001).

342. Bell, E. F. *et al.* Serum Tocopherol Levels in Very Preterm Infants After a Single Dose of Vitamin E at Birth. *PEDIATRICS* **132**, e1626–e1633 (2013).

343. Perrone, S. *et al.* Lipid and Protein Oxidation in Newborn Infants after Lutein Administration. *Oxidative Medicine and Cellular Longevity* **2014**, 1–7 (2014).

344. Costa, S. *et al.* Effects of lutein supplementation on biological antioxidant status in preterm infants: a randomized clinical trial. *The Journal of Maternal-Fetal & Neonatal Medicine* **26**, 1311–1315 (2013).

345. te Braake, F. W. *et al.* Glutathione synthesis rates after amino acid administration directly after birth in preterm infants. *The American Journal of Clinical Nutrition* **88**, 333–339 (2008).

346. McBride, J. A., Parad, R. B., Davis, J. M., Zheng, Z. & Zupancic, J. a. F. Economic evaluation of recombinant human copper zinc superoxide dismutase administered at birth to premature infants. *Journal of Perinatology* **29**, 364–371 (2009).

347. Gentyala, R. R., Ehret, D., Suresh, G. & Soll, R. Superoxide dismutase for preventing bronchopulmonary dysplasia (BPD) in preterm infants. *Cochrane Database of Systematic Reviews* (2019) doi:10.1002/14651858.CD013232.

348. Von Kohorn, I. & Ehrenkranz, R. A. Anemia in the Preterm Infant: Erythropoietin Versus Erythrocyte Transfusion—It's not that Simple. *Clinics in Perinatology* **36**, 111–123 (2009).

349. Maier, R. F. *et al.* Early treatment with erythropoietin β ameliorates anemia and reduces transfusion requirements in infants with birth weights below 1000 g. *The Journal of Pediatrics* **141**, 8–15 (2002).

350. Juul, S. E. *et al.* A Randomized Trial of Erythropoietin for Neuroprotection in Preterm Infants. *New England Journal of Medicine* (2020) doi:10.1056/NEJMoa1907423.

351. Ohlsson, A. & Aher, S. M. Early erythropoiesis-stimulating agents in preterm or low birth weight infants. *Cochrane Database of Systematic Reviews* (2017) doi:10.1002/14651858.CD004863.pub5.

352. Chaudhari, T. & McGuire, W. Allopurinol for preventing mortality and morbidity in newborn infants with hypoxic-ischaemic encephalopathy. *Cochrane Database of Systematic Reviews* (2012) doi:10.1002/14651858.CD006817.pub3.

353. Maiwald, C. A. *et al.* Effect of allopurinol in addition to hypothermia treatment in neonates for hypoxic-ischemic brain injury on neurocognitive outcome (ALBINO): study protocol of a blinded randomized placebo-controlled parallel group multicenter trial for superiority (phase III). *BMC Pediatrics* **19**, 210 (2019).

354. Reiter, R. J., Tan, D., Osuna, C. & Gitto, E. Actions of melatonin in the reduction of oxidative stress. *J Biomed Sci* **7**, 444–458 (2000).

355. Bonnefont-Rousselot, D. & Collin, F. Melatonin: Action as antioxidant and potential applications in human disease and aging. *Toxicology* **278**, 55–67 (2010).

356. Biran, V. *et al.* Melatonin Levels in Preterm and Term Infants and Their Mothers. *IJMS* **20**, 2077 (2019).

357. Merchant, N. M. *et al.* Pharmacokinetics of melatonin in preterm infants: Pharmacokinetics of melatonin in preterm infants. *Br J Clin Pharmacol* **76**, 725–733 (2013).

358. Fulia, F. *et al.* Increased levels of malondialdehyde and nitrite/nitrate in the blood of asphyxiated newborns: reduction by melatonin: Free radicals in the asphyxiated newborn. *Journal of Pineal Research* **31**, 343–349 (2001).

359. Gitto, E. *et al.* Oxidative and Inflammatory Parameters in Respiratory Distress Syndrome of Preterm Newborns: Beneficial Effects of Melatonin. *Am J Perinatol* **21**, 209–216 (2004).

360. Sinbad, O. O., Folorunsho, A. A., Olabisi, O. L., Ayoola, O. A. & Temitope, E. J. Vitamins as Antioxidants. *Journal of Food Science and Nutrition Research* **2**, 214–235 (2019).

361. Greenough, A., Shaheen, S. O., Shennan, A., Seed, P. T. & Poston, L. Respiratory outcomes in early childhood following antenatal vitamin C and E supplementation. *Thorax* **65**, 998–1003 (2010).

362. Darlow, B. A., Graham, P. J. & Rojas-Reyes, M. X. Vitamin A supplementation to prevent mortality and short- and long-term morbidity in very low birth weight infants. *Cochrane Database of Systematic Reviews* (2016) doi:10.1002/14651858.CD000501.pub4.

363. Brion, L. P., Bell, E. F. & Raghuveer, T. S. Vitamin E supplementation for prevention of morbidity and mortality in preterm infants. *Cochrane Database of Systematic Reviews* (2003) doi:10.1002/14651858.CD003665.

364. Buonocore, G., Tei, M. & Perrone, S. Lutein as protective agent against neonatal oxidative stress. *Journal of Pediatric and Neonatal Individualized Medicine* **3**, e030244 (2014).

365. Perrone, S., Tei, M., Longini, M. & Buonocore, G. The Multiple Facets of Lutein: A Call for Further Investigation in the Perinatal Period. *Oxidative Medicine and Cellular Longevity* **2016**, 1–8 (2016).

366. Romagnoli, C. *et al.* Lutein absorption in premature infants. *Eur J Clin Nutr* **64**, 760–761 (2010).

367. Papile, L.-A., Burstein, J., Burstein, R. & Koffler, H. Incidence and evolution of subependymal and intraventricular hemorrhage: A study of infants with birth weights less than 1,500 gm. *The Journal of Pediatrics* **92**, 529–534 (1978).

368. Hartnett, M. E. Pathophysiology and Mechanisms of Severe Retinopathy of Prematurity. *Ophthalmology* **122**, 200–210 (2015).

369. Islam, J. Y., Keller, R. L., Aschner, J. L., Hartert, T. V. & Moore, P. E. Understanding the Short- and Long-Term Respiratory Outcomes of Prematurity and Bronchopulmonary Dysplasia. *Am J Respir Crit Care Med* **192**, 134–156 (2015).

370. Lakshminrusimha, S., Konduri, G. G. & Steinhorn, R. H. Considerations in the management of hypoxemic respiratory failure and persistent pulmonary hypertension in term and late preterm neonates. *J Perinatol* **36**, S12–S19 (2016).

371. Neu, J. & Walker, W. A. Necrotizing Enterocolitis. *New England Journal of Medicine* **364**, 255–264 (2011).

372. Burton, G. J. Oxygen, the Janus gas; its effects on human placental development and function. *Journal of Anatomy* **215**, 27–35 (2009).

373. Bailey, D. M. *et al.* On the antioxidant properties of erythropoietin and its association with the oxidative-nitrosative stress response to hypoxia in humans. *Acta Physiol* **212**, 175–187 (2014).

374. Northway, W. H., Rosan, R. C. & Porter, D. Y. Pulmonary Disease Following Respirator Therapy of Hyaline-Membrane Disease: Bronchopulmonary Dysplasia. *N Engl J Med* **276**, 357–368 (1967).

375. Steinhorn, R. H. Neonatal pulmonary hypertension: *Pediatric Critical Care Medicine* **11**, S79–S84 (2010).

376. Check, J. *et al.* Fetal growth restriction and pulmonary hypertension in premature infants with bronchopulmonary dysplasia. *J Perinatol* **33**, 553–557 (2013).

377. Haworth, S. G. & Reid, L. Persistent fetal circulation: Newly recognized structural features. *The Journal of Pediatrics* **88**, 614–620 (1976).

378. Steinhorn, R. H. & Lakshminrusimha, S. Oxygen and pulmonary vasodilation: The role of oxidative and nitrosative stress. *Seminars in Fetal and Neonatal Medicine* **25**, 101083 (2020).

379. La Frano, M. R. *et al.* Umbilical cord blood metabolomics reveal distinct signatures of dyslipidemia prior to bronchopulmonary dysplasia and pulmonary hypertension. *American Journal of Physiology-Lung Cellular and Molecular Physiology* **315**, L870–L881 (2018).

380. Reuter, S. D. *et al.* Urinary F2-isoprostanes are poor prognostic indicators for the development of bronchopulmonary dysplasia. *J Perinatol* **27**, 303–306 (2007).

381. Terry, T. L. Fibroblastic Overgrowth of Persistent Tunica Vasculosa Lentis in Infants Born Prematurely*: III. Studies in development and regression of hyaloid artery and tunica vasculosa lentis. *American Journal of Ophthalmology* **25**, 1409–1423 (1942).

382. Chen, J. & Smith, L. E. H. Retinopathy of prematurity. *Angiogenesis* **10**, 133–140 (2007).

383. Sapieha, P. *et al.* Retinopathy of prematurity: understanding ischemic retinal vasculopathies at an extreme of life. *J Clin Invest* **120**, 3022–3032 (2010).

384. Mutlu, F. M. & Sarici, S. U. Treatment of retinopathy of prematurity:a review of conventional and promising new therapeutic options. *International Journal of Ophthalmology* **6**, 228–236 (20130422).

385. Banjac, L. Pro-Oxidants and Antioxidants in Retinopathy of Prematurity. *ACC* (2018) doi:10.20471/acc.2018.57.03.08.

386. Iadecola, C. & Anrather, J. The immunology of stroke: from mechanisms to translation. *Nat Med* **17**, 796–808 (2011).

387. Dirnagl, U., Iadecola, C. & Moskowitz, M. A. Pathobiology of ischaemic stroke: an integrated view. *Trends in Neurosciences* **22**, 391–397 (1999).

388. Garofoli, F. Oral Melatonin as Neuroprotectant in Preterm Infants. https://clinicaltrials.gov/ct2/show/NCT04235673 (2020).

389. Perrone, S. *et al.* May oxidative stress biomarkers in cord blood predict the occurrence of necrotizing enterocolitis in preterm infants? *The Journal of Maternal-Fetal & Neonatal Medicine* **25**, 128–131 (2012).

390. Tam, E. W. Y. Cerebellar injury in preterm infants. in *Handbook of Clinical Neurology* vol. 155 49–59 (Elsevier, 2018).

391. Huang, J. *et al.* Antenatal infection and intraventricular hemorrhage in preterm infants: A meta-analysis. *Medicine* **98**, e16665 (2019).

392. Ballabh, P. Intraventricular Hemorrhage in Premature Infants: Mechanism of Disease. *Pediatr Res* **67**, 1–8 (2010).

393. Kuwano, T. *et al.* Cyclooxygenase 2 is a key enzyme for inflammatory cytokine-induced angiogenesis. *FASEB j.* **18**, 300–310 (2004).

394. Szpecht, D., Wiak, K., Braszak, A., Szymankiewicz, M. & Gadzinowski, J. Role of selected cytokines in the etiopathogenesis of intraventricular hemorrhage in preterm newborns. *Childs Nerv Syst* **32**, 2097–2103 (2016).

395. Ackerman, W. E., Rovin, B. H. & Kniss, D. A. Epidermal Growth Factor and Interleukin-1β Utilize Divergent Signaling Pathways to Synergistically Upregulate Cyclooxygenase-2 Gene Expression in Human Amnion-Derived WISH Cells1. *Biology of Reproduction* **71**, 2079–2086 (2004).

396. O'Brien, J. S. & Sampson, E. L. Fatty acid and fatty aldehyde composition of the major brain lipids in normal human gray matter, white matter, and myelin. *J. Lipid Res.* **6**, 545–551 (1965).

397. Lin, P. W. & Stoll, B. J. Necrotising enterocolitis. *The Lancet* **368**, 1271–1283 (2006).

398. Hui, L. *et al.* Immunoregulation effects of different γδT cells and toll-like receptor signaling pathways in neonatal necrotizing enterocolitis: *Medicine* **96**, e6077 (2017).

399. Fusunyan, R. D., Nanthakumar, N. N., Baldeon, M. E. & Walker, W. A. Evidence for an Innate Immune Response in the Immature Human Intestine: Toll-Like Receptors on Fetal Enterocytes. *Pediatr Res* **49**, 589–593 (2001).

400. Werts, A. D. *et al.* A Novel Role for Necroptosis in the Pathogenesis of Necrotizing Enterocolitis. *Cellular and Molecular Gastroenterology and Hepatology* **9**, 403–423 (2020).

401. Akira, S., Takeda, K. & Kaisho, T. Toll-like receptors: critical proteins linking innate and acquired immunity. *Nat Immunol* **2**, 675–680 (2001).

402. Nowicki, P. T. & Nankervis, C. A. The Role of the Circulation in the Pathogenesis of Necrotizing Enterocolitis. *Clinics in Perinatology* **21**, 219–234 (1994).

403. Asehnoune, K., Strassheim, D., Mitra, S., Kim, J. Y. & Abraham, E. Involvement of Reactive Oxygen Species in Toll-Like Receptor 4-Dependent Activation of NF-κB. *J Immunol* **172**, 2522–2529 (2004).

404. Belik, J., González-Luis, G. E., Perez-Vizcaino, F. & Villamor, E. Isoprostanes in fetal and neonatal health and disease. *Free Radic. Biol. Med.* **48**, 177–188 (2010).

405. Solberg, R. *et al.* Resuscitation with supplementary oxygen induces oxidative injury in the cerebral cortex. *Free Radical Biology and Medicine* **53**, 1061–1067 (2012).

406. Morrow, J. D. *et al.* A series of prostaglandin F2-like compounds are produced in vivo in humans by a non-cyclooxygenase, free radical-catalyzed mechanism. *Proc. Natl. Acad. Sci. U.S.A.* **87**, 9383–9387 (1990).

407. Jahn, U., Galano, J.-M. & Durand, T. Beyond prostaglandins--chemistry and biology of cyclic oxygenated metabolites formed by free-radical pathways from polyunsaturated fatty acids. *Angew. Chem. Int. Ed. Engl.* **47**, 5894–5955 (2008).

408. Song, W.-L. *et al.* Neurofurans, novel indices of oxidant stress derived from docosahexaenoic acid. *J. Biol. Chem.* **283**, 6–16 (2008).

409. Tonni, G., Leoncini, S., Signorini, C., Ciccoli, L. & De Felice, C. Pathology of perinatal brain damage: background and oxidative stress markers. *Arch Gynecol Obstet* **290**, 13–20 (2014).

410. Chafer-Pericas, C. *et al.* Preliminary case control study to establish the correlation between novel peroxidation biomarkers in cord serum and the severity of hypoxic ischemic encephalopathy. *Free Radical Biology and Medicine* **97**, 244–249 (2016).

411. Lee, Y. Y. *et al.* Assessment of Isoprostanes in Human Plasma: Technical Considerations and the Use of Mass Spectrometry. *Lipids* **51**, 1217–1229 (2016).

412. Milne, G. L., Gao, B., Terry, E. S., Zackert, W. E. & Sanchez, S. C. Measurement of F2- isoprostanes and isofurans using gas chromatography-mass spectrometry. *Free Radic. Biol. Med.* **59**, 36–44 (2013).

413. De las Heras-Gómez, I. *et al.* Potential applications of lipid peroxidation products – F 4 -neuroprostanes, F 3 -neuroprostanes n-6 DPA , F 2 -dihomo-isoprostanes and F 2 -isoprostanes - in the evaluation of the allograft function in renal transplantation. *Free Radic Biol Med* **104**, 178–184 (2017).

414. Durand, T. *et al.* Total Syntheses of Four Metabolites of 15-F2t-Isoprostane. *European Journal of Organic Chemistry* **2001**, 809–819 (2001).

415. Durand, T., Cracowski, J.-L., Guy, A. & Rossi, J.-C. Syntheses and preliminary pharmacological evaluation of the two epimers of the 5-F2t-isoprostane. *Bioorganic & Medicinal Chemistry Letters* **11**, 2495–2498 (2001).

416. Durand, T., Guy, A., Vidal, J.-P., Viala, J. & Rossi, J.-C. Total synthesis of 4(RS)-F4t-isoprostane methyl ester. *Tetrahedron Letters* **41**, 3859–3862.

417. Oger, C. *et al.* The Handy Use of Brown's P2-Ni Catalyst for a Skipped Diyne Deuteration: Application to the Synthesis of a [D4]-Labeled F4t-Neuroprostane. *Chemistry – A European Journal* **16**, 13976–13980 (2010).

418. Oger, C., Bultel-Poncé, V., Guy, A., Durand, T. & Galano, J.-M. Total Synthesis of Isoprostanes Derived from Adrenic Acid and EPA. *European Journal of Organic Chemistry* **2012**, 2621–2634 (2012).

419. Guy, A. *et al.* Oxygenated Metabolites of n-3 Polyunsaturated Fatty Acids as Potential Oxidative Stress Biomarkers: Total Synthesis of 8-F3t-IsoP, 10-F4t-NeuroP and [D4]-10-F4t-NeuroP. *Chemistry – A European Journal* **20**, 6374–6380 (2014).

420. de La Torre, A. *et al.* Synthesis, Discovery, and Quantitation of Dihomo-Isofurans: Biomarkers for In Vivo Adrenic Acid Peroxidation. *Angewandte Chemie International Edition* **53**, 6249–6252 (2014).

421. de la Torre, A. *et al.* Total Syntheses and In Vivo Quantitation of Novel Neurofuran and Dihomo-isofuran Derived from Docosahexaenoic Acid and Adrenic Acid. *Chemistry - A European Journal* **21**, 2442–2446 (2015).

422. Bastani, N. E., Gundersen, T. E. & Blomhoff, R. Determination of 8-epi PGF2α concentrations as a biomarker of oxidative stress using triple-stage liquid

chromatography/tandem mass spectrometry. *Rapid Communications in Mass Spectrometry* **23**, 2885–2890 (2009).

423. VanRollins, M., Woltjer, R. L., Yin, H., Morrow, J. D. & Montine, T. J. F2-Dihomo-isoprostanes arise from free radical attack on adrenic acid. *J Lipid Res* **49**, 995–1005 (2008).

424. Milne, G. L., Yin, H., Hardy, K. D., Davies, S. S. & Roberts, L. J., 2nd. Isoprostane generation and function. *Chem. Rev.* **111**, 5973–5996 (2011).

425. Cuyamendous, C. *et al.* The novelty of phytofurans, isofurans, dihomo-isofurans and neurofurans: Discovery, synthesis and potential application. *Biochimie* **130**, 49–62 (2016).

426. Roy, J. *et al.* Non-enzymatic cyclic oxygenated metabolites of omega-3 polyunsaturated fatty acid: Bioactive drugs? *Biochimie* **120**, 56–61 (2016).

427. Catalá, Á. Lipid peroxidation modifies the assembly of biological membranes "The Lipid Whisker Model". *Front. Physiol.* **5**, (2015).

428. Martinez, M. Tissue levels of polyunsaturated fatty acids during early human development. *The Journal of Pediatrics* **120**, S129–S138 (1992).

429. Galano, J.-M. *et al.* Isoprostanes and neuroprostanes: Total synthesis, biological activity and biomarkers of oxidative stress in humans. *Prostaglandins & Other Lipid Mediators* **107**, 95–102 (2013).

430. De Felice, C. *et al.* F_2 -dihomo-isoprostanes as potential early biomarkers of lipid oxidative damage in Rett syndrome. *Journal of Lipid Research* **52**, 2287–2297 (2011).

431. Lee, Y. Y. & Lee, J. C.-Y. LC-MS/MS Analysis of Lipid Oxidation Products in Blood and Tissue Samples. in *Clinical Metabolomics* 83–92 (Humana Press, New York, NY, 2018). doi:10.1007/978-1-4939-7592-1_6.

432. Milne, G. L., Sanchez, S. C., Musiek, E. S. & Morrow, J. D. Quantification of F 2 - isoprostanes as a biomarker of oxidative stress. *Nature Protocols* **2**, 221–226 (2007).

433. Yan, Z., Mas, E., Mori, T. A., Croft, K. D. & Barden, A. E. A significant proportion of F2-isoprostanes in human urine are excreted as glucuronide conjugates. *Anal. Biochem.* **403**, 126–128 (2010).

434. Leung, K. S., Galano, J. M., Durand, T. & Lee, J. C.-Y. Current development in non-enzymatic lipid peroxidation products, isoprostanoids and isofuranoids, in novel biological samples. *Free Radical Research* **49**, 816–826 (2015).

435. Chemical Abstracts Service (CAS). SciFinder®. https://scifinder.cas.org.

436. Wheelan, P., Zirrolli, J. A. & Murphy, R. C. Electrospray ionization and low energy tandem mass spectrometry of polyhydroxy unsaturated fatty acids. *Journal of the American Society for Mass Spectrometry* **7**, 140–149 (1996).

437. Murphy, R. C. *Tandem Mass Spectrometry of Lipids: Molecular Analysis of Complex Lipids*. (Royal Society of Chemistry, 2014).

438. Martín, I. *et al.* Oxidative stress in mothers who have conceived fetus with neural tube defects: the role of aminothiols and selenium. *Clinical Nutrition* **23**, 507–514 (2004).

439. Saugstad, O. D. Oxidative stress in the newborn--a 30-year perspective. *Biol. Neonate* **88**, 228–236 (2005).

440. Erdem, M., Harma, M., Harma, I. M., Arikan, I. & Barut, A. Comparative study of oxidative stress in maternal blood with that of cord blood and maternal milk. *Archives of Gynecology and Obstetrics* **285**, 371–375 (2012).

441. Watanabe, K. *et al.* Differences in levels of oxidative stress in mothers and neonate: the impact of mode of delivery. *The Journal of Maternal-Fetal & Neonatal Medicine* **26**, 1649–1652 (2013).

442. Şimşek, Y., Karabiyik, P., Polat, K., Duran, Z. & Polat, A. Mode of delivery changes oxidative and antioxidative properties of human milk: a prospective controlled clinical investigation. *The Journal of Maternal-Fetal & Neonatal Medicine* **28**, 734–738 (2015).

443. Roy, S. *et al.* Differential oxidative stress levels in mothers with preeclampsia delivering male and female babies. *The Journal of Maternal-Fetal & Neonatal Medicine* **28**, 1973–1980 (2015).

444. Cappelletti, M., Bella, S. D., Ferrazzi, E., Mavilio, D. & Divanovic, S. Inflammation and preterm birth. *J Leukoc Biol* **99**, 67–78 (2016).

445. Winterbourn, C. C., Kettle, A. J. & Hampton, M. B. Reactive Oxygen Species and Neutrophil Function. *Annual Review of Biochemistry* **85**, 765–792 (2016).

446. Lugrin, J., Rosenblatt-Velin, N., Parapanov, R. & Liaudet, L. The role of oxidative stress during inflammatory processes. *Biological Chemistry* **395**, 203–230 (2013).

447. Mouls, L., Silajdzic, E., Haroune, N., Spickett, C. M. & Pitt, A. R. Development of novel mass spectrometric methods for identifying HOCl-induced modifications to proteins. *Proteomics* **9**, 1617–1631 (2009).

448. Perrone, S., Tataranno, M. L., Stazzoni, G. & Buonocore, G. Biomarkers of oxidative stress in fetal and neonatal diseases. *The Journal of Maternal-Fetal & Neonatal Medicine* **25**, 2575–2578 (2012).

449. Torres-Cuevas, I., Kuligowski, J., Escobar, J. & Vento, M. Determination of biomarkers of protein oxidation in tissue and plasma. *Free Radic. Biol. Med.* **75 Suppl 1**, S51 (2014).

450. Yuksel, S., Yigit, A. A., Cinar, M., Atmaca, N. & Onaran, Y. Oxidant and antioxidant status of human breast milk during lactation period. *Dairy Science & Technology* **95**, 295–302 (2015).

451. Akdag, A. *et al.* Storage at −80°C Preserves the Antioxidant Capacity of Preterm Human Milk: Antioxidant Capacity of Preterm Human Milk at − 80 ° C. *Journal of Clinical Laboratory Analysis* **28**, 415–418 (2014).

452. Zagierski, M. *et al.* Maternal smoking decreases antioxidative status of human breast milk. *Journal of Perinatology* **32**, 593–597 (2012).

453. Wilinska, M., Borszewska-Kornacka, M., Niemiec, T. & Jakiel, G. Oxidative stress and total antioxidant status in term newborns and their mothers. *Annals of Agricultural and Environmental Medicine* **22**, 736–740 (2015).

454. Tudehope, D. I. Human milk and the nutritional needs of preterm infants. *J. Pediatr.* **162**, S17-25 (2013).

455. Guo, M. 2 - Chemical composition of human milk. in *Human Milk Biochemistry and Infant Formula Manufacturing Technology* (ed. Guo, M.) 19–32 (Woodhead Publishing, 2014).

456. Collado, M. C. *et al.* Factors influencing gastrointestinal tract and microbiota immune interaction in preterm infants. *Pediatr. Res.* **77**, 726–731 (2015).

457. Tudehope, D., Vento, M., Bhutta, Z. & Pachi, P. Nutritional requirements and feeding recommendations for small for gestational age infants. *J. Pediatr.* **162**, S81-89 (2013).

458. Guo, M. & Ahmad, S. 5 - Human milk banking. in *Human Milk Biochemistry and Infant Formula Manufacturing Technology* (ed. Guo, M.) 112–138 (Woodhead Publishing, 2014).

459. Manzoni, P. Clinical Benefits of Lactoferrin for Infants and Children. *The Journal of Pediatrics* **173**, S43–S52 (2016).

460. Silvestre, D. *et al.* Antioxidant capacity of human milk: effect of thermal conditions for the pasteurization. *Acta Paediatr.* **97**, 1070–1074 (2008).

461. Elisia, I. & Kitts, D. D. Quantification of hexanal as an index of lipid oxidation in human milk and association with antioxidant components. *Journal of Clinical Biochemistry and Nutrition* **49**, 147–152 (2011).

462. Hanson, C., Lyden, E., Furtado, J., Van Ormer, M. & Anderson-Berry, A. A Comparison of Nutritional Antioxidant Content in Breast Milk, Donor Milk, and Infant Formulas. *Nutrients* **8**, (2016).

463. Marinkovic, V. *et al.* Antioxidative Activity of Colostrum and Human Milk: Effects of Pasteurization and Storage. *Journal of Pediatric Gastroenterology and Nutrition* **62**, 901–906 (2016).

464. Lam, P. M. W. *et al.* Rapid measurement of 8-oxo-7,8-dihydro-2′-deoxyguanosine in human biological matrices using ultra-high-performance liquid chromatography–tandem mass spectrometry. *Free Radical Biology and Medicine* **52**, 2057–2063 (2012).

465. De Luca, A. *et al.* Higher concentrations of branched-chain amino acids in breast milk of obese mothers. *Nutrition* **32**, 1295–1298 (2016).

466. Boskabadi, H. *et al.* The value of serum pro-oxidant/antioxidant balance in the assessment of asphyxia in term neonates. *The Journal of Maternal-Fetal & Neonatal Medicine* **30**, 1556–1561 (2017).

467. Irusen, H., Rohwer, A. C., Steyn, D. W. & Young, T. Treatments for breast abscesses in breastfeeding women. in *Cochrane Database of Systematic Reviews* (John Wiley & Sons, Ltd, 2015). doi:10.1002/14651858.CD010490.pub2.

468. Vento, M. Oxygen supplementation in the neonatal period: changing the paradigm. *Neonatology* **105**, 323–331 (2014).

469. Forman, H. J., Zhang, H. & Rinna, A. Glutathione: Overview of its protective roles, measurement, and biosynthesis. *Mol Aspects Med* **30**, 1–12 (2009).

470. Frijhoff, J. *et al.* Clinical Relevance of Biomarkers of Oxidative Stress. *Antioxid Redox Signal* **23**, 1144–1170 (2015).

471. Jones, D. P. & Sies, H. The Redox Code. *Antioxid. Redox Signal.* **23**, 734–746 (2015).

472. Giustarini, D. *et al.* Assessment of glutathione/glutathione disulphide ratio and S -glutathionylated proteins in human blood, solid tissues, and cultured cells. *Free Radical Biology and Medicine* **112**, 360–375 (2017).

473. Monostori, P., Wittmann, G., Karg, E. & Túri, S. Determination of glutathione and glutathione disulfide in biological samples: An in-depth review. *Journal of Chromatography B* **877**, 3331–3346 (2009).

474. Giustarini, D., Fanti, P., Matteucci, E. & Rossi, R. Micro-method for the determination of glutathione in human blood. *Journal of Chromatography B* **964**, 191–194 (2014).

475. Giustarini, D. *et al.* Pitfalls in the analysis of the physiological antioxidant glutathione (GSH) and its disulfide (GSSG) in biological samples: An elephant in the room. *Journal of Chromatography B* **1019**, 21–28 (2016).

476. Olmos Moya, P. M. *et al.* Simultaneous Electrochemical Speciation of Oxidized and Reduced Glutathione. Redox Profiling of Oxidative Stress in Biological Fluids with a Modified Carbon Electrode. *Anal. Chem.* **89**, 10726–10733 (2017).

477. Cialla-May, D., Zheng, X.-S., Weber, K. & Popp, J. Recent progress in surface-enhanced Raman spectroscopy for biological and biomedical applications: from cells to clinics. *Chem. Soc. Rev.* **46**, 3945–3961 (2017).

478. Le Ru, E. C., Blackie, E., Meyer, M. & Etchegoin, P. G. Surface Enhanced Raman Scattering Enhancement Factors: A Comprehensive Study. *The Journal of Physical Chemistry C* **111**, 13794–13803 (2007).

479. Santos, J. J., Toma, S. H., Corio, P. & Araki, K. Key role of surface concentration on reproducibility and optimization of SERS sensitivity. *J. Raman Spectrosc.* **48**, 1190–1195 (2017).

480. Zhang, D., Xie, Y., Deb, S. K., Davison, V. J. & Ben-Amotz, D. Isotope Edited Internal Standard Method for Quantitative Surface-Enhanced Raman Spectroscopy. *Analytical Chemistry* **77**, 3563–3569 (2005).

481. Gao, J., Zhao, C., Zhang, Z. & Li, G. An intrinsic internal standard substrate of Au@PS-b-P4VP for rapid quantification by surface enhanced Raman scattering. *The Analyst* **142**, 2936–2944 (2017).

482. Shi, C.-X., Chen, Z.-P., Chen, Y., Liu, Q. & Yu, R.-Q. Quantification of dopamine in biological samples by surface-enhanced Raman spectroscopy: Comparison of different calibration models. *Chemometrics and Intelligent Laboratory Systems* **169**, 87–93 (2017).

483. Subaihi, A. *et al.* Towards improved quantitative analysis using surface-enhanced Raman scattering incorporating internal isotope labelling. *Anal. Methods* **9**, 6636–6644 (2017).

484. Wang, W., Zhang, L., Li, L. & Tian, Y. A Single Nanoprobe for Ratiometric Imaging and Biosensing of Hypochlorite and Glutathione in Live Cells Using Surface-Enhanced Raman Scattering. *Analytical Chemistry* **88**, 9518–9523 (2016).

485. Zhou, Y. & Ding, R. Quantitative SERS Detection of Trace Glutathione with Internal Reference Embedded Au-core/Ag-shell Nanoparticles. *Nano LIFE* **06**, 1642003 (2016).

486. Huang, G. G., Hossain, M. K., Han, X. X. & Ozaki, Y. A novel reversed reporting agent method for surface-enhanced Raman scattering; highly sensitive detection of glutathione in aqueous solutions. *Analyst* **134**, 2468–2474 (2009).

487. Huang, G. G., Han, X. X., Hossain, M. K. & Ozaki, Y. Development of a heat-induced surface-enhanced Raman scattering sensing method for rapid detection of glutathione in aqueous solutions. *Anal. Chem.* **81**, 5881–5888 (2009).

488. Huang, G. G., Han, X. X., Hossain, M. K., Kitahama, Y. & Ozaki, Y. A study of glutathione molecules adsorbed on silver surfaces under different chemical environments by surface-enhanced Raman scattering in combination with the heat-induced sensing method. *Applied spectroscopy* **64**, 1100–1108 (2010).

489. Saha, A. & Jana, N. R. Detection of cellular glutathione and oxidized glutathione using magnetic-plasmonic nanocomposite-based 'turn-off' surface enhanced Raman scattering. *Anal. Chem.* **85**, 9221–9228 (2013).

490. Brambilla, A. *et al.* Adapting and testing a portable Raman spectrometer for SERS analysis of amino acids and small peptides. *Journal of Molecular Structure* **1044**, 121–127 (2013).

491. Ouyang, L., Zhu, L., Jiang, J. & Tang, H. A surface-enhanced Raman scattering method for detection of trace glutathione on the basis of immobilized silver nanoparticles and crystal violet probe. *Anal. Chim. Acta* **816**, 41–49 (2014).

492. An, H. H. *et al.* Preparation of SERS active Ag nanoparticles encapsulated by phospholipids. *Journal of Raman Spectroscopy* **45**, 292–298 (2014).

493. Ma, S. & Huang, Q. A SERS study of oxidation of glutathione under plasma irradiation. *RSC Adv.* **5**, 57847–57852 (2015).

494. Zhao, J., Zhang, K., Ji, J. & Liu, B. Sensitive and label-free quantification of cellular biothiols by competitive surface-enhanced Raman spectroscopy. *Talanta* **152**, 196–202 (2016).

495. Sheen Mers, S. V., Umadevi, S. & Ganesh, V. Controlled Growth of Gold Nanostars: Effect of Spike Length on SERS Signal Enhancement. *ChemPhysChem* **18**, 1358–1369 (2017).

496. Chinnakkannu Vijayakumar, S., Venkatakrishnan, K. & Tan, B. SERS Active Nanobiosensor Functionalized by Self-Assembled 3D Nickel Nanonetworks for Glutathione Detection. *ACS Applied Materials & Interfaces* **9**, 5077–5091 (2017).

497. Le Ru, E. C. & Etchegoin, P. G. Chapter 7 - Metallic colloids and other SERS substrates. in *Principles of Surface-Enhanced Raman Spectroscopy* 367–413 (Elsevier, 2009). doi:10.1016/B978-0-444-52779-0.00013-1.

498. Procházka, M. *Surface-enhanced raman spectroscopy: bioanalytical, biomolecular and medical applications*. (Springer, 2016).

499. Lv, M., Gu, H., Yuan, X., Gao, J. & Cai, T. Investigation of 3D silvernanodendrite@glass as surface-enhanced Raman scattering substrate for the detection of Sildenafil and GSH. *Journal of Molecular Structure* **1029**, 75–80 (2012).

500. Podstawka, E., Ozaki, Y. & Proniewicz, L. M. Part I: surface-enhanced Raman spectroscopy investigation of amino acids and their homodipeptides adsorbed on colloidal silver. *Appl Spectrosc* **58**, 570–580 (2004).

501. Lee, H., Kim, M. S. & Suh, S. W. Raman spectroscopy of sulphur-containing amino acids and their derivatives adsorbed on silver. *Journal of Raman spectroscopy* **22**, 91–96 (1991).

502. Ratcliffe, C. I. & Irish, D. E. Vibrational spectral studies of solutions at elevated temperatures and pressures. VI. Raman studies of perchloric acid. *Canadian journal of chemistry* **62**, 1134–1144 (1984).

503. Picquart, M., Grajcar, L., Baron, M. H. & Abedinzadeh, Z. Vibrational spectroscopic study of glutathione complexation in aqueous solutions. *Biospectroscopy* **5**, 328–337 (1999).

504. Carvalho, B. R. *et al.* Probing carbon isotope effects on the Raman spectra of graphene with different $^{13}\mathrm{C}$ concentrations. *Phys. Rev. B* **92**, 125406 (2015).

505. Richie, J. P., Skowronski, L., Abraham, P. & Leutzinger, Y. Blood glutathione concentrations in a large-scale human study. *Clinical Chemistry* **42**, 64–70 (1996).

Annex I. Supplementary figures and tables

AI.1 Novel free-radical mediated Lipid Peroxidation Biomarkers in Newborn Plasma

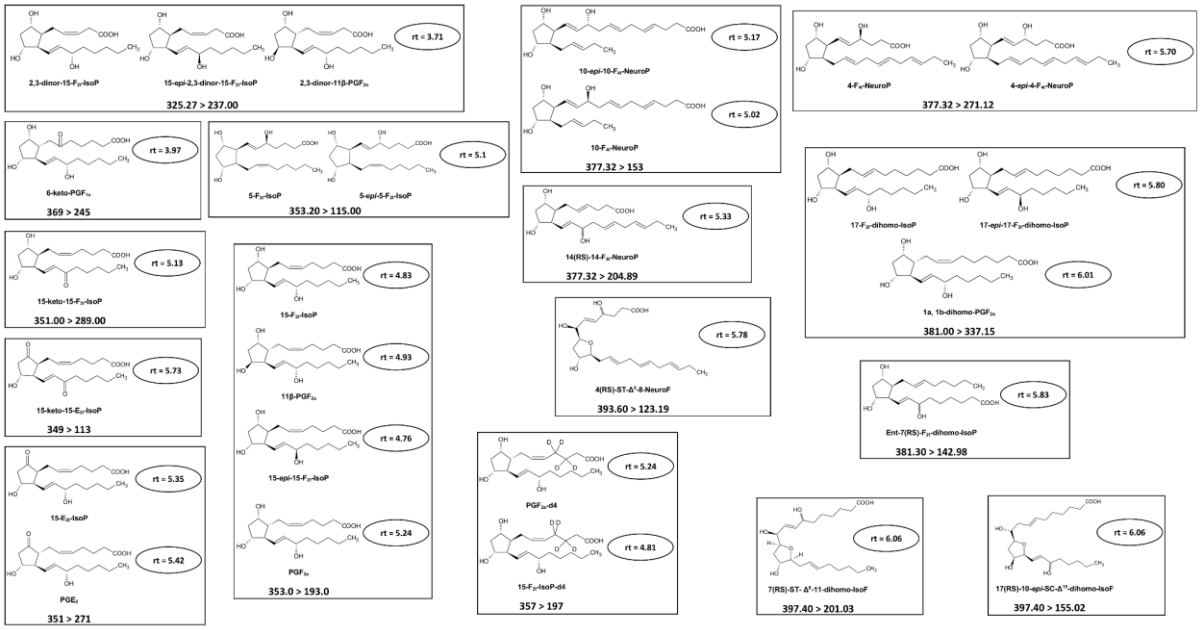

Supplementary figure AI.1.1 Chemical structures of determined isoprostanoids. Note: rt= retention time in minutes; acquired MRM transitions are given as parent ion > daughter ion; compounds acquired employing the same MRM transition were grouped in boxes.

AI.2 Adrenic acid non-enzymatic peroxidation products in biofluids of moderate preterm infants

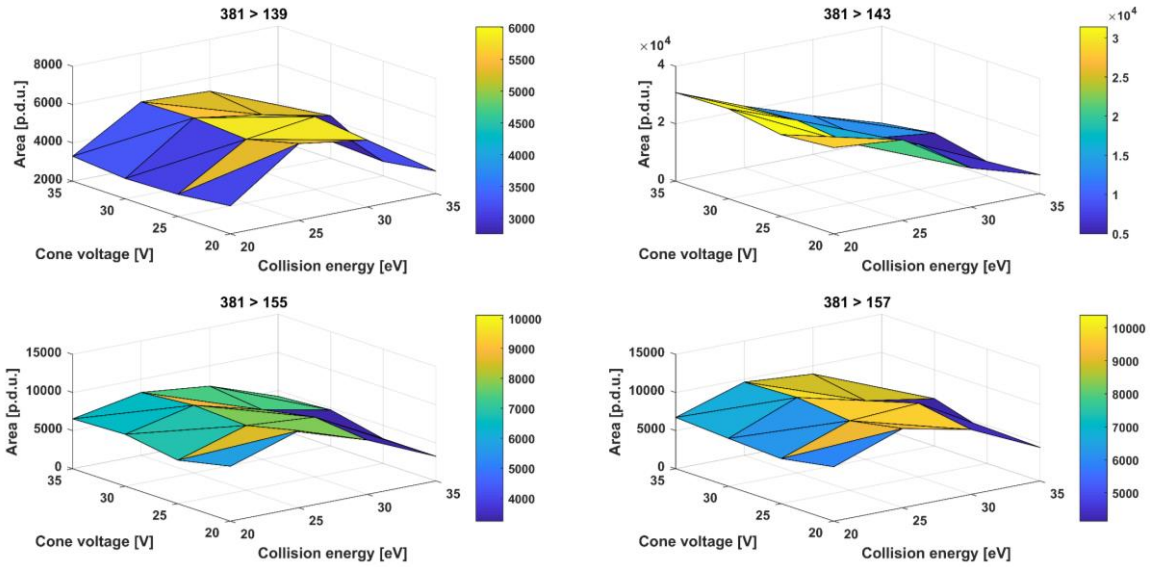

Supplementary figure AI.2.1 Optimization surfaces of dihomo-isoP ([C22H38O5 – H]-, m/z = 381) fragmentations. In each triangular surface plot is shown the corresponding values of the integrated area along the window of 5.3 – 6.5 minutes for each cone voltage and collision energy.

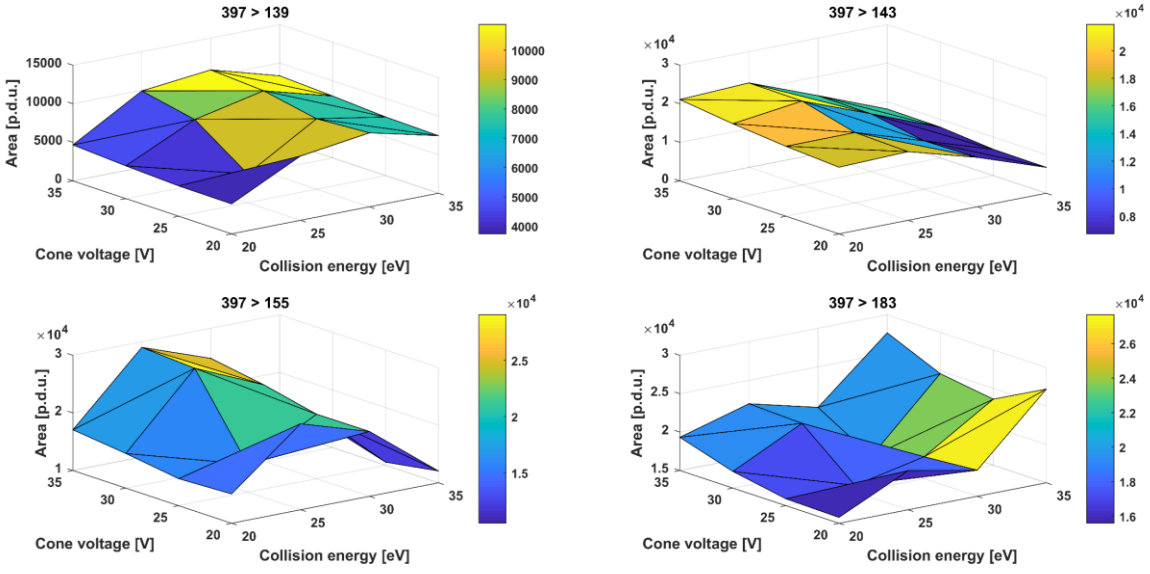

Supplementary figure AI.2.2 Optimization surfaces of dihomo-isoF ([C22H38O6 – H]-, m/z = 397) fragmentations. In each triangular surface plot is shown the corresponding values of the integrated area along the window of 3.5 – 6.5 minutes for each cone voltage and collision energy.

AI3. On-Capillary Surface-Enhanced Raman Spectroscopy: Determination of Glutathione in Whole Blood Microsamples

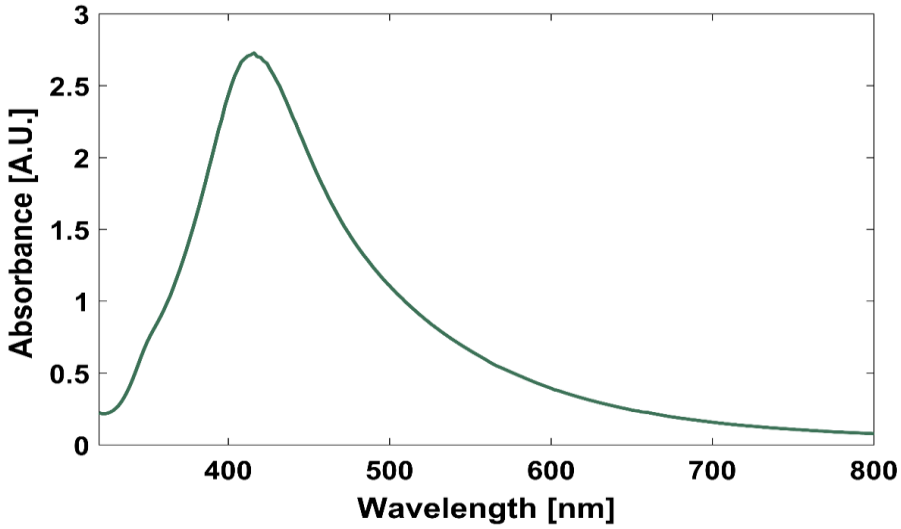

Supplementary figure AI 3.1 UV-Vis spectrum of the SERS substrate.

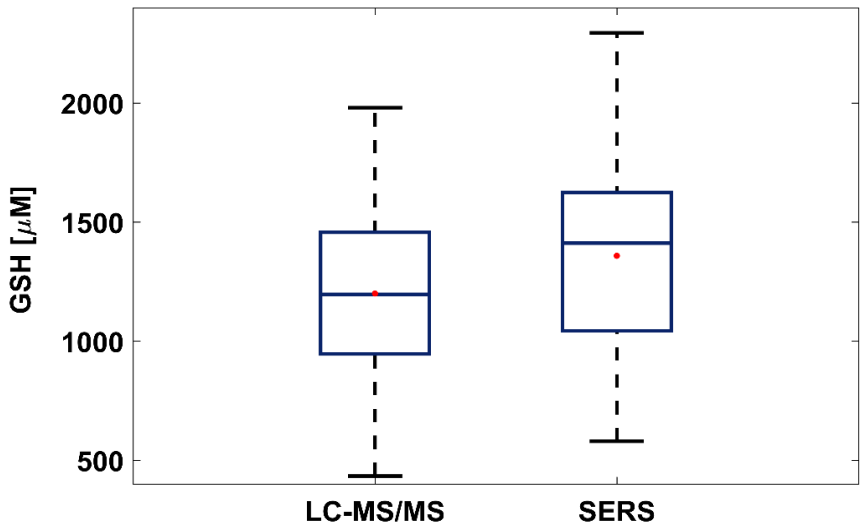

Supplementary figure AI 3.2 GSH concentrations determined in blood samples from 36 newborns employing a validated LC-MS/MS reference method and the SERS approach.

Supplementary table AI 3.1 Characteristics of adults (N=20).

Parameter	Newborns (N=36)
Weight, mean [kg] ± s	67 ± 13
Height, mean [cm] ± s	168 ± 8
Male [%]	40
Age [years] ± s	33 ± 11

Supplementary table AI 3.2 Characteristics of newborns (N=36).

Parameter	Newborns (N=36)
Gestational age, mean [weeks + days] ± s [days]	39+3 ± 2
Birthweight, mean [g] ± s	3300 ± 400
Length, mean [cm] ± s	50 ± 2
Male [%]	44
Age [h] ± s	54 ± 13

Supplementary table AI 3.3 Correlation coefficients (R) of 27 SERS spectra of standard solutions of metabolites found in blood with GSH and blank SERS spectra in the 600 to 1800 cm-1 region.

Metabolite	R with GSH spectrum	R with blank spectrum
L-alanine	0.2	0.96
L-asparagine	0.3	0.94
L- histidine	0.3	0.8
L-isoleucine	0.2	0.96
L-leucine	0.4	0.92
L-ornithine	0.3	0.93
L-proline	0.3	0.98
Sarcosine	0.3	0.93
L-serine	0.3	0.990
Taurine	0.2	0.95
L- threonine	0.2	0.94
L- tryptophan	0.3	0.90
L-valine	0.2	0.93
L-glutamine	0.3	0.96
L-arginine	0.2	0.03
Glycine	0.3	0.98
L-aspartic acid	0.3	0.93

Metabolite	R with GSH spectrum	R with blank spectrum
L-creatinine	0.3	0.8
L-cystine	0.4	0.90
L-glutamic acid	0.3	0.94
L-lysine	0.09	0.6
L-phenylalanine	0.3	0.90
L-tyrosine	0.2	0.94
L- methionine	0.2	0.91
L-homocystine	0.2	0.90
L-cystathionine	0.4	0.94
L- cysteine	0.4	0.93